# A LONG TERM PERSPECTIVE ON

# THE LWR FUEL CYCLE

by

MUSHTAQ AHMAD MALIK

M.Sc., QUAID-E-AZAM UNIVERSITY, PAKISTAN
(1977)

M.S., Massachusetts Institute of Technology
(1981)

SUBMITTED IN PARTIAL FULFILLMENT
OF THE REQUIREMENTS OF THE
DEGREE OF

DOCTOR OF PHILOSOPHY

at the

MASSACHUSETTS INSTITUTE OF TECHNOLOGY

December 1984

© Massachusetts Institute of Technology

Signature of Author _____
Department of Nuclear Engineering
December 12, 1984

Certified by _____
Prof. Michael J. Driscoll
Thesis Supervisor

Accepted by _____
Allan F. Henry, Chairman
Department Committee on Graduate Students

MASSACHUSETTS INSTITUTE OF TECHNOLOGY

APR 16 1985

LIBRARIES

ARCHIVES

# A LONG TERM PERSPECTIVE ON THE LWR FUEL CYCLE

by

MUSHTAQ AHMAD MALIK

Submitted to the Department of Nuclear Engineering on December 12, 1984 in partial fulfillment of the requirements for the Degree of Doctor of Philosophy in Nuclear Engineering.

## ABSTRACT

A comprehensive interactive computer program for strategic studies of the LWR fuel cycle has been developed, incorporating simple models for estimating material flow, correlations for discharge fuel composition (as a function of core enrichment, burnup, fuel-to-moderator ratio and number of batches), algorithms for nuclear fuel cycle economic computations, and an ore resource/cost relationship. These models have been linked together to yield fuel cycle cost equations, in terms of the unit cost of each process step, in a form suitable for estimation of breakeven costs and for sensitivity analyses.

The program has been employed in a number of case studies to evaluate the impact of the introduction of the recycle mode, extended burnup, more batches in the core, low-enrichment-cost technologies and a reduction in enrichment plant tails assay. The results of these evaluations show that:

- The recycle mode would become economic, depending on the values of various highly uncertain parameters (primarily reprocessing and enrichment costs) once uranium prices (in today's dollars) exceed approximately 80 \$/lb $U_3O_8$. Breakeven values range from \$70 to \$125/lb as individual economic and technical parameters are varied independently, but cases in which all variables assume their most likely projected values cluster around the consensus value of 80 \$/lb $U_3O_8$. Using an EPRI cost/resource projection and the author's own estimate of the rate of growth of nuclear energy usage in the U.S., breakeven is predicted to occur around the year 2050.

- The breakeven ore cost is very sensitive to reprocessing cost. An increase of 1% in the base value of the cost of reprocessing will increase the breakeven ore cost by 1 \$/lb.

ABSTRACT (Continued)

● The recycle mode is favored as burnup is extended by increasing enrichment, but cheaper enrichment and a lower tails assay defer the time at which reprocessing becomes viable.

● Optimization of system cost (which includes the effect of plant capacity factor and replacement energy cost) indicates that PWR fuel management will not profit by increasing the number of staggered-reload in-core batches from its present value of three, but 18-24 month fuel cycles are fully justified.

Based upon the present work, it is concluded that LWR units will be operated in the once-through fueling mode for many decades into the future unless a radical technological breakthrough leading to a substantial reduction in reprocessing cost can be effected. The computer program developed in the present work can be used to evaluate this and other alternative scenarios, involving different cost projections of the user's choosing.

Thesis Supervisor: Michael J. Driscoll
Title: Professor of Nuclear Engineering

DEDICATED TO

God,the Merciful,the Mercy-Giving:

"Praise be to God,Lord of the Universe,
the Merciful, the Mercy-Giving,
Ruler of the Day of Judgement,
You do we worship and from You do we seek help.
Guide us along the Straight Path ,
the path of those whome You have favored,
with whom You are not angry,nor who are lost."

Qur'an(a unique book)

# ACKNOWLEDGEMENTS

I would like to express my thanks to my thesis supervisor, Prof. Michael J. Driscoll, for his invaluable advice and encouragement during the course of this work. Also thanks to Prof. David D. Lanning, who served as the thesis reader, for his critical review and helpful suggestions.

The financial support provided by the Ministry of Education (Pakistan) is very much appreciated. Funds for computer usage and report preparation were provided under a research grant from the Westinghouse Electric Corporation. Typing of this thesis was ably handled by Vicki Law.

I sincerely acknowledge the spiritual support and cooperation of the president of the MIT Islamic Society, Br. Idrees Ibrahim (may Allah reward him for his efforts).

TABLE OF CONTENTS

page

ABSTRACT..... 2

TABLE OF CONTENTS..... 6

LIST OF FIGURES..... 10

LIST OF TABLES..... 14

CHAPTER 1. INTRODUCTION..... 20

1.1 Foreword..... 20

1.2 Background..... 22

1.3 Purpose and Outline of Present Work..... 26

CHAPTER 2. NUCLEAR FUEL CYCLE MODELS..... 29

2.1 Introduction..... 29

2.2 The Nuclear Fuel Cycle..... 31

2.3 Once-through Mode Mass Flow Submodel..... 34

2.4 Discharge Composition Submodel..... 36

2.5 Isotopic Composition of Fuel During Irradiation..... 53

2.6 Recycle Mode Mass Flow Model..... 63

2.7 Nuclear Fuel Cycle Economics..... 84

2.7.1 Assumptions..... 85

2.7.2 Direct and Carrying Charges..... 85

2.7.3 Spent Fuel Credit Scheme..... 89

2.7.4 Constant Dollar Analysis..... 89

2.7.5 Busbar and System Costs..... 90

2.8 Ore Resource Model..... 92

2.9 Chapter Summary..... 95

TABLE OF CONTENTS (Continued)


| | page |
|---|---|
| CHAPTER 3. CORRELATIONS FOR KEY PARAMETERS..... | 98 |
| 3.1 Introduction..... | 98 |
| 3.2 Reactivity Versus Burnup for Uranium Fueled Cores..... | 98 |
| 3.3 Reactivity Versus Burnup for Plutonium Cores.. | 100 |
| 3.3.1 Functional Dependence of A and $\rho_o/A$ on $X_{Puf}$..... | 103 |
| 3.3.2 Functional Dependence of $\rho_o$ and A on $V_F/V_M$..... | 109 |
| 3.3.3 Simultaneous Functional Dependence of $\rho_o/A$ on $X_{Puf}$ and $V_F/V_M$..... | 114 |
| 3.4 Relative Worth of Plutonium and U-235..... | 117 |
| 3.5 Optimum Enrichment Plant Tails..... | 125 |
| 3.6 Isotope Separation for Three Component Mixtures..... | 126 |
| 3.7 Separative Work Requirements..... | 131 |
| 3.8 Chapter Summary..... | 139 |
| CHAPTER 4. CASE STUDIES..... | 141 |
| 4.1 Introduction..... | 141 |
| 4.2 Fuel Cycle Cost for Once Through (OT) and Recycle (RC) Mode Fueling of LWRs..... | 142 |
| 4.3 Sensitivity Analysis of Fuel Cost..... | 146 |

TABLE OF CONTENTS (Continued)

page

4.4 Case Study Results..... 148

4.4.1 Once Through Versus Recycle Mode "Breakeven"..... 148

4.4.2 Extended Burnup..... 157

4.4.3 More Batches in the Core..... 171

4.4.4 Lower Enrichment Costs and Reduction in Tails Assay..... 174

4.5 Price of Ore Projection..... 180

4.6 Results and Discussion..... 186

4.7 Chapter Summary..... 191

CHAPTER 5. SUMMARY, CONCLUSIONS AND RECOMMENDATIONS... 194

5.1 Introduction..... 194

5.2 Nuclear Fuel Models..... 195

5.2.1 Once-through Mass Flow Model..... 197

5.2.2 Discharge Composition Submodel..... 198

5.2.3 Recycle Mode Scheme..... 199

5.2.4 Nuclear Fuel Cycle Economics..... 200

5.2.5 Ore Resource Model..... 200

5.3 Correlations for Key Parameters..... 201

5.3.1 Reactivity Versus Burnup for Uranium and Plutonium Cores..... 201

5.3.2 Distribution of U-236..... 205

TABLE OF CONTENTS (Continued)

page

5.4 Case Study Results..... 208

5.5 Recommendations..... 212

APPENDIX A FUNCTIONAL DEPENDENCE OF ISOTOPIC COMPOSITION OF SPENT FUEL ON VARIOUS PARAMETERS..... 215

APPENDIX B NFC COMPUTER PROGRAM..... 229

B-1 DESCRIPTION AND LISTING..... 229

B-2 SAMPLE PROBLEM..... 241

APPENDIX C VARIATION OF REACTIVITY WITH BURNUP FOR PLUTONIUM ASSEMBLIES..... 249

REFERENCES..... 267

# LIST OF FIGURES


| | | page |
|---|---|---|
| 1.1 | A Uranium Price History..... | 21 |
| 2.1 | Schematic Showing Interrelation of Submodels in the Fuel Cycle Scoping Program..... | 30 |
| 2.2 | The LWR Nuclear Fuel Cycle..... | 33 |
| 2.3 | U-235 in Discharged Fuel Versus Reload Enrichment for Various Fuel-to-Moderator Ratios (n=3)..... | 40 |
| 2.4 | U-236 in Discharged Fuel Versus Reload Enrichment for Various Fuel-to-Moderator Ratios (n=3)..... | 41 |
| 2.5 | Fissile Plutonium in Discharged Fuel Versus Reload Enrichment for Various Fuel-to-Moderator Ratios (n=3)..... | 42 |
| 2.6 | U-235 in Discharged Fuel Versus Reload Enrichment for Various Fuel-to-Moderator Ratios (n=5)..... | 43 |
| 2.7 | U-236 in Discharged Fuel Versus Reload Enrichment for Various Fuel-to-Moderator Ratios (n=5)..... | 44 |
| 2.8 | Fissile Plutonium in Discharged Fuel Versus Reload Enrichment for Various Fuel-to-Moderator Ratios (n=5)..... | 45 |
| 2.9 | Fissile Plutonium in Discharged Fuel Versus Reload Enrichment for Various n: ($V_F/V_M$ = 0.604)..... | 46 |
| 2.10 | U-235 in the Fuel Versus Burnup for Various Fuel-to-Moderator Ratios..... | 64 |
| 2.11 | U-236 in the Fuel Versus Burnup for Various Fuel-to-Moderator Ratios..... | 65 |
| 2.12 | Fissile Pu in the Fuel Versus Burnup for Various Fuel-to-Moderator Ratios..... | 66 |

LIST OF FIGURES (Continued)

page

2.13 Composition of Fuel as a Function of Burnup: $V_F/V_M$ = 0.75..... 67

2.14 U-235 in the Fuel Versus Burnup for Various Reload Enrichments..... 68

2.15 U-236 in the Fuel Versus Burnup for Various Reload Enrichments..... 69

2.16 Fissile Pu in the Fuel Versus Burnup for Various Reload Enrichments..... 70

2.17 Schematic Showing Interrelation of Blending and Credit Steps..... 81

2.18 Cash Flow Diagram for a Batch of Nuclear Fuel..... 87

3.1 Variation of $\rho_o/A$ with $V_F/V_M$ for Various U-235 Enrichments..... 101

3.2 Variation of the Slope of $\rho(B)$, A, with Fissile Plutonium Enrichment for Various Fuel-to-Moderator Ratios..... 107

3.3 Variation of $\rho_o/A$ with $X_{Puf}$ for Various Fuel-to-Moderator Ratios..... 110

3.4 Variation of $\rho_o$ with $V_F/V_M$ for Various $X_{Puf}$..... 111

3.5 Variation of the Slope of $\rho(B)$, A, with $V_F/V_M$ for Various $X_{Puf}$..... 115

3.6 Variation of $\rho_o/A$ with $V_F/V_M$ for Various $X_{Puf}$..... 118

3.7 Worth of Fissile Pu Relative to U-235 for Various Fuel-to-Moderator Ratios..... 122

3.8 Optimum Tails Assay as a Function of Ratio: Cost of Feed/Cost of SWU..... 127

LIST OF FIGURES (Continued)

page

3.9 U-236 (w/o) in Product Versus U-236 (w/o) in Feed for Various U-235 Enrichments in Product ($X_2$); for U-235 in Feed $X_1$ = 0.6 w/o..... 133

3.10 U-236 (w/o) in Product Versus U-236 (w/o) in Feed for Various U-236 Enrichments in Product ($X_2$); for U-235 in Feed $X_1$ = 0.7 w/o..... 134

3.11 U-236 (w/o) in Product Versus U-236 (w/o) in Feed for Various U-235 Enrichments in Product ($X_2$); for U-236 in Feed $X_1$ = 0.8 w/o..... 135

4.1 Breakeven Ore Cost Versus Fuel Cycle Cost for Various Enrichment and Reprocessing Costs..... 154

4.2 Breakeven Ore Cost Versus Fuel Cycle Cost for Various Enrichment and MOX Fabrication Costs..... 155

4.3 Optimum Burnup with Respect to Fuel Cycle Cost for Various Number of Batches..... 159

4.4 Optimum Burnup with Respect to Busbar and System Cost..... 160

4.5 Optimum Fuel Cycle Length as Determined by Fuel Cycle Cost..... 163

4.6 Optimum Cycle Length as Determined by System Cost for Three-batch and Five-batch Cores..... 164

4.7 Breakeven Ore Cost for Various Reload Enrichments..... 168

4.8 Breakeven Ore Cost of Once-through Versus Recycle-mode Cycle Cost as a Function of Number of Batches in the Core..... 173

4.9 Breakeven Ore Cost of Once-through Versus Recycle-mode Fuel Cycle Cost for Various Enrichment Costs: $X_w$ = 0.3 w/o..... 177

LIST OF FIGURES (Continued)

page

4.10 Breakeven Ore Cost of Once-through Versus Recycle-mode Fuel Cycle Cost for Various Enrichment Costs: $X_w$ = 0.2 w/o..... 178

4.11 Breakeven Ore Cost of Once-through Versus Recycle-mode Fuel Cycle Cost for Various Enrichment Costs: $X_w$ = 0.1 w/o..... 179

4.12 Installed Nuclear Power Estimates, Year 2000 - U.S. ..... 181

4.13 $U_3O_8$ Projected Price Versus Cumulative Demand in Constant December 1980 Dollars (0.2 tails)..... 185

5.1 Schematic Showing Interrelation of Submodels in the Fuel Cycle Scoping Program..... 196

A-1 Flowchart for the Procedure Used to Develop Isotopic Composition Relations for Discharged Fuel..... 216

A-2 Fissile Pu in Discharged Fuel Versus Discharge Burnup for Various n:($V_F/V_M$=0.75)..... 226

A-3 U-235 in Discharged Fuel Versus Discharge Burnup for Various n:($V_F/V_M$=0.75)..... 227

A-4 U-236 in Discharged Fuel Versus Discharge Burnup for Various n:($V_F/V_M$=0.75)..... 228

# LIST OF TABLES

page

2.1 Comparison of Curve-fit Values and LEOPARD Data for the Isotopic Composition of Spent Fuel: $V_F/V_M$ = 0.604; n=3..... 47

2.2 Comparison of Curve-fit Values and LEOPARD Data for the Isotopic Composition of Spent Fuel: $V_F/V_M$ = 0.75; n=3..... 48

2.3 Comparison of Curve-fit Values and LEOPARD Data for the Isotopic Composition of Spent Fuel: $V_F/V_M$ = 1.0; n=3..... 49

2.4 Comparison of Curve-fit Values and LEOPARD Data for the Isotopic Composition of Spent Fuel: $V_F/V_M$ = 0.604; n=5..... 50

2.5 Comparison of Curve-fit Values and LEOPARD Data for the Isotopic Composition of Spent Fuel: $V_F/V_M$ = 0.75; n=5..... 51

2.6 Comparison of Curve-fit Values and LEOPARD Data for the Isotopic Composition of Spent Fuel: $V_F/V_M$ = 1.0; n=5..... 52

2.7 Coefficients of Curve-fit of X-235 Versus Burnup for Various Reload Enrichments and Fuel-to-Moderator Ratios..... 55

2.8 Coefficients of Curve-fit of X-235 Versus Burnup and $X_P$ for Various Fuel-to-Moderator Ratios..... 56

2.9 Coefficients of Curve-fit of X-236 Versus Burnup for Various Reload Enrichments and Fuel-to-Moderator Ratios..... 58

2.10 Coefficients of Curve-fit of X-236 Versus Burnup and $X_P$ for Various Fuel-to-Moderator Ratios..... 59

LIST OF TABLES (Continued)

page

2.11 Coefficients of Curve-fit of $X_{Puf}$ Versus Burnup for Various Reload Enrichments and Fuel-to-Moderator Ratios..... 61

2.12 Coefficients of Curve-fit of $X_{Puf}$ Versus Burnup and Reload Enrichment for Various Fuel-to-Moderator Ratios..... 62

2.13 Comparison of Curve-fit Values and LEOPARD Data for the Concentration of U-236 in the Fuel During Irradiation: $V_F/V_M$ = 0.604..... 71

2.14 Comparison of Curve-fit Values and LEOPARD Data for the Concentration of U-236 in the Fuel During Irradiation: $V_F/V_M$ = 0.75..... 72

2.15 Comparison of Curve-fit Values and LEOPARD Data for the Concentration of U-236 in the Fuel During Irradiation: $V_F/V_M$ = 1.0..... 73

2.16 Comparison of Curve-fit Values and LEOPARD Data for the Concentration of U-235 in the Fuel During Irradiation: $V_F/V_M$ = 0.604..... 74

2.17 Comparison of Curve-fit Values and LEOPARD Data for the Concentration of U-235 in the Fuel During Irradiation: $V_F/V_M$ = 0.75..... 75

2.18 Comparison of Curve-fit Values and LEOPARD Data for the Concentration of U-235 in the Fuel During Irradiation: $V_F/V_M$ = 1.0..... 76

2.19 Comparison of Curve-fit Values and LEOPARD Data for Fissile Plutonium in the Fuel During Irradiation: $V_F/V_M$ = 0.604..... 77

2.20 Comparison of Curve-fit Values and LEOPARD Data for Fissile Plutonium in the Fuel During Irradiation: $V_F/V_M$ = 0.75..... 78

2.21 Comparison of Curve-fit Values and LEOPARD Data for Fissile Plutonium in the Fuel During Irradiation: $V_F/V_M$ = 1.0..... 79

LIST OF TABLES (Continued)

page

3.1 Comparison of Curve-fit and LEOPARD Values of $\rho_o/A$ for Various $X_P$ and $V_F/V_M$..... 102

3.2 Isotopic Composition of Spent Fuel Plutonium Used to Prepare Reload Fuel..... 104

3.3 Variation of $\rho_o$, A and $\rho_o/A$ with $X_{Puf}$ and $V_F/V_M$ for Plutonium Fueled Lattices..... 105

3.4 Coefficients of A Versus $X_{Puf}$ Curve-fit, for Various $V_F/V_M$, for Plutonium Fueled Cores..... 108

3.5 Curve-fit Coefficients of $\rho_o/A$ Versus Fissile Pu Content for Various $V_F/V_M$..... 112

3.6 Coefficients of $\rho_o$ Versus $V_F/V_M$ Curve-fit, for Various $X_{Puf}$ Values..... 113

3.7 Comparison of Curve-fit Values and LEOPARD Results of $\rho_o/A$ for Various $X_{Puf}$ and $V_F/V_M$ for Plutonium Fueled Cores..... 119

3.8 Comparison of Curve-fit and Calculated Worths of Fissile Pu Relative to U-235..... 123

3.9 Comparison of Curve-fit and Exact Values of the Optimum Tails Assay..... 128

3.10 Comparison of Curve-fit and Exact Distributions of U-236 in the Product and Tails of a Three Component Isotope Separation Plant..... 132

3.11 Coefficients of S/P Versus $X_P$ Curve-fit, for Various Values of Tails Assay..... 137

3.12 Comparison of Curve-fit and Exact Values of SWU Requirements for Various Tails Assay: U-235 in Feed = 0.711 (w/o)..... 138

LIST OF TABLES (Continued)


page

4.1 Base Case Fuel Cycle Data..... 144

4.2 Reference Case Economic Parameters..... 145

4.3 Sensitivity Parameters for Various Fuel Cycle Transactions..... 147

4.4 Recent Reprocessing Cost Estimates..... 149

4.5 Recent Mixed Oxide (MOX) Fabrication Cost Estimates..... 150

4.6 Future Enrichment Cost Estimates..... 151

4.7 Breakeven Cost of Ore as a Function of Other Transaction Costs..... 153

4.8 Fuel Cycle Cost, Busbar Cost and System Cost for a 3-batch Core on the Once Through Fuel Cycle..... 158

4.9 Energy Production Costs for the Once Through Cycle..... 162

4.10 Cost Coefficients for Various Enrichments..... 165

4.11 Coefficients of Breakeven Equation, (4.17)..... 169

4.12 Cost Coefficients as a Function of Number of Batches: $X_p$ = 3.5 w/o..... 172

4.13 Ore and Enrichment Cost Coefficients for the Fuel Cycle Cost for Various Values of $X_p$ and $X_w$..... 176

4.14 A Uranium Price History..... 183

4.15 Projected Profile of Installed Nuclear Capacity and Future Cost of Yellowcake..... 187

4.16 Summary of Breakeven Case Study Results..... 188

LIST OF TABLES (Continued)


| | | page |
|---|---|---|
| 5.1 | Worth of Fissile Plutonium Relative to U-235..... | 204 |
| 5.2 | Comparison of Curve-fit and Exact Distributions of U-236 in the Product and Tails of the Three Component Isotope Separation Plant..... | 207 |
| 5.3 | Summary of Breakeven Case Study Results..... | 209 |
| A-1 | Variation of $\rho_o$, A and $\rho_o/A$, with $X_P$ and $V_F/V_M$..... | 218 |
| A-2 | Coefficients of Curve-fit of X-236 Versus Enrichment for Various Fuel-to-Moderator Ratios..... | 220 |
| A-3 | Coefficients of Curve-fit of $X_d$-235 Versus Enrichment for Various Fuel-to-Moderator Ratios..... | 223 |
| A-4 | Coefficients of Curve-fit of $X_{Puf}$ Versus Enrichment for Various Fuel-to-Moderator Ratios..... | 224 |
| B-1 | Important Parameters in NFC Program..... | 231 |
| C-1 | Equivalent Values for Cell and Core Fuel-to-Moderator Ratios..... | 251 |
| C-2 | Reactivity Versus Burnup Data for $X_{Puf}$=3.0 w/o, and $V_F/V_M$=0.3..... | 252 |
| C-3 | Reactivity Versus Burnup Data for $X_{Puf}$=4.0 w/o, and $V_F/V_M$=0.3..... | 253 |
| C-4 | Reactivity Versus Burnup Data for $X_{Puf}$=2.5 w/o, and $V_F/V_M$=0.5..... | 254 |
| C-5 | Reactivity Versus Burnup Data for $X_{Puf}$=3.0 w/o, and $V_F/V_M$=0.5..... | 255 |
| C-6 | Reactivity Versus Burnup Data for $X_{Puf}$=4.0 w/o, and $V_F/V_M$=0.5..... | 256 |

LIST OF TABLES (Continued)

page

C-7 Reactivity Versus Burnup Data for $X_{Puf}$=6.0 w/o, and $V_F/V_M$=0.5 ..... 257

C-8 Reactivity Versus Burnup Data for $X_{Puf}$=4.0 w/o, and $V_F/V_M$=0.604 ..... 258

C-9 Reactivity Versus Burnup Data for $X_{Puf}$=6.0 w/o, and $V_F/V_M$=0.604 ..... 259

C-10 Reactivity Versus Burnup Data for $X_{Puf}$=8.0 w/o, and $V_F/V_M$=0.604 ..... 260

C-11 Reactivity Versus Burnup Data for $X_{Puf}$=4.0 w/o, and $V_F/V_M$=0.75 ..... 261

C-12 Reactivity Versus Burnup Data for $X_{Puf}$=6.0 w/o, and $V_F/V_M$=0.75 ..... 262

C-13 Reactivity Versus Burnup Data for $X_{Puf}$=8.0 w/o, and $V_F/V_M$=0.75 ..... 263

C-14 Reactivity Versus Burnup Data for $X_{Puf}$=10.0 w/o, and $V_F/V_M$=1.0 ..... 264

C-15 Reactivity Versus Burnup Data for $X_{Puf}$=12.0 w/o, and $V_F/V_M$=1.0 ..... 265

C-16 Reactivity Versus Burnup Data for $X_{Puf}$=14.0 w/o, and $V_F/V_M$=1.0 ..... 266

# CHAPTER 1

# INTRODUCTION

## 1.1 Foreword

Current indications are that light water reactors, which dominate the commercial nuclear power industry worldwide, will continue to be competitive, many decades into the future, even if they are confined to operation on a once-through fuel cycle [W1]. This possibility represents a major departure from past expectations, which were based on projections of rapid depletion of low cost uranium resources - a prospect which motivated energy planners to emphasize prompt development and deployment of fuel reprocessing/recycling facilities and breeder reactors. During the past ten years, however, the worldwide economic recession and its consequences have led to a large decrease in the rate of reactor construction; and significant uranium reserves have been confirmed, while spotmarket prices for $U_3O_8$ have dropped as shown in Fig. 1.1 [N1]. At the same time reprocessing costs have escalated substantially, and new high-performance centrifuge enrichment cascades and laser isotope enrichment devices, which promise large reductions in separative work costs, are being perfected (amid a surplus

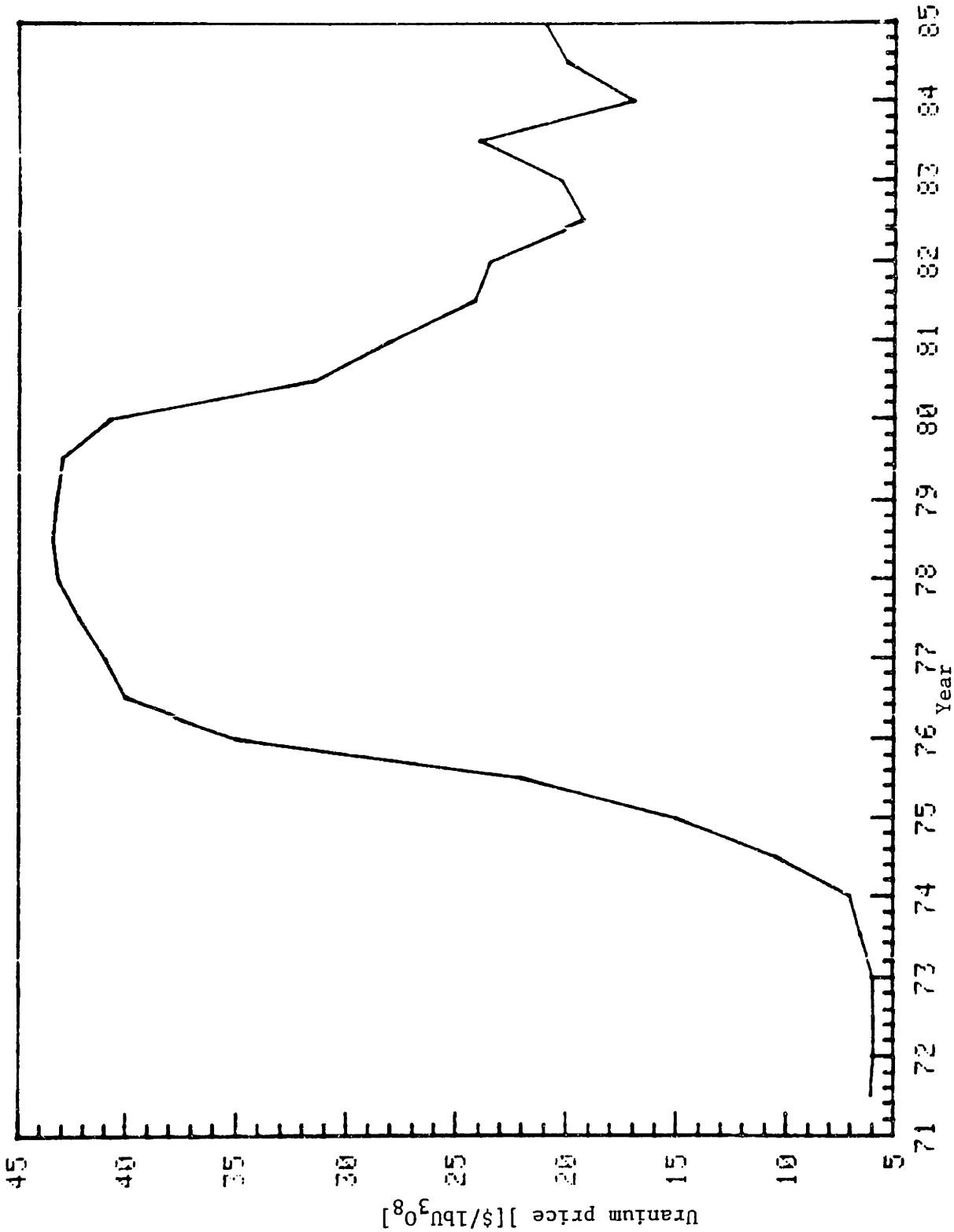


Fig.1.1 A Uranium price history .

in SWU capacity). In addition, LWR fuel is being pushed to ever higher burnup levels, with consequent savings in ore requirements.

In view of the profound changes taking place in virtually every stage of the nuclear fuel cycle it is essential that appropriate analytical tools be available to LWR nuclear fuel managers, who must devise appropriate responses to the evolving economic and technical environment. It has been the objective of the present thesis research to develop a comprehensive computational model, embodied in a computer program, which can serve this purpose.

## 1.2 Background

A considerable technical literature and many computer models exist for what might be termed "strategic" studies of the nuclear fuel cycle. Reference T1 is a recent, comprehensive review of this field, and the NASAP [N2], INFCE [I1], and IIASA [H1,I2] reports constitute benchmark analyses of this genre. Table 3.1 in reference G1 also lists a number of popular electric systems' models. These models attempt to describe the energy sector, including its electric (and nuclear-electric) subsectors, as part of the national or world economy. From these models the demand for fuels of various types are projected, and strategic plans developed to meet future needs in an optimum manner.

Typical applications include evaluation of the rationale for development and deployment of breeder reactors.

Planning models of a more specific nature also exist in the form of those used by individual utilities to decide upon the best mix of generating types for their system [T2, B1, S1].

Of interest here, however, is a class we prefer to think of as "tactical" models: those which can be used by fuel managers to plan a suitable response to an evolving economic and technical environment involving current or soon-to-be-ordered plants over their operational lifetime. The time frame of concern encompasses what some have designated as "long-range fuel management". Surprisingly little is currently available to the practitioner in this area. State-of-the-art licensing techniques for cycle-by-cycle reload analysis such as the EPRI ARMP package [E1], are generally too detailed, and hence too time consuming and expensive for long range studies, being better suited for short term fuel management.

Analytic tools for intermediate range planning studies come closer to satisfying the needs of present interest. These include the FLAC program developed by Beard [B2] and Hsieh [H2], the TJD codes of Dowmar [D1] and several other like contributions [M1, A1, L1]. While it would, in principle, be possible to stretch these codes to cover a larger range, they generally

devote too much detail to core description, and not enough to the ex-core fuel cycle. In addition some require considerable exogenous input, or deal only with neutronics, without performing a concurrent economic analysis. Thus a code focusing only on the long range would be preferable on several grounds.

Beyond merely filling a planning void, the incentive for development of a long range fuel cycle tactical model can be appreciated by considering what has transpired over the past decade in matters affecting decision-making in this area. The high ore and SWU consumption rates of LWRs have not been of particular concern in the past because such reactors were viewed as precursors of Fast Breeder Reactors (FBRs) capable of extracting 50-60 times the amount of energy from a given mass of $U_3O_8$. However, as a result of recession, diminished power demand, and rising plant costs, the US, in particular, has moved from a situation in the mid 1970s where 500 to 700 GWE installed nuclear capacity were forecast by the year 2000, to a situation in which an end-of-century installed nuclear capacity of only 125 to 150 GWE is forecast. The result is that scarcity of uranium as a driving force to deploy possible $U_3O_8$ extenders, such as recycle-mode LWRs, and FBRs, has decreased, and it is expected that LWRs will account for the bulk of nuclear capacity for at least several decades into the 21st century. The NASAP and INFCE studies have also brought to the forefront a variety of considerations which suggest that

LWR core design and fuel management strategies may be more resilient with respect to retention of a favorable competitive edge over a longer time horizon than anticipated during the original formulation of current nuclear energy programs. Among these factors are: better knowledge of the resource/cost relationship for uranium ore, the prospects for inexpensive Advanced Isotope Separation (AIS) technology, fuel designs capable of higher burnup, and escalation of reprocessing and mixed oxide fabrication costs.

In view of these circumstances it is likely that the nuclear industry will concentrate its scarce financial resources on improving existing LWR technology and in particular, over the long run, work to maintain low fuel cycle cost to offset the inherently higher capital costs of nuclear units. All of these developments promise to have profound effects on the future LWR fuel cycle. However, the impact of such current and potential developments has not been fully appreciated, due in part to the lack of comprehensive quantification. Specific case studies have too often focused on a limited set of options, or based their analysis on rapidly outdated input data. Accordingly,the present analysis addresses a broad spectrum of concerns, and casts the results in the form of a user-friendly computer program capable of running further case studies of the readers interest, as time and data change.

## 1.3 Purpose and Outline of Present Work

The basic features of the LWR fuel cycle were established many years ago. Large changes in the relative cost of uranium, SWU, fabrication and reprocessing have taken place since then. Moreover, the unpredictability of events during the last decade has made everyone look to the future with a cautious eye. The need to cope with these changing economic circumstances make it essential that nuclear fuel managers have at their disposal the means to continually update and optimize their response.

In view of the above considerations, the major objective of the present work has been to provide an uncomplicated means for the fuel manager to determine optimal responses to future economic and technical environments of his own projection. Accomplishing this task involved integration of a number of submodels into a program of sufficient scope and level of detail that it can be used to assess the incentives for adoption of alternative fuel cycles and/or for modification of the fuel design and operation of a reactor to minimize fuel cycle and overall production costs of electrical energy. In other words, this model can answer the questions surrounding many suggested policy options, by quantifying their potential economic impact. Some of the areas of current interest, which are to be addressed, include:

- Plutonium recycle
- Advanced Isotope Separation (AIS) enrichment processes

- Changes in the enrichment plant tail's assay.
- Higher fuel discharge burnup.
- Increasing the number of batches.
- The effect of escalation of reprocessing and MOX fabrication costs.

Accordingly,in Chapter 2, various submodels are developed and incorporated into a simple fuel cycle economics program. These submodels include mass flow models, both for once-through and recycle modes of LWR operation, and discharge fuel composition and ore resource models. The comprehensive nature of these models permits an analysis of the effect of all key parameters on the fuel cycle cost for a wide variety of fuel cycle scenarios in a convenient and inexpensive manner, a feature which is highly desirable when a large number of parametric studies are to be carried out.

In Chapter 3, some simple correlations for key parameters such as the reactivity of uranium and plutonium cores, the relative worth of plutonium and uranium, optimum enrichment plant tails, separative work requirements and isotope separation for three component systems are developed. These will facilitate the use of the code in a stand-alone manner, independent of outside input.

Various fuel cycles and fuel management strategies have been analyzed in Chapter 4. The case study results which are

presented and discussed cover many of the contemporary issues in LWR fuel cycle planning.

Finally, in Chapter 5, the results and conclusions of the study are summarized, together with recommendations for future work.

Appendices are included to provide supplementary material in support of the information presented in the main text. The computer program, which is the major legacy of the present effort, and a sample problem are also documented.

# CHAPTER 2

# NUCLEAR FUEL CYCLE MODELS

## 2.1 Introduction

The intent of this chapter is to provide simple models which can be used for the evaluation of various fuel management strategies and for the assessment of alternative nuclear fuel technologies that might be developed in the future. The elements of the overall model consist of submodels describing material flow throughout the LWR nuclear fuel cycle (for both the once-through and recycle modes of operation), discharge fuel composition, nuclear fuel cycle economics and the ore resource/cost relationship. Figure 2.1 shows how these components are linked up to comprise a fuel cycle scoping program.

The calculational methodology in the present work is based on relatively simple correlations in order to reduce the cost of, and time required for, the analysis of the various fuel cycle options. This is desirable for models which are to be suitable for use within a much more comprehensive description of the nuclear-electric economy, or, as in the present case, models for implementation on microcomputers. In addition, analytic simplicity provides a more transparent understanding

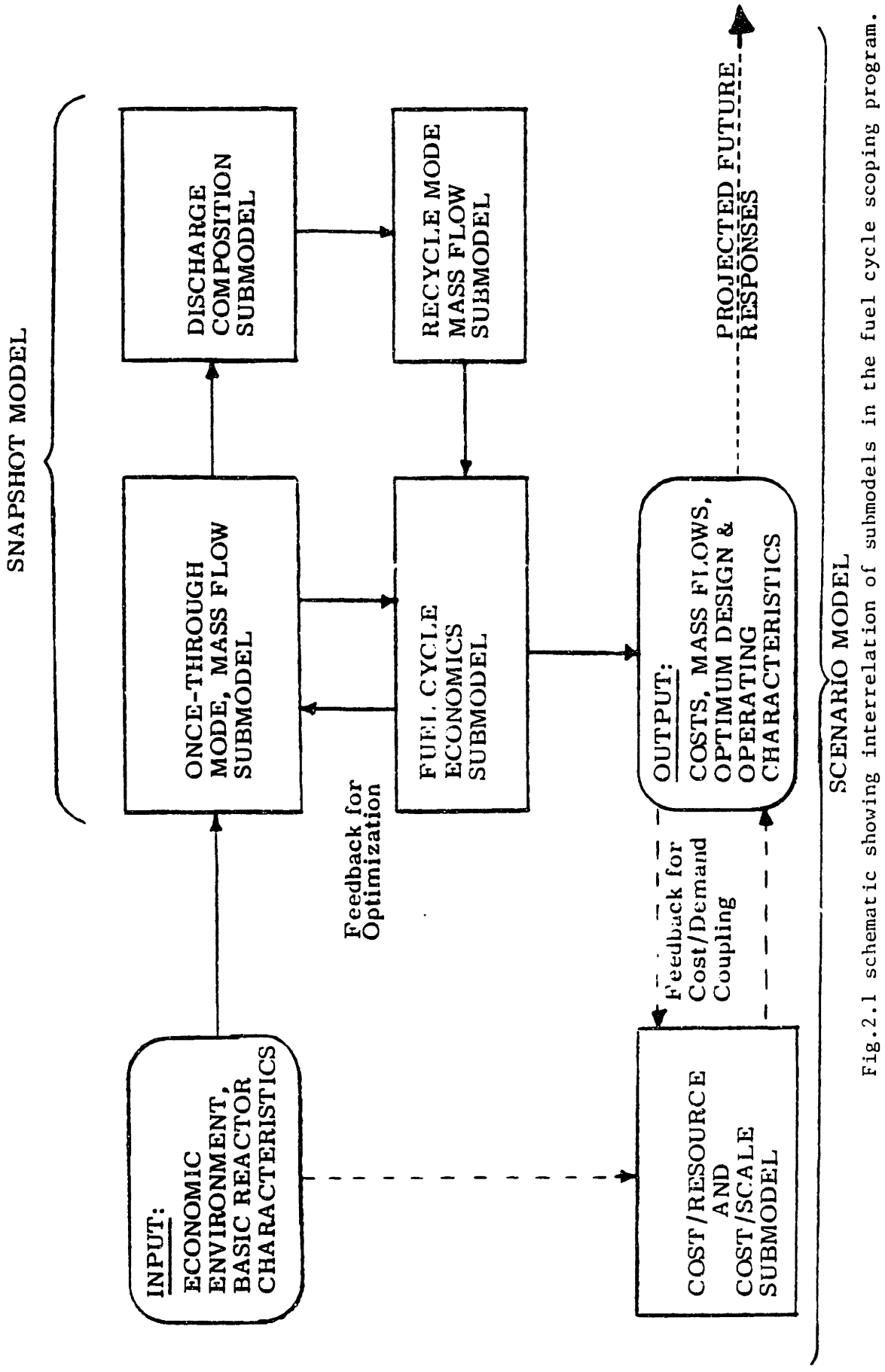


Fig.2.1 schematic showing interrelation of submodels in the fuel cycle scoping program.

of the functional interrelationships of the major variables which determine system performance. It will also be demonstrated that this can be accomplished without sacrificing any significant degree of accuracy.

## 2.2 The Nuclear Fuel Cycle

The total cost of nuclear-generated electricity consists of three major cost components: capital, operation and maintenance, and fuel cycle. Of these cost categories, the fuel cycle component is of particular interest and importance here, since the cost advantage of nuclear power over competing technologies is dependent on the saving embodied in this term. One must keep in mind, however, the effect of the fuel cycle on capital and O & M charges through the agency of the plant capacity factor, and the cost of replacement energy during refueling downtime.

The term fuel cycle refers to all steps from the time when the fuel is purchased as "yellowcake" ($U_3O_8$) to disposal of final wastes. It is sometimes further subdivided into "front end" (prior to irradiation) and "back end" (subsequent to irradiation) phases. The description here can be brief because of the availability of several comprehensive texts which describe the LWR fuel cycle in exhaustive detail [G2], [B3].

Figure 2.2 shows the fuel cycle for LWRs. After mining, the ore is concentrated as $U_3O_8$ and converted to $UF_6$. The $UF_6$ is processed through an isotope separation plant to enrich the fuel in the fissile isotope U-235. From enriched $UF_6$, $UO_2$ is prepared and fabricated into fuel elements. After the fuel elements are irradiated, they enter the back-end of the fuel cycle, which comprises storage and disposal for the once-through mode or reprocessing and waste disposal for the recycle mode.

The purchase of yellowcake and enrichment services has the greatest effect on nuclear fuel cycle costs. Therefore, variations of the unit price of ore and separative work units, SWU, will have a dominant effect on the fuel cycle cost, and hence on both the short and long-term strategy selected for fuel management and fuel cycle development. Thus these aspects are of particular significance in the modelling process in this chapter and in the subsequent parametric studies of Chapter 4.

From this brief summary it can be seen that to calculate the fuel cycle cost one needs to determine:

- The composition of the fuel loaded into the reactor.
- Ore and SWU requirements.
- Processing costs at each step and transportation costs between stages.
- The composition of discharged fuel.

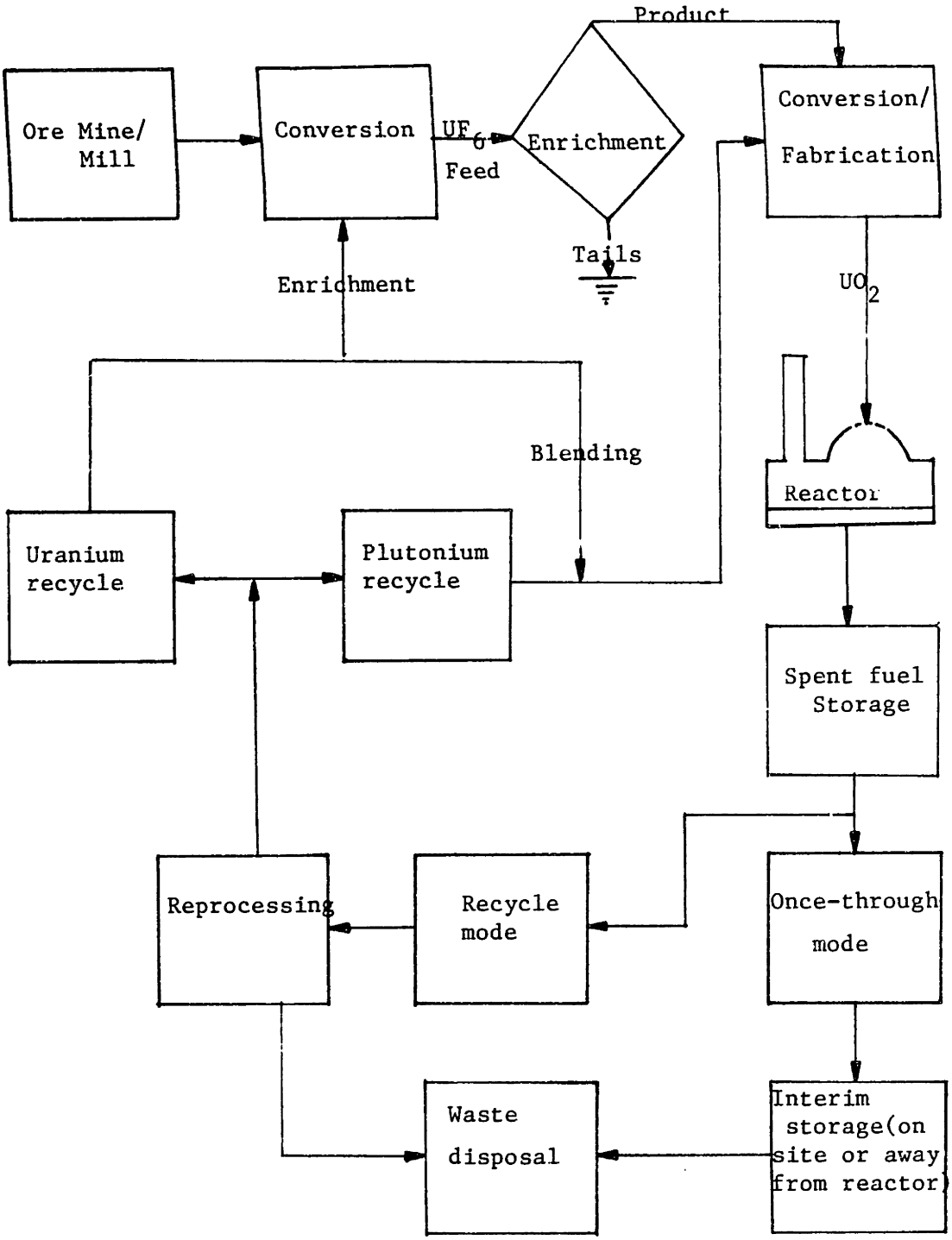


Fig.2.2 The LWR nuclear fuel cycle.

- Processing and/or disposal costs and product credits for discharged fuel.
- The time at which each cost is paid or credit is received.
- The amount of electricity generated.

In order to determine the above factors, simple submodels have been developed, as explained in the rest of this chapter.

## 2.3 Once-through Mode Mass Flow Submodel

The core heavy metal loading and composition is fixed by thermal/hydraulic and neutronic constraints. The fuel for LWR units is generally enriched in the isotope U-235 to between 2.5 and 4.5 weight percent (w/o). The quantity of feed material required can be obtained by performing a material balance on both total uranium and the U-235 isotope. A material balance around the enrichment facility yields

$$F = P + W \tag{2.1}$$

where

F = mass in feed stream

P = mass in product stream

W = mass in tails stream

Conservation of mass for the U-235 isotope gives

$$X_F F = X_P P + X_W W \tag{2.2}$$

where $X_F$, $X_P$ and $X_W$ are the weight percents of U-235 in feed, product and tails, respectively.

Eliminating W from Eqs. (2.1) and (2.2) yields

$$\frac{F}{P} = \left[\frac{X_P - X_W}{X_F - X_W}\right] \tag{2.3}$$

The mass of ore required is then calculated as

$$M_{ore} = \frac{F}{P}\left[\frac{M_b}{F_1 \cdot F_2 \cdot F_3}\right], \text{Kg of U} \tag{2.4}$$

and substituting Eq. (2.3) gives

$$M_{ore} = \frac{1.179\ M_b}{F_1 \cdot F_2 \cdot F_3}\left[\frac{X_P - X_W}{X_F - X_W}\right], \text{Kg of } U_3O_8 \tag{2.5}$$

where $M_b$ is the Kg of heavy metal required for equilibrium loading of a reactor batch, and $F_1$, $F_2$ and $F_3$ are the fractional recoveries of uranium in conversion, enrichment and fabrication plants, respectively.

The cost of enrichment is directly proportional to the separative work required per Kg of the product material, S/P, where

$$S/P = V_P + V_W\left[\frac{X_P - X_F}{X_F - X_W}\right] - V_F\left[\frac{X_P - X_W}{X_F - X_W}\right] \tag{2.6}$$

in which

$$V_i = (2X_i - 1)\ \ln\left\{\frac{X_i}{1-X_i}\right\} \tag{2.7}$$

and where $X_i$ is the fractional enrichment.

Then the SWU requirement for the equilibrium loading of a reactor batch becomes

$$M_{SWU} = \frac{M_b}{F_2 \cdot F_3}\left(\frac{S}{P}\right), \text{ Kg SWU} \tag{2.8}$$

$$M_{Fab} = \frac{M_b}{F_3} \tag{2.9}$$

and

$$M_{dis} \cong M_b \tag{2.10}$$

In Eq. (2.10) we have adopted the convention that discharged fuel is treated as equal in mass to reload fuel, neglecting the small amount of mass converted to energy.

## 2.4 Discharge Composition Submodel

The isotopic composition of spent fuel is required as input for recycle mode mass flow calculations. This composition is a function of discharge burnup, number of batches and fuel-to-moderator ratio. As shown by Montaldo-Volachec [M2] and others, the discharge burnup is, to a very good approximation, a linear function of reload enrichment, $X_p$. In the present work approximate formulas for U-235, U-236 and fissile plutonium in the discharge fuel have been formulated by fitting semi-empirical relations to the output of LEOPARD computer code-calculations [B4]. Although LEOPARD is one of the initial generation of LWR core physics programs, a recent intercomparision has confirmed that it is still equal to or better than more recent codes for applications of the type of present concern [L2]. The resulting prescriptions for discharge fuel composition are given below. (See Appendix A for a detailed discussion of the procedures

employed to develop these correlations, which the user can follow to tailor the prescriptions to fit any desired class of reactor core designs).

$$X_d - 235,\ w/o = \left(0.454 - \frac{5}{4n}\right) + \left(\frac{0.635}{n} + 0.07\right) \Big/ \left(\frac{V_F}{V_M}\right) + \left[\left(1 + \frac{0.782}{n}\right)\left(\frac{V_F}{V_M}\right) - \left(0.575 + \frac{n}{24}\right)\right] \ln X_P \qquad (2.11)$$

$$X - 236,\ w/o = \frac{1}{100}\left[\left(\frac{4 + 3n}{10}\right)\left(\frac{V_F}{V_M}\right) + 14.67 + \frac{3}{n}\right] X_P - \left[\frac{0.075}{n} + 0.09\left(\frac{V_F}{V_M}\right)\right] \qquad (2.12)$$

$$X_{Puf},\ w/o = \left(1.528 + \frac{5n}{1000}\right) + \left[1.27 + 0.05n\right] \ln\left(\frac{V_F}{V_M}\right) + \frac{1}{X_P}\left[\left(1.1 + \frac{n}{10}\right) - (3.28 + 0.073n)\ \frac{V_F}{V_M}\right] \qquad (2.13)$$

for $2 < X_P < 5$ w/o

$2 < n < 6$

$0.5 \leq \frac{V_F}{V_M} \leq 1.0$

where

$X_P \equiv$ U-235 reload enrichment, w/o

$X_d - 235 \equiv$ U-235 (w/o) in the spent fuel.

X-236 $\equiv$ U-236 (w/o) in the spent fuel.

$X_{Puf} \equiv$ Fissile Plutonium (Pu-239 + Pu-241)(w/o) in the spent fuel.

$n \equiv$ number of batches in the core

$\frac{V_F}{V_M} \equiv$ Fuel-to-moderator ratio in a unit cell of the core lattice.

Figures (2.3) through (2.8) compare the curve fit expressions of Eqs. (2.11), (2.12) and (2.13) to LEOPARD data. Selected results spanning the range of applicability are summarized in Tables (2.1) through (2.6), which also document the discrepancy between LEOPARD and the prescriptions.

Several observations are worthwhile:

a) For fixed n and $\frac{V_F}{V_M}$, the fissile fuel content of spent fuel (both U-235 and Puf) is very nearly a linear function of reload enrichment. Since reload enrichment is itself a linear function of discharge burnup, $X_{Puf}$ and X-236 also vary nearly linearly with burnup.

b) The U-236 content in the spent fuel increases very nearly linearly with discharge burnup (attained by increasing reload enrichment), which makes reprocessing less attractive for high burnup or multiply-recycled fuel.

c) The content of U-236 is almost the same (regardless of the number of batches employed) with fixed reload enrichment. Thus one can go to higher burnups by increasing the number of batches, n, without much increase in U-236 content. But, on the other hand, $X_d$-235 decreases as n increases, and so the incentive for reprocessing will decrease.

d) $X_{Puf}$ (for fixed $\frac{V_F}{V_M}$ and $X_p$) increase slightly for larger n due to the longer irradiation time (higher burnup) but it saturates for higher reload enrichments: see Fig. 2.9.

e) For a fixed n and reload enrichment, the fissile content of spent fuel (both Puf and $X_d$-235) increases, and X-236 decreases, with increasing $\frac{V_F}{V_M}$, making reprocessing more attractive for tight-pitch, hard-spectrum cores.

f) Despite their simplicity, e.g., for a conventional PWR with n = 3, $\frac{V_F}{V_M} = 0.604$ :

$$X_d\text{-}235,\ w/o = 0.502 + 0.061 \ln X_p, \qquad (2.14)$$

$$X\text{-}236, w/o = 0.1646\ X_p - 0.080, \qquad (2.15)$$

$$X_{Puf}, w/o = 0.827 - 0.714/X_p , \qquad (2.16)$$

These prescriptions are quite accurate. Discharge enrichments are predicted within an average error of less than 1% of LEOPARD results, a discrepancy far smaller than reported differences between computed and measured isotope data on spent fuel [M3].

g) For conventional PWRs, the U-235 content of spent fuel is very nearly constant, independent of reload enrichment (or burnup).

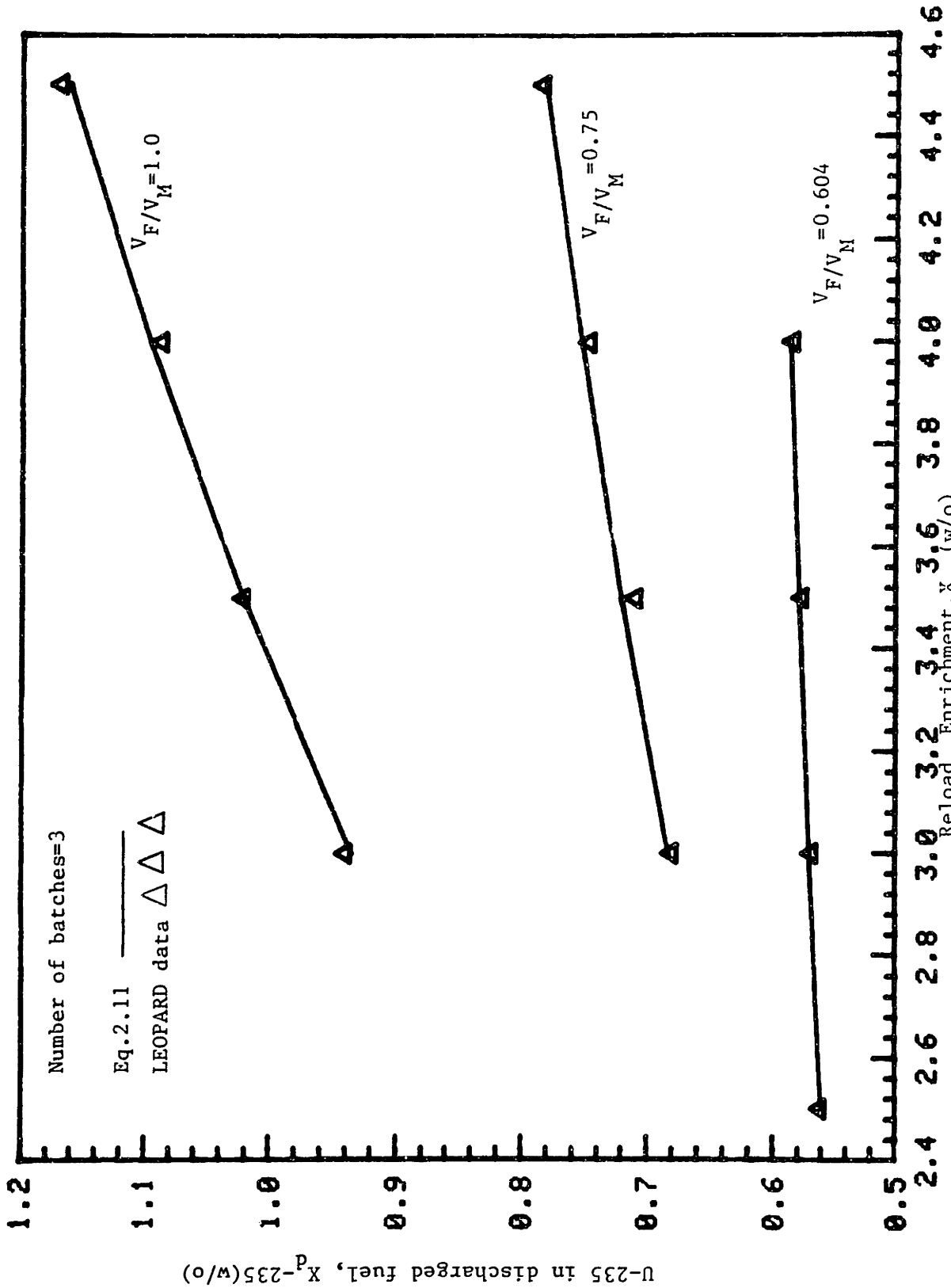


Fig.2.3 U-235 in discharged fuel $X_p$ vs. reload enrichment for various fuel-to-moderator ratios(n=3).

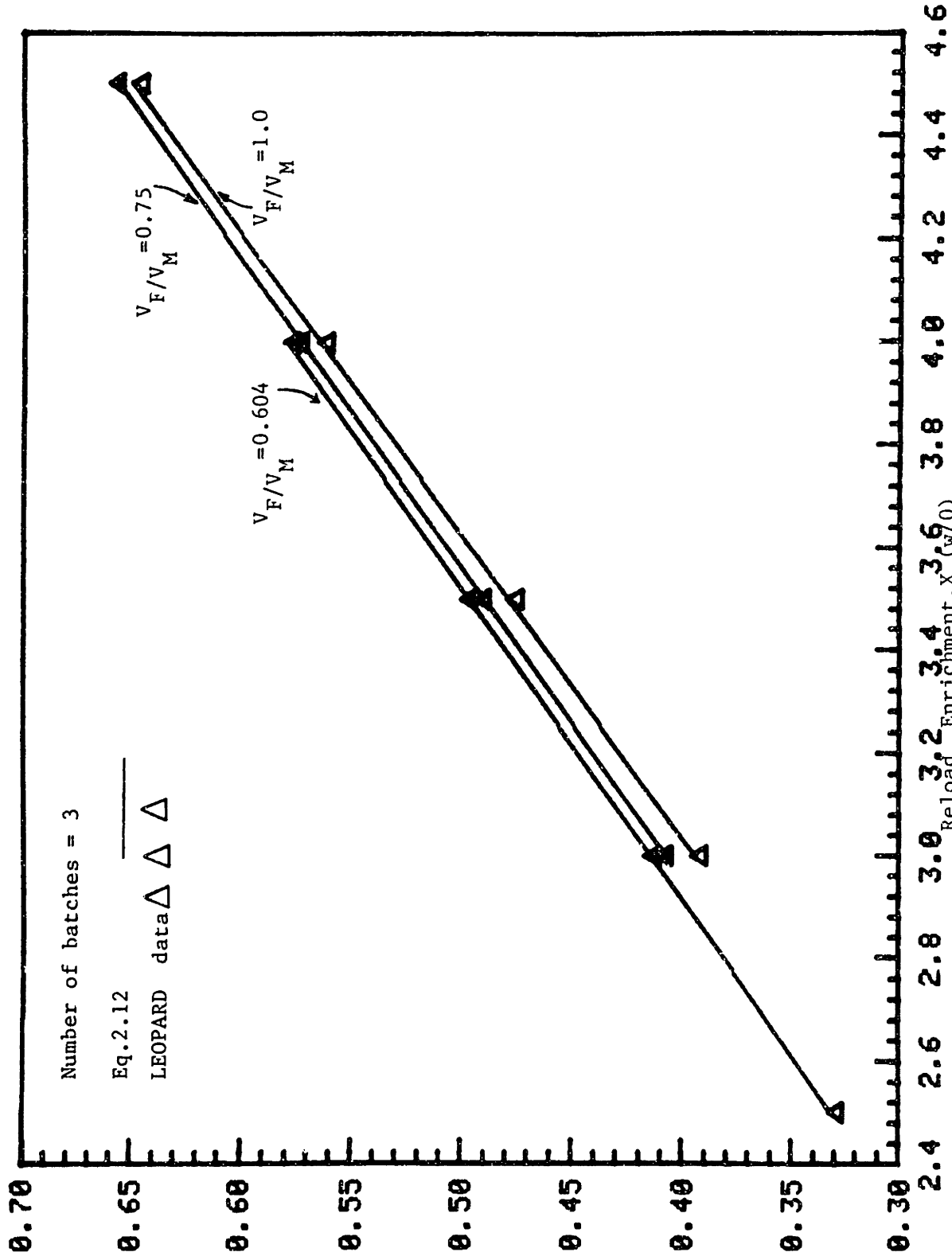


Fig.2.4 U-236 in discharged fuel$^P$vs. reload enrichment for various fuel-to-moderator ratios(n=3).

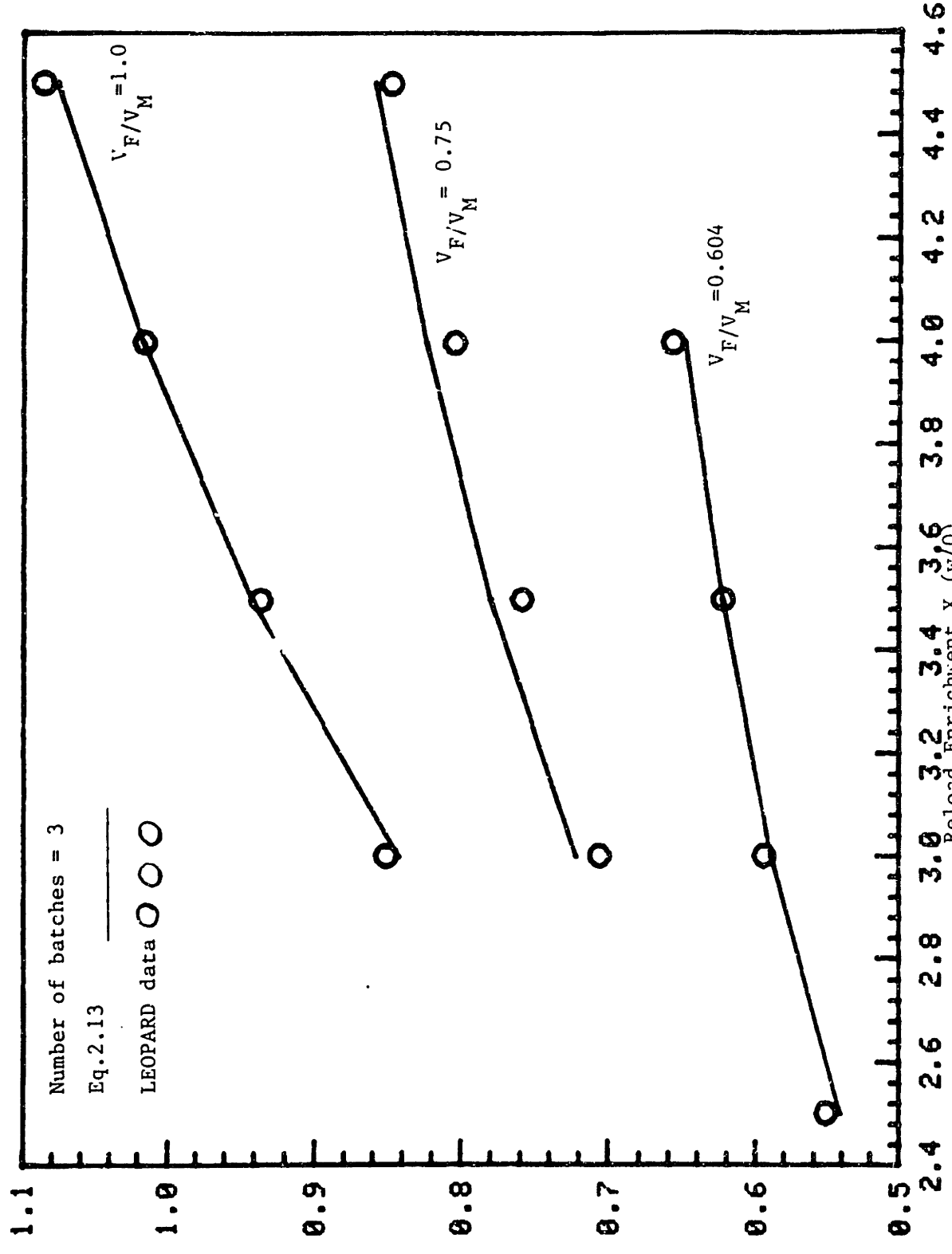


Fig. 2.5 Fissile Plutonium in $^{P}$discharged fuel vs. reload enrichment for various fuel-to-moderator ratios(n = 3).

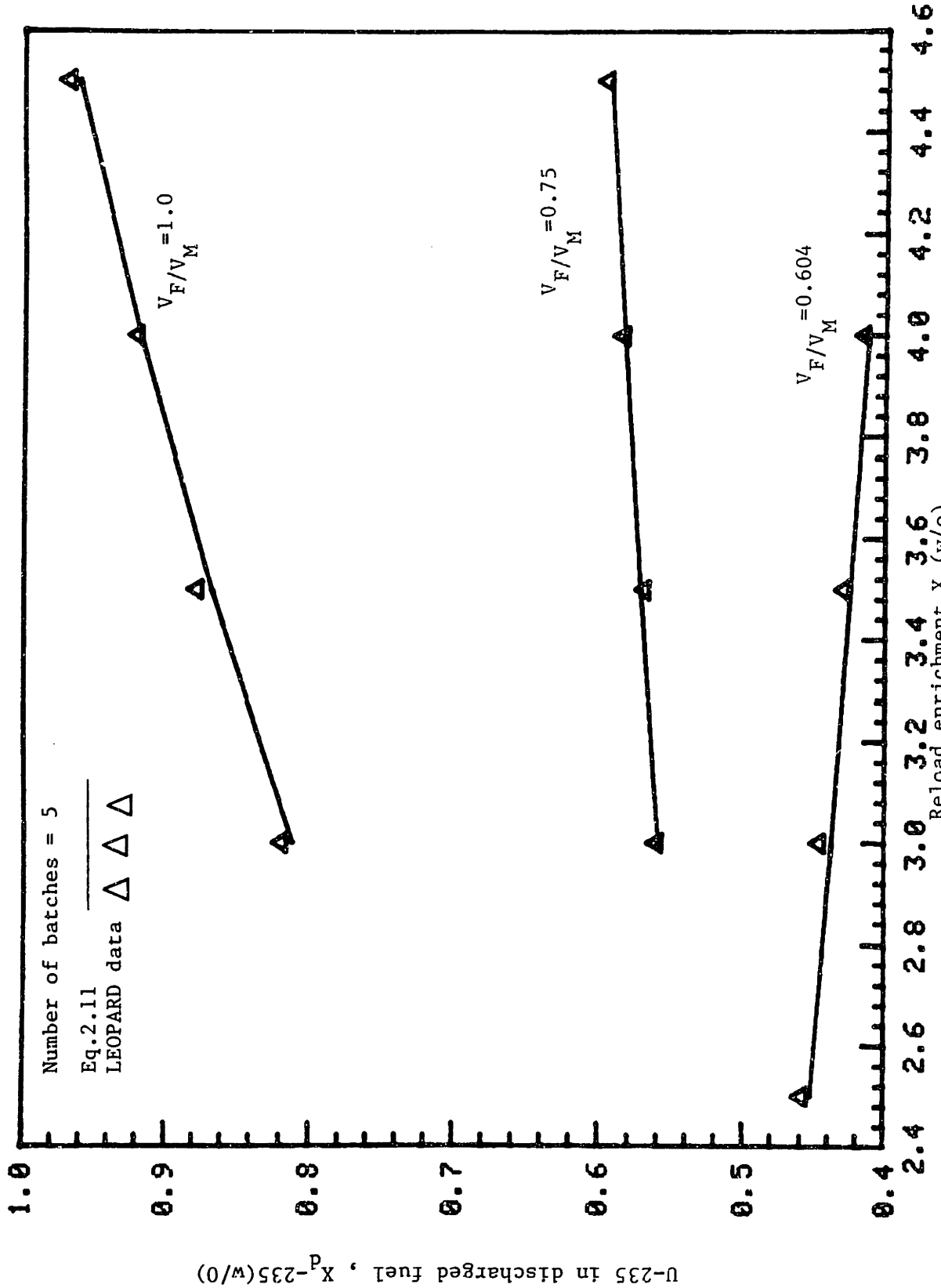


Fig.2.6 U-235 in discharged fuel vs. reload enrichment for various fuel-to-moderator ratios (n= 5).

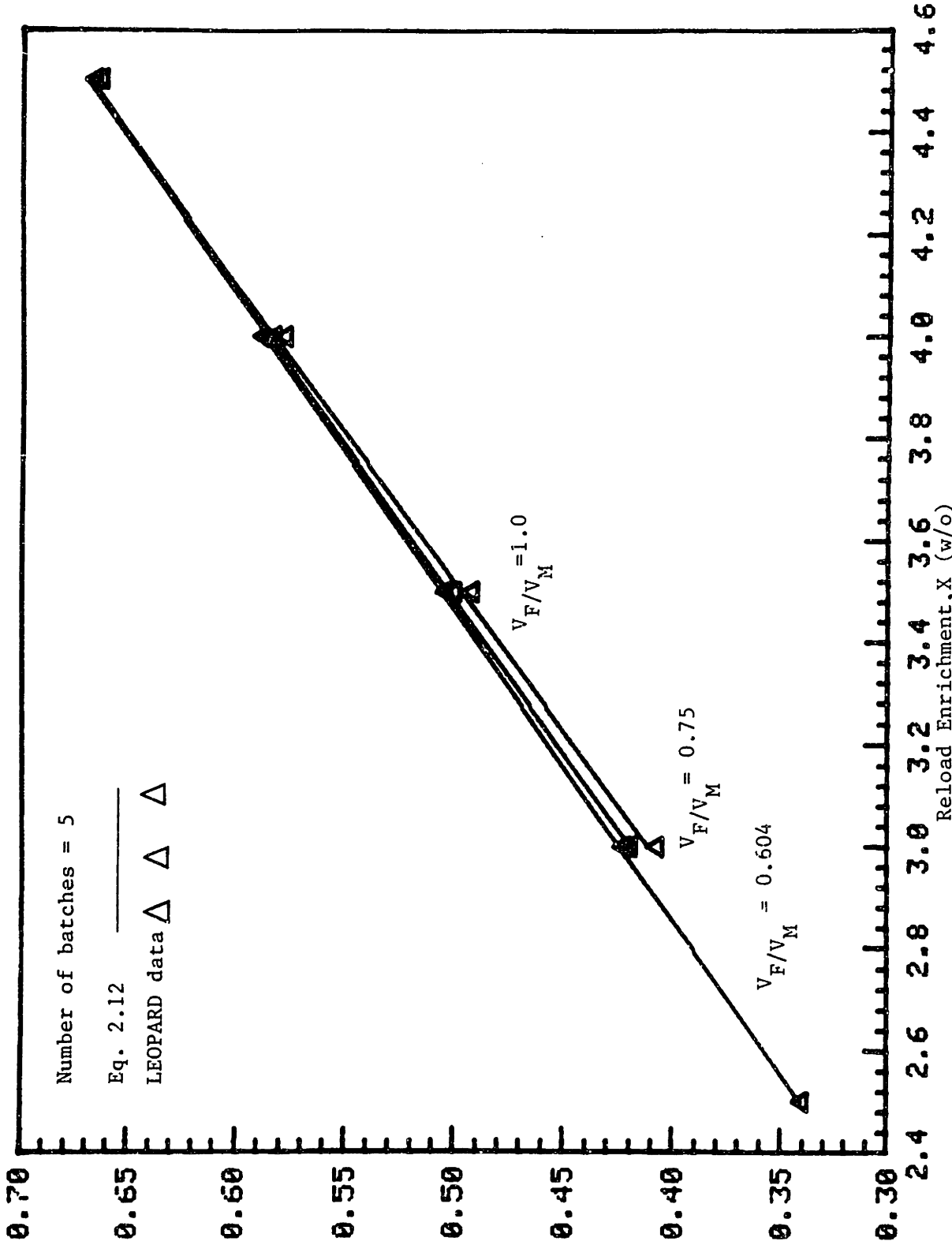


Fig.2.7 U-236 in discharged fuel vs. reload enrichment for various fuel-to-moderator ratios(n = 5).

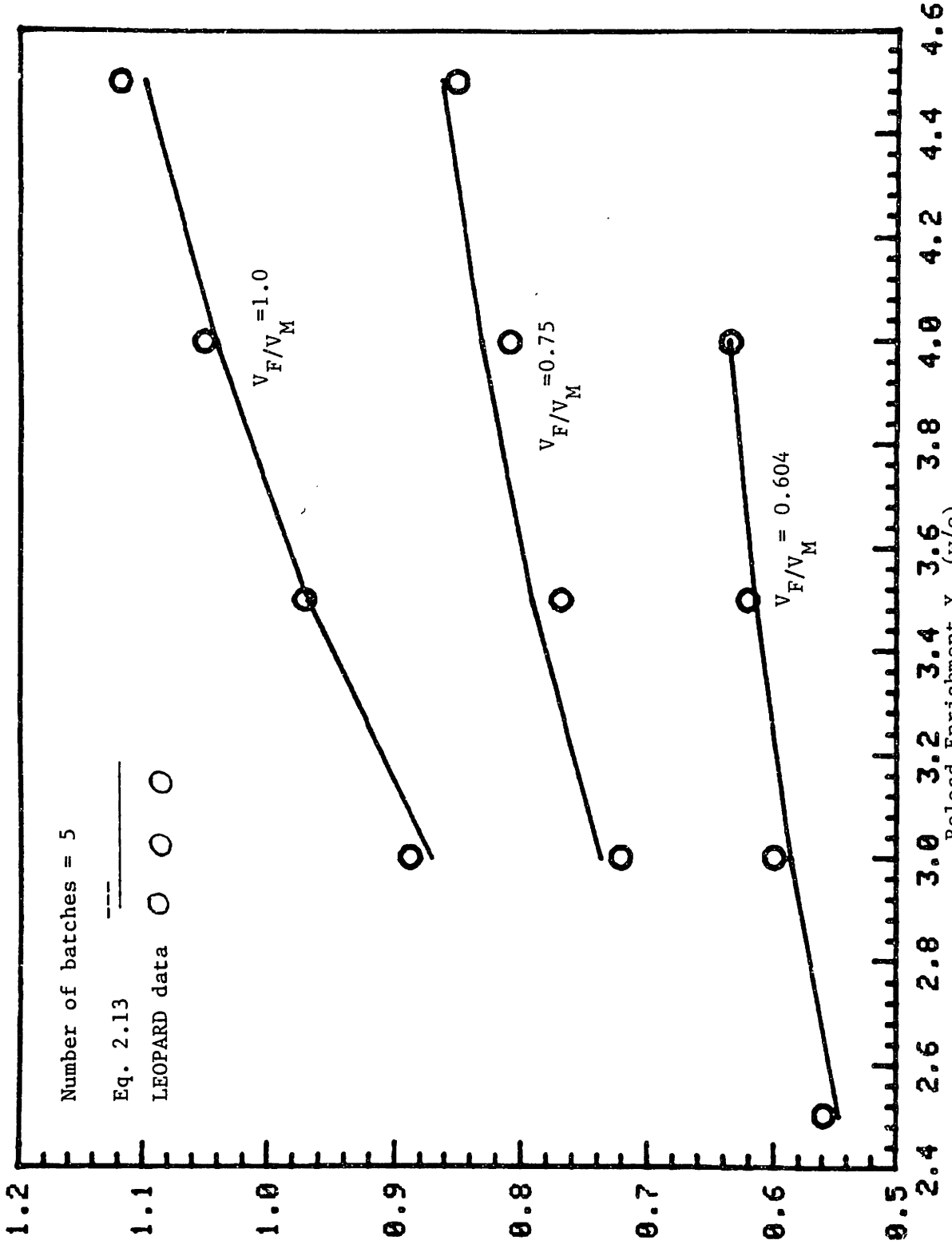


Fig.2.8 Fissile Plutonium in discharged fuel vs. reload enrichment for varicus fuel-to-moderator ratios(n=5).

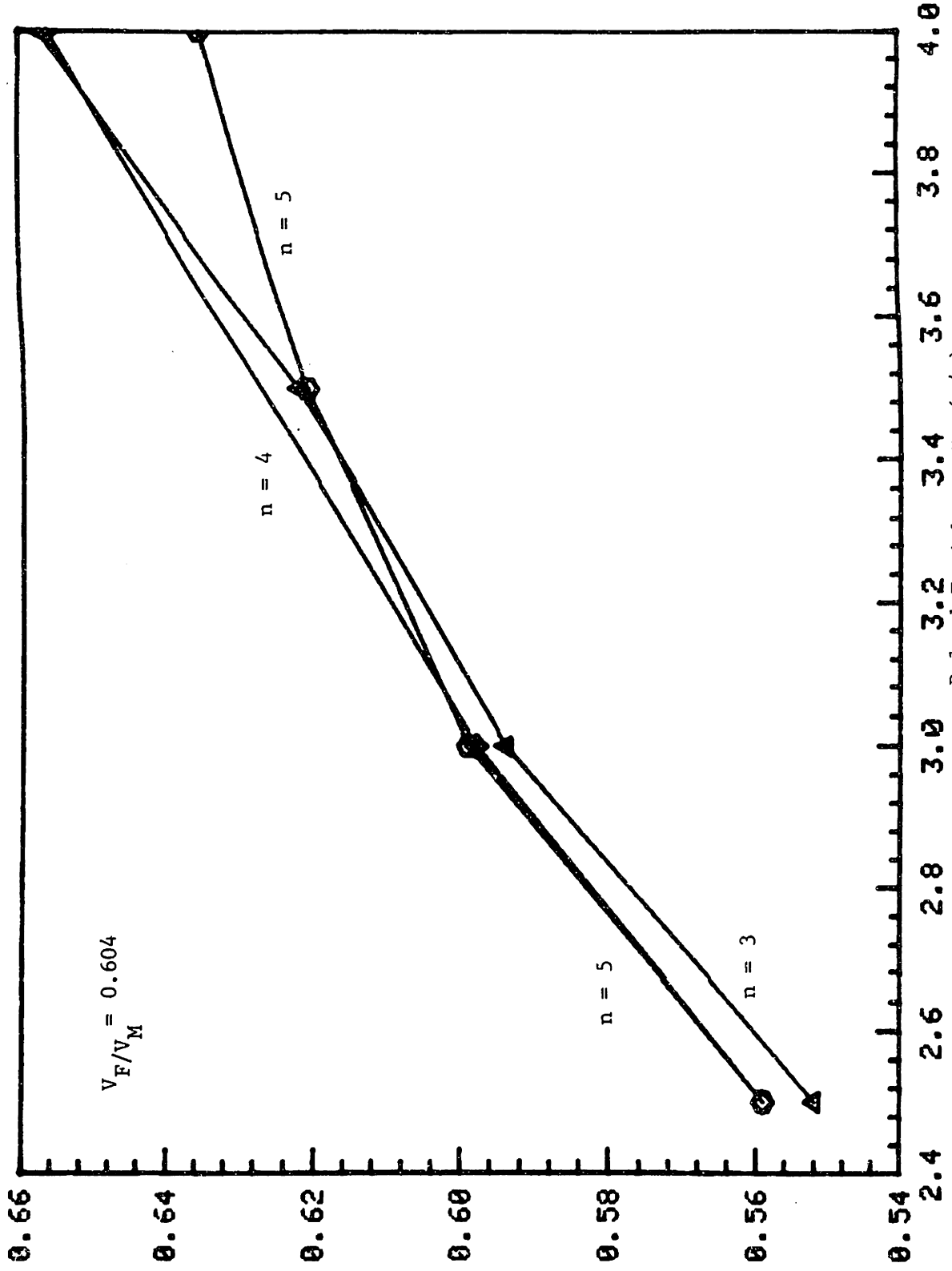


Fig.2.9 Fissile Plutonium in discharged fuel vs. reload enrichment for various n:($V_{F/V_M}$=0.604).

TABLE 2.1

Comparison of Curve-fit Values and LEOPARD Data for the Isotopic Composition of Spent Fuel: $V_F/V_M = 0.604$ ; n=3

| $X_P$ U-235 (w/o) | Puf (w/o) Fissile Pu (Pu-239+Pu-241) | | | U-235 (w/o) | | | U-236 (w/o) | | |
|---|---|---|---|---|---|---|---|---|---|
| | LEOPARD | Curve fit Formula | Error % | LEOPARD | Curve fit Formula | Error % | LEOPARD | Curve fit Formula | Error % |
| 2.5 | 0.551 | 0.541 | 1.81 | 0.561 | 0.560 | 0.18 | 0.328 | 0.332 | 1.22 |
| 3.0 | 0.594 | 0.589 | 0.84 | 0.569 | 0.571 | 0.35 | 0.412 | 0.414 | 0.48 |
| 3.5 | 0.622 | 0.623 | 0.16 | 0.576 | 0.578 | 0.35 | 0.496 | 0.497 | 0.20 |
| 4.0 | 0.657 | 0.649 | 1.22 | 0.585 | 0.587 | 0.34 | 0.576 | 0.579 | 0.52 |

TABLE 2.2

Comparison of Curve-fit Values and LEOPARD Data for the Isotopic Composition of Spent Fuel: $V_F/V_M = 0.75$ ; n=3

| $X_P$ U-235 (w/o) | Puf (w/o) Fissile Pu (Pu-239+Pu-241) | | | U-235 (w/o) | | | U-236 (w/o) | | |
|---|---|---|---|---|---|---|---|---|---|
| | LEOPARD | Curve fit Formula | Error % | LEOPARD | Curve fit Formula | Error % | LEOPARD | Curve fit Formula | Error % |
| 3.0 | 0.706 | 0.722 | 2.27 | 0.680 | 0.683 | 0.44 | 0.407 | 0.407 | 0.0 |
| 3.5 | 0.759 | 0.780 | 2.77 | 0.710 | 0.720 | 1.41 | 0.490 | 0.490 | 0.0 |
| 4.0 | 0.805 | 0.825 | 2.48 | 0.747 | 0.753 | 0.80 | 0.573 | 0.573 | 0.0 |
| 4.5 | 0.848 | 0.859 | 1.30 | 0.784 | 0.782 | 0.26 | 0.656 | 0.656 | 0.0 |

TABLE 2.3

Comparison of Curve-fit Values and LEOPARD Data for the Isotopic Composition of Spent Fuel: $V_F/V_M = 1.0$ ; n=3

| $X_P$ U-235 (w/o) | Puf (w/o) Fissile Pu (Pu-239+Pu-241) | | | U-235 (w/o) | | | U-236 (w/o) | | |
|---|---|---|---|---|---|---|---|---|---|
| | LEOPARD | Curve fit Formula | Error % | LEOPARD | Curve fit Formula | Error % | LEOPARD | Curve fit Formula | Error % |
| 3.0 | 0.851 | 0.843 | 0.94 | 0.940 | 0.935 | 0.53 | 0.391 | 0.394 | 0.77 |
| 3.5 | 0.936 | 0.942 | 0.64 | 1.022 | 1.021 | 0.10 | 0.475 | 0.479 | 0.84 |
| 4.0 | 1.016 | 1.017 | 0.10 | 1.087 | 1.096 | 0.83 | 0.561 | 0.564 | 0.53 |
| 4.5 | 1.086 | 1.076 | 0.92 | 1.169 | 1.162 | 0.60 | 0.645 | 0.649 | 0.62 |

TABLE 2.4

Comparison of Curve-fit Values and LEOPARD Data for the Isotopic Composition of Spent Fuel: $V_F/V_M$ = 0.604 ; n=5

| $X_P$ U-235 (w/o) | Puf (w/o) Fissile Pu (Pu-239+Pu-241) | | | U-235 (w/o) | | | U-236 (w/o) | | |
|---|---|---|---|---|---|---|---|---|---|
| | LEOPARD | Curve fit Formula | Error % | LEOPARD | Curve fit Formula | Error % | LEOPARD | Curve fit Formula | Error % |
| 2.5 | 0.559 | 0.546 | 2.32 | 0.458 | 0.452 | 1.31 | 0.340 | 0.341 | 0.29 |
| 3.0 | 0.599 | 0.586 | 2.32 | 0.446 | 0.437 | 2.02 | 0.422 | 0.424 | 0.47 |
| 3.5 | 0.621 | 0.615 | 0.97 | 0.429 | 0.424 | 1.16 | 0.504 | 0.506 | 0.40 |
| 4.0 | 0.635 | 0.636 | 0.16 | 0.415 | 0.412 | 0.72 | 0.588 | 0.588 | 0.000 |

TABLE 2.5

Comparison of Curve-fit Values and LEOPARD Data for the Isotopic Composition of Spent Fuel: $V_F/V_M = 0.75$ ; n=5

| $X_P$ U-235 (w/o) | Puf (w/o) Fissile Pu (Pu-239+Pu-241) | | | U-235 (w/o) | | | U-236 (w/o) | | |
|---|---|---|---|---|---|---|---|---|---|
| | LEOPARD | Curve fit Formula | Error % | LEOPARD | Curve fit Formula | Error % | LEOPARD | Curve fit Formula | Error % |
| 3.0 | 0.721 | 0.737 | 2.22 | 0.560 | 0.550 | 0.18 | 0.419 | 0.419 | 0.00 |
| 3.5 | 0.769 | 0.792 | 2.99 | 0.569 | 0.572 | 0.53 | 0.500 | 0.503 | 0.60 |
| 4.0 | 0.810 | 0.833 | 2.84 | 0.584 | 0.583 | 0.17 | 0.583 | 0.586 | 0.51 |
| 4.5 | 0.852 | 0.864 | 1.41 | 0.596 | 0.593 | 0.50 | 0.666 | 0.670 | 0.60 |

TABLE 2.6

Comparison of Curve-fit Values and LEOPARD Data for the Isotopic Composition of Spent Fuel: $V_F/V_M = 1.0$ ; n=5

| $X_P$ U-235 (w/o) | Puf (w/o) Fissile Pu (Pu-239+Pu-241) | | | U-235 (w/o) | | | U-236 (w/o) | | |
|---|---|---|---|---|---|---|---|---|---|
| | LEOPARD | Curve fit Formula | Error % | LEOPARD | Curve fit Formula | Error % | LEOPARD | Curve fit Formula | Error % |
| 3.0 | 0.888 | 0.871 | 1.91 | 0.818 | 0.811 | 0.86 | 0.407 | 0.411 | 0.98 |
| 3.5 | 0.972 | 0.969 | 0.31 | 0.878 | 0.868 | 1.14 | 0.492 | 0.497 | 1.02 |
| 4.0 | 1.051 | 1.042 | 0.86 | 0.920 | 0.918 | 0.22 | 0.578 | 0.583 | 0.86 |
| 4.5 | 1.119 | 1.099 | 1.79 | 0.969 | 0.962 | 0.72 | 0.663 | 0.669 | 0.90 |

Note that the $X_d$-235 values shown in Fig. 2.3 are somewhat lower than encountered in practice ($X_d \approx 0.7$ w/o) because the reactivity limited discharge burnup calculated using k-infinity values from LEOPARD output, even after correcting for leakage (see Appendix A for procedure) is higher than the burnup achieved in practical situations. Thus the absolute values quoted here should be considered as indicative of the general behavior of LWR units, and not as an absolute prediction of the specific performance of a given reactor design. This is particularly true of BWR units, since the present data has been computed for PWR lattices. Nevertheless, by following the procedures laid out in Appendix A, similar prescriptions can be readily developed for applications of specific interest.

Note that the discharged fuel composition relations of Eqs. (2.11), (2.12) and (2.13), unlike similar relations developed by others [M4], include the functional dependence on fuel-to-moderator ratio and number of batches - features which are essential to optimization strategy.

## 2.5 Isotopic Composition of Fuel During Irradiation

In the preceding section, correlations for the composition of fuel at the point of reactivity-limited burnup were presented. One can instead attempt to correlate composition as a function

of any intermediate burnup state: the goal explored in the present section.

Standard statistical programs for simple regression were used to curve fit the previously discussed LEOPARD data for U-235, U-236 and fissile plutonium in the fuel as a function of burnup.

The functional dependence of X-235 versus burnup, B (GWD/MT), was found to be of the form

$$\text{X-235} = a_1 + b_1 \ln (B), \text{w/o} \tag{2.17}$$

where $a_1$ and $b_1$ depend on reload enrichment, $X_P$, and can be expressed as

$$a_1 (X_P) = a_2 + b_2 X_P, \text{ w/o} \tag{2.18}$$

and

$$b_1 (X_P) = b_3 X_P, \text{ w/o} \tag{2.19}$$

combining Eqs. (2.17), (2.18) and (2.19):

$$\text{X-235} = a_2 + b_2 X_P + b_3 X_P \ln (B), \text{ w/o} \tag{2.20}$$

The coefficients of the curve fit of Eqs. (2.17) and (2.20) are listed in tables (2.7) and (2.8), respectively. Including the dependence of parameters $a_2$, $b_2$ and $a_3$ on $\frac{V_F}{V_M}$, it was found that

$$\text{X-235} = a_4 + b_4 \frac{V_F}{V_M} + \left(a_5 + b_5 \frac{V_F}{V_M}\right) X_P + X_P \left(a_6 + b_6 \frac{V_F}{V_M}\right) \ln (B) \tag{2.21}$$

TABLE 2.7

Coefficients of Curve Fit of X-235 vs Burnup for Various Reload Enrichments and Fuel-to-Moderator Ratios

| $V_F/V_M$ | $X_p$ (w/o) | X-235 = $a_1$ + $b_1$ ln (B), (w/o) | | $R^2$ |
|---|---|---|---|---|
| | | $a_1$ (w/o) | $b_1$ (w/o) | |
| 0.604 | 2.5 | 3.8976 | -1.0000 | 0.9996 |
| | 3.0 | 4.9088 | -1.2179 | 0.9993 |
| | 4.0 | 7.0801 | -1.6715 | 0.9981 |
| 0.750 | 3.0 | 4.8167 | -1.1730 | 0.9995 |
| | 3.5 | 5.8570 | -1.3897 | 0.9993 |
| | 4.0 | 6.9214 | -1.6057 | 0.9985 |
| | 4.5 | 7.9281 | -1.7969 | 0.9969 |
| 1.000 | 3.0 | 4.6891 | -1.1125 | 0.9995 |
| | 3.5 | 5.6939 | -1.3182 | 0.9994 |
| | 4.0 | 6.7166 | -1.5218 | 0.9990 |
| | 4.5 | 7.6974 | -1.7060 | 0.9973 |

The Libraries
Massachusetts Institute of Technology
Cambridge, Massachusetts 02139

Institute Archives and Special Collections
Room 14N-118
(617) 253-5688

This is the most complete text of the thesis available. The following page(s) were not included in the copy of the thesis deposited in the Institute Archives by the author:

Pg. 56

with:

$a_4 = -1.62102$ w/o  $b_4 = 0.28151$ w/o

$a_5 = 2.30733$  $b_5 = -0.29904$

$a_6 = 0.08364$  $b_6 = -0.46118$

An analogous approach was used to determine the functional dependence of X-236 and $X_{Puf}$ with burnup, $X_P$ and $\frac{V_F}{V_M}$ :

$$X\text{-}236 = a_1 + b_1/B \text{ , w/o} \tag{2.22}$$

$$a_1(X_P) = b_2 X_P \text{ , w/o} \tag{2.23}$$

$$b_1(X_P) = a_3 + b_3 X_P \text{ , w/o GWD/MT} \tag{2.24}$$

Substituting Eqs. (2.24) and (2.23) in Eq. (2.22)

$$X\text{-}236 = b_2 X_P + (a_3 + b_3 X_P)/B \tag{2.25}$$

The coefficients of the curve fit to Eqs. (2.22) and (2.25) are listed in Tables (2.9) and (2.10) respectively. The dependence of parameters $b_2$, $a_3$ and $b_3$ on $\frac{V_F}{V_M}$ was included to give:

$$X\text{-}236 = \left(a_4 + b_4 \frac{V_F}{V_M}\right) X_P + \frac{1}{B}\left[a_5 + b_5 \cdot \frac{V_F}{V_M} + c_5\left(\frac{V_F}{V_M}\right)^2 + \left\{a_6 + b_6 \cdot \frac{V_F}{V_M} + c_6\left(\frac{V_F}{V_M}\right)^2\right\} X_P\right] \tag{2.26}$$

TABLE 2.9

Coefficients of Curve-fit of X-236 Versus Burnup for Various Reload Enrichments and Fuel-to-Moderator Ratios

| $V_F/V_M$ | $X_P$ (w/o) | X-236 = $a_1 + b_1/B$, w/o | | $R^2$ |
|---|---|---|---|---|
| | | $a_1$ (w/o) | $b_1$ (w/o) MT/GWD | |
| 0.604 | 2.5 | 0.44234 | -3.20536 | 0.998 |
| | 3.0 | 0.53160 | -4.31314 | 0.995 |
| | 4.0 | 0.71527 | -6.9989 | 0.991 |
| 0.750 | 3.0 | 0.52958 | -4.20859 | 0.997 |
| | 3.5 | 0.62757 | -5.59815 | 0.997 |
| | 4.0 | 0.71868 | -6.93167 | 0.993 |
| | 4.5 | 0.80282 | -8.18659 | 0.990 |
| 1.000 | 3.0 | 0.53584 | -4.20138 | 0.999 |
| | 3.5 | 0.63331 | -5.51508 | 0.997 |
| | 4.0 | 0.72825 | -6.88576 | 0.994 |
| | 4.5 | 0.81578 | -8.14266 | 0.990 |

TABLE 2.10

Coefficients of Curve-fit of X-236 Versus Burnup and $X_P$ for Various Fuel-to-Moderator Ratios

| $V_F/V_M$ | X-236 = $a_1 + b_1/B$ , w/o | | | | |
|---|---|---|---|---|---|
| | $a_1 = b_2 X_P$ (w/o) / $b_2$ | $R^2$ | $b_1 = a_3 + b_3 X_P$ w/o $\frac{MT}{GWD}$ | | $R^2$ |
| | | | $a_3$ | $b_3$ | |
| 0.604 | 0.17755 | 0.998 | 3.24035 | -2.55142 | 0.9997 |
| 0.750 | 0.17865 | 0.998 | 3.71939 | -2.65350 | 0.9995 |
| 1.000 | 0.18101 | 0.998 | 3.70967 | -3.70967 | 0.9997 |

with:

$$a_4 = 0.17215 \; ; \; b_4 = 0.00881$$

$$a_5 = -2.548 \text{ w/o } \frac{MT}{GWD} \; ; \; b_5 = 14.655 \text{ w/o } \frac{MT}{GWD} \; ;$$

$$c_5 = -8.397 \text{ w/o } \frac{MT}{GWD}$$

$$a_6 = -1.263 \frac{MT}{GWD} \; ; \; b_6 = -3.288 \frac{MT}{GWD} \; ; \; c_6 = 1.912 \frac{MT}{GWD}$$

$$X_{Puf} = B/(a_1 + b_1 B) \quad , \text{ w/o} \tag{2.27}$$

$$a_1(X_P) = a_2 + b_2 X_P \text{ GWD/MT w/o} \tag{2.28}$$

$$b_1(X_P) = a_3 + b_3 X_P \text{ (w/o)}^{-1} \tag{2.29}$$

Substituting Eqs. (2.29) and (2.28) in Eq. (2.27)

$$X_{Puf} = B \left[ a_2 + b_2 X_P + (a_3 + b_3 X_P) \; B \right]^{-1} \text{ , w/o} \tag{2.30}$$

The coefficients of the curve fit of Eqs. (2.27) and (2.30) are listed in tables (2.11) and (2.12), respectively.

Including the dependence of parameters $a_2$, $b_2$, $a_3$ and $b_3$ on $\frac{V_F}{V_M}$, it was found that:

$$X_{Puf} = B \left[ a_4 + b_4 \frac{V_F}{V_M} + \left( a_5 + \frac{b_5}{VF/VM} \right) X_P + \left\{ a_6 + b_6 \frac{V_F}{V_M} + \left( a_7 + b_7 \frac{V_F}{V_M} \right) X_P \right\} B \right]^{-1} \text{, w/o} \tag{2.31}$$

TABLE 2.11

Coefficients of Curve-fit of $X_{Puf}$ Versus Burnup for Various Reload Enrichments and Fuel-to-Moderator Ratios

| $V_F/V_M$ | $X_P$ (w/o) | $X_{Puf} = B(a_1 + b_1 B)^{-1}$, w/o | | $R^2$ |
|---|---|---|---|---|
| | | $a_1 \frac{GWD}{MT}$ (w/o) | $b_1$ $(w/o)^{-1}$ | |
| 0.604 | 2.5 | 16.86804 | 1.15616 | 0.993 |
| | 3.0 | 18.58432 | 1.03427 | 0.980 |
| | 4.0 | 20.8695 | 0.88533 | 0.990 |
| 0.750 | 3.0 | 16.52715 | 0.92709 | 0.992 |
| | 3.5 | 17.79535 | 0.81441 | 0.994 |
| | 4.0 | 18.63356 | 0.77303 | 0.996 |
| | 4.5 | 19.68057 | 0.69359 | 0.994 |
| 1.000 | 3.0 | 14.64580 | 0.69347 | 0.9992 |
| | 3.5 | 15.57895 | 0.63232 | 0.9994 |
| | 4.0 | 16.39591 | 0.58302 | 0.9994 |
| | 4.5 | 17.15978 | 0.53720 | 0.9995 |

TABLE 2.12

Coefficients of Curve-fit of $X_{Puf}$ Versus Burnup and Reload Enrichment for Various Fuel-to-Moderator Ratios

| $V_F/V_M$ | $X_{Puf} = B(a_1 + b_1 B)^{-1}$, w/o | | | | | |
|---|---|---|---|---|---|---|
| | $a_1 = a_2 + b_2 X_P$ GWD/MT (w/o) | | $R^2$ | $b_1 = a_3 + b_3 X_P$ | | $R^2$ |
| | $a_2$ GWD/MT (w/o) | $b_2$ GWD/MT $(w/o)^{-2}$ | | $a_3 (w/o)^{-1}$ | $b_3 (w/o)^{-2}$ | |
| 0.604 | 10.5000 | 2.61307 | 0.990 | 1.58220 | -0.1760 | 0.980 |
| 0.750 | 10.43644 | 2.05935 | 0.994 | 1.358 | -.1484 | 0.980 |
| 1.000 | 9.676 | 1.672 | 0.998 | 1.000 | -0.10362 | 0.995 |

with:

$$a_4 = 11.920 \frac{GWD}{MT\ w/o} ; \quad b_4 = -2.200 \frac{GWD}{MT\ w/o}$$

$$a_5 = 0.20834 \frac{GWD}{MT\ (w/o)^2} ; \quad b_5 = 1.43381 \frac{GWD}{MT\ (w/o)^2}$$

$$a_6 = 2.46378\ w/o^{-1} ; \ b_6 = 1.46607\ w/o^{-1}$$

$$a_7 = -0.28578\ (w/o)^{-2} ; \quad b_7 = 0.18238\ (w/o)^{-2}$$

The curve fit values from Eqs. (2.21), (2,26) and (2.31) are compared to LEOPARD data in tables (2.13) through (2.21). Selected comparisons of interest are shown in Figs. 2.10 through 2.16.

If the fuel is discharged from the reactor at a burnup different from its reactivity limited capability then the above correlations can be used to determine isotopic composition of discharged fuel as a function of burnup.

## 2.6 Recycle Mode Mass Flow Submodel

In the recycle mode considered in this work, the plutonium from spent fuel is used to make up for the consumed U-235 in part of the discharged fuel, and the remaining uranium is credited both for ore and SWU. Other alternatives exist: recycle plutonium could be blended with natural uranium or with enrichment plant tails. These options were not adopted

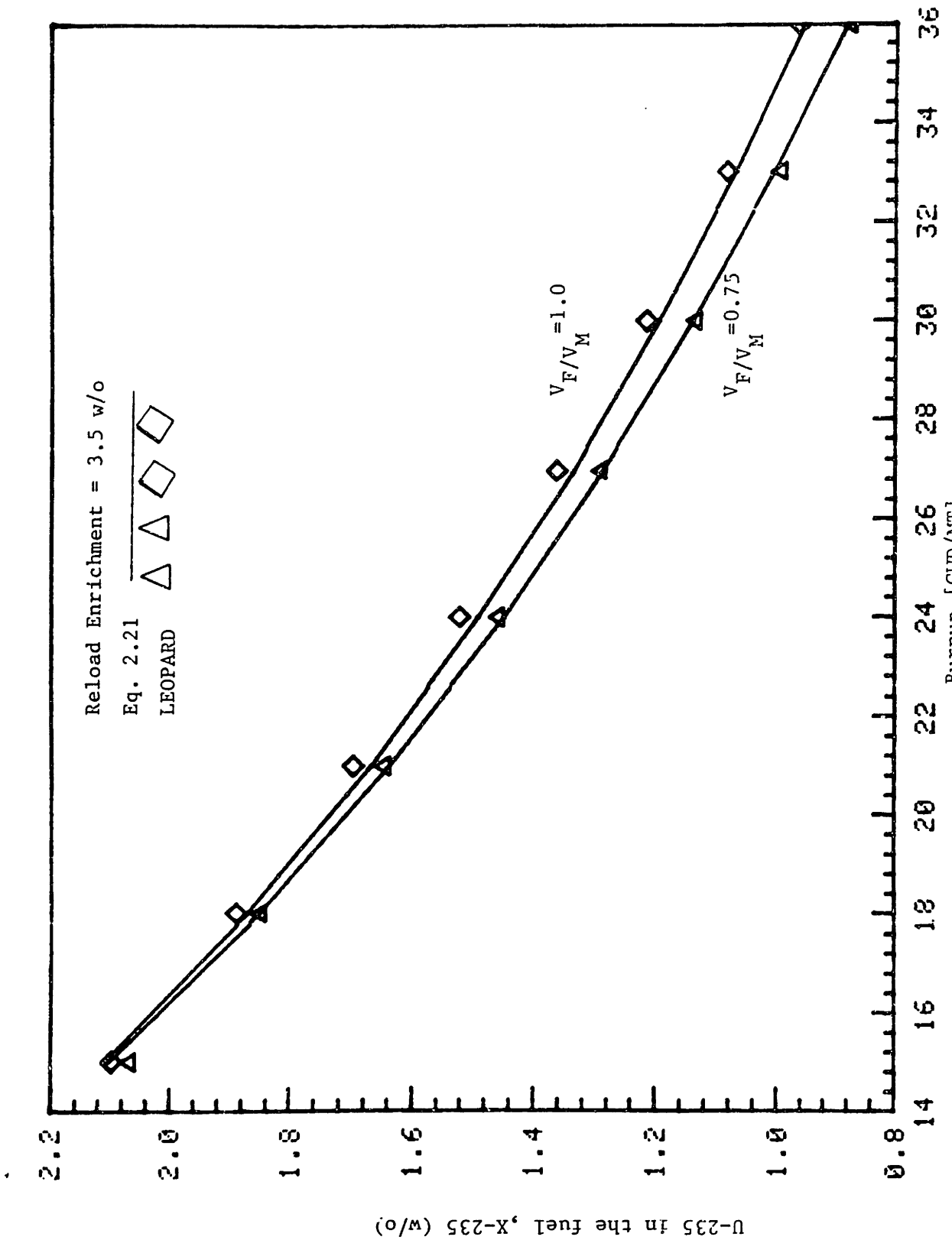


Fig.2.10.U-235 in the fuel vs burnup for various fuel to modrator ratios.

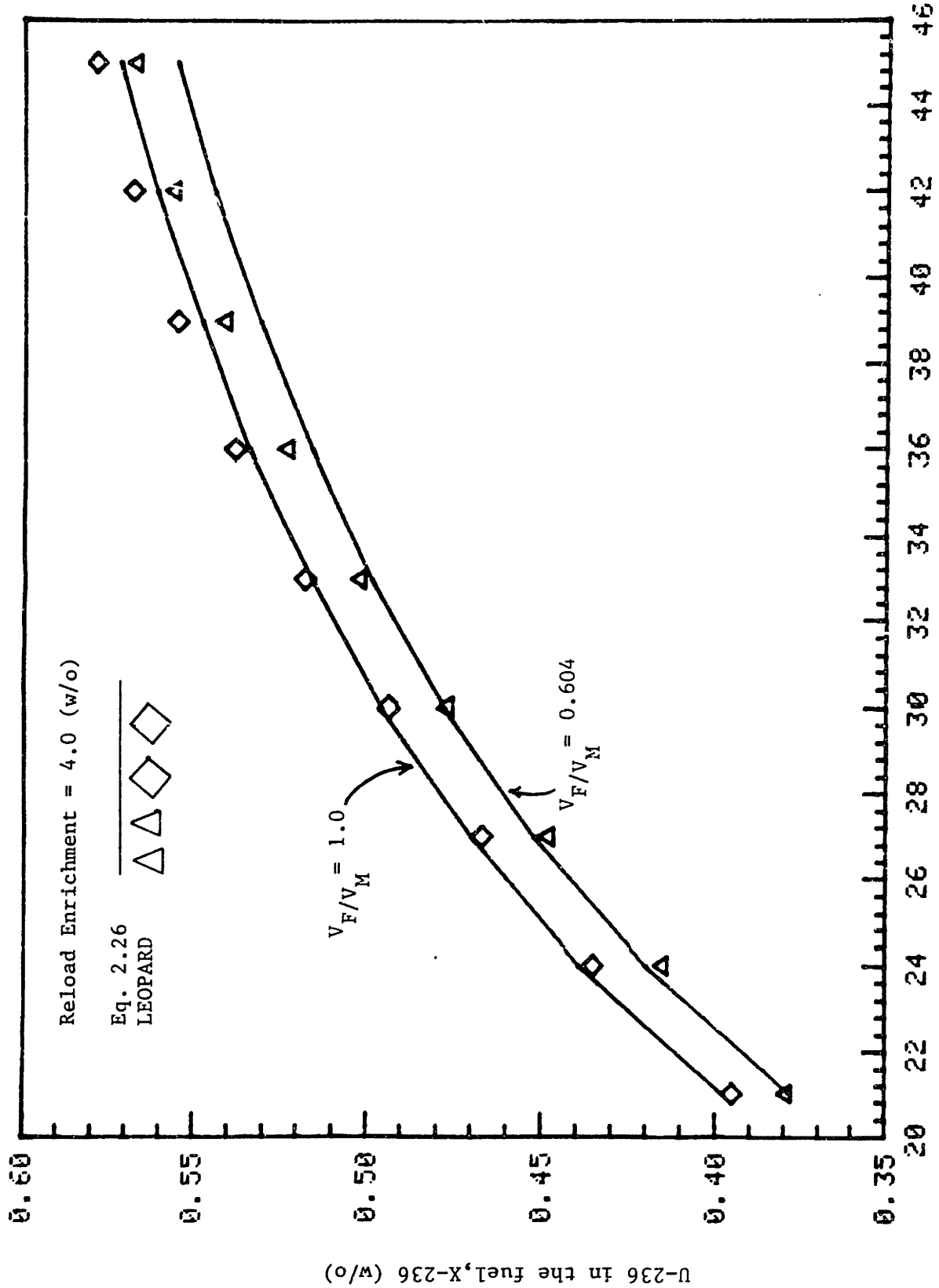


Fig.2.11. U-236 in the fuel vs burnup for various fuel to moderator ratios.

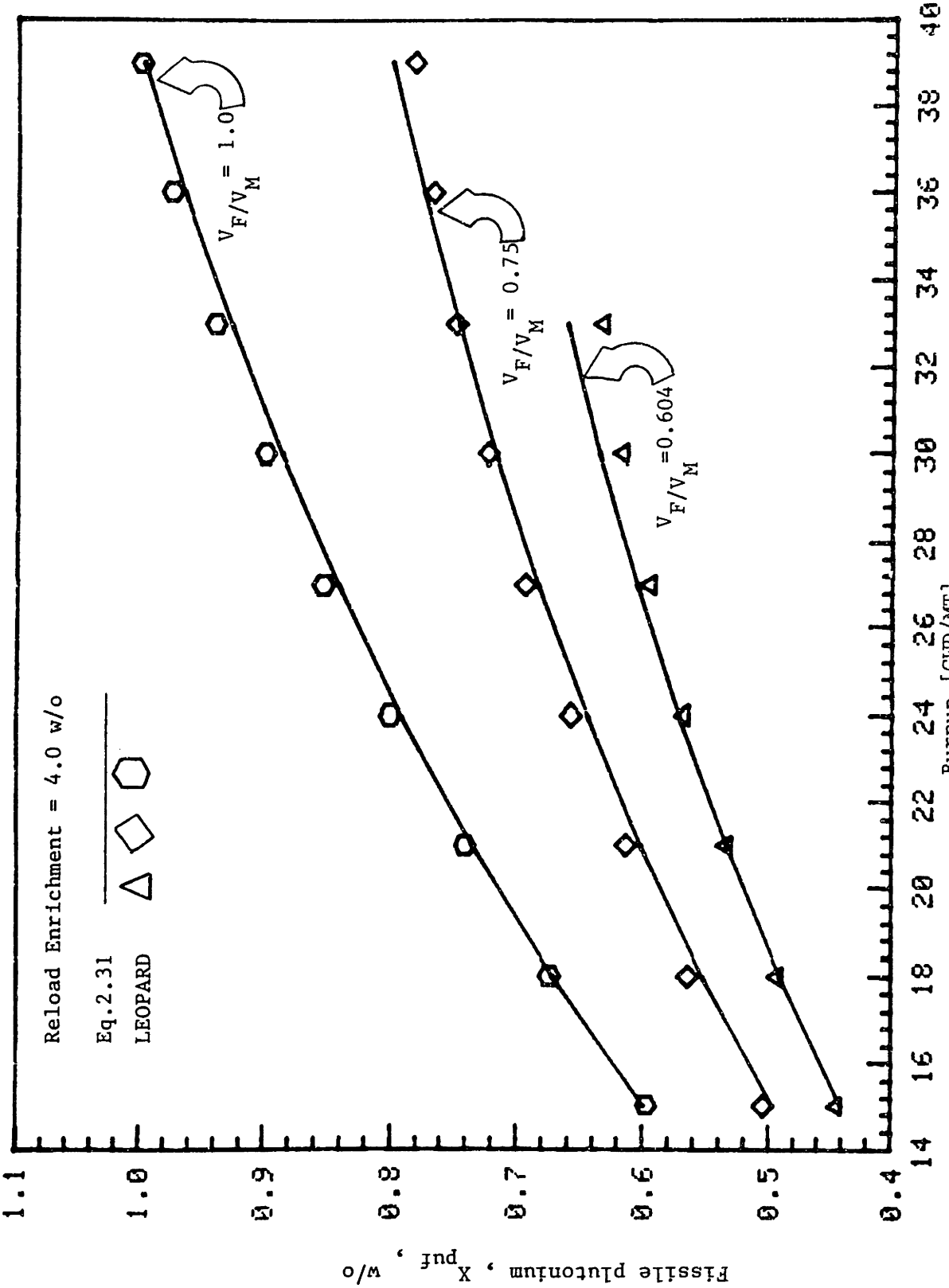


Fig.2.12. Fissile Pu in the fuel vs burnup for various fuel to moderator ratios.

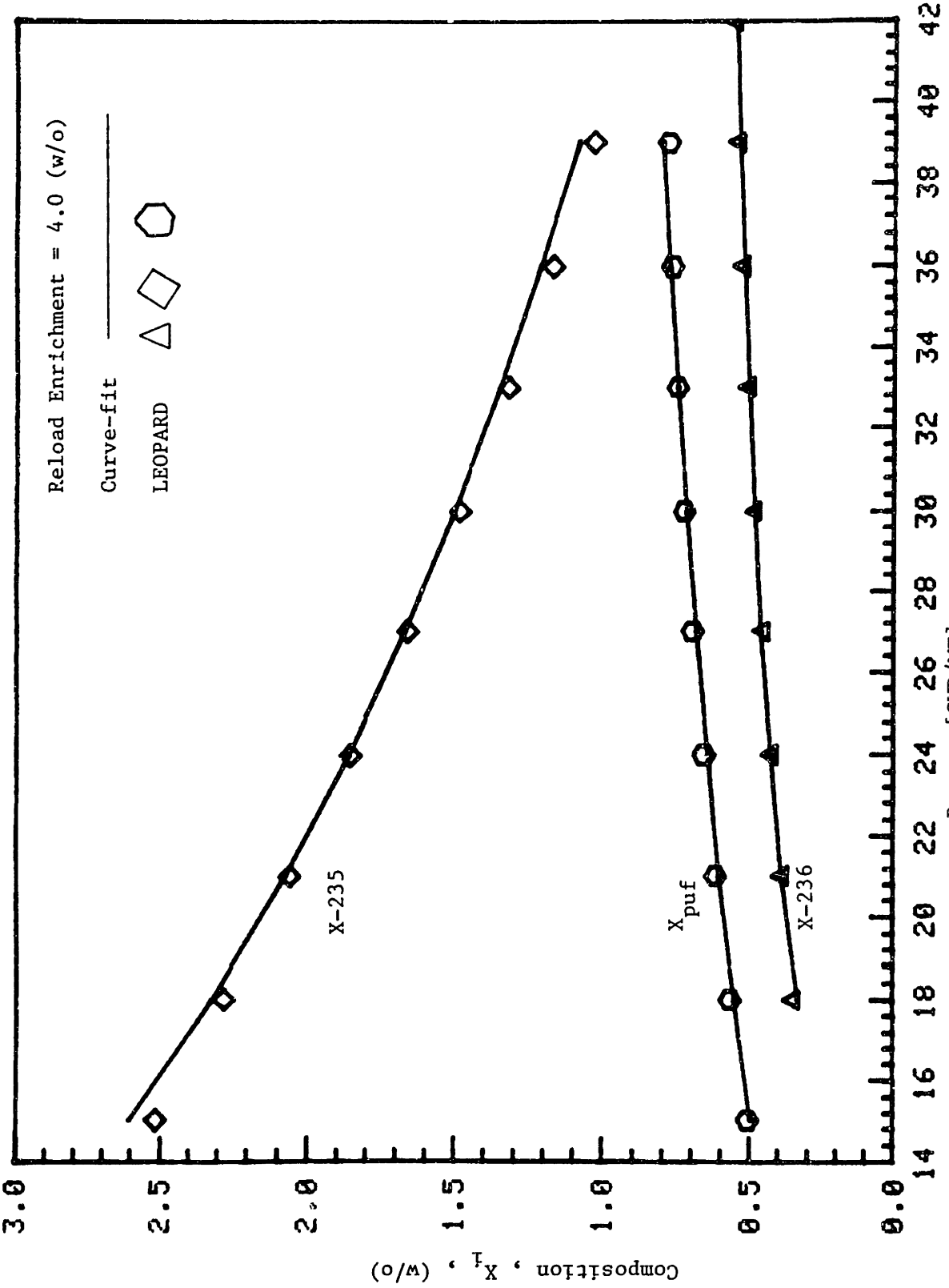


Fig.2.13. Composition of fuel as a function of burnup: $V_F/V_M$=0.75

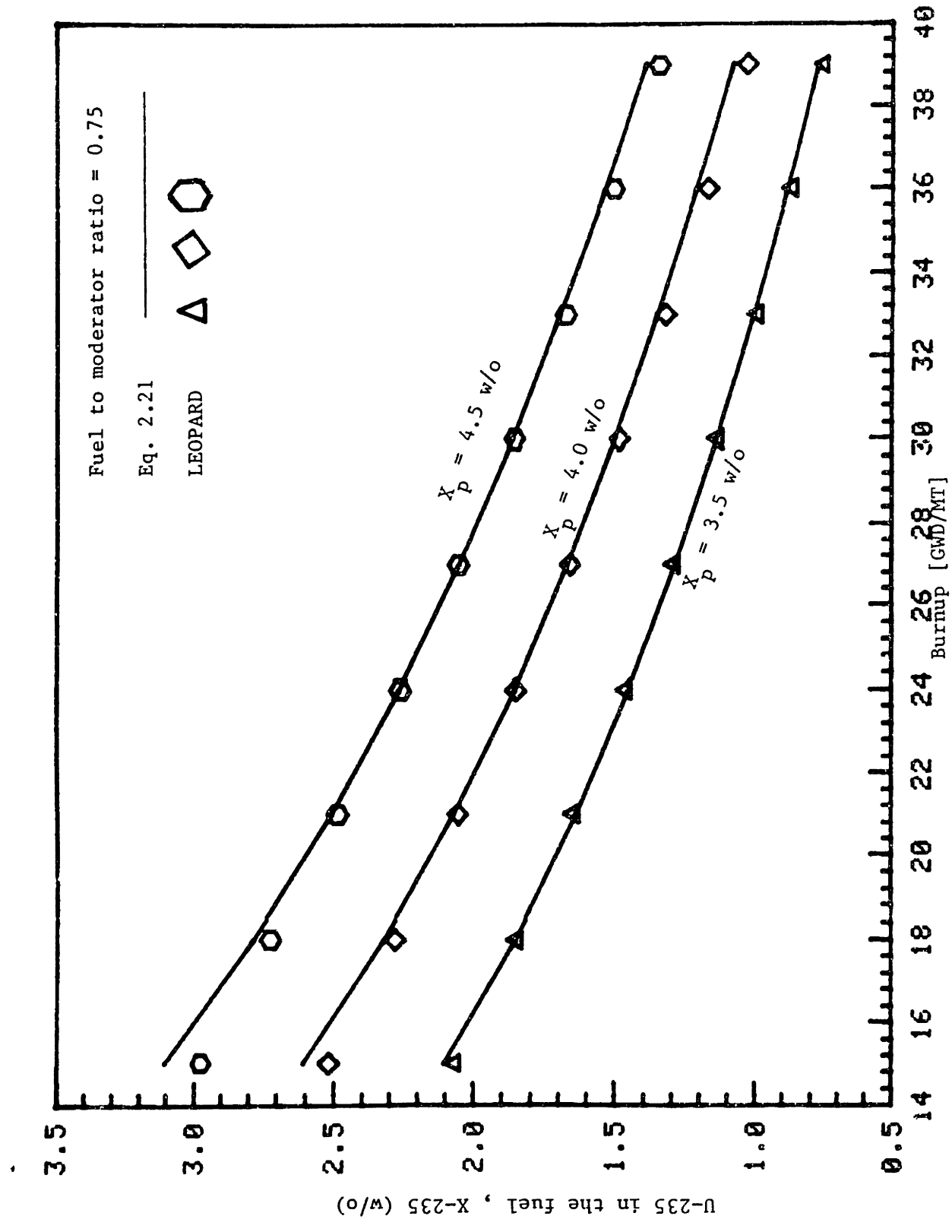


Fig.2.14 U-235 in the fuel vs burnup for various reload enrichments.

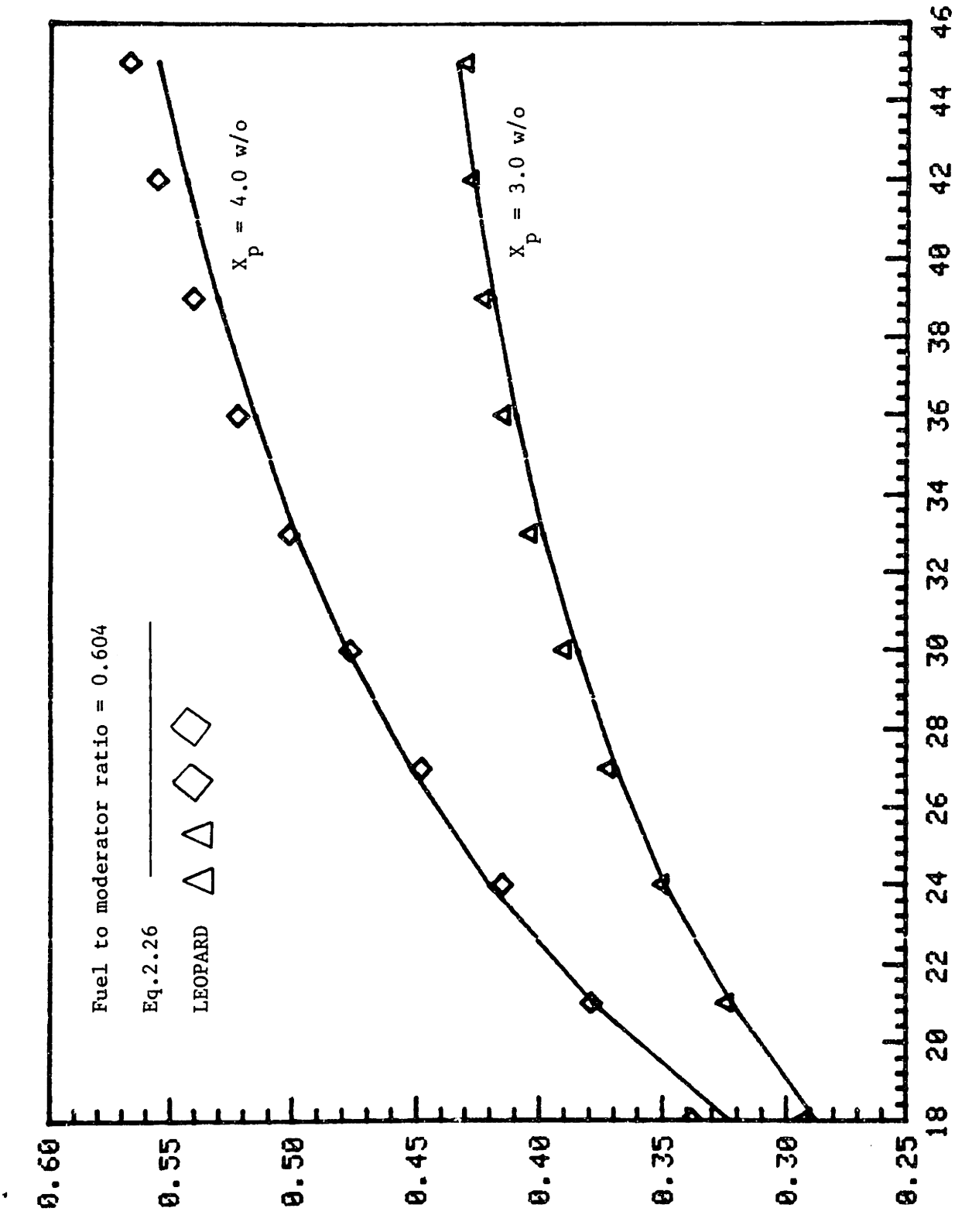


Fig. 2.15 U-236 in the fuel vs burnup for various reload enrichments.

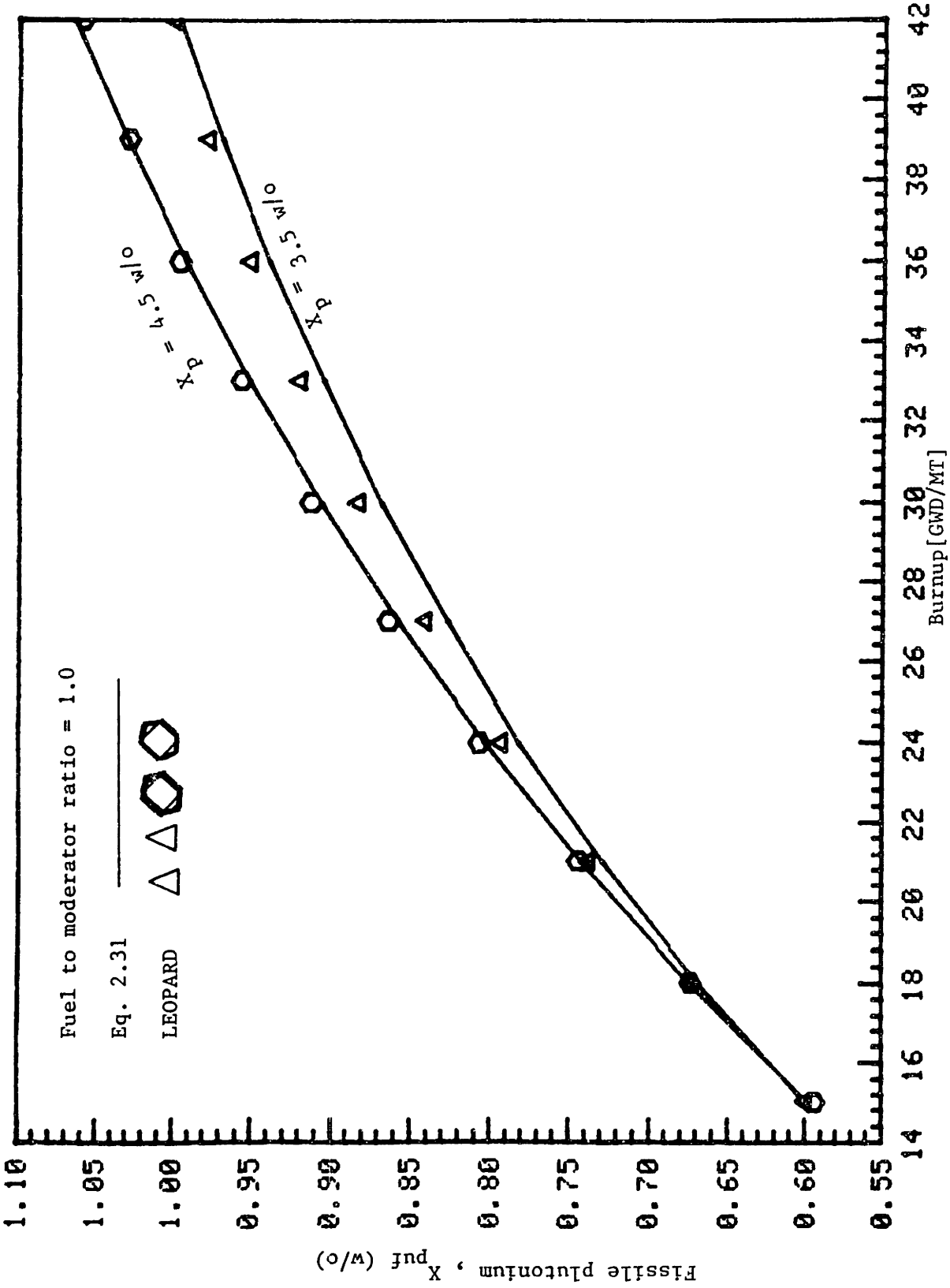


Fig. 2.16 Fissile Pu in the fuel vs burnup for various reload enrichments.

TABLE 2.13

Comparison of Curve-fit Values and LEOPARD Data for the Concentration of U-236 in the Fuel During Irradiation: $V_F/V_M = 0.604$

| Burnup GWD/MT | $X_P$ = 3.0 (w/o) X-236, w/o | | | $X_P$ = 4.0 (w/o) X-236, w/o | | |
|---|---|---|---|---|---|---|
| | Curve fit | LEOPARD | Error % | Curve fit | LEOPARD | Error % |
| 18.0 | 0.287 | 0.293 | 2.05 | 0.323 | 0.338 | 4.64 |
| 21.0 | 0.322 | 0.324 | 0.62 | 0.378 | 0.379 | 0.26 |
| 24.0 | 0.349 | 0.350 | 0.29 | 0.420 | 0.415 | 1.20 |
| 27.0 | 0.369 | 0.372 | 0.81 | 0.452 | 0.448 | 0.89 |
| 30.0 | 0.385 | 0.390 | 1.28 | 0.478 | 0.477 | 0.21 |
| 33.0 | 0.399 | 0.404 | 1.24 | 0.499 | 0.502 | 0.60 |
| 36.0 | 0.410 | 0.415 | 1.20 | 0.516 | 0.523 | 1.34 |
| 39.0 | 0.419 | 0.423 | 0.95 | 0.531 | 0.541 | 1.85 |
| 42.0 | 0.427 | 0.428 | 0.23 | 0.544 | 0.556 | 2.16 |
| 45.0 | 0.434 | 0.430 | 0.93 | 0.555 | 0.567 | 2.12 |

TABLE 2.14

Comparison of Curve-fit Values and LEOPARD Data for the Concentration of U-236 in the Fuel During Irradiation: $V_F/V_M = 0.75$

| Burnup GWD/MT | $X_P$ = 3.0 (w/o) | | | $X_P$ = 4.0 (w/o) | | |
|---|---|---|---|---|---|---|
| | Curve fit | LEOPARD | Error % | Curve fit | LEOPARD | Error % |
| 18.0 | 0.301 | 0.297 | 1.35 | 0.332 | 0.345 | 3.77 |
| 21.0 | 0.334 | 0.327 | 2.14 | 0.387 | 0.386 | 0.26 |
| 24.0 | 0.360 | 0.352 | 2.27 | 0.428 | 0.422 | 1.42 |
| 27.0 | 0.379 | 0.374 | 1.34 | 0.460 | 0.454 | 1.32 |
| 30.0 | 0.395 | 0.391 | 1.02 | 0.485 | 0.482 | 0.62 |
| 33.0 | 0.408 | 0.405 | 0.74 | 0.506 | 0.507 | 0.20 |
| 36.0 | 0.419 | 0.416 | 0.72 | 0.524 | 0.527 | 0.57 |
| 39.0 | 0.428 | 0.423 | 1.18 | 0.538 | 0.544 | 1.10 |
| 42.0 | 0.435 | 0.428 | 1.64 | 0.551 | 0.558 | 1.25 |
| 45.0 | 0.442 | 0.431 | 2.55 | 0.562 | 0.569 | 1.23 |

TABLE 2.15

Comparison of Curve-fit Values and LEOPARD Data for the Concentration of U-236 in the Fuel During Irradiation: $V_F/V_M = 1.00$

| Burnup GWD/MT | $V_F/V_M = 1.00$ | | | | | |
|---|---|---|---|---|---|---|
| | $X_P = 3.0$ (w/o) | | | $X_P = 4.0$ (w/o) | | |
| | Curve fit | LEOPARD | Error % | Curve fit | LEOPARD | Error % |
| 18.0 | 0.309 | 0.304 | 1.64 | 0.344 | 0.357 | 3.64 |
| 21.0 | 0.342 | 0.334 | 2.40 | 0.398 | 0.395 | 0.76 |
| 24.0 | 0.368 | 0.359 | 2.51 | 0.439 | 0.435 | 0.92 |
| 27.0 | 0.385 | 0.380 | 1.31 | 0.470 | 0.467 | 0.64 |
| 30.0 | 0.402 | 0.397 | 1.26 | 0.496 | 0.494 | 0.40 |
| 33.0 | 0.415 | 0.411 | 0.97 | 0.516 | 0.518 | 0.39 |
| 36.0 | 0.426 | 0.421 | 1.19 | 0.534 | 0.538 | 0.74 |
| 39.0 | 0.435 | 0.428 | 1.64 | 0.548 | 0.555 | 1.26 |
| 42.0 | 0.443 | 0.433 | 2.31 | 0.561 | 0.568 | 1.23 |
| 45.0 | 0.449 | 0.436 | 2.98 | 0.572 | 0.579 | 1.21 |

TABLE 2.16

Comparison of Curve-fit Values and LEOPARD Data for the Concentration of U-235 in the Fuel During Irradiation: $V_F/V_M = 0.604$

| Burnup (GWD/MT) | $X_P$ = 3.0 (w/o) | | | $X_P$ = 4.0 (w/o) | | |
|---|---|---|---|---|---|---|
| | $X_d$, w/o - U-235 | | | $X_d$, w/o - U-235 | | |
| | Curve fit | LEOPARD | Error % | Curve fit | LEOPARD | Error % |
| 15 | 1.593 | 1.605 | -0.75 | 2.607 | 2.493 | +4.57 |
| 18 | 1.368 | 1.399 | -2.21 | 2.308 | 2.247 | +2.71 |
| 21 | 1.178 | 1.211 | -2.72 | 2.055 | 2.017 | +1.88 |
| 24 | 1.014 | 1.042 | -2.69 | 1.835 | 1.803 | +1.77 |
| 27 | 0.869 | 0.891 | -2.47 | 1.642 | 1.603 | +2.43 |
| 30 | 0.739 | 0.756 | -2.25 | 1.469 | 1.418 | +3.60 |
| 33 | 0.622 | 0.636 | -2.20 | 1.312 | 1.246 | +5.30 |
| 36 | 0.514 | 0.531 | -3.20 | 1.169 | 1.089 | +7.35 |

TABLE 2.17

Comparison of Curve-fit Values and LEOPARD Data for the Concentration of U-235 in the Fuel During Irradiation: $V_F/V_M = 0.75$

| Burnup (GWD/MT) | $X_P$ = 3.5 (w/o) | | | $X_P$ = 4.0 (w/o) | | | $X_P$ = 4.5 (w/o) | | |
|---|---|---|---|---|---|---|---|---|---|
| | $X_d$ - 235 (w/o) | | | $X_d$ - 235 (w/o) | | | $X_d$ - 235 (w/o) | | |
| | Curve fit | LEOPARD | Error % | Curve fit | LEOPARD | Error % | Curve fit | LEOPARD | Error % |
| 15 | 2.104 | 2.067 | 1.79 | 2.606 | 2.515 | 3.62 | 3.108 | 2.975 | 4.47 |
| 18 | 1.850 | 1.847 | 0.16 | 2.316 | 2.278 | 1.67 | 2.781 | 2.723 | 2.13 |
| 21 | 1.635 | 1.644 | 0.55 | 2.070 | 2.056 | 0.68 | 2.505 | 2.485 | 0.80 |
| 24 | 1.449 | 1.458 | 0.62 | 1.857 | 1.850 | 0.38 | 2.265 | 2.262 | 0.13 |
| 27 | 1.285 | 1.289 | 0.31 | 1.669 | 1.659 | 0.60 | 2.054 | 2.053 | 0.05 |
| 30 | 1.138 | 1.134 | 0.35 | 1.501 | 1.482 | 1.28 | 1.865 | 1.857 | 0.43 |
| 33 | 1.005 | 0.993 | 1.21 | 1.350 | 1.319 | 2.35 | 1.694 | 1.674 | 1.19 |
| 36 | 0.883 | 0.867 | 1.85 | 1.211 | 1.169 | 3.59 | 1.538 | 1.503 | 2.33 |
| 39 | 0.772 | 0.753 | 2.52 | 1.083 | 1.032 | 4.94 | 1.395 | 1.345 | 3.72 |

TABLE 2.18

Comparison of Curve-fit Values and LEOPARD Data for the Concentration of U-235 in the Fuel During Irradiation: $V_F/V_M = 1.0$

| Burnup (GWD/MT) | $X_P$ = 3.5 (w/o) | | | $X_P$ = 4.0 (w/o) | | | $X_P$ = 4.5 (w/o) | | |
|---|---|---|---|---|---|---|---|---|---|
| | $X_d$ - 235 (w/o) | | | $X_d$ - 235 (w/o) | | | $X_d$ - 235 (w/o) | | |
| | Curve fit | LEOPARD | Error % | Curve fit | LEOPARD | Error % | Curve fit | LEOPARD | Error % |
| 15 | 2.111 | 2.099 | 0.57 | 2.604 | 2.544 | 2.36 | 3.097 | 3.000 | 3.23 |
| 18 | 1.870 | 1.888 | 0.95 | 2.329 | 2.315 | 0.60 | 2.787 | 2.756 | 1.12 |
| 21 | 1.666 | 1.696 | 1.77 | 2.096 | 2.104 | 0.38 | 2.525 | 2.528 | 0.12 |
| 24 | 1.490 | 1.521 | 2.04 | 1.894 | 1.908 | 0.73 | 2.299 | 2.315 | 0.69 |
| 27 | 1.334 | 1.361 | 1.98 | 1.716 | 1.727 | 0.64 | 2.098 | 2.116 | 0.85 |
| 30 | 1.195 | 1.215 | 1.65 | 1.557 | 1.560 | 0.19 | 1.919 | 1.930 | 0.57 |
| 33 | 1.069 | 1.083 | 1.29 | 1.413 | 1.406 | 0.50 | 1.758 | 1.757 | 0.06 |
| 36 | 0.954 | 0.963 | 0.93 | 1.282 | 1.265 | 1.34 | 1.610 | 1.597 | 0.81 |
| 39 | 0.849 | 0.855 | 0.70 | 1.161 | 1.136 | 2.20 | 1.474 | 1.448 | 1.76 |
| 42 | 0.751 | 0.757 | 0.79 | 1.049 | 1.018 | 3.04 | 1.348 | 1.310 | 2.90 |

TABLE 2.19

Comparison of Curve-fit Values and LEOPARD Data for Fissile Plutonium in the Fuel During Irradiation: $V_F/V_M = 0.604$

| Burnup (GWD/MT) | $X_P$ = 3.0 (w/o) | | | $X_P$ = 4.0 (w/o) | | |
|---|---|---|---|---|---|---|
| | Fissile Pu (Pu-239+Pu-241) | | | Fissile Pu (Pu-239+Pu-241) | | |
| | Curve fit | LEOPARD | Error % | Curve fit | LEOPARD | Error % |
| 15 | 0.440 | 0.445 | -1.12 | 0.440 | 0.444 | -0.90 |
| 18 | 0.483 | 0.487 | -0.82 | 0.491 | 0.493 | -0.40 |
| 21 | 0.520 | 0.521 | -0.19 | 0.534 | 0.534 | 0.00 |
| 24 | 0.551 | 0.547 | +0.73 | 0.572 | 0.568 | 0.70 |
| 27 | 0.578 | 0.566 | +2.12 | 0.606 | 0.595 | 1.85 |
| 30 | 0.601 | 0.581 | +3.44 | 0.636 | 0.617 | 3.08 |
| 33 | 0.622 | 0.590 | +5.42 | 0.662 | 0.633 | 4.58 |

TABLE 2.20

Comparison of Curve-fit Values and LEOPARD Data for Fissile Plutonium in the Fuel During Irradiation: $V_F/V_M = 0.75$

| Burnup (GWD/MT) | $X_P$ = 3.5 (w/o) | | | $X_P$ = 4.0 (w/o) | | | $X_P$ = 4.5 (w/o) | | |
|---|---|---|---|---|---|---|---|---|---|
| | Fissile Pu (239+241) | | | Fissile Pu (239+241) | | | Fissile Pu (239+241) | | |
| | Curve fit | LEOPARD | Error % | Curve fit | LEOPARD | Error % | Curve fit | LEOPARD | Error % |
| 15 | 0.495 | 0.505 | 1.98 | 0.496 | 0.504 | 1.59 | 0.496 | 0.502 | 1.19 |
| 18 | 0.548 | 0.561 | 2.32 | 0.553 | 0.564 | 1.95 | 0.557 | 0.564 | 1.24 |
| 21 | 0.593 | 0.608 | 2.47 | 0.602 | 0.614 | 1.95 | 0.611 | 0.618 | 1.13 |
| 24 | 0.633 | 0.648 | 2.31 | 0.645 | 0.658 | 1.98 | 0.658 | 0.665 | 1.05 |
| 27 | 0.668 | 0.680 | 1.76 | 0.684 | 0.694 | 1.44 | 0.701 | 0.705 | 0.57 |
| 30 | 0.698 | 0.706 | 1.13 | 0.718 | 0.724 | 0.83 | 0.739 | 0.739 | 0.00 |
| 33 | 0.725 | 0.727 | 0.28 | 0.748 | 0.749 | 0.13 | 0.773 | 0.767 | 0.78 |
| 36 | 0.749 | 0.743 | 0.80 | 0.776 | 0.768 | 1.04 | 0.804 | 0.790 | 1.77 |
| 39 | 0.771 | 0.755 | 2.07 | 0.801 | 0.783 | 2.30 | 0.832 | 0.809 | 2.84 |

TABLE 2.21

Comparison of Curve-fit Values and LEOPARD Data for Fissile Plutonium in the Fuel During Irradiation: $V_F/V_M = 1.00$

| Burnup (GWD/MT) | $X_P$ = 3.5 (w/o) | | | $X_P$ = 4.0 (w/o) | | | $X_P$ = 4.5 (w/o) | | |
|---|---|---|---|---|---|---|---|---|---|
| | Fissile Pu (239+241) | | | Fissile Pu (239+241) | | | Fissile Pu (239+241) | | |
| | Curve fit | LEOPARD | Error % | Curve fit | LEOPARD | Error % | Curve fit | LEOPARD | Error % |
| 15 | 0.600 | 0.599 | 0.17 | 0.599 | 0.597 | 0.33 | 0.598 | 0.594 | 0.67 |
| 18 | 0.669 | 0.673 | 0.59 | 0.672 | 0.674 | 0.30 | 0.674 | 0.673 | 0.15 |
| 21 | 0.729 | 0.737 | 1.09 | 0.735 | 0.741 | 0.81 | 0.742 | 0.744 | 0.27 |
| 24 | 0.781 | 0.793 | 1.51 | 0.792 | 0.801 | 1.12 | 0.803 | 0.807 | 0.50 |
| 27 | 0.827 | 0.841 | 1.66 | 0.842 | 0.854 | 1.41 | 0.858 | 0.864 | 0.69 |
| 30 | 0.869 | 0.883 | 1.59 | 0.887 | 0.900 | 1.44 | 0.907 | 0.913 | 0.66 |
| 33 | 0.905 | 0.920 | 1.63 | 0.928 | 0.940 | 1.28 | 0.952 | 0.957 | 0.52 |
| 36 | 0.939 | 0.951 | 1.26 | 0.965 | 0.975 | 1.03 | 0.992 | 0.996 | 0.40 |
| 39 | 0.969 | 0.978 | 0.92 | 0.998 | 1.000 | 0.20 | 1.030 | 1.029 | 0.10 |
| 42 | 0.996 | 1.000 | 0.40 | 1.029 | 1.031 | 0.19 | 1.064 | 1.059 | 0.47 |

here because of the subjective judgement that it would be desirable to blend with uranium from spent fuel to reduce the amount of this material subjected to re-enrichment, because of its high U-236 content.

The spent fuel required per reload batch of $M_b$ Kg heavy metal is $M_b \cdot G$, where

$$G = \frac{\text{U-235 consumed + U-236 penalty}}{\text{Fissile Pu (Pu-239 + Pu-241) produced}} \times g \quad (2.32)$$

and g is the "burnup worth" of fissile Pu relative to U-235. This worth is not merely the radio of reactivity per unit mass attributable to the two materials in question, rather it is determined by comparing $\rho(B)$ behavior over the complete life cycle, and matching attainable reactivity-limited discharge burnup, as will be explained in the next chapter.

Fissile plutonium from $G \cdot M_b$ Kg of spent fuel is blended with uranium recovered from $M_b$ Kg of spent fuel and the remaining uranium recovered from $M_b$ (G-1) Kg of spent fuel is credited for the ore and SWU savings which its reuse permits (see Fig. 2.17). Note that in the blending step, it is assumed that the U-238 destruction in $M_b$ Kg of spent fuel and losses in the conversion process are compensated by addition of Pu from $M_b \cdot G$ Kg of spent fuel. In crediting the rest of the uranium, from $M_b$ (G-1) Kg of spent fuel, the mass decrement due to U-238 destruction and fission product removal has been ignored. During irradiation of the fuel, the U-236 isotope is

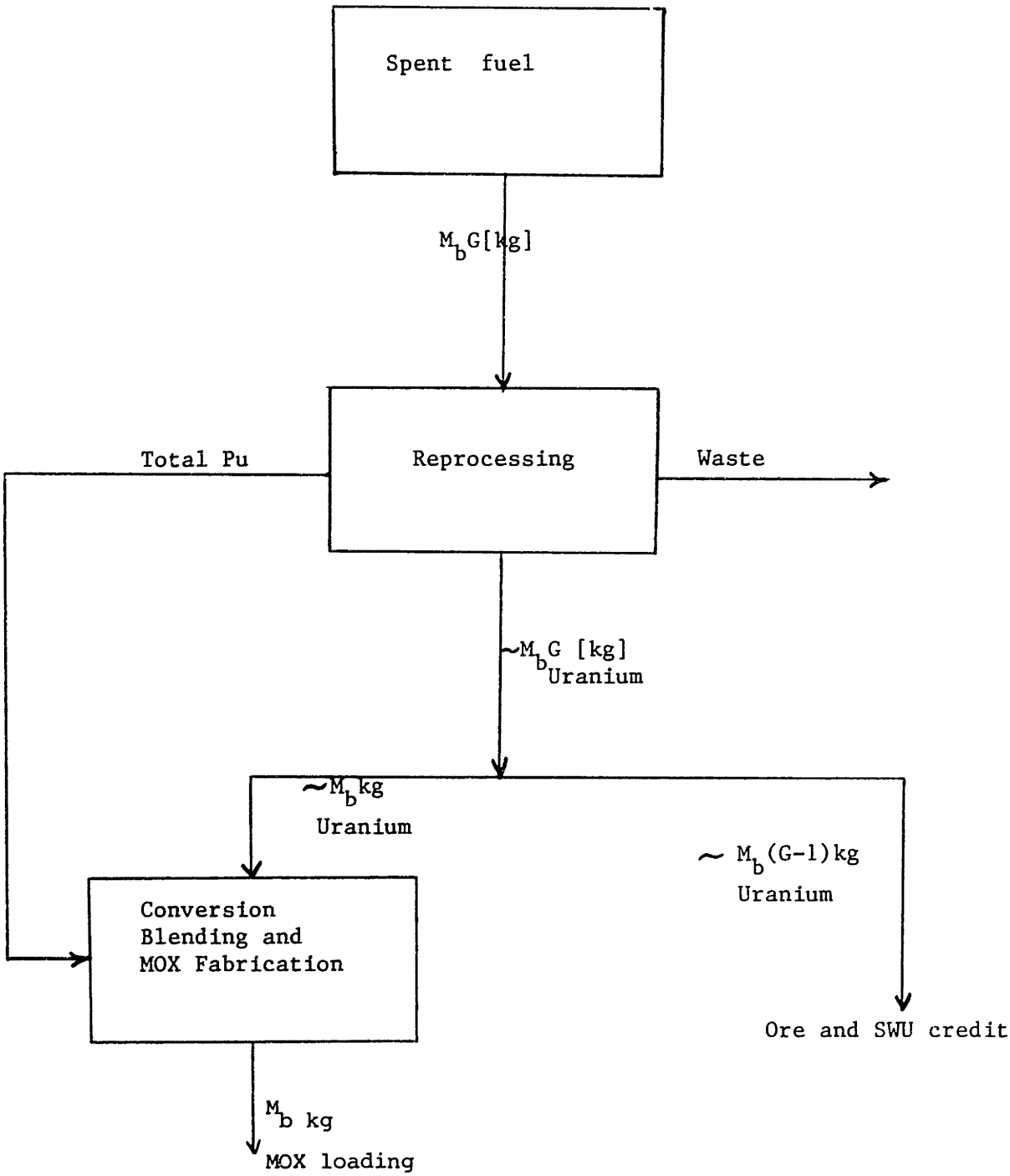


Fig. 2.17 Schematic showing interrelation of blending and credit steps.

created, which has a large capture cross-section leading to non-fissile nuclide production, and hence behaves as a poison. The presence of U-236 in fuel requires extra separative work; also, the concentration of U-235 must be greater to compensate for the negative reactivity due to the presence of residual U-236. The distribution of U-236 between the diffusion plant product and tails streams in terms of the specified fraction of U-236 in feed has been determined by De La Garza [D2]. A simple correlation to serve this purpose has been developed in the present work (see the next chapter).

Let $X_P'$ be the U-235 (w/o) required in the presence of U-236, then

$$X_P' = X_P + \Delta X_P \tag{2.33}$$

In Eq. (2.33) $\Delta X_P$ is the increase in U-235 enrichment required to offset the presence of $Y_P$ weight percent of U-236 in the product. It should be noted that $Y_P$ itself is dependent on $X_P'$. Thus an iteration is used. First $Y_F$, the wt.% of U-236 in the feed is used as $Y_P$ to estimate the penalty needed to find $X_P'$. Then for that $X_P'$, a new $Y_P$ is calculated, and this $Y_P$ is used to re-estimate the penalty, and so on until the iteration converges. The credit terms are then determined by enriching the uranium from the spent fuel to the enrichment of U-235 required for a certain burnup and comparing this case with the enriching of natural uranium to the enrichment $X_P$ ($= X_P' - \Delta X_P$) which gives the same burnup.

The separative work required per unit mass of product when three isotopes are present is calculated as

$$\frac{SW3}{P} = V\left(X_P', Y_P\right) + \left(\frac{X_P'-X_d-235}{X_d-235-X_w}\right) V\left(X_w, Y_w\right) - \frac{(X_P'-X_w)}{(X_d-235-X_w)} \quad V\ (X_d-235, Y_F) \tag{2.34}$$

where

$$V\ (x,y) = (2x-4y-1)\ \ln \frac{x}{1-x-y} \tag{2.35}$$

$X_P'$ ≡ U-235(w/o) in the product

$X_d$-235 ≡ U-235 (w/o) in the spent fuel, which is "feed" for this case

$X_w$ = U-235 (w/o) in the tails of the enrichment plant (can be specified or optimized, see Chapter 3)

$Y_F$ = U-236 (w/o) in the spent fuel

$Y_P$ = U-236 (w/o) in the product

$Y_w$ ≡ U-236 (w/o) in the tails of the enrichment plant.

Mass of product from $M_b$ (G-1) Kg uranium as feed from spent fuel is

$$M_P = M_b\ (G-1)\ \frac{(X_d-235 - X_w)}{(X_P' - X_w)} \tag{2.36}$$

Accordingly the credit for SWU is

$$M_{SWU}\Big)_{credit} = M_P \left[S/P - \frac{SW3}{P}\right] \text{Kg SWU} \tag{2.37}$$

In Eq. (2.37) S/P is the separative work required per unit of product to enrich natural uranium to enrichment $X_P$ (without a U-236 penalty) as calculated for a two isotope (U-235, U-238)

separation plant using Eq. (2.6). The corresponding credits for $UF_6$ conversion and ore are

$$M_{UF_6}\Big)_{credit} = M_P \frac{(X_P - X_W)}{(X_F - X_W)} - M_b \ (G-1), \text{Kg of U} \tag{2.38}$$

$$M_{ore}\Big)_{credit} = \frac{1.179}{F1} M_P \frac{(X_P - X_W)}{(X_F - X_W)}, \text{Kg of } U_3O_8 \tag{2.39}$$

Only one pass recycle is considered, which means that the discharged fuel from recycle mode operation is disposed of:

$$M_{dis} = M_b \tag{2.40}$$

## 2.7 Nuclear Fuel Cycle Economics

The economic analysis of the nuclear fuel cycle is not as simple and straightforward as that of fossil fueled electric generation. Uranium ore is subjected to a complex sequence of processing steps before it can be used as fuel in reactors. The cost computations are further complicated by the fact that the finished product is capitalized and depreciated, analogous to an item of machinery, rather than being expensed as a consumable (as are fossil fuels). In addition, nuclear fuel has a relatively long life history before, during and after irradiation, which means that it is particularly important to see that all transactions are discounted by an appropriate discount rate which reflects the time value of money. The economic model applied in the

present work will be described in the following subsections. Prior work by Abbaspour [A2] and Zimmermann [Z1] should be referred to for details.

### 2.7.1 Assumptions

The assumptions of the model are as follows:

1) All batches of fuel are considered equilibrium batches, having equal in-core residence time and equal charge and discharge enrichment (i.e., neglecting startup and shutdown batches)
2) The revenue and depreciation charges for each batch are represented by single payments at the middle of the irradiation interval
3) Depreciation is a linear function of time (~ burnup).
4) In-core fuel cycle operation and maintenance costs are negligible
5) The revenues received from the sale of energy generated by a batch of fuel exactly compensate for all the costs and credits associated with all steps of the fuel cycle, as well as the appropriate carrying charges for these steps.

### 2.7.2 Direct and Carrying Charges

With the above assumptions, a present worth balance can

be executed [D3],

$$\Sigma_i \, M_i \, C_i \, (P/F,x,t_i) = [R(1-\tau) + \tau D] \, (P/F,x,T/2) \tag{2.41}$$

where

$M_i$ = Transaction quantity involved in the ith step.

$C_i$ = Unit price of the ith step.

$t_i$ = Lead or lag time for step i.

$(P/F,x,t) = (1-x)^{-t}$ , the present worth factor.

$\tau$ = Equivalent tax fraction.

T = Irradiation time.

x = Discount rate (see discussion at the end of section).

R = Revenues = Electricity generated times the fuel cycle cost/kwhr (i.e., E $e_f$).

D = Depreciation, in the present instance (lump sum depreciation at the midpoint of the cycle) equal to $\Sigma_i \, M_i \, C_i$ .

Equation (2.25) can be re-arranged to give:

$$e_f = \frac{1}{E} \, \Sigma_i \, M_i \, C_i \left[ \left( \frac{1}{1-\tau} \right) \frac{(P/F,x,t_i)}{(P/F,x,T/2)} - \left( \frac{\tau}{1-\tau} \right) \right] \tag{2.42}$$

$$\text{Defining } F_i = \left( \frac{1}{1-\tau} \right) \frac{(P/F,x,t_i)}{(P/F,x,T/2)} - \left( \frac{\tau}{1-\tau} \right) \tag{2.43}$$

Equation (2.42) becomes

$$e_f = \frac{1}{E} \, \Sigma_i \, M_i \, C_i \, F_i \tag{2.44}$$

Equation (2.43) can be manipulated as follows:

$$F_i = \frac{1}{1-\tau} \left[ (1 + x)^{(T/2 - t_i)} - 1 \right] + 1 \tag{2.45}$$

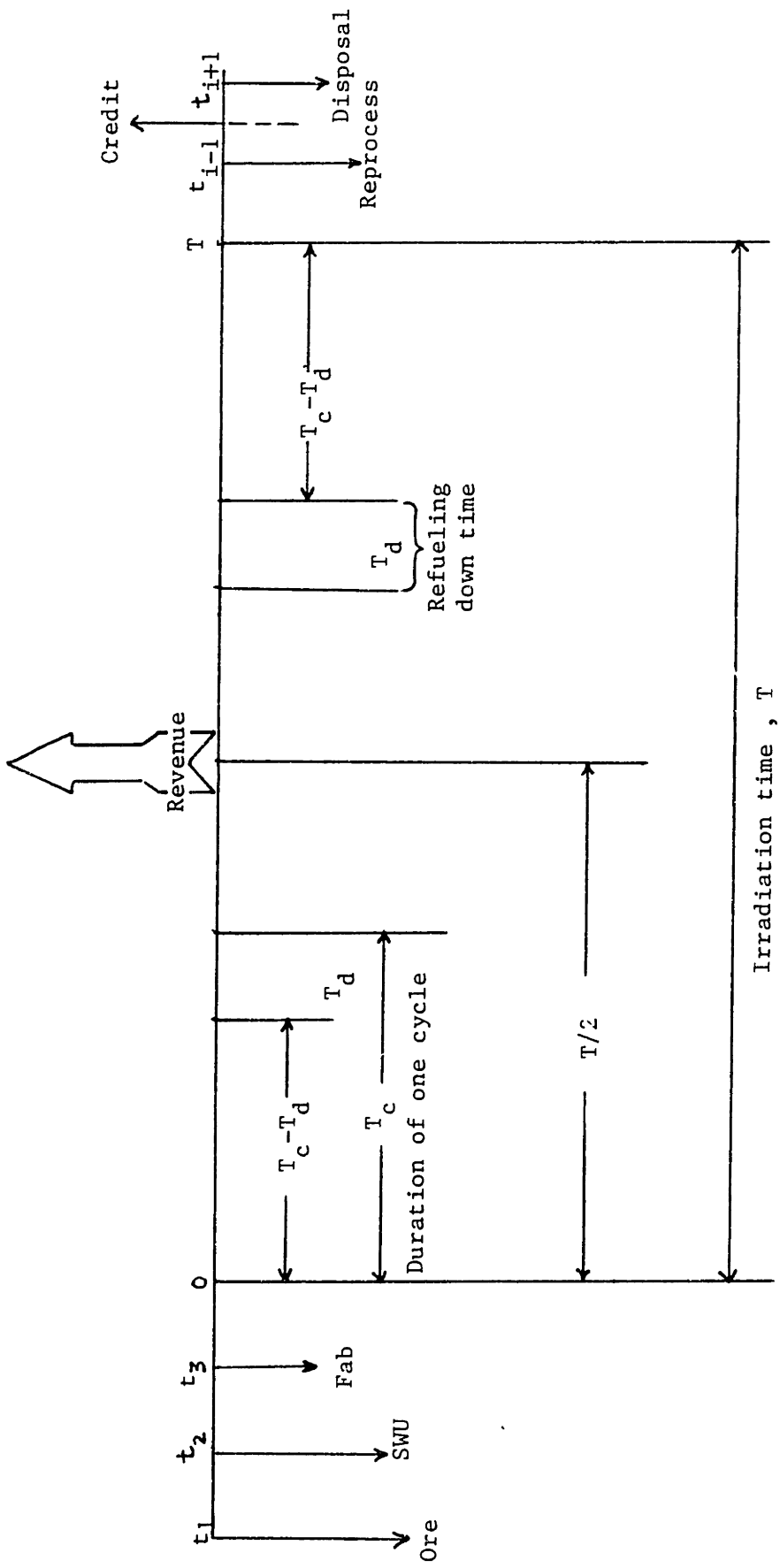


Fig.2.18 Cash flow diagrame for a batch of nuclear fuel.

which can be written in the form:

$$F_i = 1 + \phi \, \Delta T_i^* \tag{2.46}$$

where

$$\phi = \frac{x}{1-\tau} \tag{2.47}$$

and

$$\Delta T_i^* = \left[ \frac{(1 + x)^{(T/2 - t_i)} - 1}{x} \right] \tag{2.48}$$

using Equation (2.46) in Equation (2.44)

$$e_f = \frac{1}{E} \Sigma \, M_i \, C_i + \frac{1}{E} \Sigma_i \, M_i \, C_i \, \phi \, \Delta T_i^* \tag{2.49}$$

In Equation (2.49) the first term on the righthand side is the sum of the direct costs and the second term is the sum of the carrying charges, where $\phi$ is the carrying charge factor. To first order

$$\Delta T_i^* \approx (T/2 - t_i) = \Delta T \quad , \tag{2.50}$$

a simple expression often applied in back-of-the-envelope hand calculations.

It is important to note that the discount rate X in the above prescriptions is defined as [S2], [D4]

$$X = (1 - \tau) \, f_b \, r_b + f_s \, r_s \tag{2.51}$$

where

$f_b$ = Debt fraction

$f_s$ = Equity fraction = $1 - f_b$

$r_b$ = Rate of return to bond holders

$r_s$ = Rate of return to stock holders.

### 2.7.3 Spent Fuel Credit Scheme

In the recycle mode the reprocessor is credited with the avoided cost of indefinite storage for spent fuel received. He then credits his operation with this fee, and pays reprocessing, waste disposal and MOX fabrication costs (less a small credit for recovered uranium). Note that by this approach the issue of assigning an explicit value to Pu has been avoided. Actually it has been implicitly included in this methodology. Pu is recycled and the uranium is credited both for ore and SWU, as shown in Fig. (2.17).

### 2.7.4 Constant Dollar Analysis

In the present work market discount rates are employed and all transaction quantities are expressed in current dollars. This convention was adopted so that computed fuel cycle costs are of a familiar magnitude to contemporary readers. Future costs will actually be incurred in inflated dollars. As long as we deal only with successive "snapshot" values of individual fuel batch costs, and not their levelized value over the life of a reactor, the above convention does not lead to any inconsistencies. When fuel cycle and plant capital-related costs are combined to compute the system cost of energy, all costs should be lifetime levelized; and if fuel cycle costs are not escalated (inflated), then the carrying charge factor, $\phi$, should be deflated (D3, S3). Note, however, that in the system

cost equation the capital-related term appears as a constant- and therefore does not affect the location of the optimum: thus the magnitude of $\phi$ is actually immaterial.

The use of constant dollar costs for future transactions does not imply that they will be constant in magnitude in later years. Ore will escalate in constant dollar cost as resource grade declines, and other parameters, such as enrichment costs, will decrease in constant dollar cost due to improvements in technology.

### 2.7.5 Busbar and System Costs

The busbar cost of electrical energy is obtained by summing the contributions from the three main categories: capital, operation and maintenance, and fuel, which can be written as [D3]

$$e_b = \frac{1000}{8766L} \left[ \phi(I/K) + \left(\frac{O}{K}\right) \right] + e_f \qquad (2.52)$$

where

$e_b$ = Busbar cost of electricity, mills/kwhr

$L = L'(1 - T_d/T_c)$; capacity factor: total energy generated during intra-refueling interval, $T_c$, divided by the maximum energy which could have been generated during $T_c$.

$T_d$ = Refueling downtime

$L'$ = Availability-based capacity factor: the ratio

of total energy generated during time $T_c$ to the maximum energy available during normal operation.

$\phi$ = Inflation free annual fixed charge rate, $Yr^{-1}$

(I/K) = Capital cost of unit, \$/kw.

(O/K) = Lifetime levelized, constant-dollar annual operating cost, \$/kw-yr.

= Initial year value if no escalation, but only monetary inflation, is incurred.

$e_f$ = Constant-dollar fuel cycle cost, mills/kwhr.

In Equation (2.52) the capital cost and operating costs do not change with different fuel management schemes. Thus we can write,

$$e_b = \frac{A}{L} + e_f \tag{2.53}$$

where

$$A = \frac{1000}{8766} \left[\phi \left(\frac{I}{K}\right) + \left(\frac{O}{K}\right)\right] \tag{2.54}$$

and A is constant for an installed plant regardless of whether the plant is generating electricity or not. While the reactor is shut down, it may be necessary for the utility to satisfy the demand of its customers with electricity purchased or generated at a higher cost. Thus the total cost is not merely the busbar cost: the effect of the replacement energy cost must also be considered, which is included in the overall system cost $e_s$ according to the relation:

$$e_s = L\, e_b + (1-L)\, e_r \qquad (2.55)$$

where $e_r$ is the replacement energy cost, mills/kwhr (expressed in constant dollars).

## 2.8 Ore Resource Model

Nuclear power policies in the future are dependent on the price and availability of natural uranium. The cost of uranium is set by the relation between supply and demand, which is affected by the rate of the growth of the nuclear power economy and the nature and pace of changes in nuclear technology. The growth of the nuclear electric sector is itself weakly dependent on uranium prices, but the decisions to build reactors are influenced more by

- factors affecting capital costs
- regulatory conditions
- public acceptance
- the desire of utilities to maintain a mix of generation sources.

Forecasting nuclear power growth has been very uncertain and there have been drastic revisions in the projections during the last decade due to

- the worldwide economic recession
- high financing and inflation rates
- the concurrent reduction in energy demand and regulatory uncertainties.

The projections for the years 1990 and 2000 published in the IAEA 1980-83 annual reports were one-third to one-fifth of those published in its 1973-1974 annual reports. The sharp decline in the expected growth rate of nuclear capacity, together with the more promising outlook for the availability of reasonably-priced uranium resources means that uranium conservation need no longer be the overriding objective of reactor designers during the next few decades [N1]. The fuel supply outlook is further enhanced by the shift towards higher burnup fuel and the favorable prospects for advanced enrichment technologies. The current depressed uranium price is a consequence of the reduced demand projections and a large supply capability resulting from the high price level for uranium in the late 1970's.

Despite this substantial contemporary imbalance between supply and demand, and the unstable spot market which has resulted, it is necessary to look ahead at the long-term availability and long-term average price of uranium. Thus, estimation of a scarcity-related cost escalation rate for future uranium prices as a function of key variables is included in the resource-cost model described in this section, which can be directly used in fuel cycle economic analysis [G3].

The rate at which ore is being mined is $\frac{1}{x}\ \frac{d\ U(t)}{dt}$, where $x$ is the grade of the ore (i.e., wt. of $U_3O_8$ per wt. of raw ore) and $\frac{d\ U(t)}{dt}$ is the system $U_3O_8$ use rate, mass per year. The product of the unit cost of $U_3O_8$, $C$, and the grade, $x$, is the unit cost of handling raw ore; applying the scale factor method for estimating the variation of production costs with the size of the operation one obtains:

$$Cx = A \left[\frac{1}{x}\ \frac{d\ U(t)}{dt}\right]^{-\gamma} \tag{2.56}$$

In other words, the unit cost of raw ore as a function of raw ore throughput has a log-log-plot slope of $-\gamma$. The resource grade, $x$, and $U$, the cumulative amount of $U_3O_8$ content $\geq x$, is assumed to obey the following equation, based upon geostatistical considerations, as discussed by Gharamani [G3] and Drew [D5],

$$x = B\ U^{-\mu} \tag{2.57}$$

If one assumes the average long-term system growth rate is exponential, then the system capacity $E(t)$ is given by

$$E(t) = E(0)\ e^{rt} \tag{2.58}$$

where r is the growth rate of installed nuclear capacity and $E(0)$ is the installed capacity of reactors at time zero. Since the forecasts of capacity growth rates are highly uncertain, an estimated profile of year-by-year installed capacity (or variable growth rates) as a succession of uniform growth rate intervals can be employed. From the profile supplied, r can

be defined as

$$r = \ln\left(\frac{E_2}{E_1}\right) \tag{2.59}$$

where $E_1$ is the beginning of year, and $E_2$ ($> E_1$) is the end of year, installed capacity. Cumulative $U_3O_8$ consumption is given by (since use is proportional to installed capacity, Eq. (2.38)):

$$U(t) = U_{(o)} \; e^{rt} \tag{2.60}$$

Equations (2.56), (2.57) and (2.60) combine to give an expression for constant-dollar ore costs as a function of time

$$C(t) = C_{(o)} \; e^{yt} \quad \$/kg \; U_3O_8 \tag{2.61}$$

where

$$y = r \; [\mu - \gamma(\mu + 1)] \tag{2.62}$$

is the scarcity-related escalation rate.

In the above model, appropriate numerical values for the correlations employed were determined by Gharamani to be:

$$\gamma = \frac{1}{6} \quad , \quad \mu = 1.0 \quad ,$$

hence $y = \frac{2}{3} r$ .

## 2.9 Chapter Summary

In this chapter, simple models for the evaluation of various fuel management strategies were developed. These models include prescriptions for estimating the material flow through the LWR nuclear fuel cycle, correlations for discharged fuel

composition, algorithms for nuclear fuel cycle economic computations and an ore resource/cost relationship, all of which have been explained in sufficient detail for present purposes (together with references to in-depth treatments of each topic).

The approximate formulas for U-235, U-236 and fissile plutonium mass as a function of reload enrichment ($X_p$), fuel-to-moderator ratio $\left(\frac{V_F}{V_M}\right)$ and the number of staggered-reload batches, which were required as input for recycle mass flow calculations, were formulated by fitting semi-empirical relations to the output of LEOPARD computer code-calculations. The details of the procedures employed to develop these correlations are described in Appendix A. The curve fit expressions were compared to LEOPARD data in Figs. (2.3) through (2.8) and the results were documented in tables (2.1) through (2.6). The prescriptions for the discharge composition were found to be within an average error of less than 1% of LEOPARD results. A similar procedure was followed to correlate the composition of fuel as a function of any intermediate burnup state.

In the recycle mode mass flow model, plutonium from the spent fuel was used to make up for the consumed U-235 in part of the discharged fuel, and the remaining uranium was credited both for ore and SWU savings. In the calculations of SWU

credit for the reprocessed fuel, the presence of U-236 in the isotope separation plant was taken into account and the corresponding SWU penalty was included; the burnup penalty of U-236 in the resulting enriched uranium was also quantified. The issue of assigning an explicit value to plutonium was avoided by basing spent fuel value on the avoided cost of disposal.

The present worth method was applied for the calculation of fuel cost. Various cash flows were described in terms of direct plus carrying charges. The analysis was carried out using the market discount rate and transaction costs in today's (1984) dollars.

The estimation of a scarcity-related cost escalation rate for future uranium prices as a function of key variables was included in the resource-cost model.

Finally the busbar and the system cost relationships were also included in the model to permit analysis of the effect of the plant capacity factor and the cost of replacement energy during refueling downtime.

# CHAPTER 3

# CORRELATIONS FOR KEY PARAMETERS

## 3.1 Introduction

Simple correlations capable of predicting the functional dependence of key parameters on the important variables are developed in this chapter. These prescriptions permit the estimation of burnup for uranium and plutonium cores, optimum enrichment plant tails, isotope separation for three component mixtures and separative work requirements. The detailed procedures are explained in the following sections.

## 3.2 Reactivity Versus Burnup for Uranium Fueled Cores

The term "reactivity" of a particular reactor core region is defined, in the present work, in terms of its infinite medium multiplication factor ($k_\infty$ ):

$$\rho = 1 - \frac{1}{k_\infty} \tag{3.1}$$

Since the reactivity, $\rho$ , is a linear function of the burnup for reload enrichment higher than 1.5 w/o [S4], it can

be expressed as a function of burnup for a particular assembly as:

$$\rho = \rho_o - A\,B \tag{3.2}$$

where

$\rho$ = unpoisoned reactivity of a PWR assembly

$\rho_o$ = extrapolated beginning of life (BOL) reactivity

A = slope of the reactivity versus burnup curve, $[MWD/MT]^{-1}$

B = fuel burnup, [MWD/MT]

The discharge burnup of a fuel batch can be obtained by performing a reactivity balance for an n-batch steady-state core [D6],

$$Bd = \left(\frac{2n}{n+1}\right)\left(\frac{\rho_o - \rho_L}{A}\right) \tag{3.3}$$

where $\rho_L$ is the leakage reactivity.

In the present work, the values of $\rho_o$ and A are obtained from a least squares linear regression fit of reactivity, $\rho$, as a function of burnup, B, obtained using the LEOPARD code. The results are presented in Appendix A, table A-1 for various reload enrichments and fuel-to-moderator ratios. The different values of $\frac{V_F}{V_M}$ were obtained by keeping fuel pellet diameter constant and varying the pitch. The reload enrichment of fuel was varied from 2.5 w/o to 4.5 w/o U-235 in increments of 0.5 w/o. The reactivity has been computed for an infinite

medium, and the effect of leakage has been accounted for separately by subtracting an assumed value for $\rho_L$ (= 0.05 $\rho_o$).

The functional dependence of $\frac{\rho_o}{A}$ on $\frac{V_F}{V_M}$ and $X_P$ is obtained, again, by using a statistical program for simple regressions to curve fit the data presented in table (A-1). The procedure followed for correlating these parameters is similar to the one employed by Montaldo-Volachec [M2], but our expression for $\frac{\rho_o}{A}$ is much simpler than his (which was a third order polynomial in $\frac{V_F}{V_M}$):

$$\frac{\rho_o}{A} = 1.3 + \left(12.338 - 4.674 \frac{V_F}{V_M}\right) X_P - 3.5 \Big/ \left(\frac{V_F}{V_M}\right), \frac{GWD}{MT} \tag{3.4}$$

The values of $\frac{\rho_o}{A}$ obtained using Eq. (3.4) are compared to LEOPARD data in Fig. (3.1). Table (3.1) shows the results and the errors that can be expected. Note that the above correlation reproduces $\frac{\rho_o}{A}$, hence discharge burnup values, within a maximum error of 2.5% .

## 3.3 Reactivity Versus Burnup for Plutonium Cores

It has been found [L3] that the linear reactivity model is also applicable to plutonium-fueled cores. The values of extrapolated BOL reactivity, $\rho_o$, the slope of the $\rho$(B) curve fit, A, and the ratio, $\frac{\rho_o}{A}$ were obtained from reactivity versus

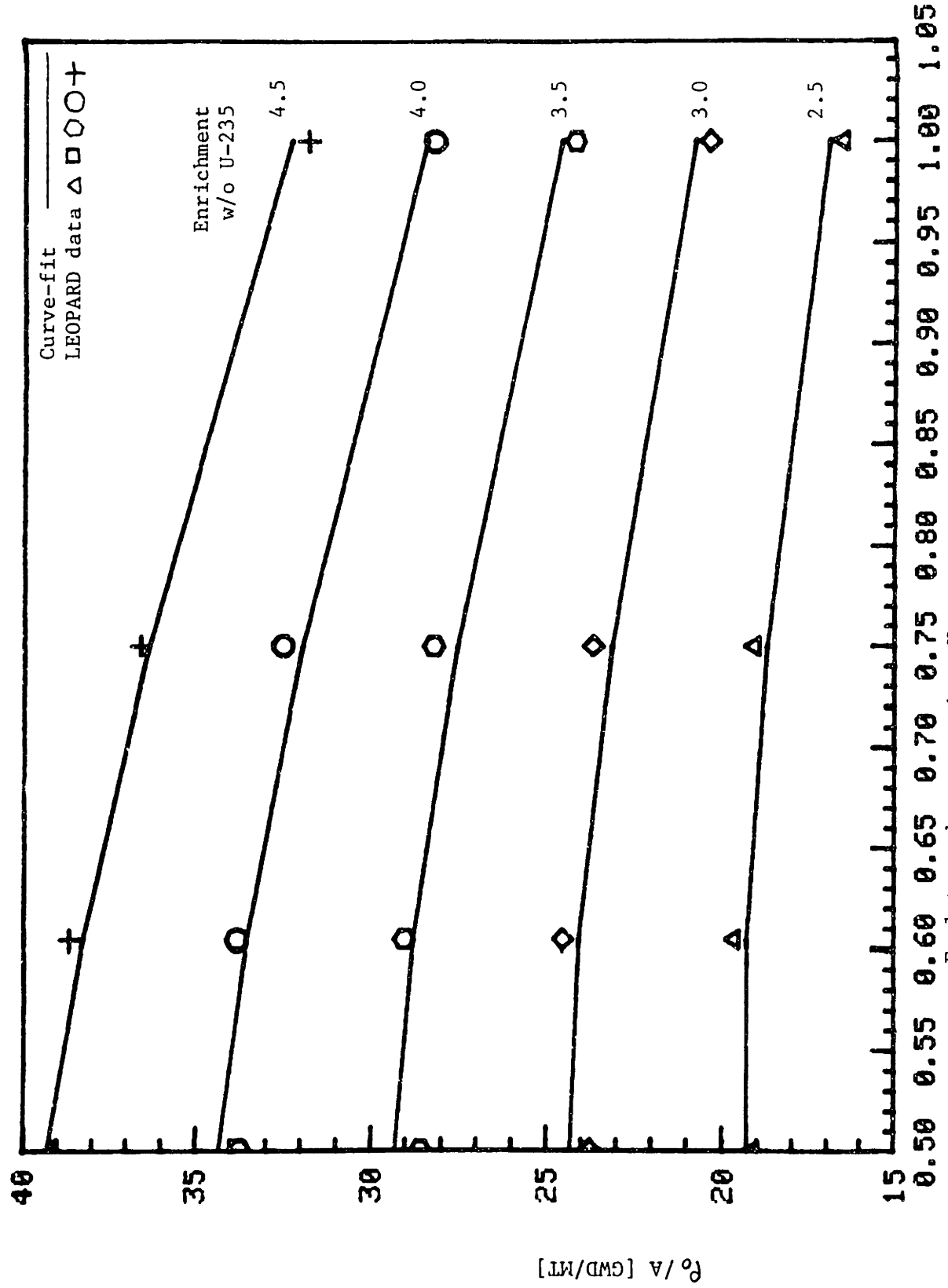


Fig. 3.1 Variation of $\rho_o$/A with $V_{F/V_M}$ for various U-235 enrichments.

TABLE 3.1

Comparison of Curve-fit and LEOPARD values of $\rho_o/A$ for Various $X_P$ and $V_F/V_M$

| $X_P$ , w/o U-235 | $V_F/V_M$ | $\rho_o/A$ [GWD/MT] | | Error % |
|---|---|---|---|---|
| | | Curve-fit | LEOPARD | |
| 2.5 | 0.500 | 19.30 | 19.09 | +1.1 |
| | 0.604 | 19.29 | 19.62 | -1.7 |
| | 0.750 | 18.71 | 19.07 | -1.9 |
| | 1.000 | 16.96 | 16.55 | +2.5 |
| 3.0 | 0.500 | 24.30 | 23.74 | +2.4 |
| | 0.604 | 24.05 | 24.52 | -1.9 |
| | 0.750 | 23.13 | 23.66 | -2.2 |
| | 1.000 | 20.78 | 20.38 | +2.0 |
| 3.5 | 0.500 | 29.30 | 28.57 | +2.5 |
| | 0.604 | 28.81 | 29.07 | -0.9 |
| | 0.750 | 27.55 | 28.24 | -2.4 |
| | 1.000 | 24.62 | 24.22 | +1.6 |
| 4.0 | 0.500 | 34.30 | 33.73 | +1.3 |
| | 0.604 | 33.56 | 33.84 | -0.8 |
| | 0.750 | 31.96 | 32.52 | -1.7 |
| | 1.000 | 28.46 | 28.24 | +0.8 |
| 4.5 | 0.500 | 39.30 | 39.18 | +0.3 |
| | 0.604 | 38.32 | 38.70 | -1.0 |
| | 0.750 | 36.38 | 36.62 | -0.6 |
| | 1.000 | 32.29 | 31.83 | +1.4 |

burnup data computed using the LEOPARD program. The isotopic composition of the plutonium used to prepare the reload fuel is shown in table 3.2 : it is representative of spent fuel from today's LWR units. The $\rho(B)$ data for various fissile plutonium contents, $X_{Puf}$ , and fuel-to-moderator ratios are presented in Appendix C.

The values of $\rho_o$ and A were obtained from a least squares fit to a polynomial of degree 1. The results for various BOL $X_{Puf}$ and $V_F/V_M$ values are shown in table 3.3 . Values of $\frac{\rho_o}{A}$ which are proportional to the discharge fuel burnup of the fuel assemblies, were obtained directly as the ratio of $\rho_o$ and A.

The different values of $V_F/V_M$ were obtained in the manner described in Appendix C, keeping fuel pellet diameter constant and varying the pitch. The BOL $X_{Puf}$ was varied from 2.5 w/o to 10 w/o , and $V_F/V_M$ was varied from 0.3 to 1.0 . The values of $R^2$ in table 3.3 indicate that the $\rho(B)$ curves for the plutonium cases are also quite linear.

### 3.3.1 Functional Dependence of A and $\frac{\rho_o}{A}$ on $X_{Puf}$

The functional dependence of A and $\frac{\rho_o}{A}$ on the fissile plutonium enrichment can be obtained for various $V_F/V_M$ by curve-fitting the data shown in table 3.3 .

TABLE 3.2

Isotopic Composition of Spent Fuel
Plutonium Used to Prepare Reload Fuel

| Isotope | w/o of Total Pu |
|---|---|
| Pu-239 | 54.22 |
| Pu-240 | 25.96 |
| Pu-241 | 13.94 |
| Pu-242 | 5.88 |

Note: Varying weights of Total Pu are mixed with depleted uranium (0.2 w/o U-235) to produce a given reload batch.

TABLE 3.3

Variation of $\rho_o$, A and $\rho_o/A$ with $X_{Puf}$ and $V_F/V_M$ for Plutonium Fueled Lattices

| $V_F/V_M$ | $X_{Puf}$ w/o | $\rho_o$ | A $\left[\frac{GWDx10^3}{MT}\right]^{-1}$ | $\rho_o/A$ [GWD/MT] | $R^2$ |
|---|---|---|---|---|---|
| 0.300 | 3.0 | 0.22553 | 9.0490 | 24.9238 | 0.985 |
| | 4.0 | 0.21427 | 5.7692 | 37.1398 | 0.990 |
| 0.500 | 2.5 | 0.13252 | 6.3143 | 20.9873 | 0.995 |
| | 3.0 | 0.13196 | 4.9860 | 26.4661 | 0.996 |
| | 4.0 | 0.12890 | 3.3647 | 38.3095 | 0.998 |
| | 6.0 | 0.12407 | 1.9637 | 63.1817 | 0.996 |
| | 8.0 | 0.11975 | 1.3053 | 91.7414 | 0.999 |
| 0.604 | 4.0 | 0.09277 | 2.6924 | 34.4515 | 0.997 |
| | 6.0 | 0.08824 | 1.5033 | 58.6975 | 0.997 |
| | 8.0 | 0.08804 | 1.0185 | 86.4408 | 0.997 |
| 0.750 | 4.0 | 0.04998 | 2.0756 | 24.0798 | 0.991 |
| | 6.0 | 0.04893 | 1.1231 | 43.5669 | 0.983 |
| | 8.0 | 0.05338 | 0.7758 | 68.8064 | 0.985 |
| 1.000 | 10.0 | 0.03696 | 0.8400 | 44.0000 | 0.997 |
| | 12.0 | 0.05840 | 1.0594 | 55.1255 | 0.998 |
| | 14.0 | 0.07979 | 1.2785 | 62.4091 | 0.996 |

Using a statistical program for simple regressions, the functional dependence of A versus $X_{Puf}$ was found to be:

$$A = a_1 + b_1/X_{Puf} \quad , \left[\frac{MT}{10^3\ GWD}\right] \tag{3.5}$$

where $a_1$ and $b_1$ are constants, the values of which are listed in table 3.4 for various $V_F/V_M$ . From table 3.3 , it can be seen that A decreases with increasing $X_{Puf}$ for $V_F/V_M < 1.0$ but for $V_F/V_M \geq 1.0$ , A increases with $X_{Puf}$. In fact for $V_F/V_M \geq 1.0$ , the BOL reactivity was very small for $X_{Puf} < 8.0\%$ and, therefore, the curve of $\rho$ versus B for $V_F/V_M \geq 1.0$ was fit for $X_{Puf} > 8.0\%$ , whereas the curve for $V_F/V_M < 1.0$ was fit for $3.0\% \leq X_{Puf} \leq 8.0\%$ . The change in the signs of the coefficients of A versus $X_{Puf}$ for $V_F/V_M = 1.0$ in table 3.4, also indicates this change of the trend in slope of $\rho(B)$ for higher $X_{Puf}$ values. A graphical representation of A versus $X_{Puf}$ , using $V_F/V_M$ as a parameter is given in Fig. 3.2 . Note, however, that LEOPARD is not as well suited for accurate plutonium calculations as some of the newer programs and the very dry lattices considered here (e.g. $V_F/V_M > 0.7$) are far outside the envelope of common experience; hence these observations should be tempered with an appreciation of their lack of pedigree.

The dependence of $\frac{\rho_o}{A}$ on $X_{Puf}$ , based on the data of table 3.3 , was found to be linear, and is described by:

$$\frac{\rho_o}{A} = a_2 + b_2\ X_{Puf} \quad , \quad [GWD/MT] \tag{3.6}$$

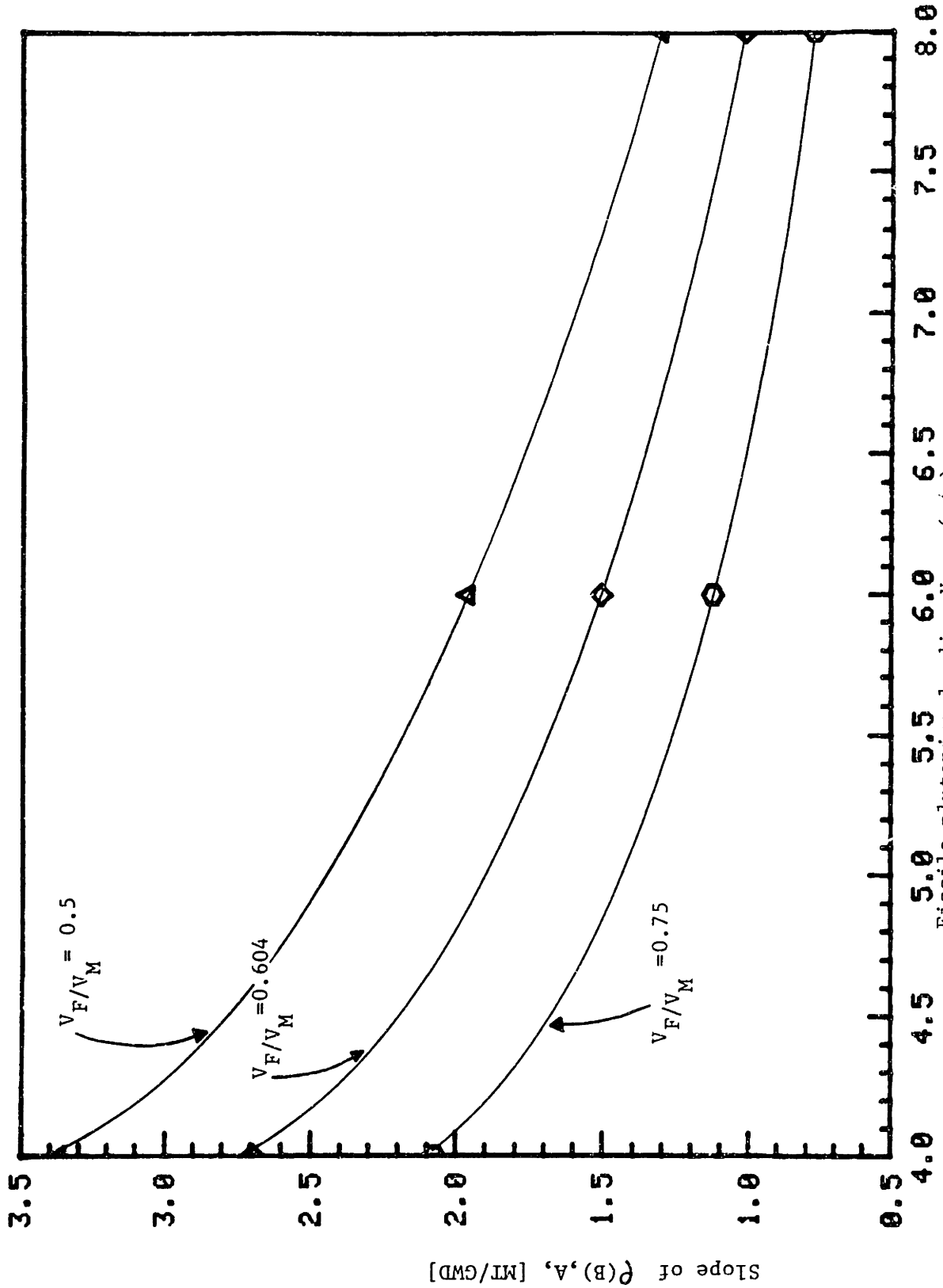


Fig.3.2 Variation of the slope of ρ(B),A, with fissile plutonium enrichment for various fuel to moderator ratios.

TABLE 3.4

Coefficients of A versus $X_{Puf}$ Curve-fit, for Various $V_F/V_M$ , for Plutonium Fueled Cores

| $V_F/V_M$ | $A = a_1 + b_1/X_{Puf}$ | | $R^2$ |
|---|---|---|---|
| | $a_1$ [MT/$10^3$ GWD] | $b_1$ [MT/($10^3$ GWD w/o)] | |
| 0.500 | -1.0630 | 18.2343 | 0.998 |
| 0.604 | -0.7024 | 13.5166 | 0.998 |
| 0.750 | -0.5793 | 10.5458 | 0.995 |
| 1.000 | 2.3507 | -15.2073 | 0.991 |

The constants $a_2$ and $b_2$ are documented in table 3.5 for various $V_F/V_M$ . The linear fit of $\frac{\rho_o}{A}$ versus $X_{Puf}$ indicates that $\frac{\rho_o}{A}$ , and consequently the discharge burnup of the fuel assemblies, increases linearly with $X_{Puf}$ for all values of $V_F/V_M$ in the interval $0.3 \leq V_F/V_M \leq 1.0$ . Figure 3.3 shows the variation of $\frac{\rho_o}{A}$ with $X_{Puf}$ for various $V_F/V_M$ values.

### 3.3.2 Functional Dependence of $\rho_o$ and A on $V_F/V_M$

The functional dependence of $\rho_o$ and A on $V_F/V_M$ was obtained by designating $V_F/V_M$ as the independent variable and $X_{Puf}$ as a parameter. A similar procedure to that described in the previous section was also applied here to curve fit the experimental data presented in table 3.3 .

The dependence of $\rho_o$ on $V_F/V_M$ was found to be linear for the interval of variation of the independent variable. In mathematical terms:

$$\rho_o = a_3 + b_3 \cdot (V_F/V_M) \qquad (3.7)$$

The constants $a_3$ and $b_3$ were obtained by fitting the data for $\rho_o$ versus $V_F/V_M$ for a given $X_{Puf}$ value. The results are presented in table 3.6 . Figure 3.4 shows the variation of $\rho_o$ as a function of $V_F/V_M$ . Note that at low $V_F/V_M$ , $\rho_o$ is higher, which is expected due to the soft spectrum at low $V_F/V_M$ , as

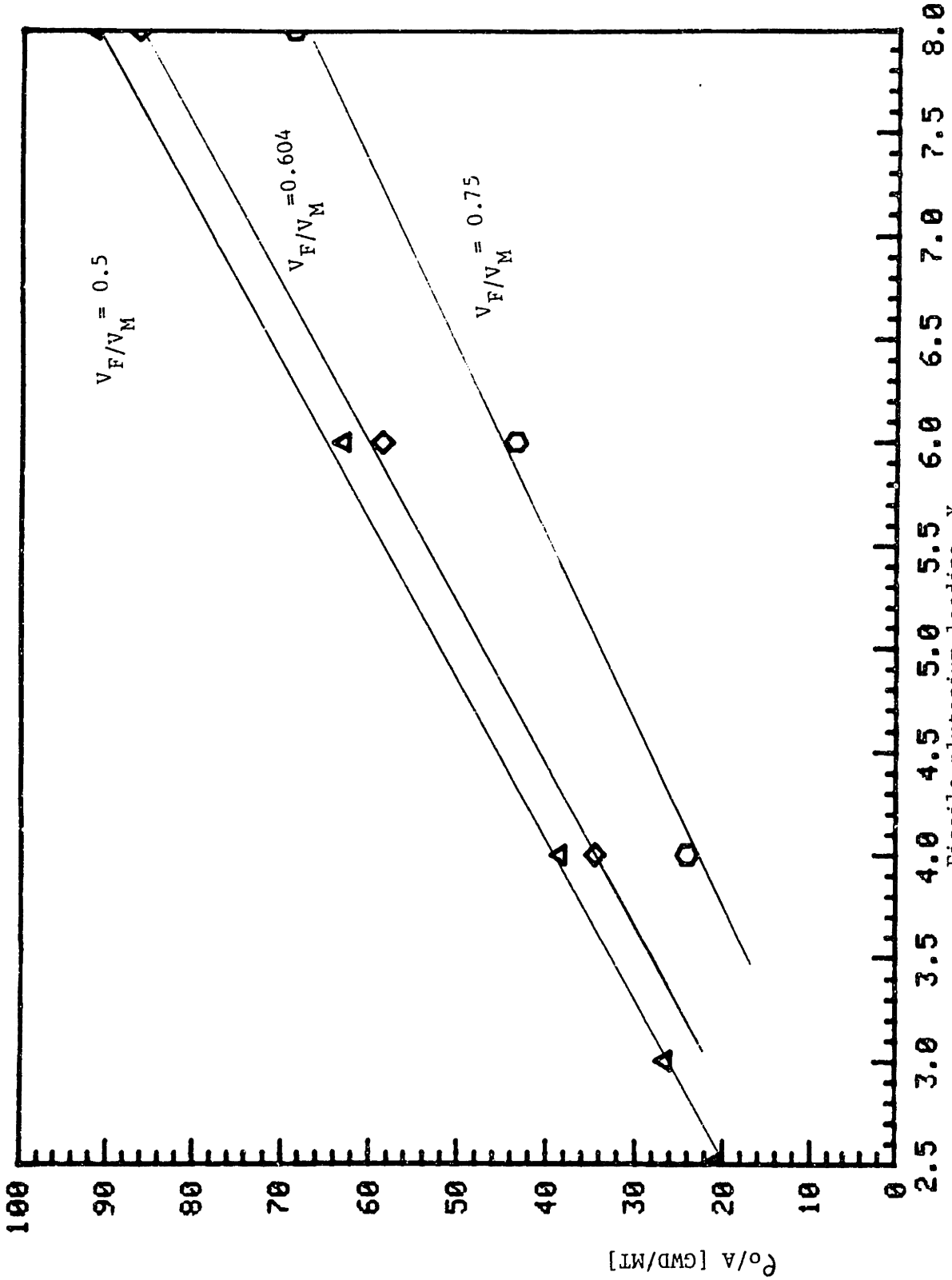


Fig. 3.3 Variation of $\rho_o/A$ with $X_{puf}$ for various fuel to moderator ratios.

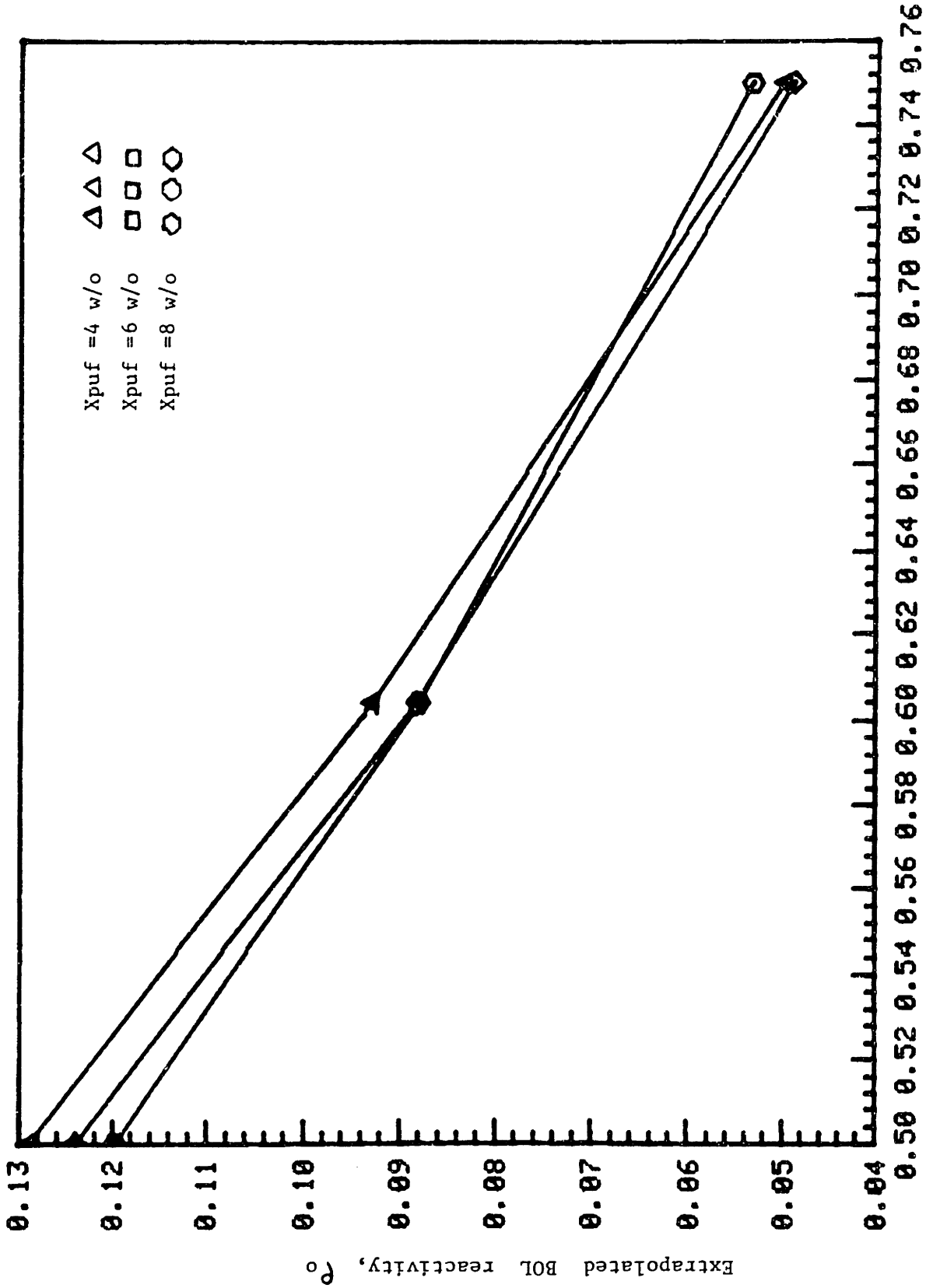


Fig. 3.4 Variation of $\rho_o$ with $V_F/V_M$ for various Xpuf.

TABLE 3.5

Curve-fit Coefficients of $\rho_o/A$ Versus Fissile Pu Content for Various $V_F/V_M$

| $V_F/V_M$ | $\rho_o/A = a_2 + b_2 X_{Puf}$ , [GWD/MT] | | $R^2$ |
|---|---|---|---|
| | $a_2$ (GWD/MT) | $b_2$ GWD/(MT*w/o) | |
| 0.300 | -1.6749 | 8.8662 | 0.999 |
| 0.500 | -12.1669 | 12.8302 | 0.998 |
| 0.604 | -18.1207 | 12.9973 | 0.998 |
| 0.750 | -21.6055 | 11.1816 | 0.994 |

TABLE 3.6

Coefficients of $\rho_o$ versus $V_F/V_M$ Curve-fit, for Various $X_{Puf}$ Values

| $X_{Puf}$ (w/o) | $\rho_o = a_3 + b_3*(V_F/V_M)$ | | $R^2$ |
|---|---|---|---|
| | $a_3$ | $b_3$ | |
| 4 | 0.2847 | -0.3142 | 0.998 |
| 6 | 0.2716 | -0.2986 | 0.995 |
| 8 | 0.2500 | -0.2637 | 0.995 |

long as we are on the "dry side" of the $k_\infty$ versus $V_F/V_M$ curve. Another observation, which was not expected, is that $\rho_o$ decreases as $X_{Puf}$ is increased (at low $V_F/V_M$). This may be due to the concurrent presence of the non-fissile isotopes of plutonium which also increase with $X_{Puf}$. However, at higher $V_F/V_M$ values, $\rho_o$ increases with $X_{Puf}$, which is due to the fact that the spectrum becomes harder at higher $V_F/V_M$ values and parasitic absorption in non-fissile isotopes decreases. Nevertheless, the decrease in BOL reactivity does not necessarily mean a decrease in discharge burnup. Indeed the discharge burnup increases with $X_{Puf}$ at all $V_F/V_M$ values, even though the BOL reactivity is less for higher $X_{Puf}$ at low $V_F/V_M$ values, since A, the decrease in reactivity per unit burnup, is also smaller for higher $X_{Puf}$ due to the greater rate of conversion of fertile isotopes into fissile isotopes.

Finally, Fig. 3.5 shows the dependence of the slope of $\rho(B)$, A, on $V_F/V_M$ for various $X_{Puf}$, indicating that its value decreases monotonically with fuel-to-moderator ratio.

### 3.3.3 Simultaneous Functional Dependence of $\frac{\rho_o}{A}$ on $X_{Puf}$ and $V_F/V_M$

Following an analogous procedure to that described in the previous sections, using the information presented in

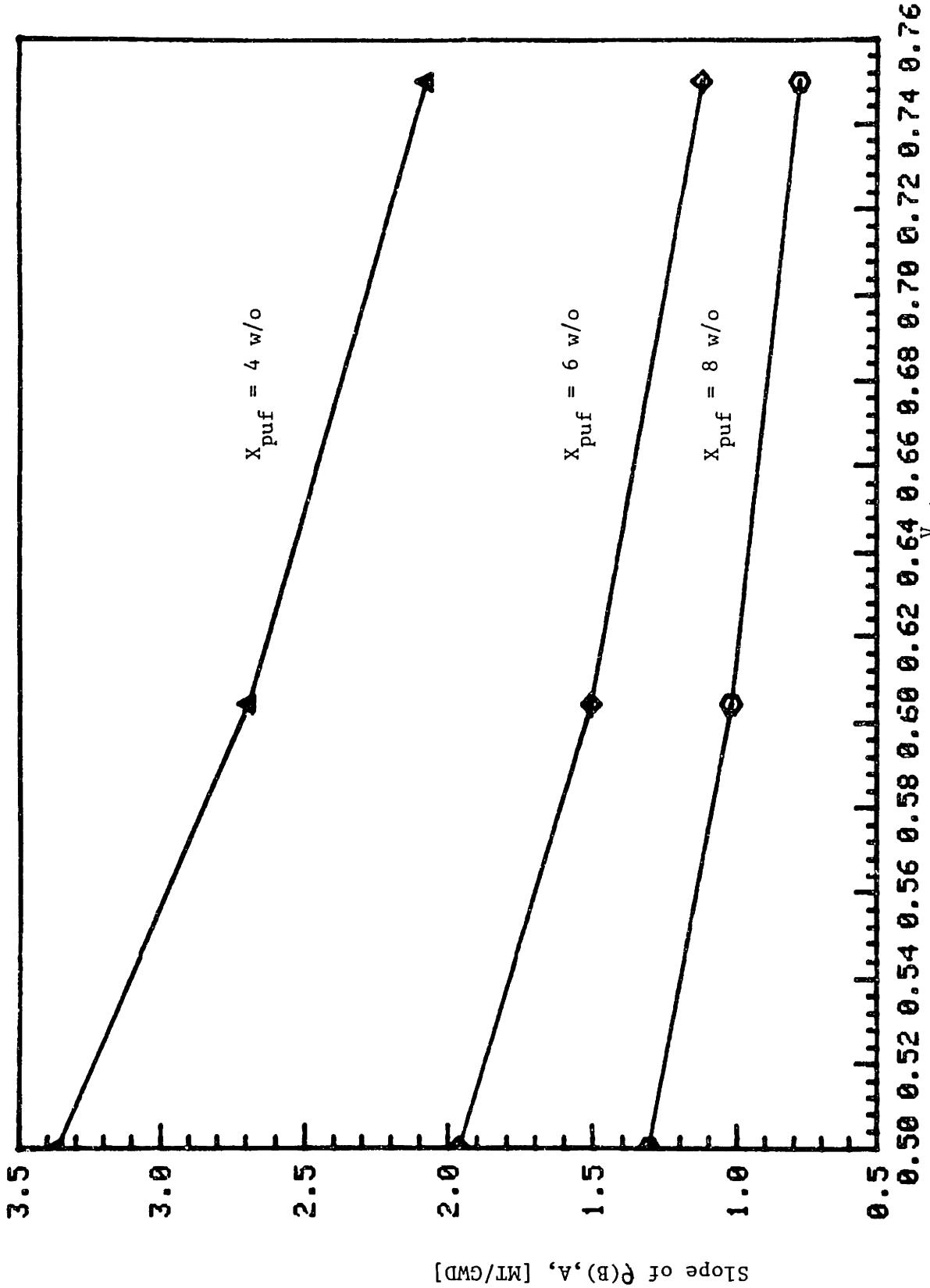


Fig. 3.5 Variation of the slope of ρ(B),A, with $V_F/V_M$ for various $X_{puf}$ (w/o).

table 3.3, the variation of $\frac{\rho_o}{A}$ with $X_{Puf}$ and $V_F/V_M$ was found to be of the form:

$$\frac{\rho_o}{A} (X_{Puf}, V_F/V_M) = F_1 (X_{Puf}) + F_2 (X_{Puf}) \frac{V_F}{V_M}, \left[\frac{GWD}{MT}\right] \tag{3.8}$$

where:

$$F_1 (X_{Puf}) = a + b * X_{Puf}, \left[\frac{GWD}{MT}\right] \tag{3.9}$$

$$F_2 (X_{Puf}) = c + d * X_{Puf}, \left[\frac{GWD}{MT}\right] \tag{3.10}$$

with:

$$a = -3.5 \left[\frac{GWD}{MT}\right]$$

$$b = 18.0 \left[\frac{GWD}{(MT * w/o)}\right]$$

$$c = 23.8 \left[\frac{GWD}{MT}\right]$$

$$d = 9.0 \left[\frac{GWD}{(MT * w/o)}\right]$$

The coefficients of determination for $F_1$ and $F_2$ were $R^2 = 0.999$ and $R^2 = 0.980$, respectively. Substituting the numerical values of a, b, c and d, Eq. (3.8) can be arranged to give:

$$\frac{\rho_o}{A} (X_{Puf}, V_F/V_M) = 9 X_{Puf} (2 - V_F/V_M) - 3.5 (1 + 6.8 V_F/V_M), \left[\frac{GWD}{MT}\right] \tag{3.11}$$

for

$$0.5 \leq V_F/V_M < 1.0 \quad ; \quad 2.5 \leq X_{Puf} \leq 10\%$$

Values of $\frac{\rho_o}{A}$ as a function of $V_F/V_M$ for various $X_{Puf}$ are shown in Fig. 3.6 . Note that values of $\frac{\rho_o}{A}$ reach a maximum within the interval of $V_F/V_M$ and $X_{Puf}$ considered. The locus of such maxima is indicated with a dotted line in Fig. 3.6 . The value of $V_F/V_M$ corresponding to the maximum of $\frac{\rho_o}{A}$ increases with $X_{Puf}$ , showing that the optimum lattice becomes drier as $X_{Puf}$ increases, a trend opposite to that observed for uranium cores [M2].

A comparison of values of $\frac{\rho_o}{A}$ obtained using Eq. (3.11) with the input data has been made to illustrate the errors that can be expected in the estimation of discharge burnup using Eq. (3.11). Table 3.7 shows the percentage error obtained when comparing values of $\frac{\rho_o}{A}$ estimated with Eq. (3.11), with those from table 3.3 for various $V_F/V_M$ and $X_{Puf}$ . Note that the simple correlation reproduces $\frac{\rho_o}{A}$ , hence discharge burnup values, within 3.0% on the average.

## 3.4 Relative Worth of Plutonium and U-235

In this work, the plutonium from the spent fuel is used to make up for the consumed U-235 in part of the discharged fuel, and the remaining uranium is credited both for ore and SWU, as shown in Fig. 2.10 . The option of limiting recycle to dedicated plutonium reactors has been adopted for the

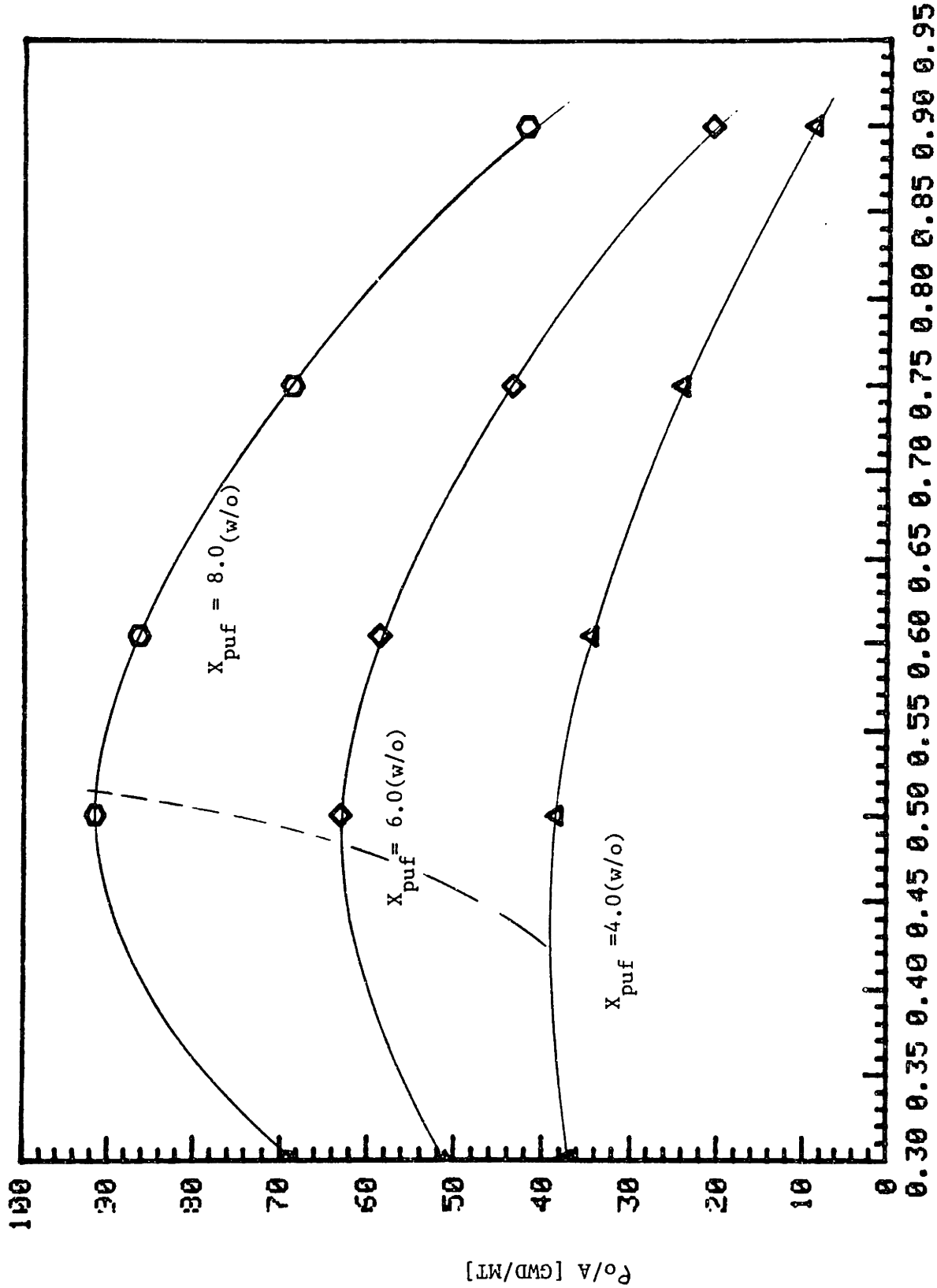


Fig.3.6 Variation of $\rho_o/A$ with $V_F/V_M$ for various $X_{puf}$ (w/o)

TABLE 3.7

Comparison of Curve-fit Values and LEOPARD Results of $\rho_o/A$ for Various $X_{Puf}$ and $V_F/V_M$ for Plutonium Fueled Cores

| $V_F/V_M$ | $X_{Puf}$ (w/o) | $\rho_o/A$ [GWD/MT] | | Error % |
|---|---|---|---|---|
| | | Curve-fit | LEOPARD | |
| 0.500 | 4.0 | 38.6 | 38.3 | +0.8 |
| | 6.0 | 65.6 | 63.2 | +3.8 |
| | 8.0 | 92.6 | 91.7 | +1.0 |
| 0.604 | 4.0 | 32.4 | 34.4 | -5.8 |
| | 6.0 | 57.5 | 58.7 | -2.0 |
| | 8.0 | 82.6 | 86.4 | -4.4 |
| 0.750 | 4.0 | 23.7 | 24.1 | -1.6 |
| | 6.0 | 46.1 | 43.6 | +5.7 |
| | 8.0 | 68.7 | 68.8 | -0.1 |

following reasons:

- By dedicating an entire reactor core to the same fuel type, the problem of power peaking at the interface between zones of different assembly type is avoided.
- Mixed oxide (MOX) fabrication costs are about a factor of 2.5 higher than that of standard $UO_2$ reactor fuel. Hence confining plutonium-containing mixed oxide to as few assemblies/fuel batches/reactors as possible is to be preferred.
- Restricting plutonium use to a select group of reactors can reduce proliferation risks.

Plutonium as a reactor fuel is more complex to evaluate than U-235. Basically this is because more isotopes are present in Pu-enriched fuel than in uranium enriched fuel. In addition, the neutron cross-sections of Pu isotopes have significant resonances at thermal and near-thermal energies, which complicate the calculation of neutron spectra in Pu-fueled cores.

The isotopic composition of plutonium has a large bearing on its reactivity worth, since the various isotopes (Pu-239, 240, 241, 242) have substantially different neutronic properties. The composition of spent fuel plutonium used to prepare MOX reload fuel in the present work is shown in table 3.2 .

Equation (3.4) gives the values of $\frac{\rho_o}{A}$ for a uranium core as a function of $X_P$ and $V_F/V_M$ . The corresponding values of $X_{Puf}$ , which will give the same values of $\frac{\rho_o}{A}$ (hence cycle and discharge burnup) in the plutonium core, as $X_P$ w/o U-235 in a uranium core can be calculated using Eq. (3.11), as:

$$X_{Puf}\ (X_P\ ,\ V_F/V_M) = \frac{\frac{\rho_o}{A}\ (X_P\ ,\ V_F/V_M) + 3.5(1+6.8\ V_F/V_M)}{9\ (\ 2\ -\ V_F/V_M)} \tag{3.12}$$

The "burnup worth" of fissile plutonium relative to $X_P$ at a particular value of $V_F/V_M$ , $g(X_P\ ,\ V_F/V_M)$ , is given by:

$$g\ (X_P\ ,\ V_F/V_M) = \frac{X_P}{X_{Puf}\ (X_P\ ,\ V_F/V_M)} \tag{3.13}$$

The results from Eq. (3.13) have been curve fit to give the following direct correlation for the equivalent worth of $Pu_f$ in terms of $X_P$ AND $V_F/V_M$ :

$$g\ (X_P\ ,\ V_F/V_M) = 1.6494-0.7042\ V_F/V_M + \frac{1}{X_P} \left\{\frac{0.3925}{(V_F/V_M)} - 1.6238\right\} \tag{3.14}$$

Curve fit values of the equivalent worth of Pu from Eq. (3.14) are compared to the input data in Fig. 3.7 . Some selected results are presented in table 3.8 .

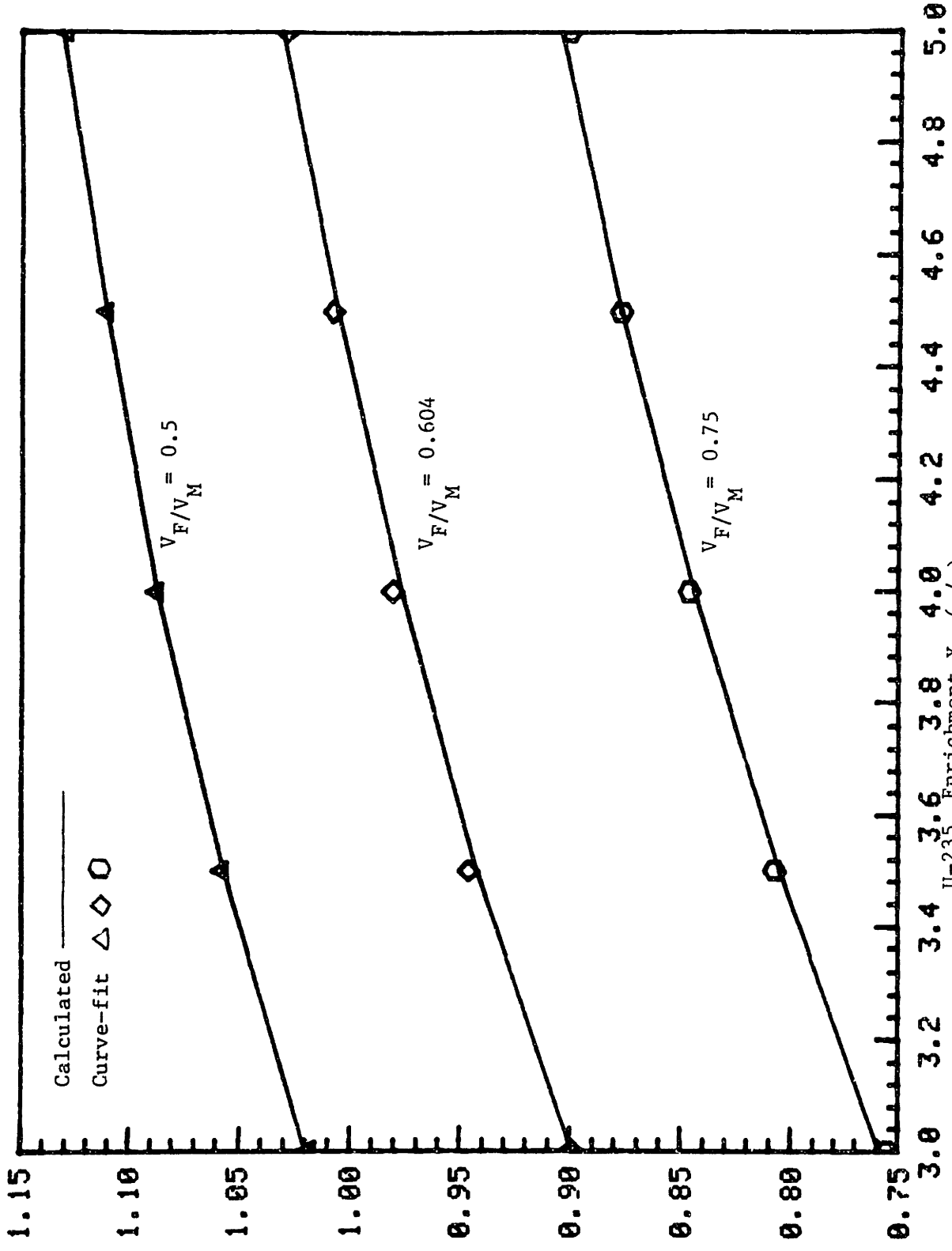


Fig. 3.7 Worth of fissile Pu relative to U-235 for various fuel-to-moderator ratios.

TABLE 3.8

Comparison of Curve-fit and Calculated Worths of Fissile Pu Relative to U-235

| $V_F/V_M$ | U-235 (w/o) $X_P$ | Fissile Pu (w/o) $X_{Puf}$ | Equivalent worth $g(X_P, V_F/V_M)$ | | Error % |
|---|---|---|---|---|---|
| | | | Calculated | Curve-fit | |
| 0.500 | 3.0 | 2.941 | 1.020 | 1.018 | -0.20 |
| | 3.5 | 3.311 | 1.057 | 1.058 | -0.09 |
| | 4.0 | 3.681 | 1.087 | 1.088 | +0.09 |
| | 4.5 | 4.052 | 1.111 | 1.111 | 0.00 |
| | 5.0 | 4.421 | 1.131 | 1.130 | -0.09 |
| 0.604 | 3.0 | 3.337 | 0.899 | 0.899 | 0.00 |
| | 3.5 | 3.716 | 0.942 | 0.946 | +0.42 |
| | 4.0 | 4.094 | 0.977 | 0.981 | +0.41 |
| | 4.5 | 4.473 | 1.006 | 1.008 | +0.20 |
| | 5.0 | 4.852 | 1.031 | 1.029 | -0.20 |
| 0.750 | 3.0 | 3.954 | 0.759 | 0.755 | -0.53 |
| | 3.5 | 4.347 | 0.805 | 0.807 | +0.25 |
| | 4.0 | 4.739 | 0.844 | 0.846 | +0.24 |
| | 4.5 | 5.132 | 0.877 | 0.877 | 0.00 |
| | 5.0 | 5.524 | 0.905 | 0.901 | -0.44 |

The burnup worth of fissile plutonium is more than that of U-235 in the wetter lattices, since, due to the much larger thermal absorption cross-section of Pu isotopes, the spectra of the Pu cores are harder than those of the corresponding uranium cores, and so the optimum lattice for a Pu core is wetter than that of a uranium-fueled core. Also, the worth of plutonium increases with $X_{Puf}$ due to a flatter reactivity swing during fuel depletion than comparable uranium fuels, as a consequence of the large Pu-240 resonance at 1.05 ev, which enables Pu-240 to behave as a burnable poison, which not only adds reactivity by its depletion, but also produces the high worth fissile isotope Pu-241.

Note in Fig. 3.7 the fortuitous circumstance for current PWR lattices ($0.5 < V_F/V_M < 0.6$ , $3\% < X_p < 4\%$) that fissile plutonium is roughly equal in worth to the U-235 it displaces on a 1:1 basis.

Finally note that "worth" as defined here refers to the capability of sustaining burnup, and not (the more common definition) the ability to provide reactivity at a fixed point in time.

## 3.5 Optimum Enrichment Plant Tails

Equations (2.3) and (2.6) determine the requirements of natural uranium feed and of separative work per unit amount of uranium enriched to $X_P$ w/o of U-235. The unit cost of enriched uranium, $C_P$ , is determined simply by the unit cost of feed material and by the unit cost of separative work, denoted by $C_F$ and $C_S$ , respectively,

$$C_P = \frac{F}{P} C_F + \frac{S}{P} C_S \quad , \quad \$/kg \tag{3.15}$$

$C_P$ can be optimized by a proper choice of tails assay, $X_W$ . Lowering the tails assay decreases the amount of feed material required and, at the same time, increases the demand for separative work.

Minimizing $C_P$ in Equation (3.15) with respect to tails assay $X_W$ yields the optimum tails assay, $X_o$ , which turns out to be independent of product enrichment $X_P$ , but depends only on the ratio $C_F/C_S$ (and the feed assay $X_F$ -- a fixed value for natural uranium). The minimizing condition $\left(\frac{\partial C_P}{\partial X_W}\right) = 0$ gives the optimum tails assay, $X_o$ , in the form of the following transcendental equation:

$$\frac{C_F}{C_S} = (2 X_F - 1) \ln\left\{\frac{X_F (1-X_o)}{X_o (1-X_F)}\right\} + \frac{(X_F - X_o)(1 - 2 X_o)}{X_o (1 - X_o)} \tag{3.16}$$

Note that the cost of feed material $C_F$ (in \$/kg of uranium), as used here, includes the cost of ore, transportation and conversion to $UF_6$ .

A simple correlation for the optimum tails assay in the range of interest is given by:

$$X_W\Big)_{opt} = [\ 2.425 + 1.925\ (C_F/C_S)\ ]^{-1} \qquad (3.17)$$

for

$$0.5 \leq C_F/C_S \leq 3$$

The actual and the curve-fit values of the optimum tails assay are compared in Fig. 3.8 , and tabulated in table 3.9 . As can be seen, Eq. 3.17 is accurate within ±1% , which is quite acceptable. Note that the above correlation, developed for a fixed value of feed assay ($X_F$ = 0.711%), cannot optimize the tails assay for the recycle case.

## 3.6 Isotope Separation for Three Component Mixtures

The isotope U-236 does not occur naturally, but it is introduced into the fuel through neutron capture accompanying the burnup of enriched uranium. U-236 has a large parasitic capture cross-section and behaves as a neutron poison. The significant effect of U-236 becomes apparent when discharged

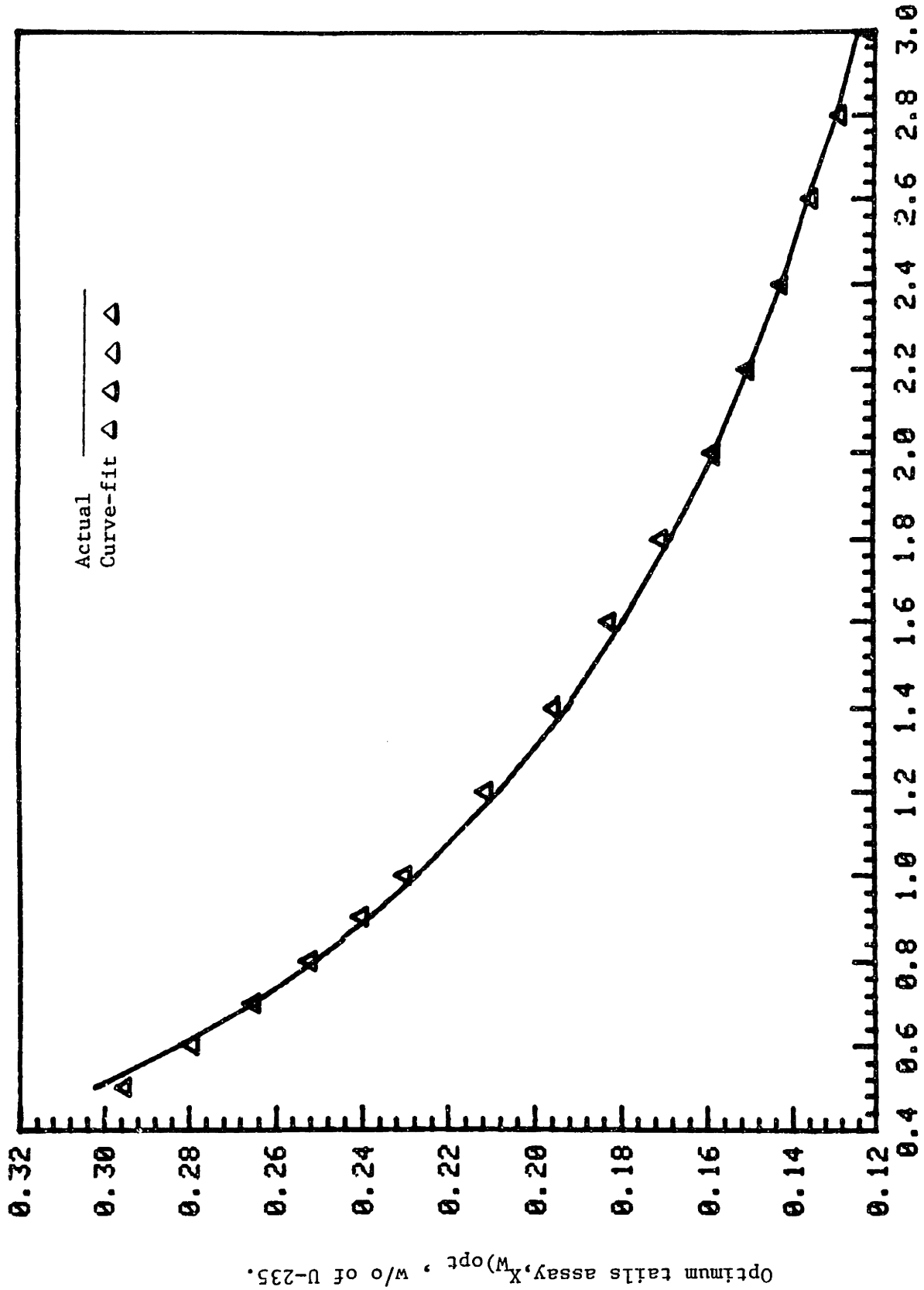


Fig 3.8 Optimum tails assay as a function of ratio : cost of feed/ cost of SWU.

TABLE 3.9

Comparison of Curve-fit and Exact Values of the Optimum Tails Assay

| $C_F/C_S$ | Optimum tails assay w/o of U-235 , $X_{W\ opt}$ | |
|---|---|---|
| | Exact | Curve-fit |
| 3.0 | 0.124 | 0.122 |
| 2.8 | 0.129 | 0.128 |
| 2.6 | 0.136 | 0.135 |
| 2.4 | 0.142 | 0.142 |
| 2.2 | 0.150 | 0.150 |
| 2.0 | 0.158 | 0.159 |
| 1.8 | 0.168 | 0.170 |
| 1.6 | 0.179 | 0.182 |
| 1.4 | 0.192 | 0.195 |
| 1.2 | 0.208 | 0.211 |
| 1.0 | 0.227 | 0.230 |
| 0.9 | 0.238 | 0.240 |
| 0.8 | 0.251 | 0.252 |
| 0.7 | 0.265 | 0.265 |
| 0.6 | 0.282 | 0.279 |
| 0.5 | 0.302 | 0.295 |

uranium, recovered in the reprocessing plant, is returned as feed for new fuel enrichment. When introduced into the separative process, the U-236 from the recycled uranium is enriched along with the U-235.

The distribution of U-236 between product and tails can be evaluated from the material balance equation [D2, B3]:

$$PY_2 + WY_3 = FY_1 \tag{3.18}$$

and application of

$$\frac{PY_2}{R_2^{1/3}} + \frac{WY_3}{R_3^{1/3}} = \frac{FY_1}{R_1^{1/3}} \tag{3 19}$$

where

$$R_i = \left( \frac{X_i}{100 - X_i - Y_i} \right) \tag{3.20}$$

$X_1$ = w/o of U-235 in Feed

$X_2$ = w/o of U-235 in Product

$X_3$ = w/o of U-235 in Tails

$Y_1$ = w/o of U-236 in Feed

$Y_2$ = w/o of U-236 in Product

$Y_3$ = w/o of U-236 in Tails.

Equations (3.18) and (3.19) can be iteratively solved to give $Y_2$ and $Y_3$ . In this section a simple but accurate empirical formula is prescribed which can be used to determine the change in the U-236 concentration per unit change in the

U-235 concentration, $\Delta Y/\Delta X$ , when recycled uranium is processed in an enrichment plant:

$$\frac{\Delta Y}{\Delta X} = Y_1 \left[ (a + b X_3) + (c + d X_3) X_2 \right]^{-1} \qquad (3.21)$$

for

$$0.4 < X_1 < 1.0 \; ; \; 2.0 < X_2 < 5.0 \; ; \; 0.1 < X_3 < 0.3 \; ;$$
$$0.2 < Y_1 < 0.6$$

where

$$a = 0.12125 + 1.0840 X_1 \qquad (3.22)$$

$$b = 0.27323 + 0.2340 X_1 \qquad (3.23)$$

$$c = 0.00521 + 0.0142 X_1 \qquad (3.24)$$

$$d = 0.06476 - 0.01044/X_1 \qquad (3.25)$$

The U-236 content in the product is given as

$$Y_2 = Y_1 + \left(\frac{\Delta Y}{\Delta X}\right) (X_2 - X_1) \text{ , w/o} \qquad (3.26)$$

and U-236 in the tails is

$$Y_3 = Y_1 - \frac{\Delta Y}{\Delta X} (X_1 - X_3) \text{ , w/o} \qquad (3.27)$$

After the determination of U-236 content in the product and tails, the separative work required per unit mass of product can be evaluated by applying the following equation:

$$\frac{SW}{P} = V(X_2 , Y_2) + \frac{W}{P} V(X_3 , Y_3) - \frac{F}{P} V(X_1 , Y_1) \qquad (3.28)$$

where

$$V(X_i , Y_i) = \left\{ \frac{2X_i}{100} + \frac{4Y_i}{100} - 1 \right\} \ln R_i \qquad (3.29)$$

is the value function for a three-component isotope separation, and

$$\frac{W}{P} = \frac{(X_2 - X_1)}{(X_1 - X_3)} \tag{3.30}$$

$$\frac{F}{P} = \frac{(X_2 - X_3)}{(X_1 - X_3)} \tag{3.31}$$

Curve-fit and exact distributions of U-236 in product and tails are compared for some representative values in table 3.10 . Figures (3.9), (3.10) and (3.11) show the content of U-236 in the product, $Y_2$ , versus the content of U-236 in feed, $Y_1$ , for various values of U-236 content in feed and product. As shown in table 3.10 , the simple empirical prescriptions err by only a few tenths of one percent: precision which is considerably better than required for present purposes.

## 3.7 Separative Work Requirements

The cost of enrichment is directly proportional to the separative work required per Kg of the product material, S/P, given by Eq. 2.6 . It is noted that for the range of enrichments of interest (2 w/o < $X_P$ < 5 w/o), S/P is an essentially linear function of product enrichment, $X_P$ , that is:

$$S/P \quad \alpha \quad + \beta \; X_P \tag{3.32}$$

where $\alpha$ and $\beta$ are functions of the tails assay, and are obtained by fitting the data for S/P versus $X_P$ ; the values

TABLE 3.10

Comparison of Curve-fit and Exact Distributions of U-236 in the Product and Tails of a Three Component Isotope Separation Plant

| U-235 (w/o) in | | | U-236 (w/o) in | | | | | | |
|---|---|---|---|---|---|---|---|---|---|
| Feed $X_1$ | Product $X_2$ | Tails $X_3$ | Feed $Y_1$ | Product, $Y_2$ | | | Tails, $Y_3$ | | |
| | | | | Exact | Empirical | Error % | Exact | Empirical | Error % |
| 0.6 | 3.0 | 0.2 | 0.3 | 1.078 | 1.079 | +0.09 | 0.1703 | 0.1701 | -0.12 |
| | | | 0.4 | 1.437 | 1.439 | +0.14 | 0.2271 | 0.2268 | -0.13 |
| | | 0.3 | 0.3 | 1.034 | 1.035 | +0.10 | 0.2082 | 0.2081 | -0.05 |
| | | | 0.4 | 1.378 | 1.380 | +0.14 | 0.2777 | 0.2775 | -0.07 |
| | 4.0 | 0.2 | 0.3 | 1.376 | 1.377 | +0.07 | 0.1735 | 0.1733 | -0.11 |
| | | | 0.4 | 1.833 | 1.836 | +0.16 | 0.2314 | 0.2311 | -0.13 |
| | | 0.3 | 0.3 | 1.311 | 1.312 | +0.08 | 0.2108 | 0.2107 | -0.05 |
| | | | 0.4 | 1.747 | 1.750 | +0.17 | 0.2811 | 0.2809 | -0.07 |
| 0.7 | 3.0 | 0.2 | 0.3 | 0.961 | 0.962 | +0.10 | 0.1563 | 0.1562 | -0.06 |
| | | | 0.4 | 1.281 | 1.282 | +0.08 | 0.2085 | 0.2082 | -0.14 |
| | | 0.3 | 0.3 | 0.926 | 0.926 | +0.00 | 0.1912 | 0.1912 | -0.00 |
| | | | 0.4 | 1.234 | 1.235 | +0.08 | 0.2550 | 0.2547 | -0.12 |
| | 4.0 | 0.2 | 0.3 | 1.226 | 1.227 | +0.08 | 0.1597 | 0.1595 | -0.12 |
| | | | 0.4 | 1.634 | 1.636 | +0.12 | 0.2131 | 0.2127 | -0.19 |
| | | 0.3 | 0.3 | 1.174 | 1.175 | +0.08 | 0.1941 | 0.1940 | -0.05 |
| | | | 0.4 | 1.564 | 1.566 | +0.13 | 0.2589 | 0.2586 | -0.12 |

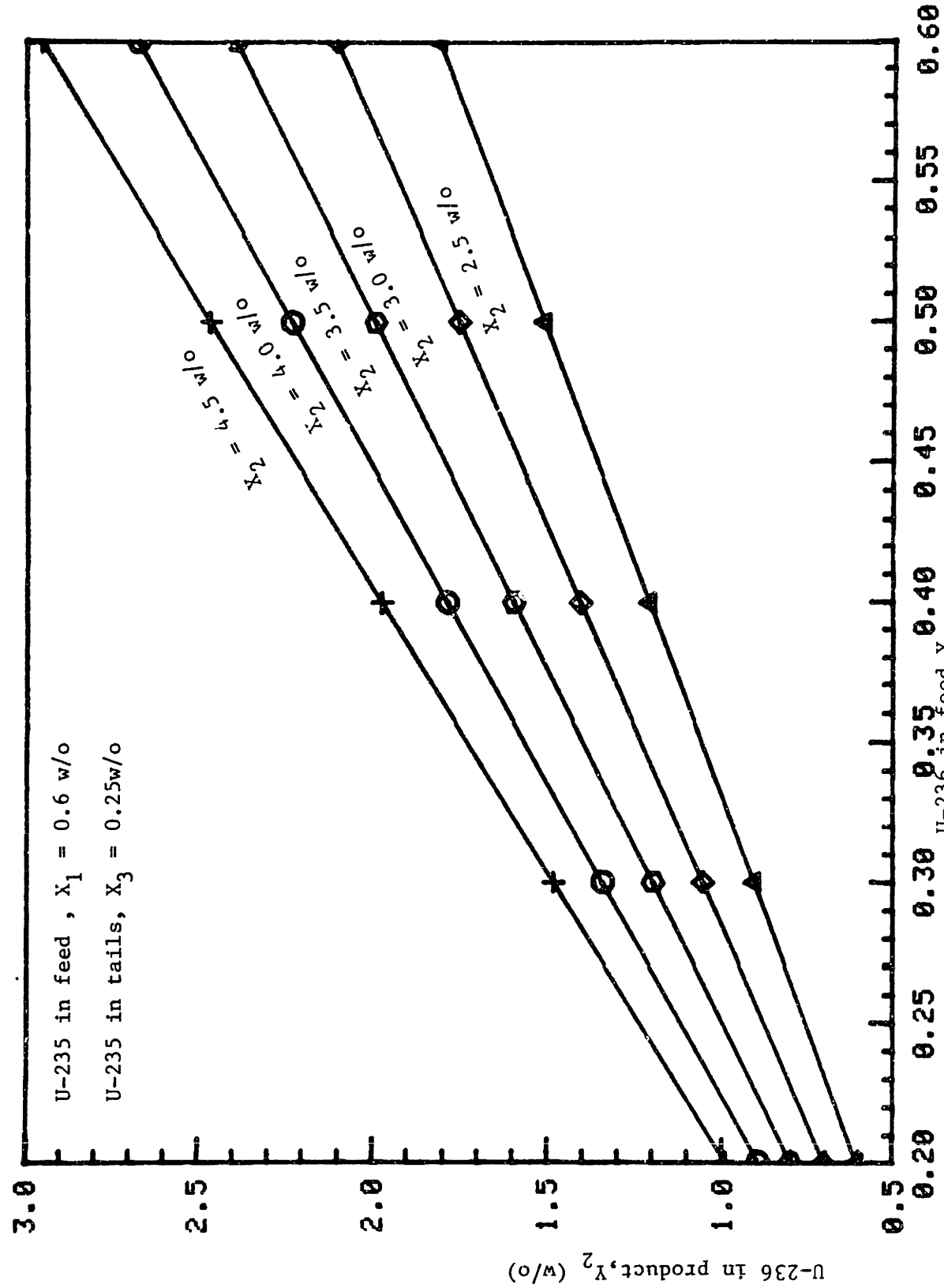


Fig 3.9 U-236(w/o) in product versus U-236(w/o) in feed for various U-235 enrichments in product($X_2$);for U-235 in feed,$X_1$=0.6 w/o.

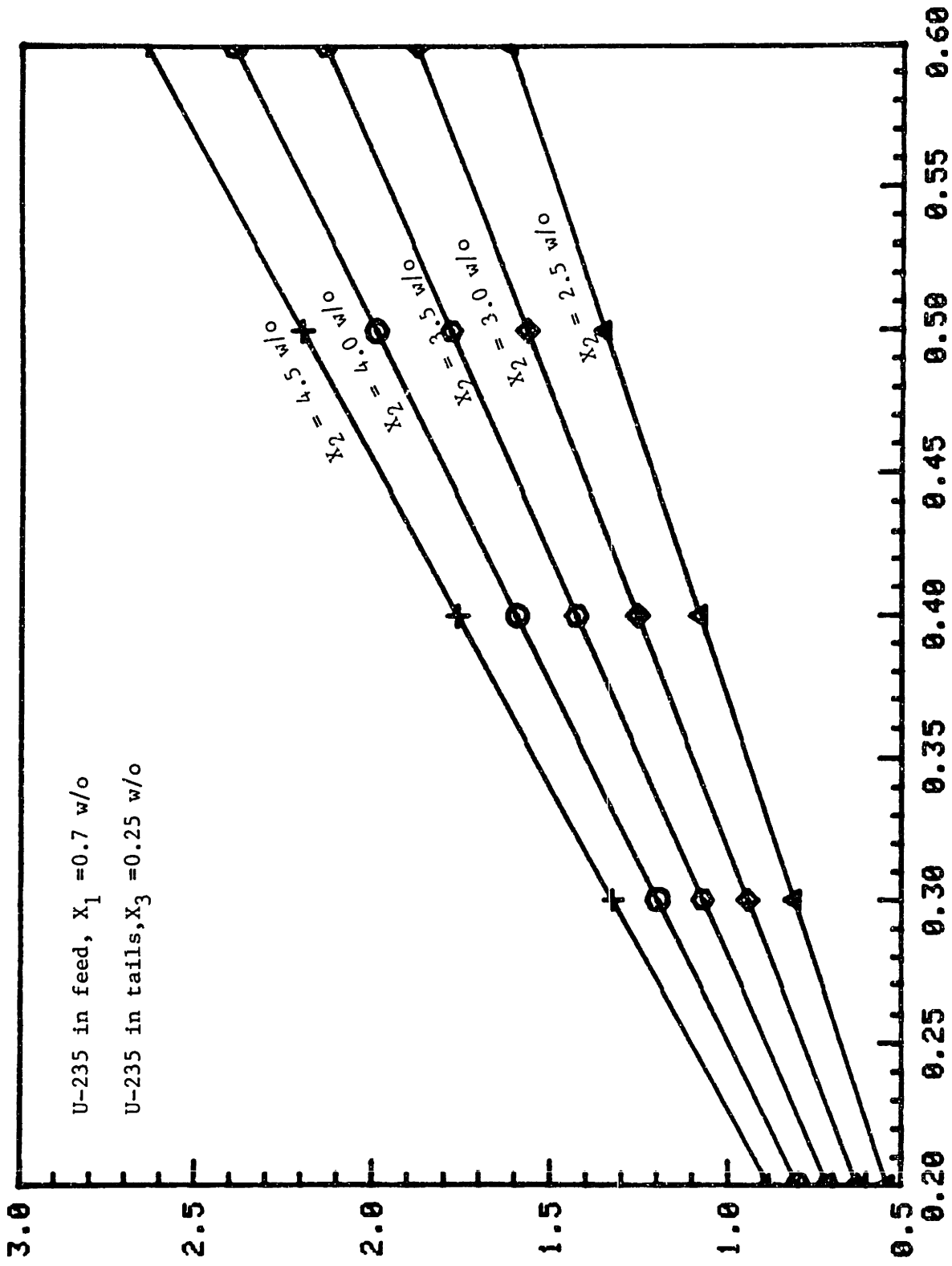


Fig. 3.10 U-236 (w/o) in product versus U-236 (w/o) in feed for various U-235 enrichments in product ($X_2$); for U-235 in feed ,$X_1$ = 0.7 w/o .

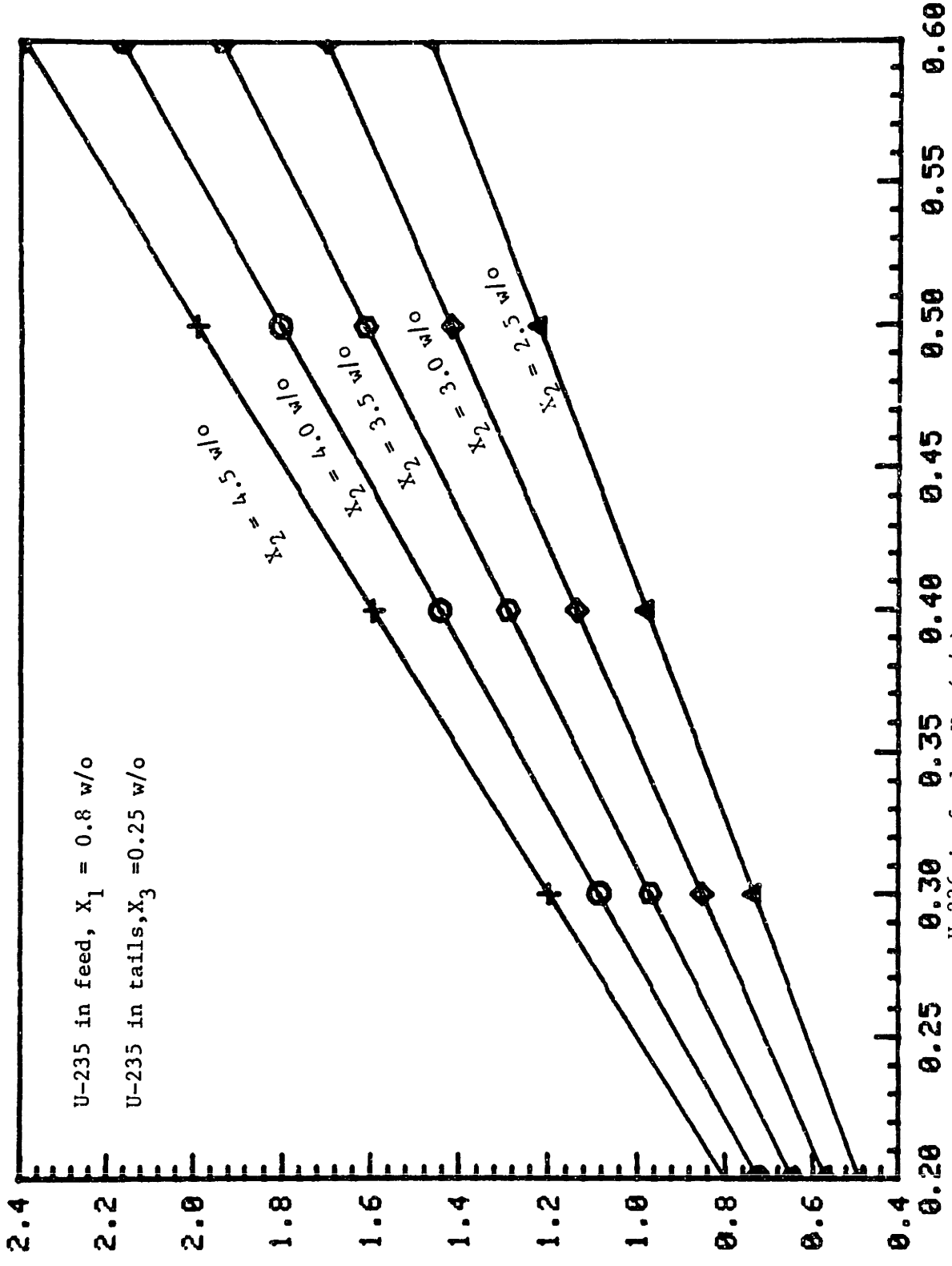


Fig. 3.11 U-236 in product versus U-236 (w/o) in feed for various U-235 enrichments in product($X_2$);for U-235 in feed,$X_1$ =0.8 w/o

of $\alpha$ and $\beta$ so obtained are listed in table 3.11 . Figure 3.12 snows the variation of S/P with $X_P$ for various tails assays. The dependence of $\alpha(X_W)$ and $\beta(X_W)$ on tails assay can be expressed as:

$$\alpha(X_W) = a_1 + b_1 X_W \qquad (3.33)$$

$$\beta(X_W) = [a_2 + b_2 X_W]^{-1} \qquad (3.34)$$

$$0.10 < X_W < 0.35 \text{ w/o}$$

with:

$$a_1 = -3.12027$$

$$b_1 = +3.29712 \text{ (w/o)}^{-1}$$

$$a_2 = +0.24412 \text{ (w/o)}$$

$$b_2 = 0.98258$$

The coefficients of determination for $\alpha$ and $\beta$ are $R^2 = 0.990$ and $R^2 = 0.998$ , respectively.

Equation (3.32) can be rewritten as:

$$S/P = (-3.12027 + 3.29712\ X_W) + \frac{X_P}{(0.24412 + 0.98258\ X_W)} \qquad (3.35)$$

In table (3.12) the curve-fit values of S/P evaluated using Eq. (3.34) are compared with the exact values of S/P. The maximum error of this empirical formula is 1.8% , which is satisfactory for the present work.

TABLE 3.11

Coefficients of S/P versus $X_p$ Curve Fit , for Various Values of Tails Assay

| Tails Assay $X_W$ (w/o) | $S/P = \alpha + \beta X_p$ | | $R^2$ |
|---|---|---|---|
| | $\alpha$ | $\beta$ | |
| 0.10 | -2.81281 | 2.95212 | 0.99992 |
| 0.15 | -2.62602 | 2.54240 | 0.99987 |
| 0.20 | -2.42068 | 2.24915 | 0.99984 |
| 0.25 | -2.28644 | 2.03695 | 0.99985 |
| 0.30 | -2.15831 | 1.86712 | 0.99980 |

TABLE 3.12

Comparison of Curve-fit and Exact Values of SWU Requirements for Various Tails Assay U-235 (w/o) in feed = 0.711

| U-235 (w/o) in tails | U-235 (w/o) in product | SWU Requirements, S/P Curve-fit | Exact | Error % |
|---|---|---|---|---|
| 0.10 | 2.5 | 4.51 | 4.54 | -0.66 |
| | 3.0 | 5.97 | 6.08 | -1.81 |
| | 4.0 | 8.89 | 8.99 | -1.11 |
| | 5.0 | 11.81 | 11.94 | -1.09 |
| 0.15 | 2.5 | 3.76 | 3.76 | 0.00 |
| | 3.0 | 5.04 | 4.98 | +1.20 |
| | 4.0 | 7.59 | 7.51 | +1.06 |
| | 5.0 | 10.14 | 10.11 | +0.30 |
| 0.20 | 2.5 | 3.21 | 3.23 | -0.62 |
| | 3.0 | 4.35 | 4.31 | +0.93 |
| | 4.0 | 6.62 | 6.54 | +1.22 |
| | 5.0 | 8.89 | 8.85 | +0.45 |
| 0.25 | 2.5 | 2.81 | 2.83 | -0.71 |
| | 3.0 | 3.83 | 3.81 | +0.52 |
| | 4.0 | 5.87 | 5.83 | +0.69 |
| | 5.0 | 7.91 | 7.92 | -0.13 |
| 0.30 | 2.5 | 2.51 | 2.54 | -1.18 |
| | 3.0 | 3.43 | 3.42 | +0.29 |
| | 4.0 | 5.29 | 5.28 | +0.20 |
| | 5.0 | 7.15 | 7.20 | -0.69 |

Note that Eq. 3.35 applies only when natural uranium feed is supplied to the enrichment plant. The same general functional relation should apply for other feed concentrations, which would permit further generalization of Eq. (3.35).

## 3.8 Chapter Summary

In this chapter, simple correlations were introduced to provide a base for the analysis of various design and fuel management strategies. These correlations provide a compact, yet accurate, means to summarize the exogenous input needed for fuel cycle studies. The simplicity of the functional dependencies demonstrated in these relations greatly reduces the number of state-of-the-art reactor physics computations needed to characterize a given reactor for such studies. They also permit rapid evaluation of the dependent variables (even using a microcomputer) - a feature essential for iterative optimization processes.

Correlations for $\frac{\rho_o}{A}$, which is directly proportional to cycle or discharge burnup have been obtained as a function of enrichment (U-235 w/o for uranium cores) and fissile plutonium w/o (for plutonium cores) and fuel-to-moderator ratio. Raw data obtained from the LEOPARD Code Output were quite accurately reproduced using such correlations.

Analysis of the $\frac{\rho_o}{A}$ curve-fits indicated that the fuel-to-moderator ratio, $V_F/V_M$ , corresponding to the maximum of $\frac{\rho_o}{A}$ decreases with increasing values of enrichment for uranium cores, whereas the optimum lattice for plutonium cores becomes drier as fissile enrichment is increased.

Using the $\frac{\rho_o}{A}$ correlations for uranium and plutonium cores, the "burnup worth" of fissile plutonium relative to U-235 was calculated and the results were curve-fit to give a correlation for the equivalent worth of Puf in terms of reload enrichment, $X_P$ , and $V_F/V_M$ . The "burnup worth" of fissile plutonium was found to be more than that of U-235 at low $V_F/V_M$ , since the optimum lattice for Pu cores is wetter than that for uranium fueled cores. For lattices of current design, however, fissile plutonium has approximately the same worth as U-235.

Simple correlations for the calculation of separative work requirements and the optimum tails assay were also developed.

Finally, an empirical formula is prescribed to determine the distribution of U-236 between the product and tails when recycled uranium is processed in an enrichment plant.

We can now move ahead and apply the models and correlations developed so far for the analysis of case studies in the next chapter.

# CHAPTER 4

# CASE STUDIES

## 4.1 Introduction

Important questions remain to be answered regarding the future course of the nuclear power economy as changes in the technical and economic environment unfold.

The integrated package of submodels described in earlier chapters permits evaluation of candidate scenarios which may characterize the user's perception of what the future holds in store. In the present chapter a number of illustrative applications are examined; they encompass many aspects of current interest to the nuclear fuel manager, e.g.:

- reprocessing and recycling spent fuel
- increasing fuel burnup
- responding to lower enrichment costs from advanced isotope separation technology
- changing the enrichment facility tails' assay
- accommodating changes in the price of uranium ore.

## 4.2 Fuel Cycle Cost for Once Through (OT) and Recycle (RC) Mode Fueling of LWRs

The spent fuel from LWRs contains fissile uranium and plutonium which can be recovered and recycled. Presently, in the U.S. the spent fuel is stored and the reactors operate in the once-through mode. However, strong sentiment remains for eventual reprocessing of this fuel when political and economical circumstances permit. Furthermore, a vigorous program to recycle fuel exists abroad, all of which invites a thorough comparison between the two options.

In the recycle mode of operation the plutonium and the residual uranium contained in the spent fuel can be recovered and recycled in various ways. In this analysis it was assumed that the plutonium from the spent fuel is used to make up for the consumed U-235 in part of the discharged fuel, and the remaining uranium is credited both for ore and SWU.

It is important to note that fuel cycle cost (mills/kwhr) varies linearly with the unit cost of all transactions [W2]. Hence we can write the general equations for the fuel cycle cost for the once-through and recycle modes in terms of the unit cost of each step as follows:

$$e_f\ (OT) = \sum_{i=1}^{5} a_i\ C_i \quad , \text{ mills/kwhr} \tag{4.1}$$

$$e_f\ (RC) = \sum_{i=6}^{13} a_i\ C_i \quad , \text{ mills/kwhr} \qquad (4.2)$$

where $C_i$ is the unit cost of the ith step (as numbered in table 4.1 , in which base case fuel cycle data are given) and the $a_i$'s are the cost coefficients, which depend on design parameters (e.g. $X_P$ , $V_F/V_M$ , number of batches, etc.)

From the output of the computer program developed during this study, the cost coefficients, $a_i$ (mills/kwhr per unit cost of the ith step), for a standard lattice 3- batch core with $X_P$ = 3.5 w/o were determined, as given below:

$a_1 = 0.10615$

$a_2 = 0.0376$

$a_3 = 0.03155$

$a_4, \ldots, a_9 = 0.00536$

$a_5, \ldots, a_{13} = 0.00198$

$-a_6, a_7 = 0.02758$

$a_8 = 0.02361$

$a_{10} = -0.00266$

$a_{11} = -0.0058$

$a_{12} = -0.06284$

TABLE 4.1

Base Case Fuel Cycle Data

| Step # | Transaction | Unit cost ($C_i$) | Lead or Lag time* $t_i$ (Yrs) |
|---|---|---|---|
| 1 | Yellowcake ($U_3O_8$) purchase | 25 $/lb | -1.5 |
| 2 | Conversion to $UF_6$ | 5 $/kg | -1.0 |
| 3 | Enrichment | 140 $/kg SWU | -1.0 |
| 4 | Fabrication | 200 $/kg | -0.5 |
| 5 | Indefinite storage | 150 $/kg | +1.0 |
| 6 | Credit for elimination of indefinite storage | 150 $/kg | -1.5 |
| 7 | Reprocessing (including transportation) | 600 $/kg | -1.5 |
| 8 | Disposal of wastes from reprocessed fuels | 150 $/kg | -0.5 |
| 9 | MOX fabrication | 570 $/kg | -0.5 |
| 10 | Enrichment credit | 140 $/kg | -0.5 |
| 11 | Conversion credit | 5 $/kg | -0.5 |
| 12 | $U_3O_8$ credit | 25 $/lb | -0.5 |
| 13 | Indefinite storage | 150 $/kg | +1.0 |

*Lead time (-) is time before start of irradiation and lag time (+) is time after end of irradiation.

TABLE 4.2

Reference Case Economic Parameters

| | |
|---|---|
| Tax rate, $\tau$ | 50% |
| Bond-holder fraction, $f_b$ | 0.5 |
| Stock-holder fraction, $f_s$ | 0.5 |
| Return to Bond-holder, $r_b$ | 10% |
| Return to Stock-holder, $r_s$ | 15% |
| Discount rate*, X | 10% |

* $X = (1-\tau)\ f_b\ r_b + f_s\ r_s$

These cost coefficients represent the relative importance of various processes to fuel cycle cost, as explained in the following section.

## 4.3 Sensitivity Analysis of Fuel Cost

To examine how sensitive the fuel cycle is to each cost component, a sensitivity study was performed using the equations developed in the previous section. The relative importance of various processes to fuel cycle cost was determined by calculating the price increase, $\Delta C_i$ , in each process that would raise fuel cycle cost by 1 mill/kwhr. Sensitivity coefficients, $S_i$ , were then defined as

$$S_i = \frac{\Delta C_i}{C_i} \times 100 \quad , \tag{4.3}$$

which is the percent increase in $C_i$ that would increase $e_f$ by 1 mill/kwhr. The sensitivity parameters determined in this manner for the important steps in the LWR fuel cycle are shown in table (4.3).

From these sensitivity coefficients we can see that fuel cycle cost is very sensitive to reprocessing cost. A change of only 6% in the base value of the cost of reprocessing will change the fuel cycle cost by 1 mill/kwhr. Enrichment and MOX fabrication follow reprocessing in order of relative importance to fuel cycle cost. Estimates for these costs reported in

TABLE 4.3

Sensitivity Parameters for Various Fuel Cycle Transactions*

| Transaction | Change in unit cost to change fuel cost by 1 mill/kwhr $\Delta C_i$ | Sensitivity Coefficient $Si = \frac{\Delta C_i}{C_i} \times 100$ (%) |
|---|---|---|
| Ore ($U_3O_8$) purchase | 9.42 $/lb | 37.68 |
| Enrichment | 31.70 $/kg SWU | 22.64 |
| $UO_2$ Fabrication | 186.57 $/kg HM | 93.28 |
| Reprocessing | 36.26 $/kg HM | 6.04 |
| MOX Fabrication | 186.57 $/kg HM | 32.73 |
| $U_3O_8$ Credit in recycle mode | 15.91 $/lb | 63.64 |
| Waste disposal | 505.05 $/kg HM | 336.67 |

*Base case unit cost values are given in table 4.1.

the recent literature are documented in tables (4.4), (4.5) and (4.6). The effects of variation in these costs on the once-through and recycle modes are illustrated in the following "breakeven" case studies.

## 4.4 Case Study Results

### 4.4.1 Once-through Versus Recycle Mode "Breakeven"

The question here is whether the added cost of recovering and recycling the plutonium and uranium would be more or less than the saving that results from the reduced requirement for uranium and enrichment. To answer this question, which depends on a number of economic and technical parameters, the results of a "breakeven" comparison of the once-through and recycle modes are presented in this section, the breakeven point being defined in terms of the value of a selected variable which results in equivalence between the alternatives.

The breakeven cost of any transaction can be calculated by treating the cost of that step as variable and specifying all other unit costs. Then, equating the fuel cycle cost from Eqs. (4.1) and (4.2) will give the breakeven cost of the key variable.

TABLE 4.4

Recent Reprocessing Cost Estimates*

| Unit Cost, $/kg | Reference |
|---|---|
| 650 | British Nuclear Fuel LTD (BNFL), Nuclear Fuel (NF), March 15, 82 |
| 560 | French, NF, Nov. 8, 82 |
| 800 | BNFL, NF, March 28, 83 |
| 936 | French, NF, Nov. 21, 83 |
| 8000 | German, NF, Nov. 7, 83 |
| 666-to-888 | Japanese, NF, March 26, 84 |
| 400 | BNFP (US), NF, April 23, 84 (Expected) |
| 800 | EPRI case study, NF, April 23, 84 |
| 1000 | Bertram Wolfe's estimate, NF, Jan. 31, 83 |
| 700 | BNFL, NF, May 21, 84 |
| 900 | French current price, NF, July 16, 84 |
| 600 | Base case for present studies |

*Exact contractual reprocessing costs are generally confidential.

TABLE 4.5

Recent Mixed Oxide (MOX) Fabrication Cost Estimates

| Unit Cost ($/kg HM) | Reference |
|---|---|
| 500 + $UO_2$ Fabrication cost | German, NF, Nov. 22, 82 |
| 4.5 times $UO_2$ Fabrication | Belgian, NF, May 10, 82 |
| 3.5 times the $UO_2$ Fabrication cost | Bertram Wolfe, NF, Jan. 31, 83 |
| Two to three times the cost of $UO_2$ fuel fabrication | EPRI Studies, NF, Aug. 1, 83 |
| 770 | EPRI reference fuel cost, Sandberg's analysis, NF, April 23, 84 |
| 570 | Base case for present studies |

TABLE 4.6

Future Enrichment Cost Estimates

| Cost ($/kg SWU) | Process | Reference |
|---|---|---|
| 25 to 30 | AVLIS | DOE, NF, May 10, 82 |
| 25 to 60 | AVLIS | DOE, NF, March 28, 83 |
| 30 to 40 | AVLIS | Manson Benedict (MIT), NF, Dec. 19, 83 |
| 50 to 60 | GCEP Set V | Manson Benedict (MIT), NF, Dec. 19, 83 |
| 25 | AVLIS | John Simpson (Westinghouse report), NF, Feb. 13, 84 |
| 16 to 33 (most probable 20) | AVLIS | Emmett (Lawrence Livermore), NF, March 12, 84 |
| 60 (in 1986 dollars) | GD | John Longnecker (DOE), NF, Sept. 10, 84 |

As an example, the fuel cycle cost as a function of ore cost for the once-through and recycle modes can be written as

$$e_f\ (OT) = b_1 + 0.10615\ C_1 \qquad (4.4)$$

$$e_f\ (RC) = b_2 - 0.06284\ C_1 \qquad (4.5)$$

where $b_1$ and $b_2$ are independent of ore cost, but linearly dependent on the other unit costs (as in Eqs. (4.1) and (4.2) ).

Thus the breakeven cost of ore, $C_{1b}$ , is

$$C_{1b} = (b_2 - b_1) \ / \ 0.169 \quad \$/lb\ U_3O_8 \qquad (4.6)$$

The values of $b_1$ , $b_2$ and $C_{1b}$ , for different enrichments, reprocessing and MOX fabrication costs have been calculated, as shown in table (4.7). Figures (4.1) and (4.2) also show the breakeven ore cost (point of intersection) for various unit cost values in the range of interest.

It can be seen from table 4.7 that for an equal incremental change in the cost of a particular transaction, the breakeven point moves by a fixed amount irrespective of the cost of other transactions. This is because the transaction costs are linearly independent in Eqs. 4.1 and 4.2 . Thus, for example, the lines representing fuel cycle cost versus ore cost in Figures 4.1 and 4.2 are parallel. A decrease of 4.94 \$/kg SWU in SWU cost or an increase of 6.13 \$/kg HM in reprocessing cost or a 31.75 \$/kg HM increase in MOX fabrication cost will increase the breakeven cost by 1 \$/lb $U_3O_8$ . The

TABLE 4.7

Breakeven Cost of Ore as a Function of Other Transaction Costs

| Enrichment cost $/kg SWU ($C_3$) | Reprocessing cost $/kg HM ($C_7$) | MOX Fabrication cost $/kg HM ($C_9$) | $b_1$ in Eq.4.4 mills/kwhr | $b_2$ in Eq.4.5 mills/kwhr | Breakeven cost of ore $C_{1b}$ $/lb $U_3O_8$ |
|---|---|---|---|---|---|
| 140 | 600 | 500 | 5.972 | 18.513 | 74.20 |
| | | 700 | 5.972 | 19.579 | 80.51 |
| | 900 | 500 | 5.972 | 26.787 | 123.17 |
| | | 700 | 5.972 | 27.853 | 129.47 |
| 100 | 600 | 500 | 4.711 | 18.620 | 82.30 |
| | | 700 | 4.711 | 19.686 | 88.61 |
| | 900 | 500 | 4.711 | 26.894 | 131.26 |
| | | 700 | 4.711 | 27.960 | 137.57 |
| 50 | 600 | 500 | 3.134 | 18.754 | 92.43 |
| | | 700 | 3.134 | 19.820 | 98.73 |
| | 900 | 500 | 3.134 | 27.028 | 141.38 |
| | | 700 | 3.134 | 28.094 | 147.67 |

Unit costs of transactions not specified in the above table are the base case values given in table 4.1.

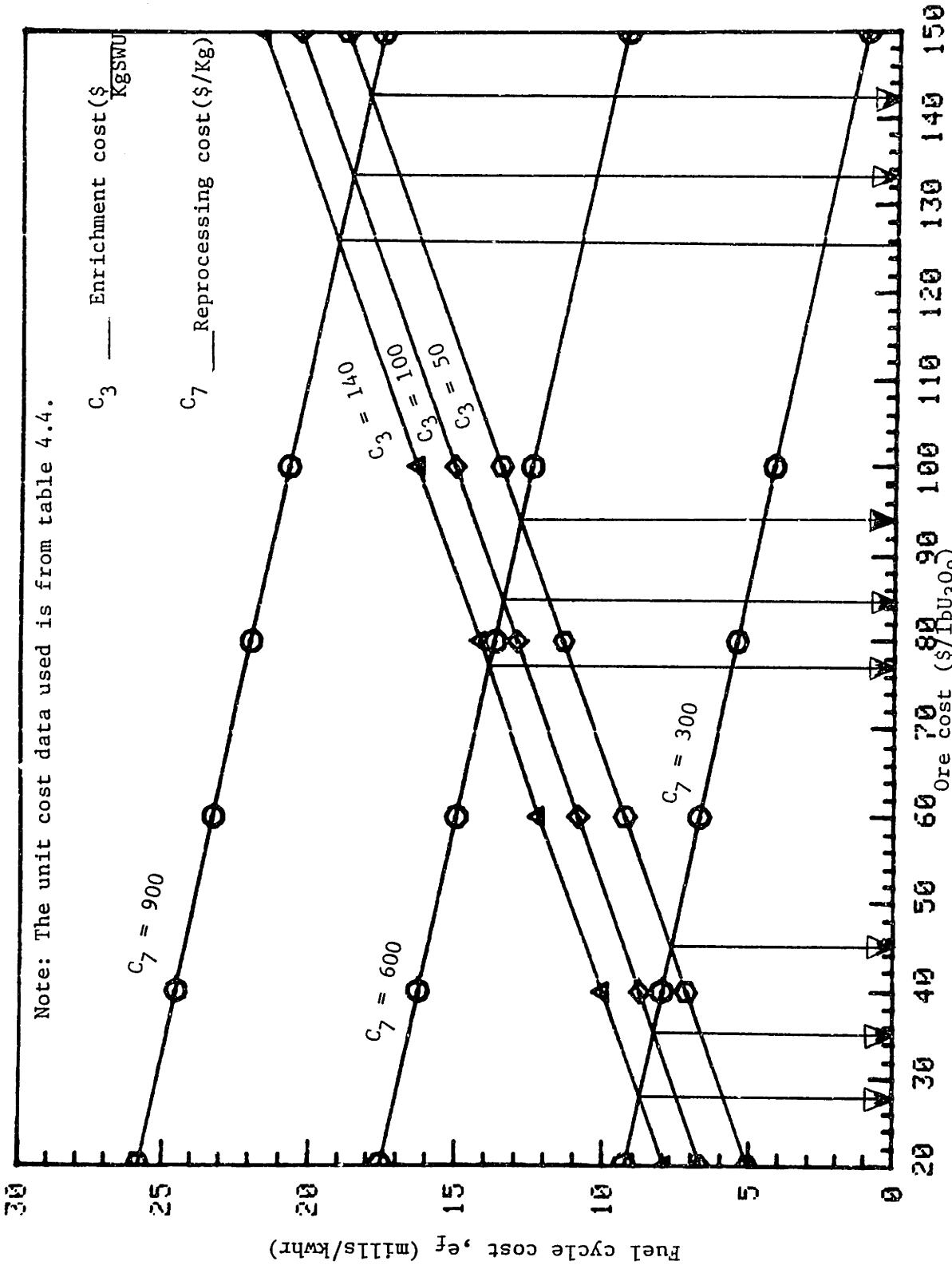


Fig. 4.1 Breakeven ore cost versus fuel cycle cost for various enrichment and reprocessing costs.

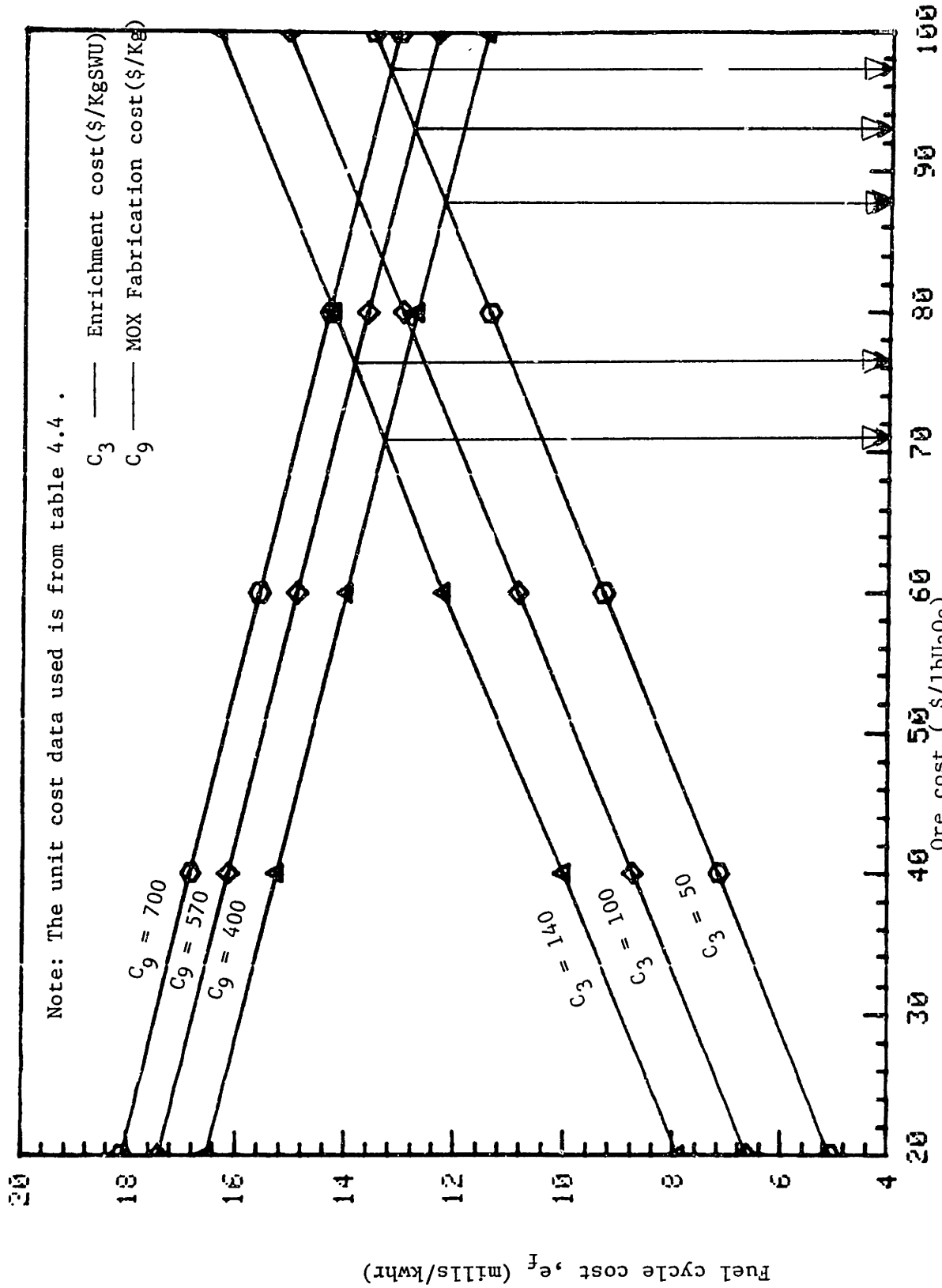


Fig. 4.2 Breakeven ore cost versus fuel cycle cost for various enrichment and MOX fabrication costs.

following equation gives the breakeven cost of ore as a function of the cost of the individual process steps:

$$C_{1b} = \frac{C_7}{6.13} + \frac{C_9}{31.75} - \frac{C_3}{4.94} - 11.09 \ , \ \$/lb\ U_3O_8 \tag{4.7}$$

The denominators on the righthand side of Eq. (4.7) can be calculated as:

$$di = \frac{a_1 - a_{12}}{a_i} \ , \ \frac{\$/kg}{\$/lb\ U_3O_8} \tag{4.8}$$

Note, however, that for calculation of $d_3$ the value of $a_i$ is not simply $a_3$ , it is rather $a_3 - a_{10}$ , to include the credit from SWU savings.

It can be seen from Fig. (4.1), and can also be calculated from Eq. (4.7), that recycling (using our base case cost data) will not be economic unless the ore cost is more than 76.4 \$/lb $U_3O_8$ : about four times todays spot market value. Equation (4.7) is a useful relation for predicting the break-even cost of ore as future unit costs evolve; and this break-even value can be translated (with an ore resource/cost model - to be discussed later in this chapter) into the time at which recycling makes economic sense.

Similarly, we can make trade-off studies for other fuel cycle processing costs by treating the cost in question as an unknown, and solving Eqs. (4.1) and (4.2) for the breakeven

value of this variable: the value for which both of these equations give the same fuel cycle cost.

### 4.4.2 Extended Burnup

At present, fuel is discharged from a typical LWR after it has achieved a batch-average burnup ranging between 30 and 35 GWD/MT . The optimum burnup with respect to fuel cycle cost also lies in this range, as shown in Fig. 4.3 . Beyond this optimum point the fuel cycle cost increases due to the increase in carrying charges, which can be seen from table 4.8 . Thus the incentive to extend the burnup is not the decrease in fuel cost; it is, rather, to increase the plant capacity factor and to thereby improve the overall economics of the energy generation system. Analyzed from this perspective, the benefits from increased reactor availability exceed the penalty due to carrying charges, up to the point where the carrying charges on the more highly enriched fuel offset the saving in the replacement energy cost. Figure 4.4 shows that the optimum burnup with respect to busbar and system cost is much higher than the current burnup levels.

A straightforward method to increase burnup is to increase the fuel residence time in the core. This can be accomplished either by increasing the cycle length and maintaining the batch size (which requires increasing reload enrichment), or

TABLE 4.8

Fuel Cycle Cost, Busbar Cost and System Cost for a 3-batch Core on the Once-through Fuel Cycle

| B $\left(\frac{GWD}{MT}\right)$ | $X_p$ (w/o) | L | Direct Cost DC mills/kwhr | Carrying Charges CC mills/kwhr | $e_f$ mills/kwhr | $e_b$ mills/kwhr | $e_s$* mills/kwhr |
|---|---|---|---|---|---|---|---|
| 10 | 1.74 | 0.5648 | 9.58 | 2.14 | 11.72 | 55.98 | 59.91 |
| 20 | 2.48 | 0.6621 | 6.63 | 2.30 | 8.93 | 46.69 | 52.88 |
| 30 | 3.22 | 0.7025 | 5.71 | 2.67 | 8.38 | 43.96 | 50.22 |
| 33 | 3.44 | 0.7104 | 5.55 | 2.79 | 8.34 | 43.53 | 49.75 |
| 35 | 3.59 | 0.7149 | 5.45 | 2.88 | 8.33 | 43.30 | 49.48 |
| 40 | 3.96 | 0.7246 | 5.27 | 3.10 | 8.37 | 42.87 | 48.97 |
| 50 | 4.33 | 0.7322 | 5.02 | 3.58 | 8.60 | 42.45 | 48.35 |
| 60 | 5.44 | 0.7481 | 4.86 | 4.08 | 8.95 | 42.36 | 48.07 |
| 70 | 6.18 | 0.7551 | 4.76 | 4.62 | 9.38 | 42.48 | 48.00 |
| 75 | 6.55 | 0.7580 | 4.71 | 4.90 | 9.61 | 42.59 | 48.02 |

*Replacement energy cost, $e_r$ = 65 mills/kwhr.

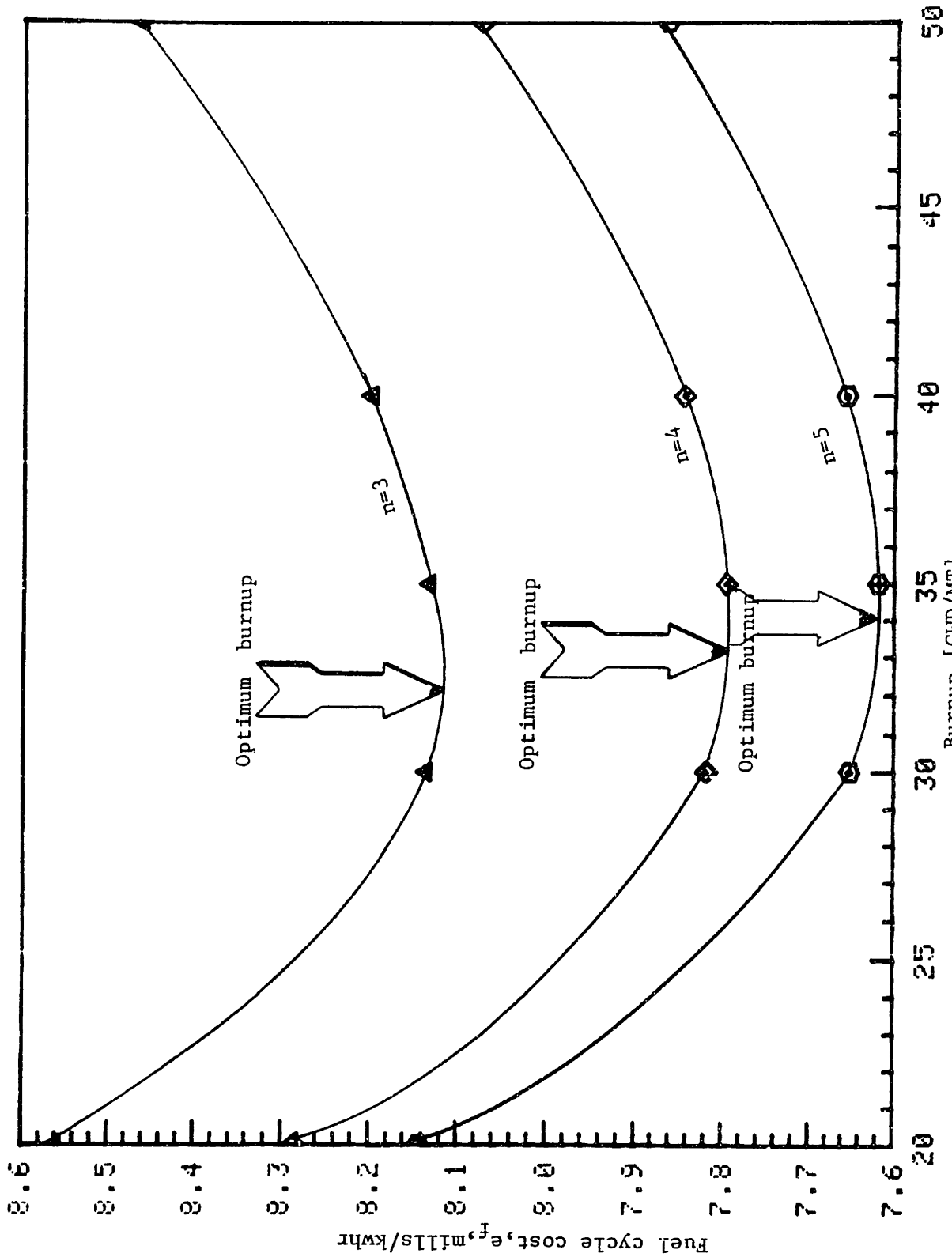


Fig.4.3 Optimum burnup with respect to fuel cycle cost for various number of batches.

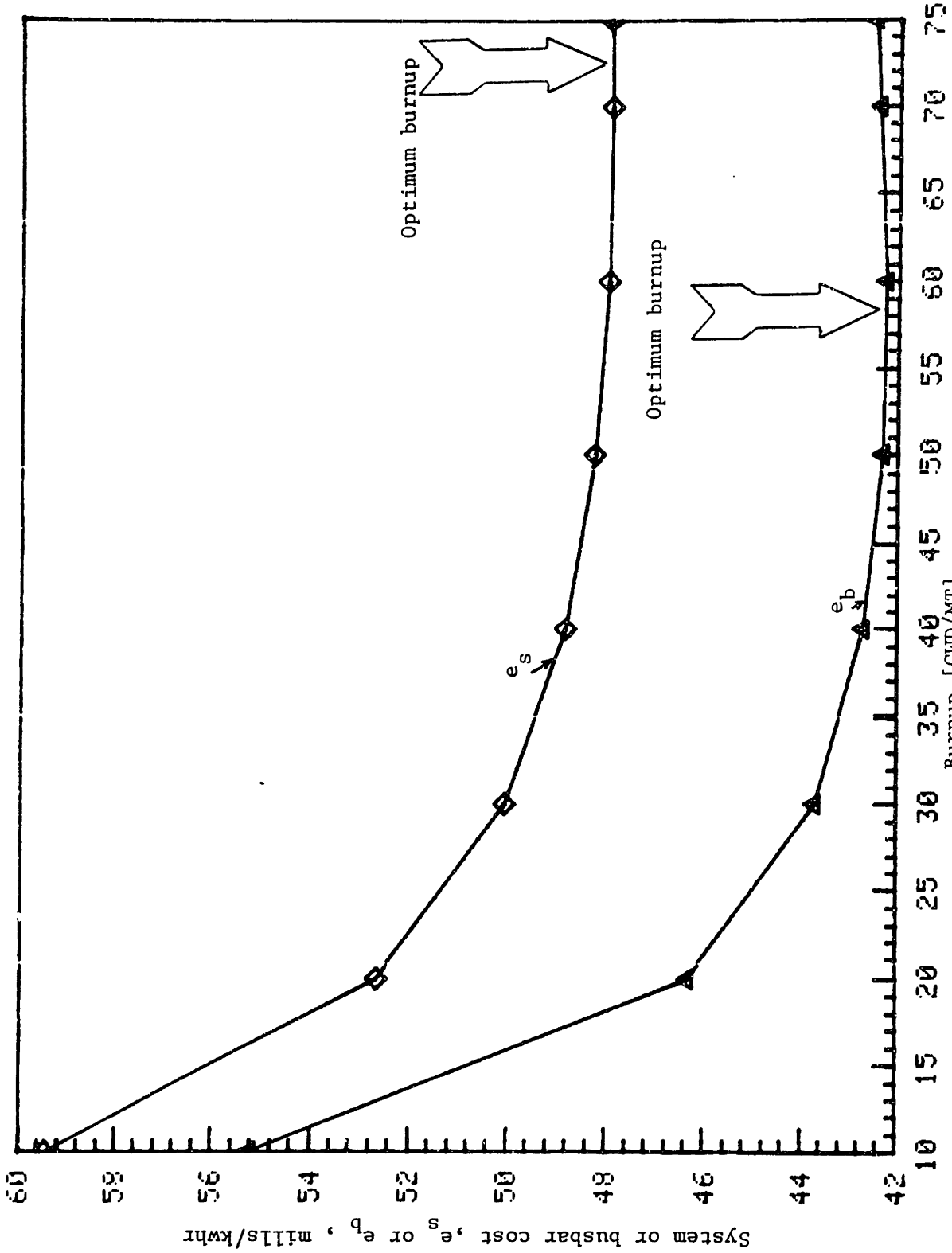


Fig.4.4 Optimum burnup with respect to busbar and system cost.

maintaining the cycle length and increasing the number of batches (at fixed enrichment). More batches (with shorter cycles) will reduce carrying charges, and prove advantageous if the only intent is to decrease fuel cycle cost, as shown in Fig. 4.5 . But the concurrent increase in refueling frequency introduces undesireable downtime, and the system cost increases, as shown in Fig. 4.6 . Since utilities aim to minimize overall system cost, it is doubtful that utilities would adopt options that sacrifice availability.

In view of the above considerations, the alternative that has been considered for burnup extension in the remainder of this discussion is an increase in fuel enrichment. In this regard, it would be very useful to provide the reactor fuel manager with a simple methodology to assess the impact of changes in the economical and technical variables on the extended burnup cycles, as was done for an average burnup cycle in the previous section.

The cost coefficients ($a_i$) in Eqs. (4.1) and (4.2) for various enrichments are tabulated in table 4.10 . As mentioned earlier, these cost coefficients represent the relative importance of various processes to fuel cycle cost, and can be used to determine the breakeven cost of any process, the change in the breakeven value resulting from a specified change in the cost of a particular transaction, and many like applications.

TABLE 4.9

Energy Production Costs for the Once-through Cycle

| n number of batches | $T_c$ ($Y_r$) | $X_P$ w/o | B GWD/MT | $e_f$ mills/kwhr | $e_b$ mills/kwhr | $e_s$ mills/kwhr | L |
|---|---|---|---|---|---|---|---|
| 3 | 0.5 | 1.93 | 12.50 | 10.20 | 51.86 | 57.12 | 0.60 |
| | 1.0 | 3.16 | 29.15 | 8.43 | 44.15 | 50.40 | 0.70 |
| | 1.5 | 4.39 | 45.80 | 8.65 | 42.74 | 48.67 | 0.73 |
| | 2.0 | 5.63 | 62.46 | 9.29 | 42.62 | 48.21 | 0.75 |
| 4 | 0.5 | 2.16 | 16.65 | 8.97 | 50.64 | 56.39 | 0.60 |
| | 1.0 | 3.70 | 38.86 | 8.11 | 43.83 | 50.18 | 0.70 |
| | 1.5 | 5.20 | 61.07 | 8.78 | 42.87 | 48.77 | 0.73 |
| | 2.0 | 6.78 | 83.28 | 9.83 | 43.16 | 48.62 | 0.75 |
| 5 | 0.5 | 2.39 | 20.82 | 8.33 | 50.00 | 56.00 | 0.60 |
| | 1.0 | 4.24 | 48.58 | 8.12 | 43.83 | 50.18 | 0.70 |
| | 1.5 | 6.09 | 76.34 | 9.20 | 43.21 | 49.08 | 0.73 |
| | 2.0 | 7.94 | 104.10 | 10.67 | 44.00 | 49.25 | 0.75 |

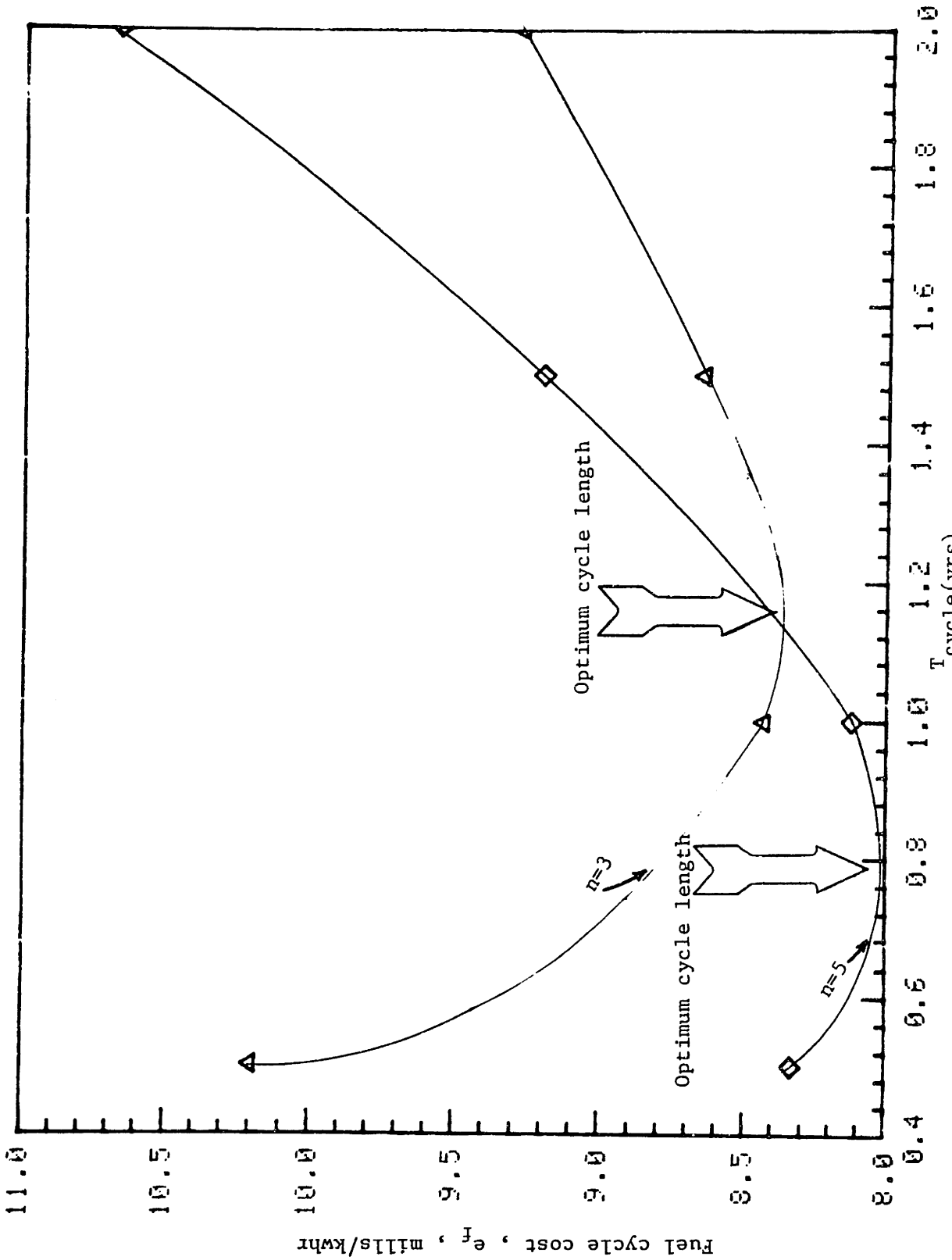


Fig. 4.5 Optimum fuel cycle length as determined by fuel cycle cost.

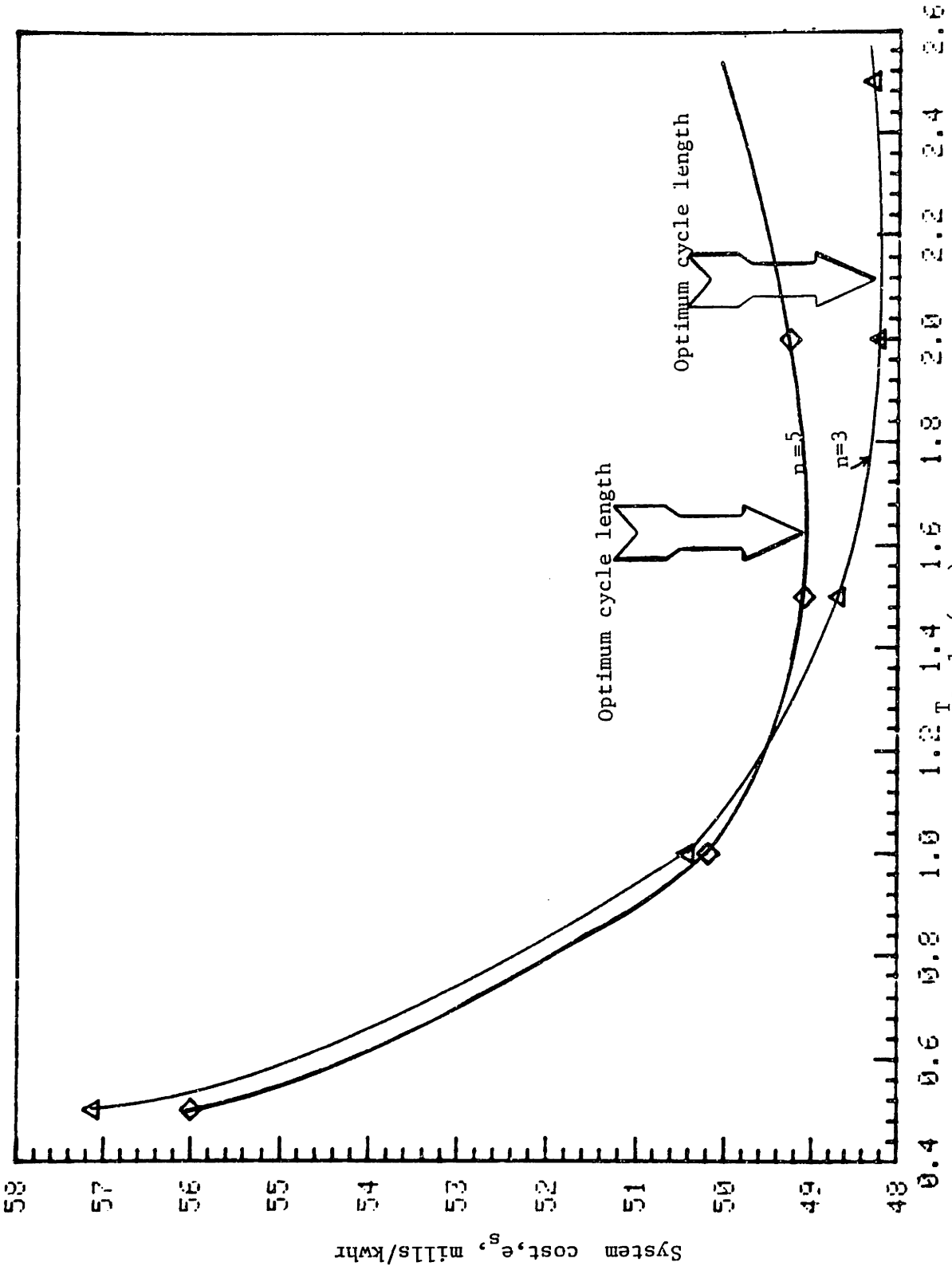


Fig.4.6 Optimum cycle length as determined by system cost for three-batch and five-batch cores.

TABLE 4.10

Cost Coefficients for Various Enrichments

| Enrichment (w/o) / Coefficients | 2.5 | 3.0 | 3.5 | 4.0 | 4.5 | 5.0 |
|---|---|---|---|---|---|---|
| $a_1$ | 0.11232 | 0.10748 | 0.10615 | 0.10660 | 0.10812 | 0.11036 |
| $a_2$ | 0.03980 | 0.03800 | 0.03760 | 0.03780 | 0.03840 | 0.03920 |
| $a_3$ | 0.02848 | 0.02991 | 0.03155 | 0.03330 | 0.03512 | 0.03700 |
| $a_4$, $a_9$ | 0.00808 | 0.00637 | 0.00536 | 0.00468 | 0.00421 | 0.00386 |
| $a_5$, $a_{13}$ | 0.00386 | 0.00268 | 0.00198 | 0.00151 | 0.00119 | 0.00095 |
| $-a_6$, $a_7$ | 0.04179 | 0.03261 | 0.02758 | 0.02436 | 0.02205 | 0.02022 |
| $a_8$ | 0.03555 | 0.02784 | 0.02361 | 0.02091 | 0.01898 | 0.01745 |
| $a_{10}$ | +0.00130 | -0.00179 | -0.00266 | -0.00288 | -0.00264 | -0.00204 |
| $a_{11}$ | -0.00140 | -0.00440 | -0.00580 | -0.00620 | -0.00580 | -0.00500 |
| $a_{12}$ | -0.07568 | -0.06792 | -0.06284 | -0.05844 | -0.05384 | -0.04876 |

Correlations for these cost coefficients in terms of enrichment have been developed by curve-fitting the data from table 4.1 as follows:

$$a_1(X_P) = 0.211842 - 0.07424\,X_P - 0.016743\,X_P^2 - 0.00119\,X_P^3 \qquad (R^2 = 0.997) \qquad (4.9)$$

$$a_3(X_P) = 0.02184\,e^{0.10539\,X_P} \qquad (R^2 = 0.9998) \qquad (4.10)$$

$$\left.\begin{matrix} a_4(X_P) \\ a_9(X_P) \end{matrix}\right\} = -0.0005 + \frac{0.021}{X_P} \qquad (R^2 = 0.992) \qquad (4.11)$$

$$\left.\begin{matrix} a_5(X_P) \\ a_{13}(X_P) \end{matrix}\right\} = 0.02457\,X_P^{-2.01506} \qquad (R^2 = 0.9999) \qquad (4.12)$$

$$\left.\begin{matrix} a_6(X_P) \\ a_7(X_P) \end{matrix}\right\} = -0.00194 + \frac{0.10656}{X_P} \qquad (R^2 = 0.990) \qquad (4.13)$$

$$a_8(X_P) = -0.00115 + \frac{0.08943}{X_P} \qquad (R^2 = 0.990) \qquad (4.14)$$

$$a_{12}\ (X_P) = -0.11447\ e^{-0.16957} \qquad (R^2 = 0.996) \qquad (4.15)$$

$$\text{For } 2.5 \leq X_p \leq 5.0 \text{ (w/o)}$$

In the calculation of the breakeven ore cost, $a_1$ and $a_{12}$ appear in sum form; the following simple curve-fit formula gives the value of $a_1 + a_{12}$ as a function of $X_P$ ,

$$a_1 + a_{12} = \frac{X_P}{a + b\ X_P} \qquad (4.16)$$

in which a = -4.61836 and b = 7.20532. This expression is quite accurate: the goodness of fit measure $R^2 = 0.991$.

For breakeven calculation a general form of Eq. 4.7 can be devised:

$$C_{1b} = \frac{C_7}{d_7} + \frac{C_9}{d_9} - \frac{C_3}{d_3} - C_o \quad , \$/\text{lb } U_3O_8 \qquad (4.17)$$

The values of $d_i$ , $C_o$ and $C_{1b}$ for various enrichments are documented in table (4.11).

The breakeven cost of ore for the once-through and recycle modes for various enrichments (hence burnups) is shown in Fig. 4.7. As can be seen, the breakeven cost of ore is lower for higher burnup values (attained through increased enrichments) i.e., recycle will be likely to turn a profit sooner compared to low burnup fueling, since uranium prices need to rise to a lower value before the breakeven price is reached.

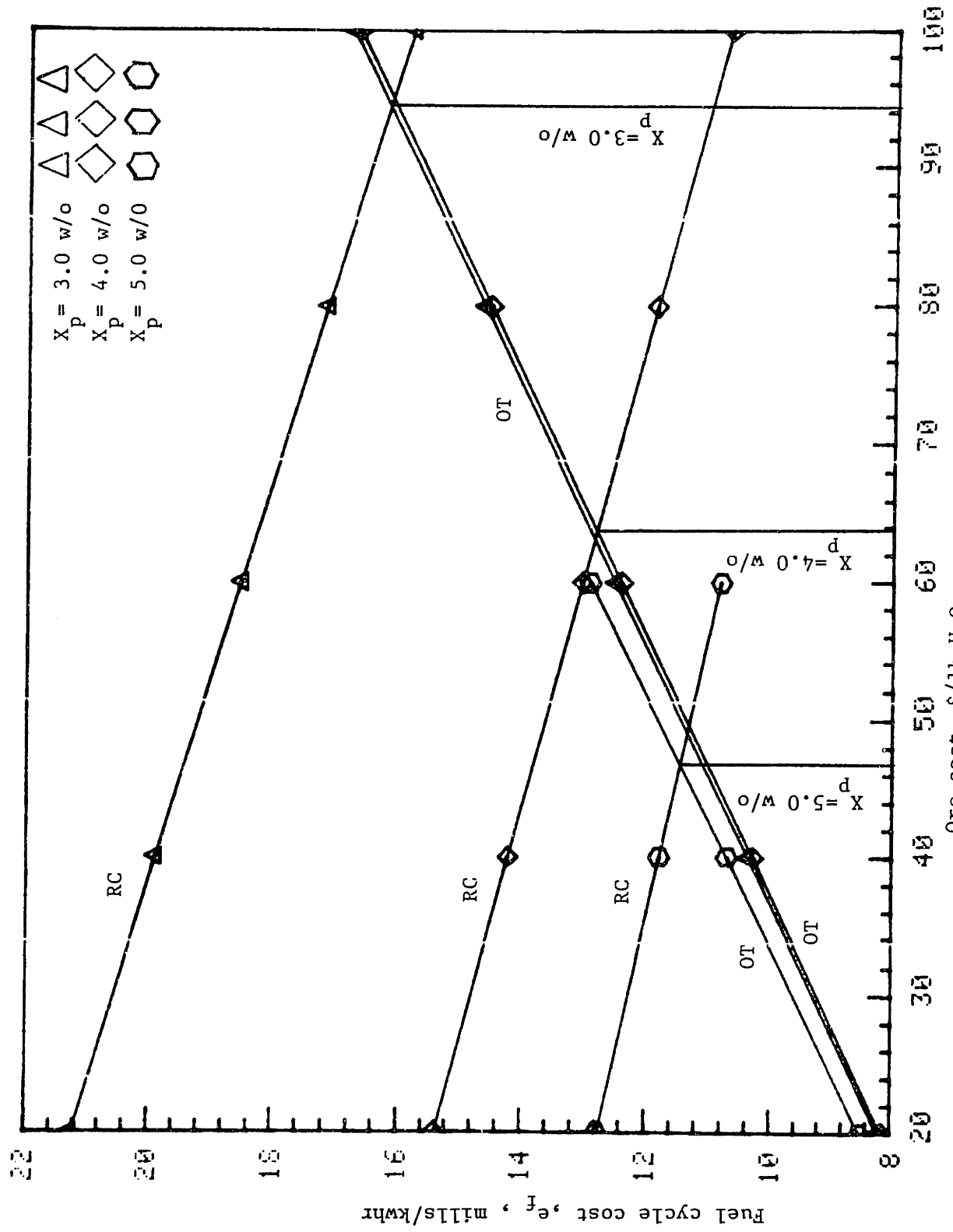


Fig.4.7 Breakeven ore cost for various reload enrichments.

Table. 4.11

Coefficients of breakeven equation,(4.17).

| $X_p$ w/o | $d_3$ | $d_7$ | $d_9$ | $C_0$ |
|---|---|---|---|---|
| | \$/kg / \$/lb $U_3O_8$ | | | \$/lb $U_3O_8$ |
| 3.0 | 5.53 | 5.38 | 27.53 | 12.55 |
| 3.5 | 4.94 | 6.13 | 31.53 | 11.15 |
| 4.0 | 4.56 | 6.77 | 35.26 | 10.14 |
| 4.5 | 4.29 | 7.35 | 38.47 | 9.41 |
| 5.0 | 4.08 | 7.87 | 41.22 | 8.85 |

This is because the fissile content of high burnup discharged fuel is higher, due to the presence of more fissile plutonium and a higher content of unburned U-235. Also, for high enrichments, plutonium is worth more than at low enrichments, as explained in Chapter 3. Thus, comparatively less fuel needs to be reprocessed to reconstitute a reload batch, which is indicated by a decrease in the cost coefficient of reprocessing, $a_7$ , in table 4.1 as enrichment increases.

Table 4.11 shows that the breakeven cost of ore for high burnup cases is more sensitive to enrichment cost and less sensitive to reprocessing and MOX fabrication costs, as compared to the low burnup case.

From table 4.10, the coefficient weighting the waste disposal cost for $X_p$ = 3.0 (w/o) is 0.00268 , which means that the 1 mill/kwhr disposal fee corresponds to paying 373.13 $/kghm. The waste disposal cost coefficient for a high burnup case, say for $X_p$ = 5.0 (w/o) , is 0.00095 , in which case a 1 mill/kwhr fee corresponds to 1052.6 $/kghm. Thus we can see that a 1 mill/kwhr fee constitutes a large disincentive for extending burnup.

### 4.4.3 More Batches in the Core

One way of increasing burnup as mentioned in the previous section, is to increase the number of batches in the core. More batches (at fixed enrichment) will reduce both fixed and carrying charges per unit energy and, hence, improve the fuel cycle cost. However, increasing the refueling frequency will penalize the overall cost of this option, unless refueling downtime can be reduced to maintain high reactor availability.

Fuel cycle cost coefficients as a function of the number of batches are shown in table 4.12. Figure 4.11 shows that the breakeven ore cost for the once-through versus the recycle-mode will be increased by increasing the number of batches in the core. In other words, the once-through mode is favored when more staggered reload batches are employed in the core fuel management scheme. This is not likely to prove to be an important factor in future strategic decision-making because, as previously noted, more batches mean more (and costly) refueling downtime.

TABLE 4.12

Cost Coefficients as a Function of Number of Batches: $X_p$ = 3.5 w/o

| Cost Coefficients | n=3 | n=4 | n=5 | n=6 |
|---|---|---|---|---|
| $a_1$ | 0.106150 | 0.10200 | 0.099830 | 0.098700 |
| $a_2$ | 0.037631 | 0.03620 | 0.035435 | 0.035040 |
| $a_3$ | 0.031548 | 0.03030 | 0.029707 | 0.029373 |
| $a_4$ , $a_9$ | 0.005360 | 0.00516 | 0.005050 | 0.004500 |
| $a_5$ , $a_{13}$ | 0.001980 | 0.00177 | 0.001640 | 0.001550 |
| $-a_6$ , $a_7$ | 0.027580 | 0.02674 | 0.026320 | 0.026110 |
| $a_8$ | 0.023610 | 0.02292 | 0.022590 | 0.022430 |
| $a_{10}$ | 0.002660 | 0.00041 | -0.000830 | -0.001610 |
| $a_{11}$ | 0.005780 | 0.00247 | 0.000480 | -0.000850 |
| $a_{12}$ | 0.062860 | 0.05300 | 0.047150 | 0.043390 |

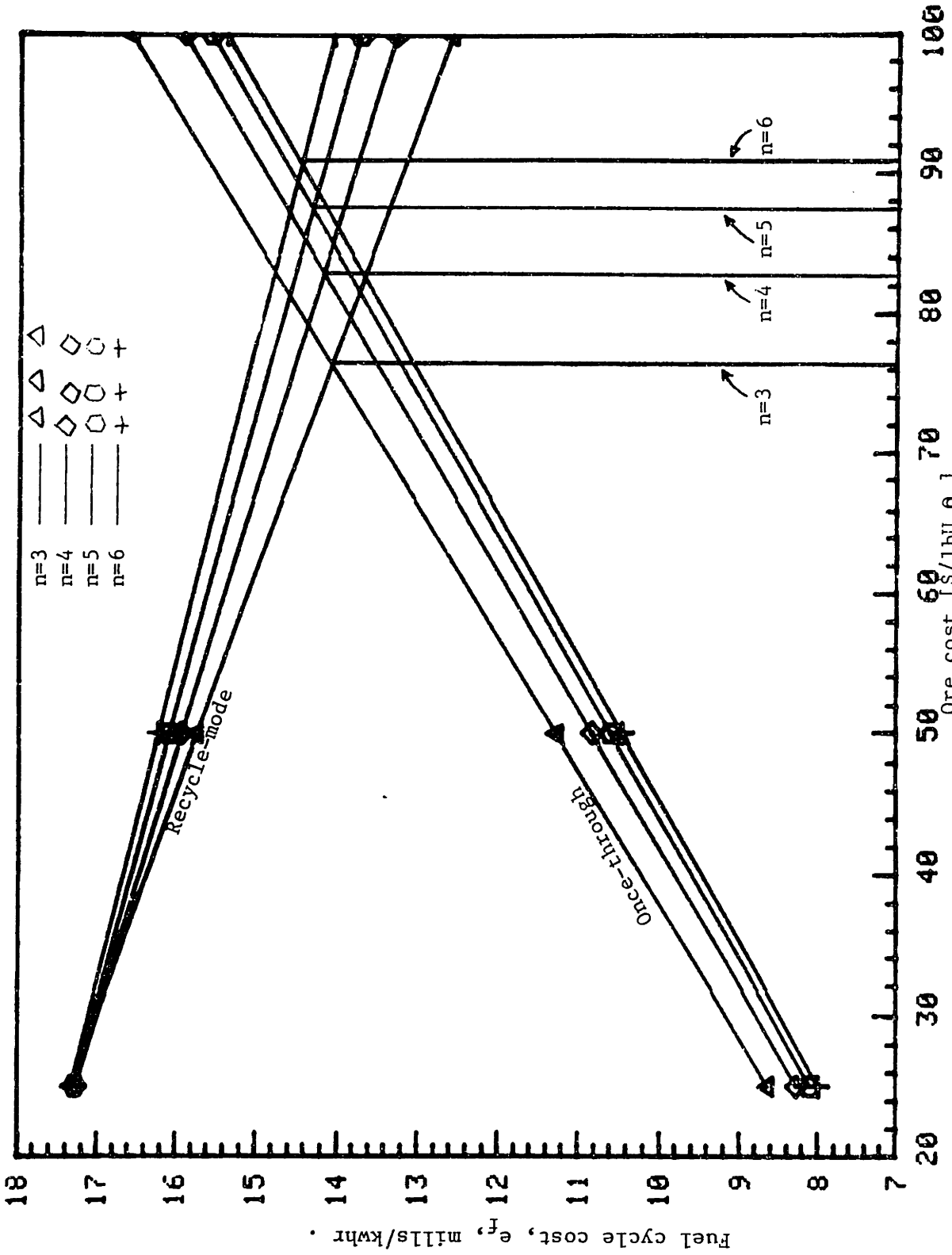


Fig. 4.8 Breakeven ore cost of once-through vs recycle-mode fuel cycle cost as a function of number of batches in the core .

### 4.4.4 Lower Enrichment Costs and Reduction in Tails Assay

Current enrichment technology commercially available in the U.S. is based on the gaseous diffusion method. Active research and development programs on gas centrifuge and advanced laser isotope separation (LIS) methods are underway. First generation centrifuge cascades are operational in Europe and under construction in the U.S. A centrifuge plant requires only 5% of the energy needed to run a diffusion plant of equal separative work output. The LIS process has lower capital costs and is highly selective as compared to either diffusion or centrifuge plants. Hence, while the cost of SWU from advanced centrifuges and LIS are not yet established, it is expected that these costs would be far below that of gaseous diffusion plants. Various recent estimates from the literature are presented in table 4.6.

One significant additional advantage of low cost LIS is that (because LIS is a one-stage process) it is ideal for further stripping the large stockpile of tails from gaseous diffusion plants to 0.047 w/o tails assay (from 0.2-0.3 w/o U-235).

In this section the effect of low enrichment costs and a reduction in tails' assay on the competitiveness of the

once-through LWR with its recycle mode of operation will be analyzed. The parameter "$d_i$" defined in Eq. 4.8 can be used to predict the variation of the breakeven cost of ore as a function of a change in the unit cost of the ith transaction. The cost coefficients $a_1$ , $a_3$ , $a_{10}$ and $a_{12}$ , required for the calculation of $d_3$ , are tabulated in table 4.13. Parameter $d_3$ , as defined earlier, is the change required in SWU cost to shift the breakeven ore cost by 1 \$/lb . For example, in our base case unit cost data, with $X_P = 3.5$ and $X_W = 0.2$ ; the breakeven cost of ore was calculated to be 76.4 \$/lb $U_3O_8$ . If the cost of enrichment is decreased to 50 \$/kg SWU , then the breakeven point will be increased by $\frac{140-50}{4.94} = 18.22$ \$/lb $U_3O_8$ and the new breakeven cost will be 94.62 \$/lb $U_3O_8$ .

In table 4.13, the pattern of variation of $d_3$ indicates that the breakeven ore cost is more sensitive to SWU cost at lower tails' assay and higher enrichments.

The shift in the breakeven cost of ore for various SWU costs at different tails' assay is shown in Figs. (4.9), (4.10) and (4.11) . As can be seen, the combination of cheap SWU and low tails assay can lead to breakeven ore cost in excess of 100 \$/lb $U_3O_8$ , which is over five times todays spot market price.

TABLE 4.13

Ore and Enrichment Cost Coefficients for the Fuel Cycle Cost for Various Values of $X_P$ and $X_w$

| $X_P$ (w/o) | $X_w$ (w/o) | $a_1$ mills/kwhr $/lb $U_3O_8$ | $a_3$ mills/kwhr $/kg SWU | $a_{10}$ mills/kwhr $/kg SWU | $a_{12}$ mills/kwhr $/lb $U_3O_8$ | $d_3 = \frac{a_1 - a_{12}}{a_3 - a_{10}}$ $\frac{\$/kg\ SWU}{\$/lb\ U_3O_8}$ |
|---|---|---|---|---|---|---|
| | 0.30 | 0.12888 | 0.02378 | -0.00118 | -0.07177 | 8.039 |
| | 0.25 | 0.11703 | 0.02647 | -0.00144 | -0.06963 | 6.688 |
| 3.0 | 0.20 | 0.10750 | 0.02991 | -0.00179 | -0.06790 | 5.533 |
| | 0.15 | 0.09966 | 0.03457 | -0.00228 | -0.06648 | 4.509 |
| | 0.10 | 0.09311 | 0.04154 | -0.00303 | -0.06528 | 3.554 |
| | 0.30 | 0.12798 | 0.02529 | -0.00181 | -0.06753 | 7.214 |
| | 0.25 | 0.11588 | 0.02803 | -0.00218 | -0.06494 | 5.985 |
| 3.5 | 0.20 | 0.10615 | 0.03155 | -0.00266 | -0.06286 | 4.940 |
| | 0.15 | 0.09816 | 0.03631 | -0.00333 | -0.06114 | 4.019 |
| | 0.10 | 0.09147 | 0.04344 | -0.00437 | -0.05970 | 3.162 |
| | 0.30 | 0.12905 | 0.02685 | -0.00198 | -0.06334 | 6.673 |
| | 0.25 | 0.11661 | 0.02968 | -0.00237 | -0.06062 | 5.530 |
| 4.0 | 0.20 | 0.10660 | 0.03330 | -0.00288 | -0.05844 | 4.562 |
| | 0.15 | 0.09838 | 0.03820 | -0.00359 | -0.05663 | 3.709 |
| | 0.10 | 0.09150 | 0.04554 | -0.00468 | -0.05511 | 2.919 |
| | 0.30 | 0.13131 | 0.02845 | -0.00182 | -0.05859 | 6.274 |
| | 0.25 | 0.11846 | 0.03138 | -0.00217 | -0.05596 | 5.199 |
| 4.5 | 0.20 | 0.10813 | 0.03512 | -0.00263 | -0.05384 | 4.291 |
| | 0.15 | 0.09964 | 0.04019 | -0.00328 | -0.05208 | 3.490 |
| | 0.10 | 0.09254 | 0.04778 | -0.00428 | -0.05060 | 2.750 |

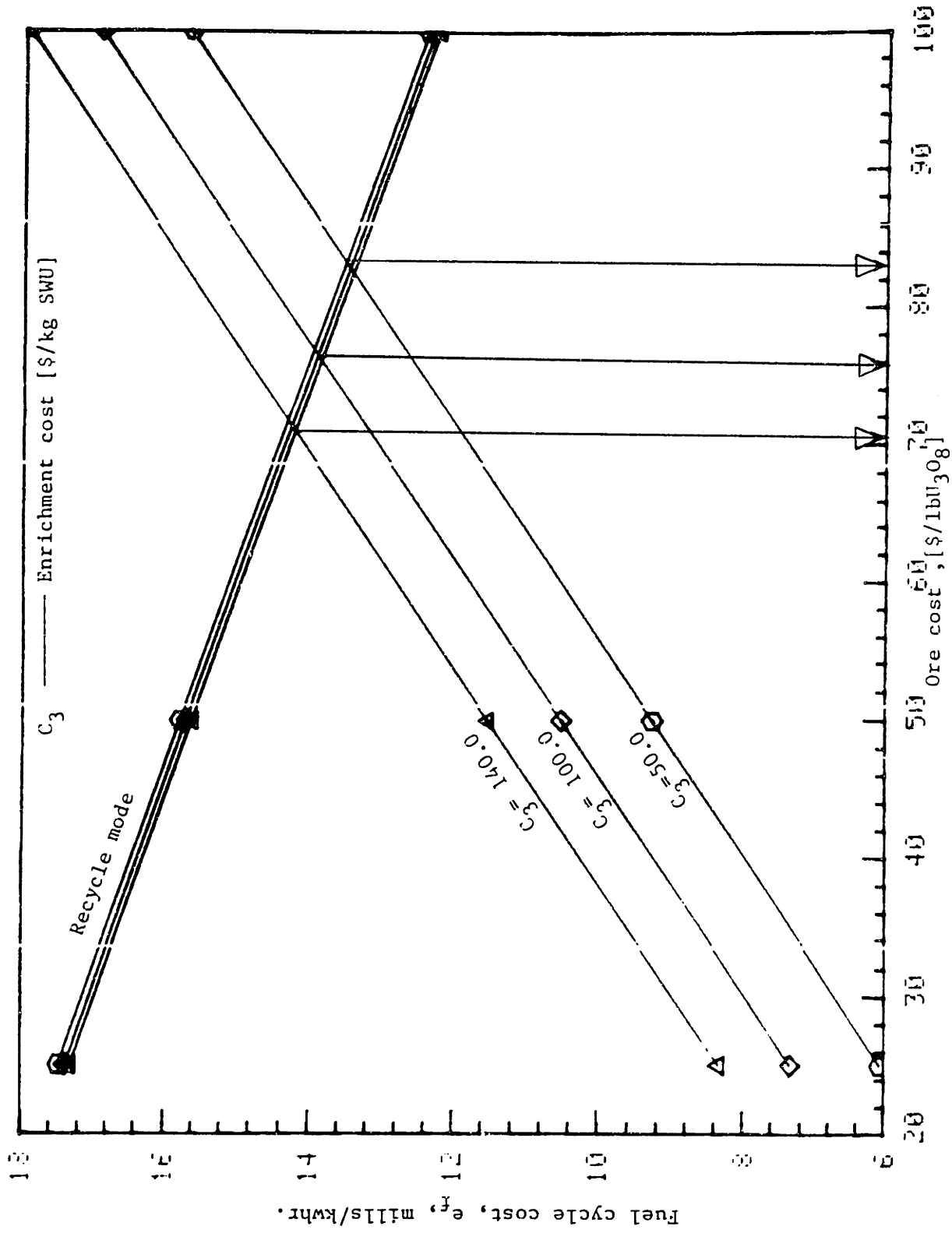


Fig.4.9 Breakeven ore cost of once-through vs recycle-mode fuel cycle cost for various enrichment costs; $X_w$= 0.3 w/o .

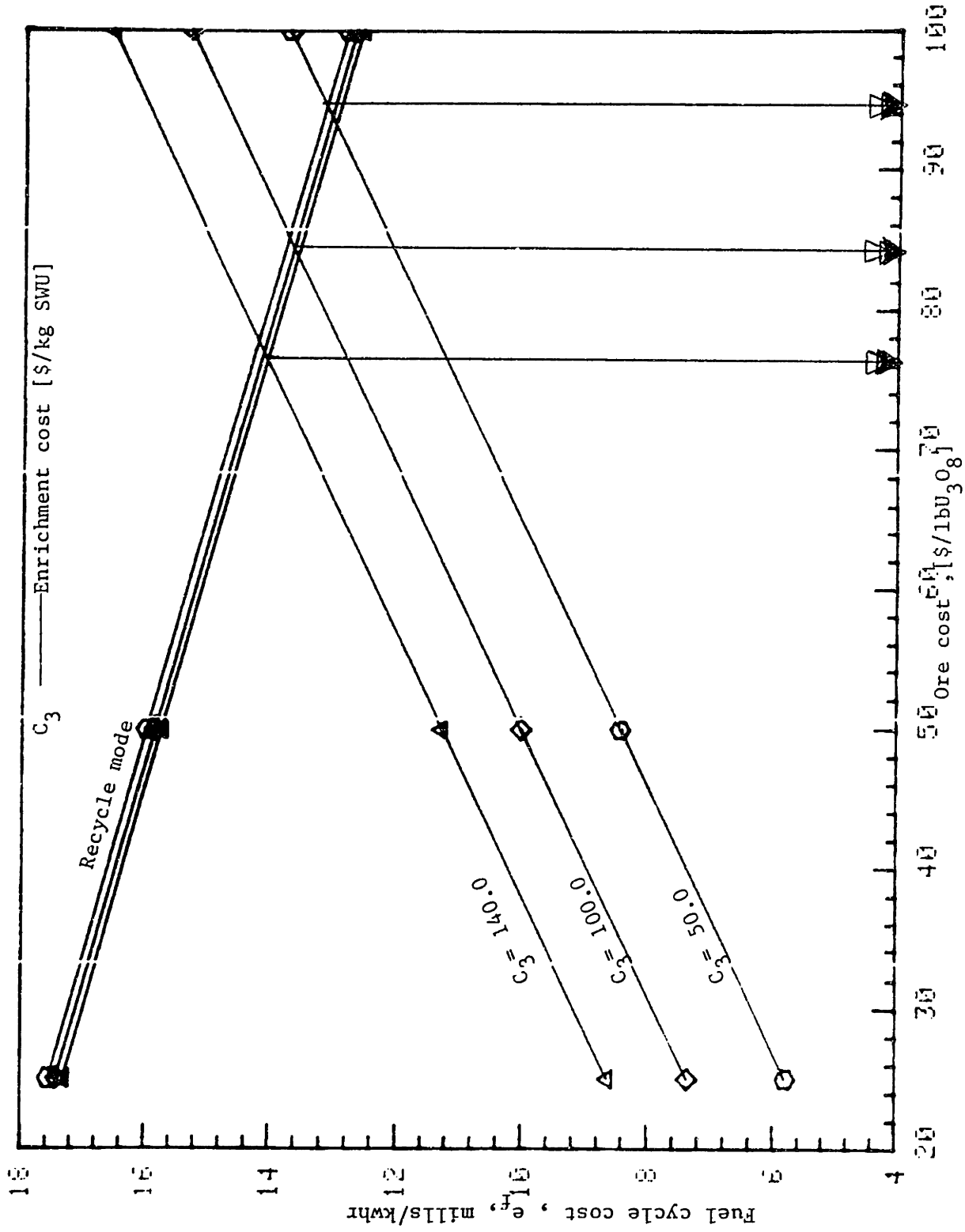


Fig.4.10Breakeven ore cost of once-through vs recycle-mode fuel cycle cost for various enrichment costs: $X_w$ = 0.2 w/o .

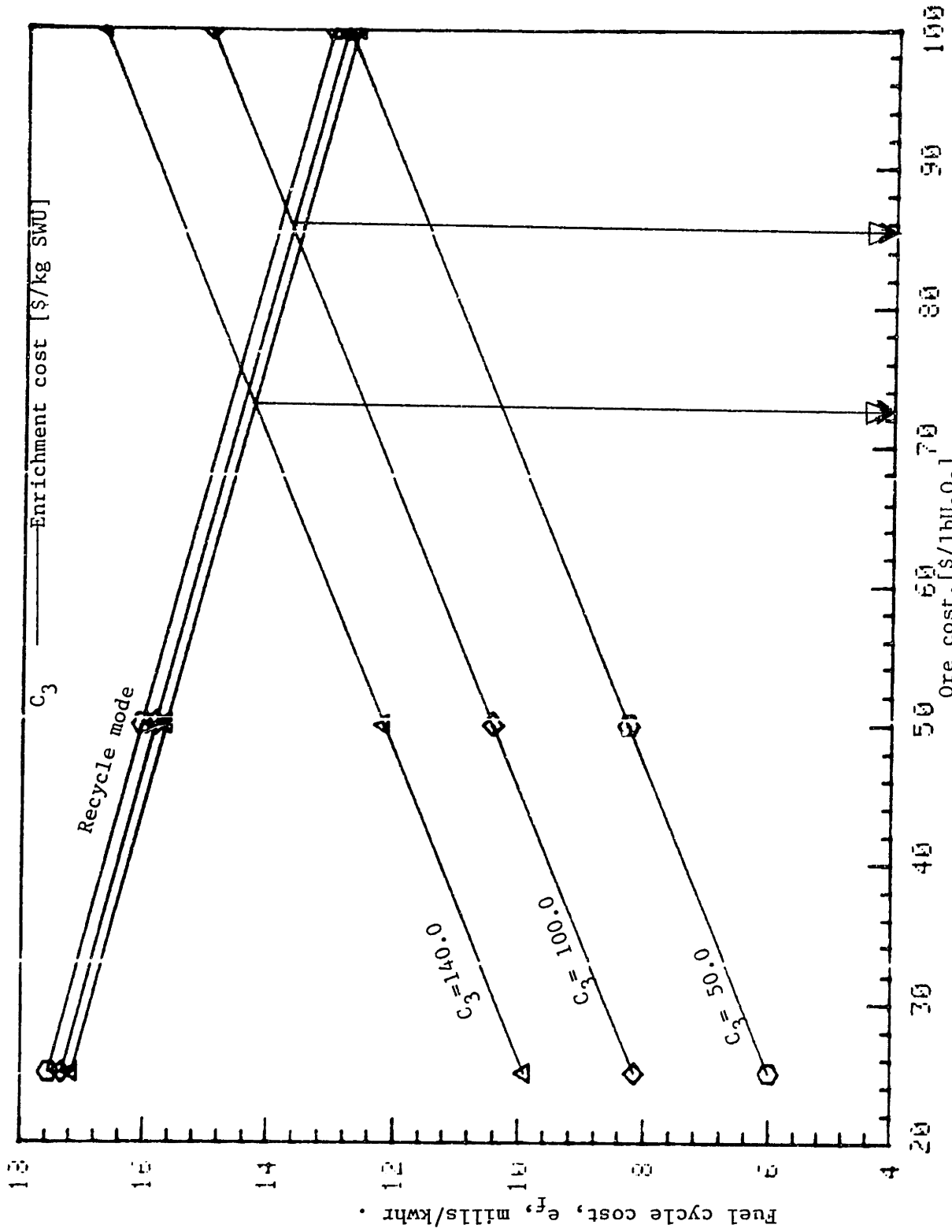


Fig. 4.11 Breakeven ore cost of once-through vs recycle-mode fuel cycle cost for various enrichment costs: $X_w$=0.1 w/o .

The following formulas have been curve fit to calculate $d_3$ for any enrichment and tails assay within the range of present interest:

$$d_3(X_P, X_W) = \frac{X_P}{1.96275\ X_P - 2.57161} + \left(7.91407 + \frac{43.0266}{X_P}\right) X_W \ , \frac{\$/kg\ SWU}{\$/lb\ U_3O_8} \qquad (4.18)$$

## 4.5 Price of Ore Projection

The cost of uranium is a key variable that affects the costs and timing of various nuclear options. In particular, the need for a LWR recycle mode and breeder reactors depends upon what uranium will cost in the decades ahead. Uranium prices are generally coupled to cumulative consumption and thus to the rate of installation of nuclear power plants, which in turn depends upon many economic, technical and political factors. The interdependence of these factors makes future projections very complex. Furthermore, due to the rapidly changing conditions affecting energy and economic growth, there have been drastic revisions in projections of nuclear load growth during the last decade. Figure 4.12 (from ref. W1) shows the changing projections for the end-of-century installed nuclear capacity in the U.S.

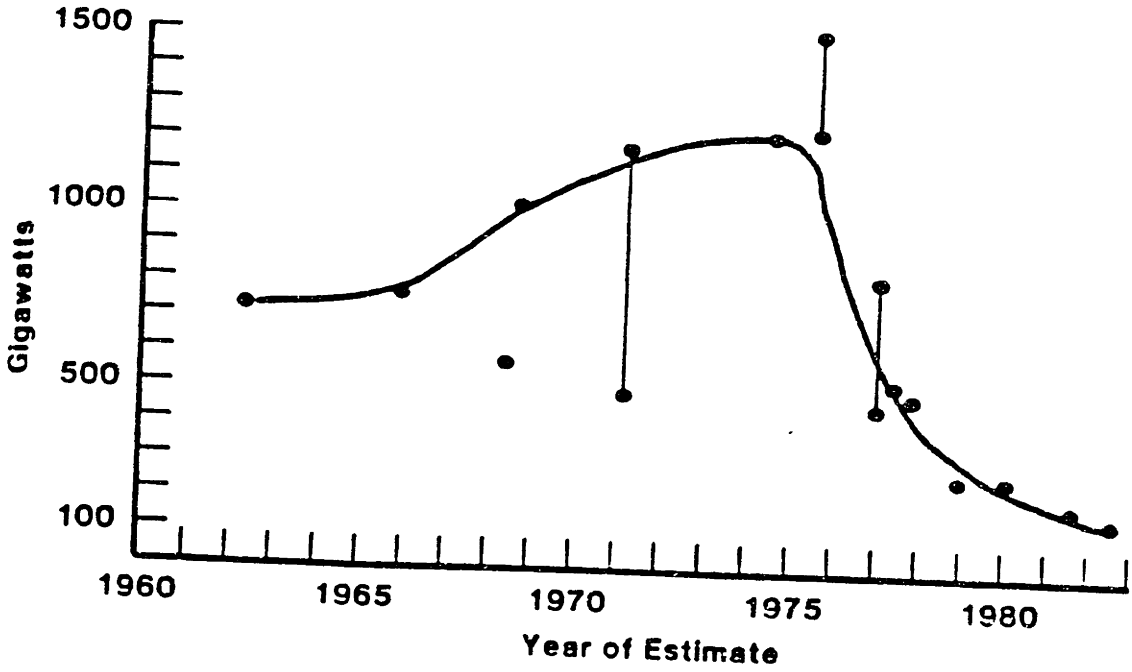


Fig.4.12. Installed nuclear power estimates, year 2000—U.S.

From ref. [W1]

The spot market price of uranium has fallen over the past several years, which reflects the current overcapacity and smaller demand for uranium than projected earlier. Table 4.14 shows the history of uranium price development in the past. Optimistic end-of-century requirements projections and the ensuing rapid build up in demand in the early 70's led to a nearly tenfold increase in uranium prices between 1972 and 1977. Substantial delays, deferrals, and cancellations of nuclear plants in the past several years, however, resulted in a sharp reduction in the demand for uranium. Dramatic price reductions followed, with current levels holding below 20 \$/lb $U_3O_8$ .

Since a major focus of our case study analyses deals with comparisons of once-through and recycle mode fuel cycle costs as a function of ore cost, it is necessary to relate current knowledge of uranium resources to long term projections of installed nuclear capacity and the resulting price of ore. The estimation of a scarcity-related cost escalation rate for future uranium prices as a function of key variables can be made using the resource-cost model described in section 2.8. The model simulates the manner in which cumulative consumption leads to the depletion of uranium ore grade, which increases the cost of uranium production. An estimate of nuclear power demand and its corresponding consumption are combined with

TABLE 4.14

A Uranium Price History*

| Year | Nominal Price $/lb $U_3O_8$ | Year | Nominal Price $/lb $U_3O_8$ |
|---|---|---|---|
| 6-71 | 6.05 | 6-80 | 31.50 |
| 12-71 | 5.95 | 12-80 | 28.00 |
| 6-72 | 5.95 | 6-81 | 24.25 |
| 12-72 | 5.95 | 12-81 | 23.50 |
| 6-73 | 6.50 | 6-82 | 19.25 |
| 12-73 | 7.00 | 12-82 | 20.25 |
| 6-74 | 10.50 | 6-83 | 24.00 |
| 12-74 | 15.00 | 12-83 | 17.00 |
| 6-75 | 22.00 | 6-84 | 20.00 |
| 12-75 | 35.00 | 12-84 | 23.00 |
| 6-76 | 40.00 | | |
| 12-76 | 41.00 | | |
| 6-77 | 42.25 | | |
| 12-77 | 43.20 | | |
| 6-78 | 43.40 | | |
| 12-78 | 43.25 | | |
| 6-79 | 43.00 | | |
| 12-79 | 40.75 | | |

*ref [N1]: in then-current dollars.

the $U_3O_8$ price/supply relationship to give an expression for constant dollar ore costs as a function of time. In the model in questions, the scarcity-related escalation rate is given by $r\theta$ , where r is the demand growth rate and $\theta$ is a function of of $\mu$ and $\gamma$ , as given in Eq. 2.62 of Chapter 2.

In Fig. 4.13 ore price versus resource projections are compared from two references. The dotted line is that predicted by Gharamani in 1978 [G3] , using $\theta = 2/3$ . The other curve is from a recent EPRI report published in 1982 The same mathematical form, but with $\theta \sim 0.5$ , provides a good representation of this more authoritative projection. In addition to showing a projected most probable value, the EPRI plot also shows the large uncertainty (shaded area) associated with such projections.

In the present work, we have used $\theta = 0.5$ , and, since the forecasts of capacity growth rates have been highly uncertain, instead of using demand growth at a constant rate r , an estimated profile of year-by-year installed capacity is employed. From the profile supplied, r for a given year is defined

$$r = \ln \left( \frac{E_2}{E_1} \right) \tag{4.20}$$

where $E_1$ is the beginning of year and $E_2$ is the end of year comulative installed capacity.

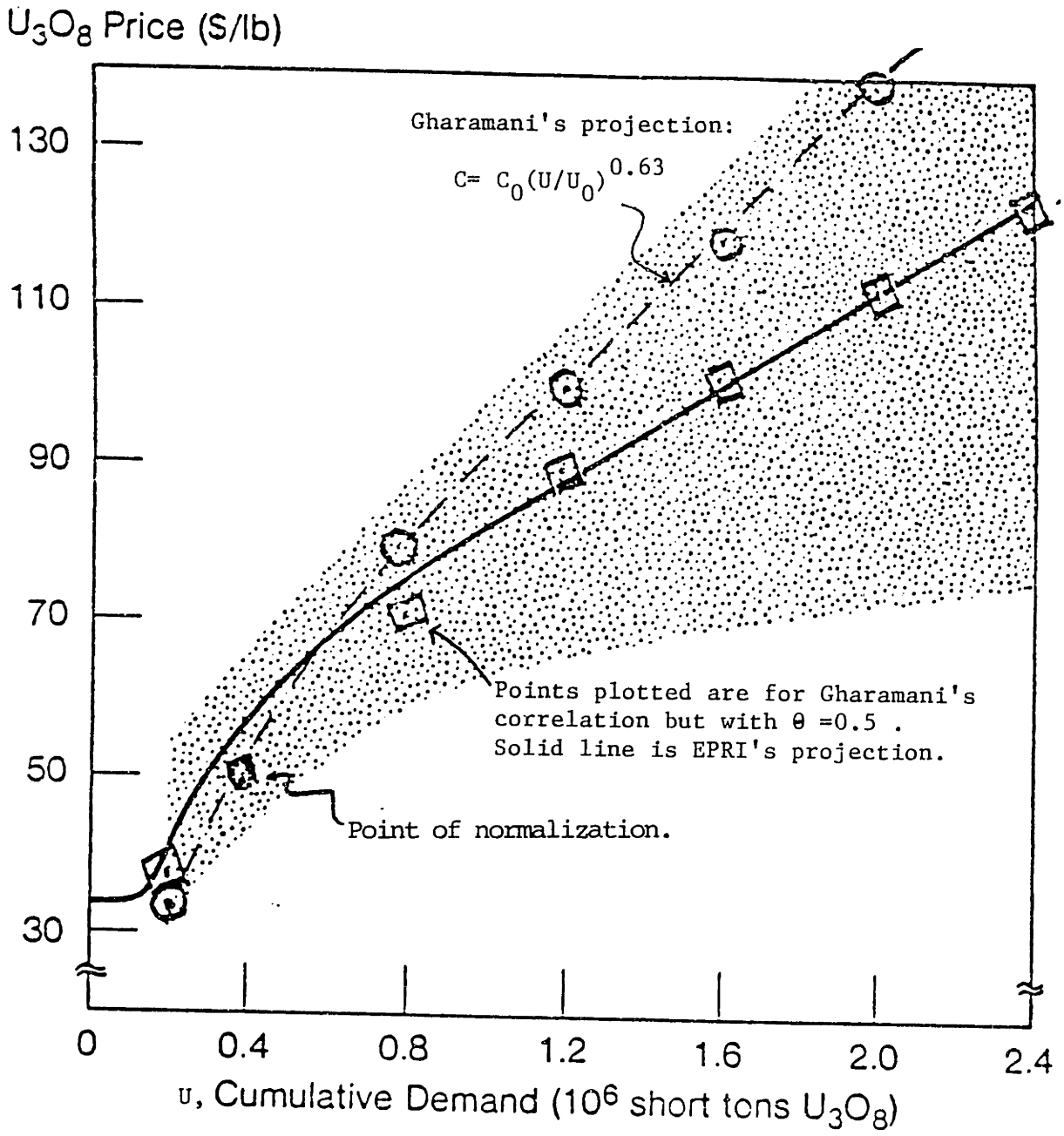


Fig.4.13 $U_3O_8$ Projected Price Versus Cumulative Demand in Constant December 1980 Dollars (0.2 tails) [from Ref. E2 ,with added details ].

A profile projected (by the author) for U.S. nuclear capacity growth up to the middle of the next century is listed in table 4.15. The capacity up to 1990 is based on current commercial operation dates as shown in AIF's 1984 status report of U.S. reactors. After 1990 the rate of growth of installed nuclear capacity, r, is assumed to be i%, where i is the number of decades after 1990. Table 4.15 also gives the projected ore cost, in constant dollars as of December 1984, calculated by applying the resource-cost model discussed in Chapter 2.

The same procedure can be followed to develop a cost history projection for any scenario of one's choice, and the time to reach breakeven estimated. For example, in table 4.15 the 76.4 \$/lb $U_3O_8$ level beyond which recycle is favored in our reference case of section 4.4.1 is not reached until the year 2049.

## 4.6 Results and Discussion

The breakeven case study results of this chapter are summarized in table 4.16. These results show that:

(1) There is no clear answer as to when recycle could be economically competitive (except that it appears to be many decades hence); depending upon the values of various uncertain

TABLE 4.15

Projected Profile of Installed Nuclear Capacity and Future Cost of Yellowcake

| Year | Beginning of year installed capacity | Ore price* ($/lb $U_3O_8$) |
|---|---|---|
| 1984 | 60.00 | 20.00 |
| 1985 | 80.00 | 23.09 |
| 1986 | 93.00 | 24.90 |
| 1987 | 104.00 | 26.33 |
| 1988 | 110.00 | 27.08 |
| 1989 | 114.00 | 27.57 |
| 1990 | 118.00 | 28.05 |
| 1995 | 124.05 | 28.76 |
| 2000 | 130.41 | 29.49 |
| 2005 | 144.13 | 31.00 |
| 2010 | 159.28 | 32.59 |
| 2015 | 185.06 | 35.13 |
| 2020 | 215.00 | 37.86 |
| 2025 | 262.60 | 41.84 |
| 2030 | 320.74 | 46.24 |
| 2035 | 411.84 | 52.40 |
| 2040 | 528.81 | 59.37 |
| 2045 | 713.82 | 68.98 |
| 2050 | 963.55 | 80.14 |

*In constant dollars.

$$c = c_o\, e^{r\theta t} \quad ; \quad r = \ln\left(\frac{E_2}{E_1}\right) ; \quad \theta = 0.5$$

TABLE 4.16

Summary of the "Breakeven" Case Study Results

| Parameter | Case* | Value | Breakeven ore ** cost $/lb $U_3O_8$ |
|---|---|---|---|
| Reprocessing cost [$/kg HM] | H | 900 | 125.0 |
| | B | 600 | 76.4 |
| | L | 300 | 27.5 |
| Enrichment cost [$/kg SWU] tails assay=0.2% | H | 200 | 64.3 |
| | B | 140 | 76.4 |
| | L | 50 | 94.6 |
| Tails assay [w/o U-235] for enrichment cost $\frac{50\$}{kg\ SWU}$ | H | 0.3 | 83.2 |
| | B | 0.2 | 94.6 |
| | L | 0.1 | 101.2 |
| MOX Fabrication cost [$/kg HM] | H | 800 | 83.6 |
| | B | 570 | 76.4 |
| | L | 350 | 69.5 |
| Enrichment, w/o (Burnup, GWD/MT) | H | 4.0 (40.50) | 63.4 |
| | B | 3.5 (33.75) | 76.4 |
| | L | 3.0 (27.00) | 94.4 |
| Number of batches | H | | 87.5 |
| | B | | 76.4 |

Composite case + 86.62

Base case 76.4

*H-High; B-Base; L-Low.

**Price of $U_3O_8$ at which the once through and recycle mode have the same fuel cycle cost.

+Reprocessing cost=700 $/kg HM; Enrichment cost=60 $/kg SWU; $X_p$=4.5; MOX Fabrication Cost=500 $/kg.

parameters, recycle would be economic over a range of $U_3O_8$ prices ranging from \$70 to \$125/lb.

(2) For the base case values the price of uranium has to rise to about four times today's spot market value to reach breakeven for the recycle mode, which is predicted to occur (for a reasonable estimated profile of installed capacity, shown in table 4.15) around 2050. Thus, the once through cycle is apparently economically preferable for nearly seven decades. However, since many uncertainties exist, a reliable forecast is not feasible that far into the future.

(3) It is highly unlikely that reprocessing can be economically justified in the near future unless there is a significant reduction in reprocessing costs, e.g., if the Barnwell Nuclear Fuel Plant (BNFP) could be completed and reprocessing charges kept below 300 \$/kg, the $U_3O_8$ price would have to rise to only \$27.5/lb for reprocessing to become economically attractive.

(4) Improvements in enrichment technology (development of better gas centrifuges or laser-based methods) and a corresponding reduction in the U-235 content of enrichment plant tailings would (by increasing the breakeven price of ore to ~100 \$/lb $U_3O_8$) defer the time at which reprocessing becomes viable.

(5) The breakeven ore cost is very sensitive to reprocessing cost. An increase of only 1% in the base value of the cost of reprocessing will increase the breakeven ore cost by 1 \$/lb.

(6) Enrichment cost follows reprocessing cost in order of relative importance to breakeven ore cost. A decrease of 3.53% in the base value of enrichment cost will increase the breakeven ore cost by 1 $/lb.

(7) Substantial increases in MOX fabrication charges have an effect on breakeven ore cost that is noticeable, but not substantial.

(8) The breakeven ore cost will further increase if we extend burnup by adopting the option of using more batches to manage the core. At low tails assay, $X_w$, and for high U-235 enrichment, $X_p$, the breakeven ore cost becomes more sensitive to enrichment cost. For example, in table 4.13, for $X_p$=3.0 w/o U-235 and $X_w$=0.25% the breakeven ore cost is increased by 1 $/lb for a decrease of 6.7 $/kg SWU in enrichment cost; whereas, for $X_p$=4.0 w/o and $X_w$=0.1% an enrichment cost decrease of 2.92 $/kg SWU can increase the breakeven ore cost by 1 $/lb.

(9) Recycle is favored as burnup is increased, and the once-through cycle is benefitted by cheap SWU and lower tail's assay. If, as is generally forseen, 18 month cycle/3 batch cores are eventually achieved in PWRs, the breakeven cost will decrease to 54.5 $/lb $U_3O_8$ (a decrease of 22 $/lb $U_3O_8$ from the base case breakeven cost). On the other hand, if the cost of separative work decreases to 60 $/kg SWU and the tails assay is reduced to 0.15%, the increase in the breakeven cost would be 22.9 $/lb $U_3O_8$ (see last column of table 4.13), more than enough to offset the decrease in breakeven cost incurred by going to higher burnup.

(10) For dry lattices, plutonium is worth less than in wet lattices, due to their harder spectra. Thus, comparatively more spent fuel from convential lattices needs to be reprocessed to constitute a reload batch. Therefore, since we have considered only single-pass recycle, there is no incentive to use drier lattices despite their higher conversion ratio. Moreover the relative amounts of Pu-240 and Pu-242 are increased in the fuel discharged from multipass recycle, and thus a greater mass of plutonium would be required to meet fissile feed requirements. Thus, while not examined in depth here, one must question the economic prospects of tight pitch cores in LWRs even if multipass recycle is allowed.

## 4.7 Chapter Summary

The integrated package of submodels described in the earlier chapters was applied to develop the equations for the once-through and recycle mode fuel cycle cost in terms of the unit costs of each process step. A sensitivity study was performed, using the fuel cycle cost equations, to examine how sensitive the fuel cycle cost is to each cost component. The fuel cycle cost was found to be very sensitive to reprocessing cost. An increase of only 6% in the base value of reprocessing could increase the fuel cycle cost by 1 mill/kwhr.

Enrichment and MOX fabrication followed reprocessing in order of relative importance to fuel cycle cost.

The results of a breakeven comparison of the once through and recycle modes were presented. A general equation for the breakeven cost of ore as a function of important process steps was also prescribed. The sensitivity analysis was extended to analyze the effect of changes in the various parameters on breakeven ore cost. For the base case, it was found that recycling will not be economic unless the ore cost is more than 76.4 \$/lb $U_3O_8$.

The case studies analyzed cover extended burnup (by increasing reload enrichment), more batches in the core, low enrichment cost technologies and reduction in enrichment plant tails assay. Correlations for the cost coefficients in terms of enrichment were developed by curve fitting the output data from the computer program. The breakeven cost of ore was found to be lower for higher burnup values (attained through increased enrichments). It was shown that the current 1 mill/kwhr disposal fee constitutes a large disincentive for extending burnup. The combination of cheap SWU and low tails assay was found to lead to a breakeven ore cost higher than 100 \$/lb $U_3O_8$.

An estimated profile of nuclear capacity up to the middle of the next century was combined with the $U_3O_8$ price/supply relationship projecting ore cost as a function of time. For the base case, breakeven time was predicted to be around 2050, which could further be deferred for a few decades through enrichment technology improvements and U-235 content reductions in enrichment plant tailings. On the other hand, the recycle mode could be economically justified in the near future if there is a substantial reduction in reprocessing costs.

# CHAPTER 5

# SUMMARY, CONCLUSIONS AND RECOMMENDATIONS

## 5.1 Introduction

During the past ten years, as a result of economic recession, diminished power demand, and rising plant costs, there has been a large decrease in the rate of reactor construction; and significant uranium reserves have been confirmed, while spot-market prices for $U_3O_8$ have dropped. At the same time reprocessing and MOX fabrication costs have escalated substantially, and new high-performance centrifuge enrichment cascades and inexpensive laser isotope enrichment devices are being perfected. In addition, LWR fuel is being pushed to ever higher burnup levels, with consequent savings in ore requirements. The result is that scarcity of uranium as a driving force to deploy possible $U_3O_8$ extenders, such as recycle mode LWRs, and FBRs, has decreased, and it is expected that LWRs will continue to be competitive, many decades into the future, even if they are confined to operation on a once-through fuel cycle.

In view of the above considerations, the major objective of the present work has been to provide an uncomplicated

means for the fuel manager to determine optimal responses to future economic and technical environments of his own projection. Accomplishing this task involved integration of a number of submodels into a model that can answer the questions surrounding many suggested policy options, by quantifying their potential economic impact. Some of the areas of current interest, which are addressed, include:

- o Plutonium recycle
- o The effect of escalation of reprocessing and MOX fabrication costs
- o AIS enrichment processes
- o Changes in the enrichment plant tail's assay
- o Extended fuel discharge burnup
- o Increasing the number of batches.

## 5.2 Nuclear Fuel Cycle Models

Simple models for the evaluation of various fuel management strategies were developed. The elements of the overall model consist of submodels describing material flow through the LWR nuclear fuel cycle, discharged fuel composition, nuclear fuel economics and the ore resource/cost relationship. Figure 5.1 shows how these components are linked up to comprise a fuel cycle scoping program.

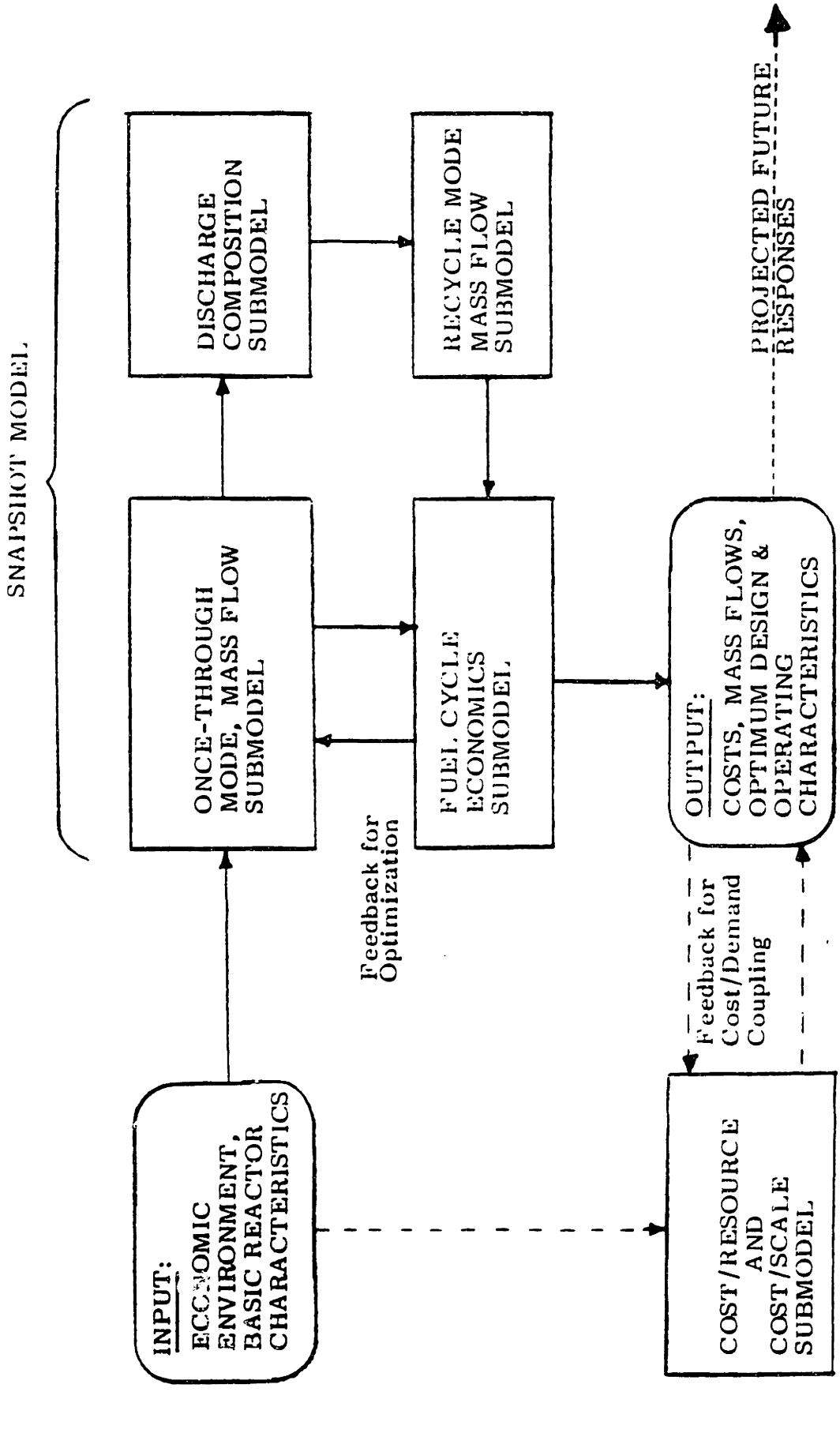


Fig 5.1 schematic showing interrelation of submodels in the fuel cycle scoping program.

### 5.2.1 Once-through Mass Flow Model

The quantity of feed material required to prepare low enrichment fuel batches was obtained by performing a material balance on both total uranium and the U-235 isotope around the enrichment facility. Simple correlations in the range of interest for the calculation of the separative work required per Kg of the product material, S/P, and the optimum tails assay, $X_w$, were developed, as follows:

$$S/P = (a_1 + b_1 X_w) + \frac{X_P}{(a_2 + b_2 X_w)} \qquad (5.1)$$

with:

$$a_1 = -3.12027$$
$$b_1 = 3.29712 \ (w/o)^{-1}$$
$$a_2 = 0.24412 \ (w/o)$$
$$b_2 = 0.98258$$

$$X_w)_{opt} = \frac{1}{[2.425 + 1.925 \ C_F/C_S]} \ , \ w/o \qquad (5.2)$$

$$\text{for } 0.5 \leq C_F/C_S \leq 3$$

where $C_F/C_S$ is the ratio of the cost of feed ($/kg U) to the cost of enrichment ($/kg SWU).

### 5.2.2 Discharge Composition Submodel

The approximate formulas for U-235, U-236 and fissile plutonium mass as a function of reload enrichment, burnup and fuel-to-moderator ratio ($V_F/V_M$), which were required as input for recycle mass flow calculations, were formulated by fitting semi-empirical relations to the output of LEOPARD computer code calculations. The resulting prescriptions are given below:

$$\text{X-235} = a_4 + b_4 \frac{V_F}{V_M} + \left(a_5 + b_5 \frac{V_F}{V_M}\right) X_P + X_P \left\{ a_6 + b_6 \frac{V_F}{V_M} \right\} \ln (B) \qquad (5.3)$$

with: $a_4 = -1.62102$ w/o $\quad a_5 = 2.30733 \quad a_6 = 0.08364$

$b_4 = 0.28151$ w/o $\quad b_5 = -0.29904 \quad b_6 = -0.46118$

$$\text{X-236} = \left(a_4 + b_4 \frac{V_F}{V_M}\right) X_P + \frac{1}{B} \left[ a_5 + b_5 \frac{V_F}{V_M} + c_5 \left(\frac{V_F}{V_M}\right)^2 + \left\{ a_6 + b_6 \frac{V_F}{V_M} + c_6 \left(\frac{V_F}{V_M}\right)^2 \right\} X_P \right] \qquad (5.4)$$

with: $a_4 = 0.17215$ ; $b_4 = 0.00881$

$a_5 = -2.548$ w/o MT/GWD ; $b_5 = 14.655$ w/o MT/GWD;

$c_5 = -8.397$ w/o MT/GWD

$a_6 = -1.263$ MT/GWD ; $b_6 = -3.288$ MT/GWD ;

$c_6 = 1.912$ MT/GWD

$$X_{Puf} = B \left[ a_4 + b_4 \; V_F/V_M + \left( a_5 + \frac{b_5}{V_F/V_M} \right) X_P + \left\{ a_6 + b_6 \; V_F/V_M + \left( a_7 + b_7 \; V_F/V_M \right) X_P \right\} B \right]^{-1} \qquad (5.5)$$

with: $a_4 = 11.920 \; \frac{GWD}{MT \; w/o}$ $\qquad b_4 = -2.200 \; \frac{GWD}{MT \; w/o}$

$a_5 = 0.20834 \; \frac{GWD}{MT \; (w/o)^2}$ $\qquad b_5 = 1.43381 \; \frac{GWD}{MT \; (w/o)^2}$

$a_6 = 2.46378 \; (w/o)^{-1}$ $\qquad b_6 = 1.46607 \; (w/o)^{-1}$

$a_7 = -0.28578 \; (w/o)^{-2}$ $\qquad b_7 = 0.18238 \; (w/o)^{-2}$

### 5.2.3 Recycle Mode Scheme

In the recycle mode considered in this work, the plutonium from spent fuel was used to make up for the consumed U-235 in part of the discharged fuel, and the remaining uranium is credited both for ore and SWU savings.

The burnup worth of fissile plutonium relative to U-235 was determined by comparing $\rho(B)$ behavior over the complete life cycle, and matching attainable reactivity-limited discharge burnup. The presence of U-236 in the isotope separation plant was taken into account, and the corresponding penalty in the resulting enriched uranium was quantified and included in the model.

### 5.2.4 Fuel Cycle Economics

The present worth method was applied for the calculation of fuel cost. Various cash flows were described in terms of direct plus carrying charges. The analysis was carried out using the market discount rate and transaction costs in today's (1984) dollars. Busbar and system cost relationships were also included in the model to permit analysis of the effect of the plant capacity factor and the cost of replacement energy during refueling downtime. The issue of assigning an explicit value to plutonium was avoided by basing spent fuel value on the avoided cost of disposal.

### 5.2.5 Ore Resource/Cost Model

The estimation of a scarcity-related cost escalation rate for future uranium prices as a function of key variables was included in the resource-cost model. The model simulates the manner in which cumulative consumption leads to the depletion of uranium ore grade, which increases the cost of uranium production. A projected profile of nuclear capacity up to the middle of the next century was combined with the $U_3O_8$ price/supply relationship to predict ore cost as a function of time.

## 5.3 Correlations for Key Parameters

Simple correlations capable of predicting the functional dependence of the key parameters on the important variables were developed. These correlations provide a compact, yet accurate, means to summarize the exogenous input needed for fuel cycle studies. Some of the more important prescriptions are summarized in the following sections.

### 5.3.1 Reactivity Versus Burnup for Uranium and Plutonium Cores

The discharge burnup of a fuel batch can be obtained by performing a reactivity balance for an n-batch steady-state core,

$$B_d = \frac{2n}{n+1}\left\{\frac{\rho_o - \rho_L}{A}\right\} \tag{5.6}$$

where

$\rho_o$ = Extrapolated beginning of life reactivity

A = Slope of reactivity versus burnup curve, $\left[\frac{MWD}{MT}\right]^{-1}$

$\rho_L$ = Leakage reactivity.

In this work, the values of $\rho_o$ and A were calculated from a least squares linear regression fit of reactivity, $\rho$, as a

function of burnup, B, obtained using the LEOPARD code. Correlations for $\rho_o/A$, which is directly proportional to discharge burnup, were developed as a function of enrichment, $X_P$, (U-235 w/o for uranium cores) and fissile plutonium, $X_{Puf}$ (for plutonium cores), and fuel-to-moderator ratio, $V_F/V_M$, by using a statistical program for simple regressions to curve fit the data obtained from the LEOPARD code:

$$\frac{\rho_o}{A}\left( X_P, \frac{V_F}{V_M}\right) = 1.3 + \left\{12.338-4.674 \frac{V_F}{V_M}\right\} X_P - \frac{3.5}{V_F/V_M}, \frac{GWD}{MT} \qquad (5.7)$$

$$\frac{\rho_o}{A}\left( X_{Puf}, \frac{V_F}{V_M}\right) = 9\ X_{Puf}\left( 2- \frac{V_F}{V_M}\right) - 3.5 \left(1+6.8 \frac{V_F}{V_M}\right), \frac{GWD}{MT} \qquad (5.8)$$

for $0.5 \leq V_F/V_M \leq 1.0$ ; $2.5 \leq X_P \leq 5.0$ w/o

$2.5 \leq X_{Puf} \leq 10.0$ w/o.

These simple correlations reproduce $\rho_o/A$ within an average error of 3.0%.

Analysis of the $\rho_o/A$ curve-fits indicated that the fuel-to-moderator ratio corresponding to the maximum $\rho_o/A$ decreases with increasing values of enrichment for uranium cores, whereas the optimum lattice for plutonium cores becomes drier as fissile enrichment is increased. Using the $\rho_o/A$ correlations for uranium and plutonium cores, the value of $X_{Puf}$,

which will give the same value of $\rho_o/A$ (hence discharge burnup) in the plutonium core, as $X_P$ w/o U-235 in the uranium core is given by:

$$X_{Puf}\left(X_P, \frac{V_F}{V_M}\right) = \frac{\frac{\rho_o}{A}\left(X_P, \frac{V_F}{V_M}\right) + 3.5\left(1 + 6.8\frac{V_F}{V_M}\right)}{9\left(2 - \frac{V_F}{V_M}\right)}, \text{ w/o} \quad (5.9)$$

The "burnup worth" (capability of sustaining burnup) of fissile plutonium relative to $X_P$ at a particular value of $V_F/V_M$ , $g(X_P , V_F/V_M)$ is calculated as:

$$g\ (X_P, V_F/V_M) = \left\{\frac{X_P}{X_{Puf}\ (X_P , V_F/V_M)}\right\} \quad (5.10)$$

Some selected results of the equivalent worth of plutonium from Eq. 5.10 are presented in table 5.1. Note that fissile plutonium has roughly the same worth as U-235 in the range of current interest.

The burnup worth of fissile plutonium is more than that of U-235 in the wetter lattices, since, due to the much larger thermal absorption cross-sections of Pu isotopes, the spectra of Pu cores are harder than those of the corresponding uranium cores, and so the optimum lattice for a Pu core is wetter than that of a uranium-fueled core. Also, the worth

TABLE 5.1

Equivalent Worth of Fissile Pu Relative to U-235

| $V_F/V_M$ | U-235 (w/o) $X_P$ | Fissile Pu (w/o) $X_{Puf}$ | Equivalent Worth |
|---|---|---|---|
| 0.500 | 3.0 | 2.941 | 1.020 |
| | 3.5 | 3.311 | 1.057 |
| | 4.0 | 3.681 | 1.087 |
| | 4.5 | 4.052 | 1.111 |
| | 5.0 | 4.421 | 1.131 |
| 0.604 | 3.0 | 3.337 | 0.899 |
| | 3.5 | 3.716 | 0.942 |
| | 4.0 | 4.094 | 0.977 |
| | 4.5 | 4.473 | 1.006 |
| | 5.0 | 4.852 | 1.031 |
| 0.750 | 3.0 | 3.954 | 0.759 |
| | 3.5 | 4.347 | 0.805 |
| | 4.0 | 4.739 | 0.844 |
| | 4.5 | 5.132 | 0.877 |
| | 5.0 | 5.524 | 0.905 |

of plutonium increases with $X_{Puf}$ due to a flatter reactivity swing during fuel depletion than comparable uranium fuels. This difference is due, in part, to the large Pu-240 resonance at 1.05 ev, which enables Pu-240 to behave as a burnable poison, which not only adds reactivity by its depletion, but also produces the high-worth fissils isotope Pu-241.

### 5.3.2 Distribution of U-236

During irradiation the U-236 isotope is created, which has a large parasitic capture cross-section and behaves as a neutron poison. When introduced into an isotope enrichment plant, the U-236 from the recycled uranium is enriched along with the U-235. The presence of U-236 in fuel requires extra separative work; also, the concentration of U-235 in recycled fuel must be greater to compensate for the negative reactivity due to the presence of U-236.

In the present work, a simple but accurate empirical formula has been prescribed which can be used to determine the change in U-236 concentration per unit change in U-235, $\Delta Y/\Delta X$, when recycled uranium is processed in an enrichment plant:

$$\frac{\Delta Y}{\Delta X} = Y_1 \left\{(a + b\,X_3) + (c + d\,X_3)\,X_2\right\}^{-1} \qquad (5.11)$$

for

$$0.4 \leq X_1 \leq 1.0 \quad ; \quad 2.0 \leq X_2 \leq 5.0$$

$$0.1 < X_3 < 0.3 \quad ; \quad 0.2 < Y_1 < 0.6$$

where

$a = 0.12125 + 1.0840\,X_1$

$b = 0.27323 + 0.2340\,X_1$

$c = 0.00521 + 0.0142\,X_1$

$d = 0.06476 - 0.01044/X_1$

$X_1$ = w/o of U-235 in Feed

$X_2$ = w/o of U-235 in Product

$X_3$ = w/o of U-235 in Tails

$Y_1$ = w/o of U-236 in Feed

$Y_2$ = w/o of U-236 in Product

$Y_3$ = w/o of U-236 in Tails

The U-236 content in the product and tails is given as:

$$Y_2 = Y_1 + \Delta Y/\Delta X\,(X_2 - X_1),\ \text{w/o} \qquad (5.12)$$

and

$$Y_3 = Y_1 - \Delta Y/\Delta X\,(X_1 - X_3),\ \text{w/o} \qquad (5.13)$$

Curve-fit and exact distributions of U-236 in product and tails are compared for some representative values in table 5.2: as can be seen, the error averages only ~0.1%.

TABLE 5.2

Comparison of Curve-fit and Exact Distributions of U-236 in the Product and Tails of a Three Component Isotope Separation Plant

| U-235 (w/o) in | | | U-236 (w/o) in | | | | | | |
|---|---|---|---|---|---|---|---|---|---|
| Feed $X_1$ | Product $X_2$ | Tails $X_3$ | Feed $Y_1$ | Product, $Y_2$ | | | Tails, $Y_3$ | | |
| | | | | Exact | Empirical | Error % | Exact | Empirical | Error % |
| 0.6 | 3.0 | 0.2 | 0.3 | 1.078 | 1.079 | +0.09 | 0.1703 | 0.1701 | -0.12 |
| | | | 0.4 | 1.437 | 1.439 | +0.14 | 0.2271 | 0.2268 | -0.13 |
| | | 0.3 | 0.3 | 1.034 | 1.035 | +0.10 | 0.2082 | 0.2081 | -0.05 |
| | | | 0.4 | 1.378 | 1.380 | +0.14 | 0.2777 | 0.2775 | -0.07 |
| | 4.0 | 0.2 | 0.3 | 1.376 | 1.377 | +0.07 | 0.1735 | 0.1733 | -0.11 |
| | | | 0.4 | 1.833 | 1.836 | +0.16 | 0.2314 | 0.2311 | -0.13 |
| | | 0.3 | 0.3 | 1.311 | 1.312 | +0.08 | 0.2108 | 0.2107 | -0.05 |
| | | | 0.4 | 1.747 | 1.750 | +0.17 | 0.2811 | 0.2809 | -0.07 |
| 0.7 | 3.0 | 0.2 | 0.3 | 0.961 | 0.962 | +0.10 | 0.1563 | 0.1562 | -0.06 |
| | | | 0.4 | 1.281 | 1.282 | +0.08 | 0.2085 | 0.2082 | -0.14 |
| | | 0.3 | 0.3 | 0.926 | 0.926 | +0.00 | 0.1912 | 0.1912 | -0.00 |
| | | | 0.4 | 1.234 | 1.235 | +0.08 | 0.2550 | 0.2547 | -0.12 |
| | 4.0 | 0.2 | 0.3 | 1.226 | 1.227 | +0.08 | 0.1597 | 0.1595 | -0.12 |
| | | | 0.4 | 1.634 | 1.636 | +0.12 | 0.2131 | 0.2127 | -0.19 |
| | | 0.3 | 0.3 | 1.174 | 1.175 | +0.08 | 0.1941 | 0.1940 | -0.05 |
| | | | 0.4 | 1.564 | 1.566 | +0.13 | 0.2589 | 0.2586 | -0.12 |

## 5.4 Case Study Results

The models and correlations described earlier (as embodied in a program written for minicomputer use-see Appendix B) were applied to develop fuel cycle cost equations for the once through and recycle mode fuel cycles in terms of the unit costs of each process step. A sensitivity study was performed, using the fuel cycle cost equations. A general equation for the breakeven cost of ore for once-through versus recycle mode cost equalization, as a function of important process steps was also developed. Trade-off studies for other fuel cycle processing costs can also be made by treating the cost in question as an unknown and solving the fuel cost equations for the once through and recycle modes for the breakeven value of this variable: the value for which both alternatives give the same fuel cycle cost.

The case studies analyzed cover extended burnup, more batches in the core, low-enrichment-cost technologies and reduction in enrichment plant tails assay. The results of these evaluations, summarized in table 5.3, show that:

(1) There is no clear answer as to when recycle could be economically competitive (except that it appears to be many decades hence); depending on the value of various uncertain parameters, recycle would be economic over a range of $U_3O_8$ prices ranging from \$70 to \$125/lb.

TABLE 5.3

Summary of the "Breakeven" Case Study Results

| Parameter | Case* | Value | Breakeven ore ** cost $/lb $U_3O_8$ |
|---|---|---|---|
| Reprocessing cost [$/kg HM] | H | 900 | 125.0 |
| | B | 600 | 76.4 |
| | L | 300 | 27.5 |
| Enrichment cost [$/kg SWU] tails assay=0.2% | H | 200 | 64.3 |
| | B | 140 | 76.4 |
| | L | 50 | 94.6 |
| Tails assay [w/o U-235] for enrichment cost $\frac{50\$}{kg\ SWU}$ | H | 0.3 | 83.2 |
| | B | 0.2 | 94.6 |
| | L | 0.1 | 101.2 |
| MOX Fabrication cost [$/kg] | H | 800 | 83.6 |
| | B | 570 | 76.4 |
| | L | 350 | 69.5 |
| Enrichment, w/o (Burnup, GWD/MT) | H | 4.0 (40.50) | 63.4 |
| | B | 3.5 (33.75) | 76.4 |
| | L | 3.0 (27.00) | 94.4 |
| Number of batches | H | | 87.5 |
| | B | | 76.4 |

Composite case + 86.62

Base case 76.4

*H-High; B-Base; L-Low.

**Price of $U_3O_8$ at which the once through and recycle mode have the same fuel cycle cost.

+Reprocessing cost=700 $/kg HM; Enrichment cost=60 $/kg SWU; $X_p$=4.5; MOX Fabrication Cost=500 $/kg.

(2) For the base case values the price of uranium has to rise to about four times today's spot market value to reach breakeven for the recycle mode, which is predicted to occur (for a reasonable estimated profile of installed capacity) around 2050. Thus, the once through cycle is apparently economically preferable for nearly seven decades. However, since many uncertainties exist, a reliable forecast is not feasible that far into the future.

(3) It is highly unlikely that reprocessing can be economically justified in the near future unless there is a significant reduction in reprocessing costs, e.g., if the Barnwell Nuclear Fuel Plant (BNFP) could be completed and reprocessing charges kept below 300 $/kg, the $U_3O_8$ price would have to rise to only $27.5/lb for reprocessing to become economically attractive.

(4) Improvements in enrichment technology (development of better gas centrifuges or laser-based methods) and a corresponding reduction in the U-235 content of enrichment plant tailings would (by increasing the breakeven price of ore to ~100 $/lb $U_3O_8$) defer the time at which reprocessing becomes viable.

(5) The breakeven ore cost is very sensitive to reprocessing cost. An increase of only 1% in the base value of the cost of reprocessing will increase the breakeven ore cost by 1 $/lb.

(6) Enrichment cost follows reprocessing cost in order of relative importance to breakeven ore cost. A decrease of 3.53% in the base value of enrichment cost will increase the breakeven ore cost by 1 $/lb.

(7) Substantial increases in MOX fabrication charges have an effect on breakeven ore cost that is noticeable, but not substantial.

(8) The breakeven ore cost will further increase if we extend burnup by adopting the option of using more batches to manage the core. At low tails assay, $X_w$, and for high U-235 enrichment, $X_p$, the breakeven ore cost becomes more sensitive to enrichment cost. For example, for $X_p$ = 3.0 w/o U-235 and $X_w$ = 0.25% the breakeven ore cost is increased by 1 $/lb for a decrease of 6.7 $/kg SWU in enrichment cost; whereas, for $X_p$ = 4.0 w/o and $X_w$ = 0.1% an enrichment cost decrease of 2.92 $/kg SWU can increase the breakeven ore cost by 1 $/lb.

(9) Recycle is favored as burnup is increased for the same number of batches, and the once-through cycle is benefitted by cheap SWU and lower tail's assay. If, as is generally forseen, 18 month cycle/3 batch cores are eventually achieved in PWRS, the breakeven cost will decrease to 54.5 $/lb $U_3O_8$ (a decrease of 22 $/lb $U_3O_8$ from the base case breakeven cost). On the other hand, if the cost of separative work decreases to 60 $/kg SWU and the tails assay is reduced to 0.15%, the increase in the breakeven cost would be 22.9 $/lb $U_3O_8$, more than enough to offset the decrease in breakeven cost incurred by going to higher burnup.

(10) For dry lattices, plutonium is worth less than in wet lattices, due to their harder spectra. Thus, comparatively more spent fuel from convential lattices needs to be reprocessed to constitute a reload batch. Therefore, since we have considered only single-pass recycle, there is no incentive to use drier lattices despite their higher conversion ratio. Moreover the relative amounts of Pu-240 and Pu-242 are increased in the fuel discharged from multipass recycle, and thus a greater mass of plutonium would be required to meet fissile feed requirements. Thus, while not examined in depth here, one must question the economic prospects of tight pitch cores in LWRs even if multipass recycle is allowed.

## 5.5 Recommendations

During the course of present work a number of technical/ economic aspects of the LWR fuel cycle were identified as deserving of additional evaluation:

- Use of recycled uranium could entail some difficulties beyond those accounted for in the present work. In addition to U-236, recycled uranium can contain small amounts of U-232 and U-234 as well as trace amounts of transuranics and fission products, all of which will make operations and maintenance

more difficult in an enrichment facility. It was assumed in the present study that recycled uranium would be accepted as feed material in an enrichment plant. This assumption should be examined, since it is possible that enrichment plants will either restrict feed material to natural uranium or charge a premium for handling recycled material (e.g. the diseconomy of scale incurred by a dedicated facility). The uranium savings credited to the recycle mode will be significantly reduced if re-enrichment is not permitted. On the other hand, the potentially beneficial introduction of laser isotope separation, which could selectively reject these detrimental isotopes, and which could better accommodate higher activity feed stock and permit rapid turn around between campaigns, should be assessed. Similarly, beneficiation of mixed isotopes of plutonium could also be contemplated.

- The reprocessed uranium-plutonium mixture from LWR discharged fuel would appear to be a premium reload fuel for CANDU reactors, without the need for re-enrichment. Hence its value for this use should be evaluated against natural uranium feed to provide a second pricing basis for recovered MOX.

- A critical review of cost projections for the back end of the fuel cycle is needed, to address the following issues:
    - the long term cost of reprocessing taking into account potential restrictions on C-14, H-3,

Kr-85 and other radionuclide releases; and the safeguards costs of sequestering plutonium.

- o the cost differential between the disposal of intact fuel assemblies and reprocessed waste.
- c reduction in MOX refabrication costs through the introduction of advanced robotics and other innovations.
- o and, as previously noted, the use of LIS to upgrade isotopic content.

- While not a finding unique to the present study, it is nevertheless clear that continuing attention to improvement of the projected cost/resource relation for $U_3O_8$ is essential, in as much as it is the principal determinant of whether and when LWR recycle or the introduction of breeder reactors are economically viable.

- Finally, although all of the correlations developed in this work should remain valid as to functional form, it would be useful to up-grade the numerical value of the curve-fit constants using state-of-the-art data and computer methods as they become available. In particular, LEOPARD-based results can undoubted be improved upon for plutonium-recycle cases, particularly in tight-pitch cores.

# APPENDIX A

## Functional Dependence of Isotopic Composition of Spent Fuel on Various Parameters

Both experimental data and computed results for LWR reprocessed fuel indicate that there exists predictable functional dependencies for the isotopic composition of spent fuel over a range of reactor operating conditions and burnup [K1]. Considerable use has been made of such correlations by the safeguards community. In the present work approximate formulae for the content of U-235, U-236 and fissile plutonium in the discharged fuel have been formulated by fitting semi-empirical relations to the output of LEOPARD computer code calculations, following the procedure shown in flow chart form in Fig. (A-1).

Reactivity versus burnup data was computed for various enrichments, $X_P$ , and fuel-to-moderator ratios, $V_F/V_M$ , using the LEOPARD program for fuel representative of Main Yankee assemblies. The intercept ($\rho_o$) and slope (A) of the $\rho(B)$ correlations were determined from the results of a linear least squares curve fit, using a standard statistical package of simple regressions on a minicomputer. The values of $\rho_o$ , A and $\frac{\rho_o}{A}$ are tabulated for various $X_P$ and $V_F/V_M$ values in

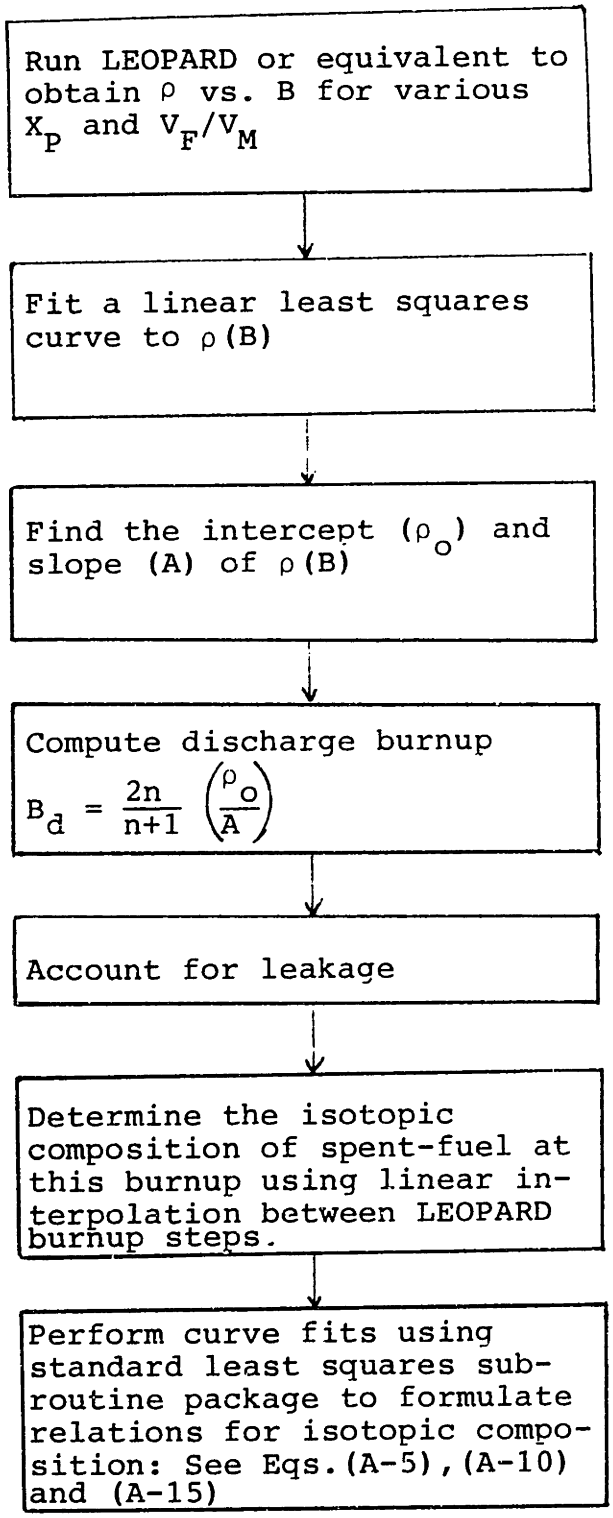


Fig. A-1. Flowchart for the procedure used to develop isotopic composition relations for discharged fuel.

Table (A-1). Reactivity-limited discharge fuel burnup was calculated by applying the following equation

$$B_d = \frac{2n}{n+1} \frac{\rho_o}{A} \qquad \text{(A-1)}$$

Note that the values of $\rho_o$ determined using data directly from LEOPARD output are the infinite medium values. The system values of $\rho_o$ in a finite reactor can be calculated by subtracting a leakage reactivity component $\rho_L$ from $\rho_o$. The neutron loss via leakage is normally on the order of $\leq$ 5% in a large modern LWR, hence in the current procedure a leakage allowance of $\rho_L = 0.05 \rho_o$ was assumed to calculate the reactivity-limited discharge burnup for a finite system. The isotopic composition of spent fuel at this discharge burnup was determined by interpolating linearly between LEOPARD burnup steps. Using standard statistical programs for simple regressions, the data were curve fit, keeping the enrichment, $X_p$, as the independent variable and $V_F/V_M$ as a parameter and treating X-236, $X_d$-235 and $X_{Puf}$ as the dependent variables. In each case a variety of candidate functional representations were evaluated (selected using insight gained from reviewing the results of prior work in this area in the previously cited literature) and the best in terms of goodness of fit, simplicity and compatibility with the expected theoretical variation were selected.

The functional dependence of X-236 versus $X_p$ was found to be of the form

$$\text{X-236 } (X_p) = a_1 + b_1 X_p \qquad \text{(A-2)}$$

TABLE A-1

Variation of $\rho_o$, A and $\rho_o/A$, with $X_p$ and $V_F/V_M$

| $X_p$ (w/o) | $V_F/V_M$ | $\rho_o$ | A $MT/10^3 GWD$ | $\rho_o/A$ GWD/MT | $R^2$ |
|---|---|---|---|---|---|
| 2.5 | 0.604 | 0.1963 | 10.0036 | 19.6226 | 0.999 |
| | 0.750 | 0.1738 | 9.1154 | 19.0655 | 0.998 |
| | 1.000 | 0.1382 | 8.3527 | 16.5472 | 0.992 |
| 3.0 | 0.604 | 0.2220 | 9.0538 | 24.5170 | 1.000 |
| | 0.750 | 0.1995 | 8.4314 | 23.6638 | 0.998 |
| | 1.000 | 0.1658 | 8.1364 | 20.3764 | 0.997 |
| 3.5 | 0.604 | 0.2429 | 8.3572 | 29.0671 | 1.000 |
| | 0.750 | 0.2174 | 7.7005 | 28.2359 | 0.998 |
| | 1.000 | 0.1844 | 7.6119 | 24.2242 | 0.999 |
| 4.0 | 0.604 | 0.2570 | 7.5942 | 33.8448 | 0.999 |
| | 0.750 | 0.2320 | 7.1345 | 32.5250 | 0.999 |
| | 1.000 | 0.1972 | 6.9825 | 28.2420 | 0.999 |
| 4.5 | 0.604 | 0.2676 | 6.9151 | 38.7014 | 0.999 |
| | 0.750 | 0.2440 | 6.6633 | 36.6206 | 0.999 |
| | 1.000 | 0.2092 | 6.5724 | 31.8317 | 0.998 |

where $a_1$ and $b_1$ depend on $V_F/V_M$ , and can be expressed as

$$a_1 \ (V_F/V_M) = a_2 + b_2 \ V_F/V_M \qquad \text{(A-3)}$$

and

$$b_1 \ (V_F/V_M) = a_3 + b_3 \ V_F/V_M \qquad \text{(A-4)}$$

The parameters, $a_2$ , $a_3$ , $b_2$ and $b_3$ are constants which depend on the number of batches (since, for a fixed reload enrichment, the number of staggered-reload batches determines the reactivity-limited discharge burnup). Combining Eqs. (A-2), (A-3) and (A-4),

$$\text{X-236}\left(X_P \ , \ \frac{V_F}{V_M}\right) = \left(a_2 + b_2 \ \frac{V_F}{V_M}\right) + \left(a_3 + b_3 \ \frac{V_F}{V_M}\right) X_P \qquad \text{(A-5)}$$

with:

$a_2 = -0.025$ $\qquad$ $b_2 = 0.0917$ $\qquad$ $R^2 = 0.98$

$a_3 = 0.1567$ $\qquad$ $b_3 = 0.0128$ $\qquad$ $R^2 = 0.98$

Following a similar procedure, the variation of X-236 with $X_P$ and $V_F/V_M$ was obtained for n = 4 and n = 5 . Including the dependence of X-236 on n , it was found that:

$$\text{X-236}\left(X_P \ , \ \frac{V_F}{V_M} \ , \ n\right) = \frac{1}{100}\left[\left(\frac{4 + 3n}{10}\right)\left(\frac{V_F}{V_M}\right) + \left(14.67 + \frac{3}{n}\right)\right] X_P - \left[\frac{0.075}{n} + 0.09 \quad (V_F/V_M)\right] \qquad \text{(A-6)}$$

The coefficients of the curve fit of Eq. (A-2) for various fuel-to-moderator ratios are listed in Table A-2. The values of $R^2$ are the coefficients of determination corresponding to

TABLE A-2

Coefficients of Curve Fit of X-236 Versus Enrichment for Various Fuel-to-Moderator Ratios

| Number of batches n | $V_F/V_M$ | X-236 = $a_1$ + $b_1$ $X_P$ | | $R^2$ |
|---|---|---|---|---|
| | | $a_1$ w/o | $b_1$ | |
| 3 | 0.604 | -0.08280 | 0.16467 | 1.000 |
| | 0.750 | -0.08995 | 0.16582 | 1.000 |
| | 1.000 | -0.11810 | 0.16962 | 1.000 |
| 4 | 0.604 | -0.07621 | 0.16493 | 1.000 |
| | 0.750 | -0.07723 | 0.16420 | 1.000 |
| | 1.000 | -0.11110 | 0.17015 | 1.000 |
| 5 | 0.604 | -0.07269 | 0.16507 | 1.000 |
| | 0.750 | -0.07285 | 0.16390 | 0.999 |
| | 1.000 | -0.10530 | 0.17072 | 1.000 |

the curve fit of the function under study. They give an indication of how good a match to the data has been obtained: $R^2$ is the fraction of total variance accounted for by the subject relation, hence a value of $R^2 = 1$ indicates that a perfect fit has been achieved. In general $R^2$ was $\geq 0.98$ for all the correlations in the present work - which is an indication of exceptionally good agreement.

An analogous approach was used to determine the functional dependence of $X_d$-235 and $X_{Puf}$ on $X_P$ and $V_F/V_M$ for n = 3, 4 and 5.

$$X_d\text{-}235 = a_4 \ (V_F/V_M) + b_4 \ (V_F/V_M) \ \ln X_P \tag{A-7}$$

$$a_4 \ (V_F/V_M) = a_5 + b_5 \Big/ (V_F/V_M) \tag{A-8}$$

$$b_4 \ (V_F/V_M) = a_6 + b_6 (V_F/V_M) \tag{A-9}$$

Substituting Eqs. (A-8) and (A-9) in Eq. (A-7)

$$X_d\text{-}235 \ (X_P \ , \ V_F/V_M) = a_5 + b_5 \Big/ (V_F/V_M) + \left[a_6 + b_6 \ (V_F/V_M)\right] \ \ln X_P \tag{A-10}$$

with:

$a_5 = 0.037$ ; $b_5 = 0.281$ ; $R^2 = 0.98$

$a_6 = -0.701$ ; $b_6 = 1.261$ ; $R^2 = 0.999$

Similarly $a_5$ , $a_6$ , $b_5$ and $b_6$ were determined for n=4 and n=5 to give

$$X_d\text{-}235\left(X_P\ ,\ \frac{V_F}{V_M}\ ,\ n\right) = \left(0.454 - \frac{5}{4n}\right) + \left(\frac{0.635}{n} + 0.07\right)\Big/\left(\frac{V_F}{V_M}\right) + \left[\left(1 + \frac{0.782}{n}\right)\left(\frac{V_F}{V_M}\right) - \left(0.575 + \frac{n}{24}\right)\right] \ln X_P \qquad \text{(A-11)}$$

The coefficients of curve fit of Eq. (A-7) for various fuel-to-moderator ratios are listed in table (A-3).

$$X_{Puf} = a_7\ (V_F/V_M) + b_7\ \ (V_F/V_M)\Big/ X_P \qquad \text{(A-12)}$$

$$a_7\ (V_F/V_M) = a_8 + b_8\ \ln\ (V_F/V_M) \qquad \text{(A-13)}$$

$$b_7\ (V_F/V_M) = a_9 + b_9\ (V_F/V_M) \qquad \text{(A-14)}$$

Table (A-4) shows the coefficients of curve fit of Eq. (A-12) for various fuel-to-moderator ratios. Equations (A-12), (A-13) and (A-14) give

$$X_{Puf}\ (X_P\ ,\ V_F/V_M) = a_8 + b_8\ \ln(V_F/V_M) + \left[a_9 + b_9\ (V_F/V_M)\right]\Big/ X_P \qquad \text{(A-15)}$$

with:

$a_8 = 1.543$ ; $b_8 = 1.419$ ; $R^2 = 0.999$

$a_9 = 1.40$ ; $b_9 = -3.5$ ; $R^2 = 0.999$

Including the dependence of $a_8$ , $b_8$ , $a_9$ and $b_9$ on n , Eq. (A-15) becomes

$$X_{Puf}\left(X_P\ ,\ \frac{V_F}{V_M}\ ,\ n\right) = \left(1.528 + \frac{5n}{1000}\right) + (1.27 + 0.05n)\ \ln X_P + \frac{1}{X_P}\left[\left(1.1 + \frac{n}{10}\right) - (3.28 + 0.073n)\ \frac{V_F}{V_M}\right] \qquad \text{(A-16)}$$

TABLE A-3

Coefficients of Curve Fit of $X_d$-235 Versus Enrichment for Various Fuel-to-Moderator Ratios

| Number of batches | $V_F/V_M$ | $X_d\text{-}235=a_4 + b_4 \ln X_P$ | | $R^2$ |
|---|---|---|---|---|
| | | $a_4$ w/o | $b_4$ w/o | |
| 3 | 0.604 | 0.51149 | 0.05308 | 0.994 |
| | 0.750 | 0.39613 | 0.25510 | 0.990 |
| | 1.000 | 0.32664 | 0.55526 | 0.995 |
| 4 | 0.604 | 0.51400 | -0.01984 | 0.997 |
| | 0.750 | 0.43970 | 0.14838 | 0.986 |
| | 1.000 | 0.36709 | 0.45148 | 0.993 |
| 5 | 0.604 | 0.52378 | -0.07110 | 0.998 |
| | 0.750 | 0.46671 | 0.08350 | 0.992 |
| | 1.000 | 0.39006 | 0.38839 | 0.995 |

TABLE A-4

Coefficients of Curve Fit of $X_{Puf}$ Versus Enrichment for Various Fuel-to-Moderator Ratios

| Number of batches n | $V_F/V_M$ | $X_{Puf} = a_7 + b_7/X_P$ | | $R^2$ |
|---|---|---|---|---|
| | | $a_7$ w/o | $b_7$ $(w/o)^2$ | |
| 3 | 0.604 | 0.83221 | -0.70539 | 0.998 |
| | 0.750 | 1.12550 | -1.26830 | 0.994 |
| | 1.000 | 1.54653 | -2.10452 | 0.994 |
| 4 | 0.604 | 0.81652 | -0.64795 | 0.996 |
| | 0.750 | 1.11234 | -1.19902 | 0.991 |
| | 1.000 | 1.56388 | -2.08705 | 0.990 |
| 5 | 0.604 | 0.81429 | -0.64033 | 0.995 |
| | 0.750 | 1.07507 | -1.06521 | 0.992 |
| | 1.000 | 1.57165 | -2.06732 | 0.997 |

Comparisons of results obtained from Eqs. (A-6), (A-11) and (A-16) with the input data are made in Chapter 2.

The contents of X-235, X-236 and $X_{Puf}$ in the spent fuel versus the reactivity-limited discharge burnup for various numbers of batches are plotted in Figs. (A-2), (A-3) and (A-4). It can be seen that for the same $X_P$ , $X_{Puf}$ is slightly higher for larger n , corresponding to the higher burnup achieved, but for progressively larger $X_P$ , $X_{Puf}$ tends to saturate. These figures also show the interdependence of B , $X_P$ and n , indicating that one can work in any set of variables of ones' choice. Again note that the burnup plotted is the reactivity-limited discharge burnup and that the correlations developed here do not apply for intermediate burnups (see section 2.5 for such broader scope correlations).

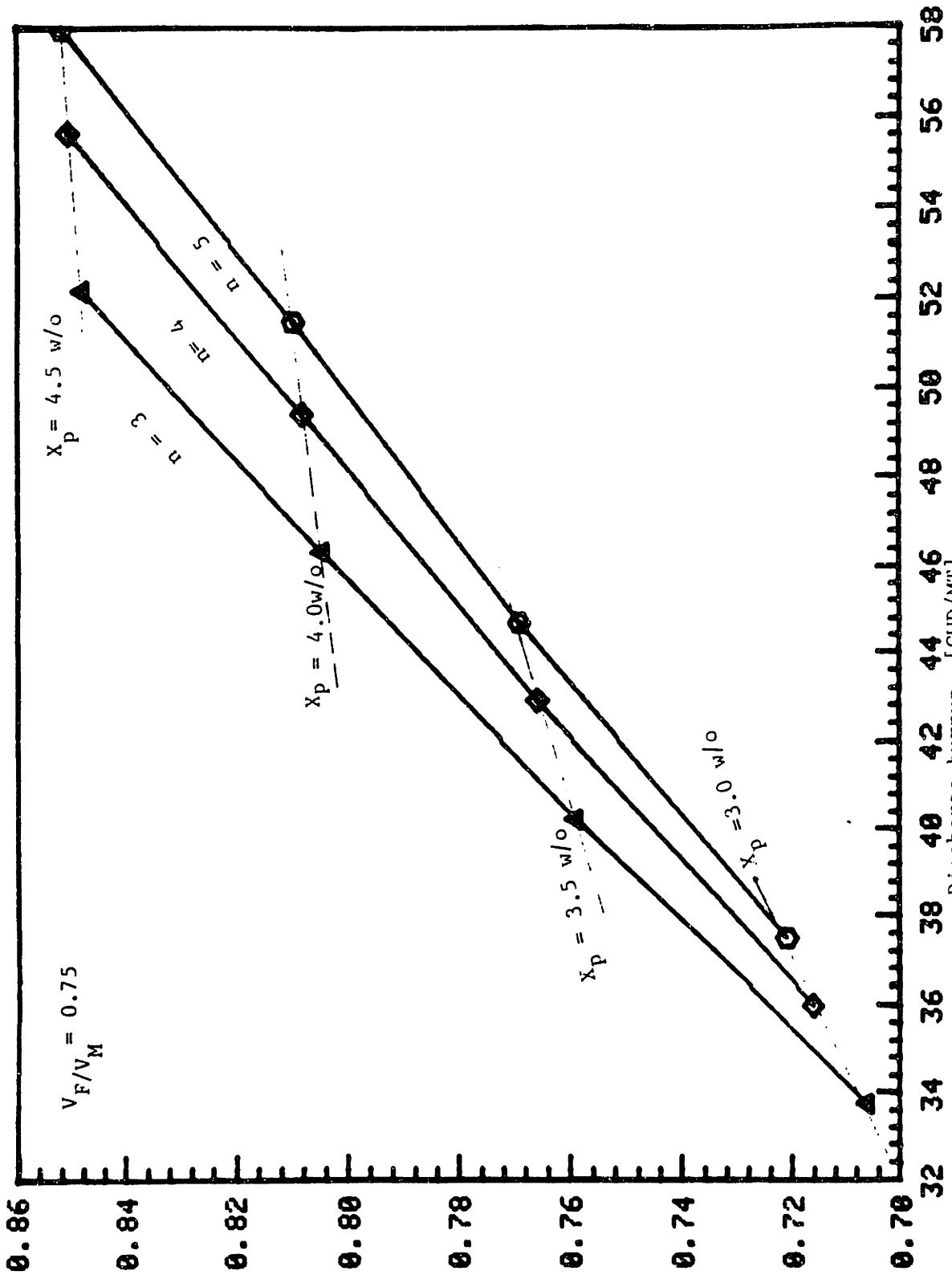


Fig.A-2.Fissile Pu in discharged fuel vs discharge burnup for various n:($V_{F/V_M}$=0.75).

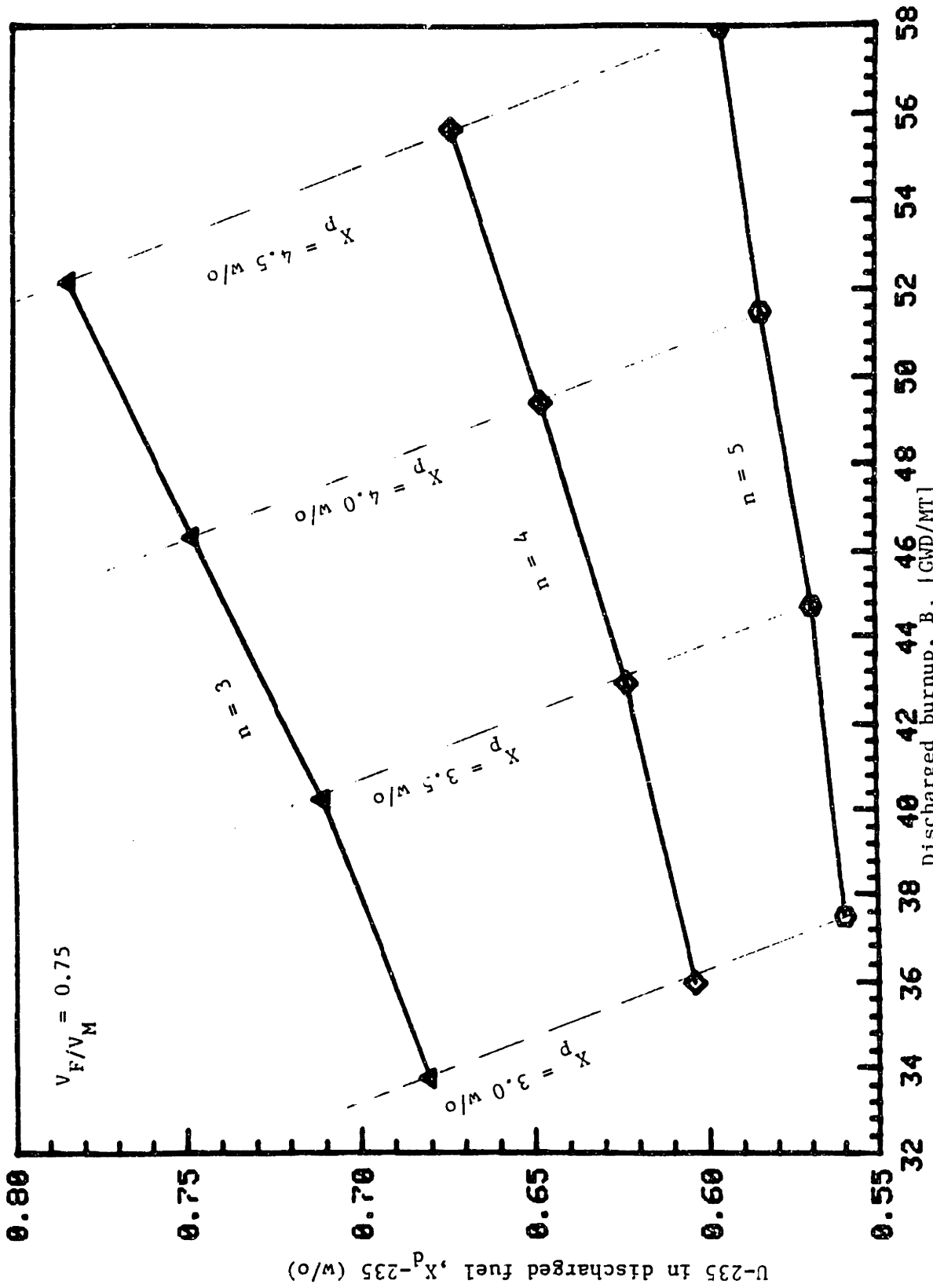


Fig.A-3 U-235 in discharged fuel vs discharge burnup for various n ($V_{F/V_M}$=0.75).

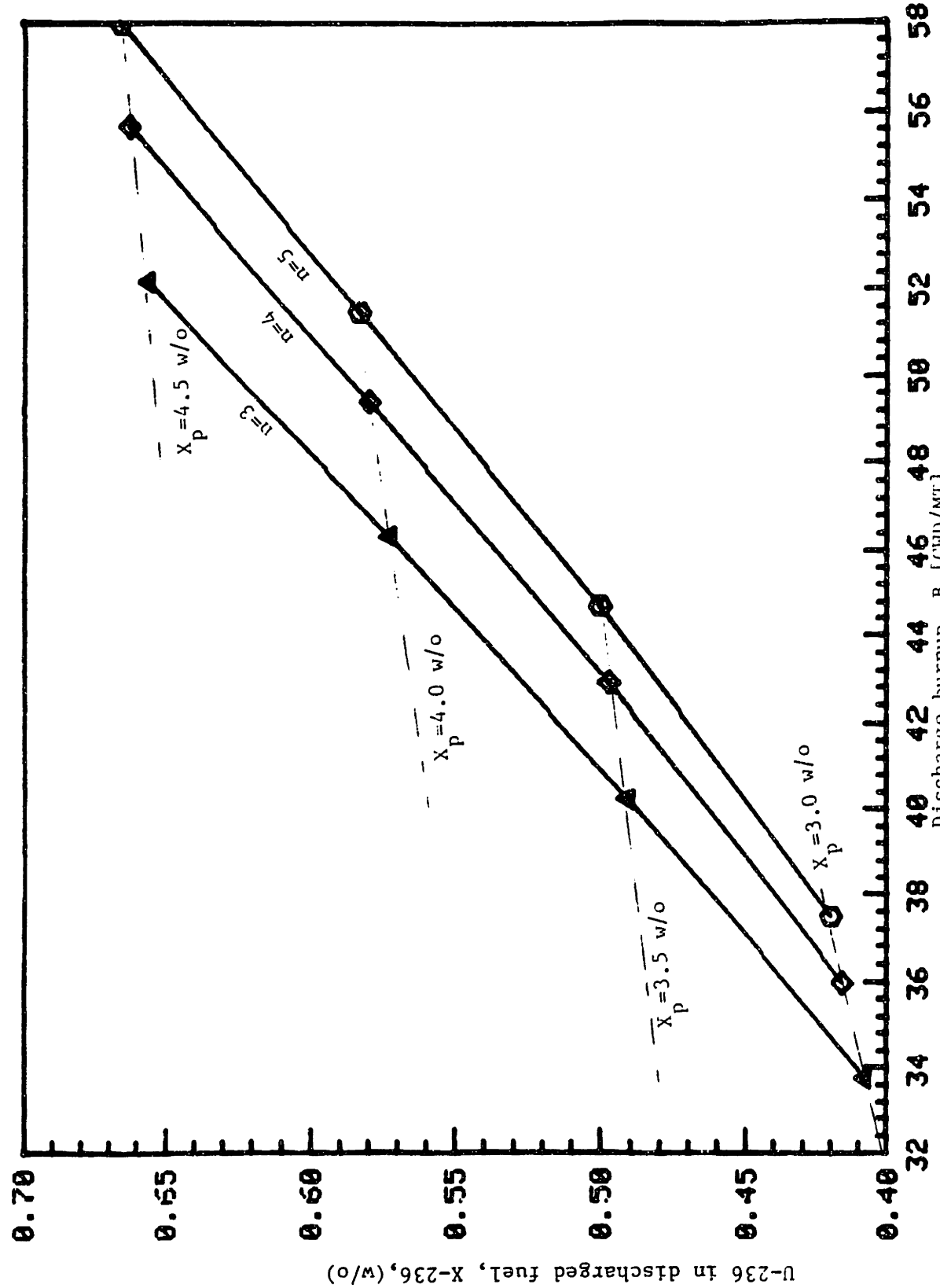


Fig.A-4. U-236 in discharged fuel vs discharge burnup for various n ( $V_F/V_M$=0.75)

# APPENDIX B

## Computer Program

### B-1 Description and Listing

This appendix documents the Nuclear Fuel Cycle (NFC) program. It is written in the BASIC Language for the TEKTRONIX Model 4051, 32K RAM minicomputer. The program is interactive in nature and hence very simple to use. It has default values built in for various parameters, and prompts the user to make changes prior to executing a run. It also contains a large number of interspersed REMARK statements, which should facilitate the insertion of modifications by the user. The total program is only about 250 lines, and it can be accommodated by most of the microcomputer brands now on the market.

The interrelation of various submodels in the program is shown in Fig. 5.1. The subject program has the following major characteristics:

- The calculational methodology is based on simple semi-empirical correlations developed during this work.
- Batch enrichment, fuel-to-moderator ratio, discharge burnup and number of batches can be varied: the program

calculates the isotopic composition of spent fuel needed for recycle mode calculations from curve-fit correlations.

- The option of using the cost-optimum tails assay is available.
- Various cash flows are described in terms of direct plus carrying charges.
- The value of plutonium is implicitly included by basing spent fuel value on the avoided cost of disposal.
- The presence of U-236 in the isotope separation plant is taken into account, and corresponding SWU and burnup penalties are included.
- The estimation of a scarcity-related cost escalation rate for future uranium prices, as a function of key variables, is included.
- The busbar and the system cost relationship are also included to permit analysis of the effect of the plant capacity factor and the cost of replacement energy during refueling downtime.
- The output includes all input data, information on each reload; and discharge burnup, fuel cycle, busbar and system costs for once-through and recycle mode operation, as well as uranium price projections.

Important parameters are given in table B-1, following which the program listing is appended.

TABLE B-1

Important Parameters in the NFC Program

| | |
|---|---|
| A(I) | Ith cost coefficient in the fuel cycle cost equation. |
| B0 | Discharge Burnup [GWD(th)/MT]. |
| C(I) | Unit cost of Ith transaction [$/kg or $/lb]. |
| E0 | Replacement energy cost [mills/kwhre]. |
| E1 | Energy produced per Batch, kwhrs(electric). |
| E(I) | Year-by-Year Installed Nuclear Capacity [MWE]. |
| F0 | Spent Fuel required per Kg of Plutonium reload. |
| F1 | Conversion Yield Fraction. |
| F2 | Enrichment Yield Fraction. |
| F3 | Fabrication Yield Fraction. |
| H1 | Rated thermal power [MW]. |
| L | Availability-based capacity factor. |
| L0 | Capacity factor |
| M(I) | Mass of Ith transaction, Kg or lb. |
| N0 | Number of Batches. |
| R | Fuel-to-Moderator Ratio. |
| R0 | $\rho_o/A$ [GWD/MT]. |
| T1 | Irradiation time [Yrs]. |
| T2 | Refueling down-time [Yrs]. |
| T3 | Cycle length [Yrs]. |
| X | Discount rate. |
| X1 | U-235 (w/o) in the enrichment plant Feed. |

X2 U-235 (w/o) in the enrichment plant Product.

X3 U-235 (w/o) in the enrichment plant tails.

X4 Fissile Plutonium (w/o) in the spent fuel.

X5 U-235 (w/o) in the spent fuel.

X6 U-236 (w/o) in the spent fuel.

Y2 U-236 (w/o) in the enriched uranium produced from the spent fuel.

```
90 REMARK NUCLEAR FUEL CYCLE (NFC)PROGRAM
95 N=13
100 DIM M(N),C(N),T(N),P(N),P1(N),U(N),H(N),Q1(N)
110 X1=0.711
120 M1=100
130 N1=0.34
140 PRINT "enter the # of batchs"
150 INPUT N0
160 N2=2*N0/(N0+1)
170 PRINT "ENTER FUEL TO MODRATER RATIO FOR CELL"
180 INPUT R
190 L=0.8
200 T2=0.125
210 H1=3800
220 PRINT "enter 1 to input burnup or 2 to input enrichment"
230 PRINT "or 3 to input cycle length"
240 INPUT I0
250 GO TO I0 OF 260,350,300
260 PRINT "ENTER     BURNUP (GWD/MT)"
270 INPUT B0
280 X2=B0/9/N2+1
290 GO TO 380
300 PRINT "ENTER CYCLE LENGTH"
310 INPUT T3
320 B0=(T3-T2)*N0*365.25*L*H1/M1/1000
330 X2=B0/9/N2+1
340 GO TO 390
350 PRINT "ENTER ENRICHMENT"
360 INPUT X2
370 B0=9*N2*(X2-1)
380 T3=B0*M1/(365.25*L*H1*N0)*1000+T2
390 R0=1.3+(12.338-4.674*R)*X2-3.5/R
400 L0=L*(1-T2/T3)
410 T1=N0*T3
```

```
420 E1=24*N1*B0*M1/N0*1000000
430 F1=0.995
440 F2=0.995
450 F3=0.995
460 F4=0.5
470 X=0.1
480 REMARK DISCHARGE FUEL COMPOSITION
490 X4=11.92-2.2*R+(0.20834+1.43381/R)*X2
500 X4=(X4+(2.46378-1.46607*R+(0.18238*R-0.28578)*X2)*B0)↑-1*B0
510 X5=-1.62102+0.28151*R+(2.30733-0.29904*R)*X2
520 X5=X5+X2*(0.08364*R-0.46118)*LOG(B0)
530 X6=(0.17215+0.00881*R)*X2
540 Y1=X6+(-2.548+14.655*R-8.397*R↑2+X2*(-1.263-3.288*R+1.912*R↑2))/B0
550 X7=(R0+3.5*(1+6.8*R))/(2-R)/9
560 X8=X5-0.2*Y1
570 F0=(X7-X8)/X4
580 A0=25
590 E0=65
600 GOSUB 1980
610 REMARK C(I) IS UNIT COST OF DIFFERENT TRANSACTIONS
620 REMARK T(I) IS LEAD OR LAG TIME FOR EACH TRANCTION
630 RESTORE 650
640 READ C
650 DATA 25,5,140,200,150,-150,600,150,570,-140,-5,-25,150
660 RESTORE 680
670 READ T
680 DATA -1.5,-1,-1,-0.5,1,-1.5,-1.5,-0.5,-0.5,-0.5,-0.5,-0.5,1
690 T(5)=T(5)+T1
700 T(13)=T(13)+T1
710 PRINT "ENTER THE ITEM # TO CHANGE THE UNIT COST OR 0 TO CONTINUE"
720 INPUT I0
730 IF I0=0 THEN 770
740 PRINT "INPUT THE NEW COST OF THIS ITEM"
750 INPUT C(I0)
760 GO TO 710
```

```
770 PRINT "enter the item # to change its lead or lag time or 0 to cont"
780 INPUT I0
790 IF I0=0 THEN 830
800 PRINT "enter new lead or lag time of this item "
810 INPUT T(I0)
820 GO TO 770
830 C(10)=-C(3)
840 C(6)=-C(5)
850 C(8)=C(5)
860 C(12)=-C(1)
870 C(11)=-C(2)
880 C(13)=C(5)
890 PRINT "ENTER 0 IF YOU WANT TO USE OPTIMUM TAIL'S ASSAY"
900 PRINT "OTHERWISE ENTER THE TAIL'S  ASSAY   YOU WANT TO USE"
910 INPUT X3
920 IF X3>0 THEN 990
930 REMARK OPTIMUM TAIL'S SUBROUTINE
940 C1=2.599*C(1)/F1*(1+(T(2)-T(1))*0.1)+C(2)
950 R1=C1/C(3)
960 X3=(2.425+1.925*R1)↑-1
970 PRINT "OPTIMUM TAILS ASSAY=";X3
980 REMARK MASS FLOW FOR ONCE-THROUGH CYCLE
990 M(5)=M1/M0*1000
1000 M(4)=M(5)/F3
1010 DEF FNS(X)=(X/50-1)*LOG(X/100/(1-X/100))
1020 S1=FNS(X2)+(X2-X1)/(X1-X3)*FNS(X3)-(X2-X3)/(X1-X3)*FNS(X1)
1030 M(3)=M(4)/F2*S1
1040 M(2)=M(4)/F2*(X2-X3)/(X1-X3)
1050 M(1)=2.6*M(2)/F1
1060 PRINT "ENTER 1,5  FOR ONCE-THROUGH MODE AND 6,13 FOR RECYCLE MODE "
1070 INPUT I1,I2
1080 IF I1=1 THEN 1430
1090 REMARK MASS FLOW FOR RECYCLE MODE
1100 M(5)=M1/M0*1000
1110 M(6)=F0*M(5)
```

```
1120 M(7)=M(6)
1130 M(8)=M(6)
1140 M(9)=M(5)
1150 REMARK U-236 PENALTY CALCULATIONS
1160 N4=0
1170 A=0.12125+1.084*X5
1180 B=0.27323+0.234*X5
1190 C0=0.00521+0.0142*X5
1200 D=0.06476-0.01044/X5
1210 X6=X2+0.2*Y1
1220 D0=(A+B*X3+(C0+D*X3)*X6)/Y1
1230 Y2=Y1+(X6-X5)/D0
1240 Y3=Y1-(X5-X3)/D0
1250 X9=X2+0.2*Y2
1260 IF ABS(X9-X6)<0.05 OR N4>10 THEN 1300
1270 N4=N4+1
1280 X6=X9
1290 GO TO 1220
1300 REMARK SWU CALCULATIONS FOR THREE ISOTOPES
1310 Z1=X5/(100-X5-Y1)
1320 Z2=X9/(100-X9-Y2)
1330 Z3=X3/(100-X3-Y3)
1340 S2=(X9/50+Y2/25-1)*LOG(Z2)+(X9-X5)/(X5-X3)*(X3/50+Y3/25-1)*LOG(Z3)
1350 S2=S2-(X9-X3)/(X5-X3)*(X5/50+Y1/25-1)*LOG(Z1)
1360 S3=S1-S2
1370 M(10)=M(5)*(F0-1)*(X5-X3)/(X9-X3)*F2*S3
1380 M(11)=M(10)/S3*(X2-X3)/(X1-X3)-M(5)*(F0-1)
1390 M(12)=2.6*M(10)/S3/F1*(X2-X3)/(X1-X3)
1400 M(13)=M(5)
1410 REMARK DIRECT+CARRYING CHARGES FOR ONCE-THROUGH-CYCLE
1420 REMARK      AND RECYCLE MODE
1430 P9=0
1440 U9=0
1450 H9=0
1460 FOR I0=I1 TO I2
```

```
1470 P1(I0)=M(I0)*C(I0)
1480 P(I0)=P1(I0)/E1*1000
1490 P9=P9+P(I0)
1500 U(I0)=P(I0)/(1-F4)*((1+X)↑(T1/2-T(I0))-1)
1510 U9=U9+U(I0)
1520 H(I0)=P(I0)+U(I0)
1525 Q1(I0)=H(I0)/C(I0)
1530 H9=H9+H(I0)
1540 NEXT I0
1550 E2=A0/L0+H9
1560 E3=E2*L0+E0*(1-L0)
1570 PAGE
1580 IF I1=1 THEN 1610
1590 PRINT USING "FA":"OUTPUT FOR RECYCLE MODE "
1600 GO TO 1630
1610 PRINT USING 1620:"OUTPUT FOR ONCE THROUGH CYCLE: TAILS ASSAY=",X3
1620 IMAGE 5X,45A,FD.5D
1630 GOSUB 2130
1640 PRINT
1650 PRINT USING 1660:"STEP","MASS    ","UNIT COST ","DIRECT COST","LAG"
1660 IMAGE 5A,5X,8A,25T,12A,41T,11A,55T,3A
1670 FOR J0=I1 TO I2
1680 PRINT USING 1690:J0,M(J0),C(J0),P1(J0),T(J0)
1690 IMAGE 2D,10T,4E,25T,6D.2D,40T,4E,55T,2D.4D
1700 NEXT J0
1710 PRINT
1720 PRINT USING "FA":"   COST IN MILLS/Kwhr  "
1730 GOSUB 2130
1740 PRINT
1750 PRINT USING 1760:"STEP","DIRECT","CARRYING","DIRECT+CARRYING","Qis"
1760 IMAGE 5A,5X,15A,5X,8A,5X,18A,2x,3a
1770 FOR J0=I1 TO I2
1780 PRINT USING 1790:J0,P(J0),U(J0),H(J0),Q1(J0)
1790 IMAGE 2D, 9T,3D.4D,25T,3D.4D,40T,4D.3D,54t,2d.6d
1800 NEXT J0
```

```
1810 PRINT
1820 PRINT USING 1830:"TOTAL ef",P9,U9,H9
1830 IMAGE 9A,10T,2D.4D,26T,2D.4D,40T,4D.3D
1840 IMAGE 5X,30A,2X,FD.4D,50T,FA
1850 IMAGE 5X,25A,2X,4E,50T,FA
1855 GOSUB 2130
1857 PRINT
1860 PRINT USING 1840:"busbar cost =",E2,"mills/kwhr"
1865 GOSUB 2130
1867 PRINT
1870 PRINT USING 1840:"system cost =",E3,"mills/kwhr"
1875 GOSUB 2130
1877 PRINT
1880 PRINT "DO YOU WANT TO RUN ANOTHER CASE (Y OR N)?";
1890 INPUT J$
1900 IF J$="N" THEN 2180
1910 PRINT "do you want to run recycle mode for the same data(y or n)"
1920 INPUT I$
1930 IF I$="Y" THEN 1060
1940 PRINT "DO YOU WANT TO CHANGE # OF BATCHES OR Xp OR F/M(Y OR N)?"
1950 INPUT K$
1960 IF K$="Y" THEN 140
1970 GO TO 710
1975 GOSUB 2130
1977 PRINT
1980 PRINT USING 1840:"FUEL ENRICHMENT",X2,"WT%"
1990 PRINT USING 1840:"CAPACITY FACTOR",L0,"-----"
2000 PRINT USING 1840:"IRRADIATION TIME",T1,"Yrs"
2010 PRINT USING 1840:"BURNUP  ",B0,"GWD/MT"
2020 PRINT USING 1850:"ENERGY PER BATCH",E1,"Kwhrs"
2030 PRINT USING 1840:"TAX FRACTION Ta ",F4,"-----"
2040 PRINT USING 1840:"YIELD FRACTION  ",F1,"-----"
2050 PRINT USING 1840:"DISCOUNT RATE X ",X,"PER Yr"
2060 PRINT USING 1840:"A IN eb=A/L+ef IS =",A0,"Mills/kwhr"
```

```
2070 PRINT USING 1840:"REPLACEMENT POWER COST=",E0,"mills/kwhr"
2075 PRINT USING "fa":" COMPOSITION OF SPENT FUEL"
2080 PRINT USING 1840:"U-235 IN SPENT FUEL=",X5,"WT%"
2090 PRINT USING 1840:"FISSILE PU IN SPENT FUEL=",X4,"WT%"
2100 PRINT USING 1840:"U-236 IN SPENT FUEL =",Y1,"WT%"
2110 PRINT USING 1840:"SPENT FUEL REQUIRED/KG HM=",F0,"KG"
2115 GOSUB 2130
2117 PRINT
2120 RETURN
2130 FOR K0=1 TO 60
2140 PRINT "-";
2150 NEXT K0
2160 RETURN
2170 REMARK SUBROUTINE TO CALCULATE PRICE OF ORE IN FUTURE
2180 PRINT "ENTER THE # OF YEARS OF FORCASTING PERIOD"
2185 INIT
2190 INPUT K
2200 DIM E(100)
2210 PRINT "ENTER DATA "
2220 FOR I=1 TO K
2230 J=1983+I
2240 PRINT J
2250 INPUT E(I)
2260 NEXT I
2270 PAGE
2280 PRINT USING "fa":"forcasted price of ore "
2290 GOSUB 2130
2300 PRINT
2310 PRINT USING 2320:"year","Installed capacity","Price of U3O8($/lb)"
2320 IMAGE 5a,5x,20a,5x,20a
2330 C0=20
2340 FOR I=1 TO K-1
2350 R=LOG(E(I+1)/E(I))
2360 C2=C0*EXP(0.5*R)
2370 J=1983+I
```

```
2380 GOSUB 2130
2390 PRINT
2400 PRINT USING 2410:J,E(I),C0
2410 IMAGE 4d,15t,6d.2d,37t,6d.2d
2420 C0=C2
2430 NEXT I
2440 END
```

## B-2 Sample Problem

A sample problem based on default values of transaction costs and their lead and lag time, as shown in table 4.1, follows.

```
run
enter the # of batchs
3
ENTER FUEL TO MODRATER RATIO FOR CELL
.6
enter 1 to input burnup or 2 to input enrichment
or 3 to input cycle length
2
ENTER ENRICHMENT
3.5
     FUEL ENRICHMENT                    3.5000       WT%
     CAPACITY FACTOR                    0.7121       -----
     IRRADIATION TIME                   3.4146       Yrs
     BURNUP                             33.7500      GWD/MT
     ENERGY PER BATCH                9.1800E+009     Kwhrs
     TAX FRACTION Ta                    0.5000       -----
     YIELD FRACTION                     0.9950       -----
     DISCOUNT RATE X                    0.1000       PER Yr
     A IN eb=A/L+ef IS =                25.0000      Mills/kwhr
     REPLACEMENT POWER COST=            65.0000      mills/kwhr
 COMPOSITION OF SPENT FUEL
     U-235 IN SPENT FUEL=               0.9336       WT%
     FISSILE PU IN SPENT FUEL=          0.6450       WT%
     U-236 IN SPENT FUEL =              0.4523       WT%
     SPENT FUEL REQUIRED/KG HM=         4.4287       KG
-------------------------------------------------------------
ENTER THE ITEM # TO CHANGE THE UNIT COST OR 0 TO CONTINUE
0
enter the item # to change its lead or lag time or 0 to cont
0
ENTER 0 IF YOU WANT TO USE OPTIMUM TAIL'S ASSAY
OTHERWISE ENTER THE TAIL'S  ASSAY   YOU WANT TO USE
.2
ENTER 1,5  FOR ONCE-THROUGH MODE AND 6,13 FOR RECYCLE MODE
1,5
```

OUTPUT FOR ONCE THROUGH CYCLE: TAILS ASSAY= 0.20000

| STEP | MASS | UNIT COST | DIRECT COST | LAG |
|---|---|---|---|---|
| 1 | 5.6817E+005 | 25.00 | 1.4204E+007 | -1.5000 |
| 2 | 2.1743E+005 | 5.00 | 1.0872E+006 | -1.0000 |
| 3 | 1.8229E+005 | 140.00 | 2.5520E+007 | -1.0000 |
| 4 | 3.3501E+004 | 200.00 | 6.7002E+006 | -0.5000 |
| 5 | 3.3333E+004 | 150.00 | 5.0000E+006 | 4.4146 |

COST IN MILLS/Kwhr

| STEP | DIRECT | CARRYING | DIRECT+CARRYING | Qis |
|---|---|---|---|---|
| 1 | 1.5473 | 1.1065 | 2.654 | 0.106151 |
| 2 | 0.1184 | 0.0697 | 0.188 | 0.037631 |
| 3 | 2.7800 | 1.6367 | 4.417 | 0.031548 |
| 4 | 0.7299 | 0.3418 | 1.072 | 0.005358 |
| 5 | 0.5447 | -0.2477 | 0.297 | 0.001979 |
| TOTAL ef | 5.7202 | 2.9070 | 8.627 | |

busbar cost = 43.7326 mills/kwhr

system cost = 49.8546 mills/kwhr

DO YOU WANT TO RUN ANOTHER CASE (Y OR N)?y
do you want to run recycle mode for the same data(y or n)
y
ENTER 1,5 FOR ONCE-THROUGH MODE AND 6,13 FOR RECYCLE MODE
6,13

OUTPUT FOR RECYCLE MODE

| STEP | MASS | UNIT COST | DIRECT COST | LAG |
|---|---|---|---|---|
| 6 | 1.4762E+005 | -150.00 | -2.2143E+007 | -1.5000 |
| 7 | 1.4762E+005 | 600.00 | 8.8573E+007 | -1.5000 |
| 8 | 1.4762E+005 | 150.00 | 2.2143E+007 | -0.5000 |
| 9 | 3.3501E+004 | 570.00 | 1.9095E+007 | -0.5000 |
| 10 | 1.6646E+004 | -140.00 | -2.3304E+006 | -0.5000 |
| 11 | 3.6114E+004 | -5.00 | -1.8057E+005 | -0.5000 |
| 12 | 3.9301E+005 | -25.00 | -9.8253E+006 | -0.5000 |
| 13 | 3.3333E+004 | 150.00 | 5.0000E+006 | 4.4146 |

COST IN MILLS/Kwhr

| STEP | DIRECT | CARRYING | DIRECT+CARRYING | Qis |
|---|---|---|---|---|
| 6 | -2.4121 | -1.7249 | -4.137 | 0.027580 |
| 7 | 9.6485 | 6.8998 | 16.548 | 0.027580 |
| 8 | 2.4121 | 1.1296 | 3.542 | 0.023611 |
| 9 | 2.0801 | 0.9741 | 3.054 | 0.005358 |
| 10 | -0.2539 | -0.1189 | -0.373 | 0.002662 |
| 11 | -0.0197 | -0.0092 | -0.029 | 0.005776 |
| 12 | -1.0703 | -0.5012 | -1.571 | 0.062860 |
| 13 | 0.5447 | -0.2477 | 0.297 | 0.001979 |
| TOTAL ef | 10.9295 | 6.4014 | 17.331 | |

busbar cost = 52.4363 mills/kwhr

system cost = 56.0529 mills/kwhr

DO YOU WANT TO RUN ANOTHER CASE (Y OR N)?

forcasted price of ore

| year | Installed capacity | Price of U308($/lb) |
|---|---|---|
| 1984 | 60.00 | 20.00 |
| 1985 | 80.00 | 23.09 |
| 1986 | 93.00 | 24.90 |
| 1987 | 104.00 | 26.33 |
| 1988 | 110.00 | 27.08 |
| 1989 | 114.00 | 27.57 |
| 1990 | 118.00 | 28.05 |
| 1991 | 119.19 | 28.19 |
| 1992 | 120.38 | 28.33 |
| 1993 | 121.59 | 28.47 |
| 1994 | 122.82 | 28.61 |
| 1995 | 124.05 | 28.76 |
| 1996 | 125.30 | 28.90 |
| 1997 | 126.56 | 29.05 |
| 1998 | 127.83 | 29.19 |
| 1999 | 129.11 | 29.34 |

| | | |
|---|---|---|
| 2000 | 130.41 | 29.49 |
| 2001 | 133.04 | 29.78 |
| 2002 | 135.73 | 30.08 |
| 2003 | 138.47 | 30.38 |
| 2004 | 141.27 | 30.69 |
| 2005 | 144.13 | 31.00 |
| 2006 | 147.04 | 31.31 |
| 2007 | 150.00 | 31.62 |
| 2008 | 153.04 | 31.94 |
| 2009 | 156.13 | 32.26 |
| 2010 | 159.28 | 32.59 |
| 2011 | 164.13 | 33.08 |
| 2012 | 169.13 | 33.58 |
| 2013 | 174.28 | 34.09 |
| 2014 | 179.59 | 34.60 |
| 2015 | 185.06 | 35.12 |
| 2016 | 190.69 | 35.65 |

| | | |
|---|---|---|
| 2017 | 196.50 | 36.19 |
| 2018 | 202.48 | 36.74 |
| 2019 | 208.65 | 37.30 |
| 2020 | 215.00 | 37.86 |
| 2021 | 223.77 | 38.62 |
| 2022 | 232.91 | 39.40 |
| 2023 | 242.41 | 40.20 |
| 2024 | 252.30 | 41.01 |
| 2025 | 262.60 | 41.84 |
| 2026 | 273.32 | 42.69 |
| 2027 | 284.47 | 43.55 |
| 2028 | 296.08 | 44.43 |
| 2029 | 3.80 | 5.03 |
| 2030 | 320.74 | 46.24 |
| 2031 | 337.18 | 47.41 |
| 2032 | 354.47 | 48.61 |
| 2033 | 372.65 | 49.84 |
| 2034 | 391.75 | 51.10 |

| | | |
|---|---|---|
| 2035 | 411.84 | 52.40 |
| 2036 | 432.95 | 53.72 |
| 2037 | 455.15 | 55.08 |
| 2038 | 478.49 | 56.48 |
| 2039 | 503.02 | 57.91 |
| 2040 | 528.81 | 59.38 |
| 2041 | 561.51 | 61.18 |
| 2042 | 596.23 | 63.05 |
| 2043 | 633.10 | 64.97 |
| 2044 | 672.25 | 66.95 |
| 2045 | 713.82 | 68.98 |
| 2046 | 757.96 | 71.08 |
| 2047 | 804.83 | 73.25 |
| 2048 | 854.60 | 75.48 |
| 2049 | 907.44 | 77.78 |

# APPENDIX C

## Variation of Reactivity with Burnup for Plutonium Fueled Assemblies

This appendix documents the reactivity versus burnup data computed using the LEOPARD program for plutonium fueled assemblies. The isotopic composition of plutonium fuel, representative of spent fuel, used in the following cases, is shown in table 3.2 .

In evaluating fuel-to-moderator ratios, the following geometric dimensions were kept constant:

- Fuel pellet diameter, $D_f$ = 0.3765 inches
- Clad outer diameter, $D_c$ = 0.440 inches

The different values of $V_F/V_M$ for hexagonal (≡ triangular) lattices were obtained by varying the lattice pitch, p , in the following relation,

$$V_F/V_M = \frac{\pi/4 \quad D_f^2}{( \sqrt{3}/2 \; P^2 - \pi/4 \; D_c^2)} \qquad \text{(C-1)}$$

Although a hexagonal configuration was used, no substantial difference from the more conventional square lattice used in todays' PWR's (other than those of Russian design, which do use hexagonal pitch) is to be expected. Triangular pitch has been specified because square pitch is impractical in the

drier end of the range of $V_F/V_M$ values considered. In this work $V_F/V_M$ was defined using cold lattice parameters for a unit cell. The hot lattice $V_F/V_M$ used by LEOPARD is adjusted (automatically, within the program) for thermal expansion. The cell $V_F/V_M$ value is in turn directly related to the core $V_F/V_M$ value - the difference being the amount of water in the extra region, as discussed by Montaldo [M2].

Fuel-to-moderator values corresponding to the cold cell, hot cell and hot core are presented in table (C-1).

The values of $\rho_o$ and A were obtained from the least squares linear regression fit to the data presented as pairs of tabulated $\rho$, B values (from LEOPARD output). In the following tables, the values of $k_\infty$ cited are the values taken directly from the LEOPARD output. They are the infinite medium value and not the system k value, which includes a leakage component determined by the input buckling value.

It is observed that the largest loss in reactivity takes place in the burnup interval between 0 and 150 MWD/MT . This reflects the buildup of the saturating fission products Xenon and Samarium. The second largest loss occurs between 150 and 850 MWD/MT . In consequence, these initial points were excluded from the set used in the curve fitting procedure.

Table. C-1

Equivalent values for cell and core fuel-to-moderator ratios.

Fuel-to-moderator ratios.

| Cold cell* | Hot cell | Hot core |
|---|---|---|
| 0.500 | 0.4986 | 0.4148 |
| 0.604 | 0.6012 | 0.4934 |
| 0.750 | 0.7457 | 0.6003 |
| 1.000 | 0.9921 | 0.7736 |

* Convention adopted in the present work.

Table. C- 2

Reactivity versus Burnup data for

$X_{puf} = 3.0$ w/o , and $V_{F/V_M} = 0.3$

| Burnup [GWD/MT] | $k_\infty$ | $\rho_\infty$ |
|---|---|---|
| 0.0 | 1.29089 | 0.22534 |
| 0.15 | 1.25957 | 0.20608 |
| 1.0 | 1.23541 | 0.19055 |
| 5.0 | 1.19490 | 0.16311 |
| 10.0 | 1.15011 | 0.13052 |
| 15.0 | 1.10601 | 0.09585 |
| 20.0 | 1.06107 | 0.05756 |
| 25.0 | 1.01442 | 0.01422 |
| 30.0 | 0.96566 | -0.03557 |
| 35.0 | 0.91516 | -0.09271 |
| 40.0 | 0.86370 | -0.15782 |

Table. C-3

Reactivity versus Burnup data for

$X_{puf}$ =4.0 w/o , and $V_{F/V_M}$ = 0.3

| Burnup [GWD/MT] | $k_\infty$ | $\rho_\infty$ |
|---|---|---|
| 0.0 | 1.29752 | 0.22930 |
| 0.15 | 1.26962 | 0.21236 |
| 1.0 | 1.24788 | 0.19864 |
| 5.0 | 1.21545 | 0.17726 |
| 10.0 | 1.18209 | 0.15404 |
| 15.0 | 1.14978 | 0.13027 |
| 20.0 | 1.11749 | 0.10514 |
| 25.0 | 1.08429 | 0.07774 |
| 30.0 | 1.04938 | 0.04706 |
| 35.0 | 1.01225 | 0.01210 |
| 40.0 | 0.97283 | -0.02793 |

Table. C- 4

Reactivity versus Burnup data for

$X_{puf}$ = 2.5w/o , and $V_{F/V_M}$ = 0.5

| Burnup [GWD/MT] | $k_\infty$ | $\rho_\infty$ |
|---|---|---|
| 0.0 | 1.18452 | 0.15578 |
| 0.15 | 1.15678 | 0.13553 |
| 1.0 | 1.13780 | 0.12111 |
| 5.0 | 1.10663 | 0.09636 |
| 10.0 | 1.07396 | 0.06887 |
| 15.0 | 1.04321 | 0.04142 |
| 20.0 | 1.01298 | 0.01281 |
| 25.0 | 0.98228 | -0.01804 |
| 30.0 | 0.95055 | -0.05203 |
| 35.0 | 0.91778 | -0.08958 |
| 40.0 | 0.88407 | -0.13113 |

Table. C- 5

Reactivity versus Burnup data for

$X_{puf} = 3.0\,w/o$ , and $V_{F/V_M} = 0.5$

| Burnup [GWD/MT] | $k_\infty$ | $\rho_\infty$ |
|---|---|---|
| 0.0 | 1.18475 | 0.15594 |
| 0.15 | 1.15944 | 0.13751 |
| 1.0 | 1.14200 | 0.12434 |
| 5.0 | 1.11532 | 0.10340 |
| 10.0 | 1.08827 | 0.08111 |
| 15.0 | 1.06297 | 0.05924 |
| 20.0 | 1.03813 | 0.03673 |
| 25.0 | 1.01283 | 0.01267 |
| 30.0 | 0.98650 | -0.01369 |
| 35.0 | 0.95890 | -0.04287 |
| 40.0 | 0.92958 | -0.07575 |

Table. C-6

Reactivity versus Burnup data for

$X_{puf}$ =4.0 w/o , and $V_{F/V_M}$ = 0.5

| Burnup [GWD/MT] | $k_\infty$ | $\rho_\infty$ |
|---|---|---|
| 0.0 | 1.18077 | 0.15309 |
| 0.15 | 1.15938 | 0.13747 |
| 1.0 | 1.14464 | 0.12636 |
| 5.0 | 1.12316 | 0.10965 |
| 10.0 | 1.10349 | 0.09378 |
| 15.0 | 1.08526 | 0.07856 |
| 20.0 | 1.06744 | 0.06318 |
| 25.0 | 1.04970 | 0.04735 |
| 30.0 | 1.03112 | 0.03018 |
| 35.0 | 1.01154 | 0.01141 |
| 40.0 | 0.99071 | -0.00937 |

Table. C- 7

Reactivity versus Burnup data for

$X_{puf}$ = 6.0 w/o , and $V_{F/V_M}$ = 0.5

| Burnup [GWD/MT] | $k_\infty$ | $\rho_\infty$ |
|---|---|---|
| 0.0 | 1.17018 | 0.14543 |
| 0.15 | 1.15433 | 0.13370 |
| 1.0 | 1.14346 | 0.12546 |
| 5.0 | 1.12671 | 0.11246 |
| 10.0 | 1.11433 | 0.10260 |
| 15.0 | 1.10313 | 0.09349 |
| 20.0 | 1.09246 | 0.08463 |
| 25.0 | 1.08160 | 0.07544 |
| 30.0 | 1.07068 | 0.06601 |
| 35.0 | 1.05929 | 0.05597 |
| 40.0 | 1.04729 | 0.04515 |

Table. C- 8

Reactivity versus Burnup data for

$X_{puf} = 4.0$ w/o , and $V_{F/V_M} = 0.604$

| Burnup [GWD/MT] | $k_\infty$ | $\rho_\infty$ |
|---|---|---|
| 0.0 | 1.13140 | 0.11614 |
| 0.15 | 1.11275 | 0.10133 |
| 1.0 | 1.10060 | 0.09140 |
| 5.0 | 1.08386 | 0.07737 |
| 10.0 | 1.06946 | 0.06495 |
| 15.0 | 1.05575 | 0.05281 |
| 20.0 | 1.04229 | 0.04057 |
| 25.0 | 1.02848 | 0.02769 |
| 30.0 | 1.01394 | 0.01375 |
| 35.0 | 0.99856 | -0.00143 |
| 40.0 | 0.98215 | -0.01818 |

Table. C- 9

Reactivity versus Burnup data for

$X_{puf}$ = 6.0 w/o , and $V_{F/V_M}$ = 0.604

| Burnup [GWD/MT] | $k_\infty$ | $\rho_\infty$ |
|---|---|---|
| 0.0 | 1.12142 | 0.10827 |
| 0.15 | 1.10817 | 0.09761 |
| 1.0 | 1.09970 | 0.09066 |
| 5.0 | 1.08680 | 0.07987 |
| 10.0 | 1.07831 | 0.07262 |
| 15.0 | 1.07048 | 0.06584 |
| 20.0 | 1.06270 | 0.05900 |
| 25.0 | 1.05457 | 0.05175 |
| 30.0 | 1.04617 | 0.04413 |
| 35.0 | 1.03701 | 0.03569 |
| 40.0 | 1.02711 | 0.02639 |

Table. C- 10

Reactivity versus Burnup data for

$X_{puf}$ = 8.0 w/o , and $V_{F/V_M}$ = 0.604

| Burnup [GWD/MT] | $k_\infty$ | $\rho_\infty$ |
|---|---|---|
| 0.0 | 1.11766 | 0.10527 |
| 0.15 | 1.10772 | 0.09724 |
| 1.0 | 1.10149 | 0.09214 |
| 5.0 | 1.09013 | 0.08268 |
| 10.0 | 1.08372 | 0.07725 |
| 15.0 | 1.07839 | 0.07269 |
| 20.0 | 1.07322 | 0.06822 |
| 25.0 | 1.06759 | 0.06331 |
| 30.0 | 1.06176 | 0.05817 |
| 35.0 | 1.05532 | 0.05242 |
| 40.0 | 1.04847 | 0.04623 |

Table. C- 11

Reactivity versus Burnup data for

$X_{puf}$ = 4.0w/o , and $V_{F/V_M}$ = 0.75

| Burnup [GWD/MT] | $k_\infty$ | $\rho_\infty$ |
|---|---|---|
| 0.0 | 1.07345 | 0.06842 |
| 0.15 | 1.05803 | 0.05485 |
| 1.0 | 1.04906 | 0.04677 |
| 5.0 | 1.03788 | 0.03650 |
| 10.0 | 1.02938 | 0.02854 |
| 15.0 | 1.02041 | 0.02000 |
| 20.0 | 1.01085 | 0.01073 |
| 25.0 | 1.00066 | 0.00066 |
| 30.0 | 0.98962 | -0.01049 |
| 35.0 | 0.97760 | -0.02291 |
| 40.0 | 0.96453 | -0.03677 |

Table. C- 12

Reactivity versus Burnup data for

$X_{puf} = 6.0$ w/o , and $V_{F/V_M} = 0.75$

| Burnup [GWD/MT] | $k_\infty$ | $\rho_\infty$ |
|---|---|---|
| 0.0 | 1.06767 | 0.06338 |
| 0.15 | 1.05729 | 0.05419 |
| 1.0 | 1.05141 | 0.04890 |
| 5.0 | 1.04279 | 0.04103 |
| 10.0 | 1.03852 | 0.03709 |
| 15.0 | 1.03408 | 0.03296 |
| 20.0 | 1.02908 | 0.02826 |
| 25.0 | 1.02333 | 0.02280 |
| 30.0 | 1.01677 | 0.01649 |
| 35.0 | 1.00950 | 0.00940 |
| 40.0 | 1.00128 | 0.00128 |

Table. C- 13

Reactivity versus Burnup data for

$X_{puf} = 8.0$ w/o , and $V_{F/V_M} = 0.75$

| Burnup [GWD/MT] | $k_\infty$ | $\rho_\infty$ |
|---|---|---|
| 0.0 | 1.07027 | 0.06566 |
| 0.15 | 1.06279 | 0.05908 |
| 1.0 | 1.05869 | 0.05544 |
| 5.0 | 1.05083 | 0.04837 |
| 10.0 | 1.04700 | 0.04489 |
| 15.0 | 1.04397 | 0.04212 |
| 20.0 | 1.04060 | 0.03902 |
| 25.0 | 1.03661 | 0.03532 |
| 30.0 | 1.03209 | 0.03109 |
| 35.0 | 1.02684 | 0.02614 |
| 40.0 | 1.02090 | 0.02047 |

Table. C-14

Reactivity versus Burnup data for

$X_{puf}$ =10.0w/o , and $V_{F/V_M}$ = 1.0

| Burnup [GWD/MT] | $k_\infty$ | $\rho_\infty$ |
|---|---|---|
| 0.0 | 1.04550 | 0.04352 |
| 0.15 | 1.04192 | 0.04023 |
| 1.0 | 1.03999 | 0.03845 |
| 5.0 | 1.03384 | 0.03273 |
| 10.0 | 1.02883 | 0.02802 |
| 15.0 | 1.02470 | 0.02410 |
| 20.0 | 1.02094 | 0.02051 |
| 25.0 | 1.01691 | 0.01663 |
| 30.0 | 1.01256 | 0.01240 |
| 35.0 | 1.00771 | 0.00765 |
| 40.0 | 1.00246 | 0.00245 |

Table. C- 15

Reactivity versus Burnup data for

$X_{puf}$ =12.0w/o , and $V_{F/V_M}$ = 1.0

| Burnup [GWD/MT] | $k_\infty$ | $\rho_\infty$ |
|---|---|---|
| 0.0 | 1.06976 | 0.06521 |
| 0.15 | 1.06689 | 0.06278 |
| 1.0 | 1.06501 | 0.06104 |
| 5.0 | 1.05740 | 0.05428 |
| 10.0 | 1.04984 | 0.04747 |
| 15.0 | 1.04365 | 0.04182 |
| 20.0 | 1.03797 | 0.03658 |
| 25.0 | 1.03268 | 0.03165 |
| 30.0 | 1.02745 | 0.02672 |
| 35.0 | 1.02215 | 0.02167 |
| 40.0 | 1.01659 | 0.01632 |

Table. C- 16

Reactivity versus Burnup data for

$X_{puf}$ = 14.0w/o , and $V_{F/V_M}$ = 1.0

| Burnup [GWD/MT] | $k_\infty$ | $\rho_\infty$ |
|---|---|---|
| 0.0 | 1.09489 | 0.08667 |
| 0.15 | 1.09251 | 0.08468 |
| 1.0 | 1.09031 | 0.08283 |
| 5.0 | 1.08120 | 0.07510 |
| 10.0 | 1.07165 | 0.06686 |
| 15.0 | 1.06349 | 0.05970 |
| 20.0 | 1.05619 | 0.05320 |
| 25.0 | 1.04941 | 0.04708 |
| 30.0 | 1.04296 | 0.04119 |
| 35.0 | 1.03675 | 0.03545 |
| 40.0 | 1.03053 | 0.02963 |

# REFERENCES


A1 Agnew, M., et al. "MESSAGE: A MODEL FOR ENERGY SUPPLY SYSTEMS ALTERNATIVES AND THEIR GENERAL ENVIRONMENTAL IMPACT," RM-78-26, Laxenburg, Austria: IIASA, (1978).

A2 Abbaspour, A.T. and Driscoll, M.J., "THE FUEL CYCLE ECONOMICS OF IMPROVED URANIUM UTILIZATION IN LIGHT WATER REACTORS," MIT-EL 79-001, MIT NE-224, (January 1979).

B1 Bukovsky, J., Martel, E., "REFUEL - NUCLEAR REFUELING SCHEDULE GENERATOR," Commonwealth Edison Co., (1971).

B2 Beard, C.L., "AN IMPROVED LONG RANGE FUEL MANAGEMENT PROGRAM," MITNE-216, MIT, (1978).

B3 Benedict, M., Pigford, T. and Levi, H., "NUCLEAR CHEMICAL ENGINEERING," 2nd ed., McGraw-Hill, (1981).

B4 Barry, R.F., "LEOPARD - A SPECTRUM DEPENDENT NON-SPATIAL DEPLETION CODE," WCAP-3269-26, (September 1963).

D1 Downar, T.J., "AN INTEGRATED METHOD FOR MID-RANGE IN-CORE PWR FUEL MANAGEMENT AND CORE DESIGN," Ph.D. Thesis, Dept. of Nucl. Eng., MIT, (May 1984).

D2 De La Garza, A., Garrett, G.A. and Murphy, J.E., "VALUE FUNCTIONS FOR MULTICOMPONENT ISOTOPE SEPARATION," AEC, R & D report K-1455, (July 1960).

D3 Driscoll, M.J., class notes, MIT subject no. 22.35, Fuel Management, Spring 1982.

D4 Delene, J.G. and Hermann, O.W., "REFCO-83 USERS MANUAL," ORNL/TM-9186, (June 1984).

D5 Drew, M.W., "US URANIUM DEPOSITS, A GEOSTATISTICAL MODEL," Resource Policy, Vol. 3, No. 1, (March 1977).

D6 Driscoll, M.J., Pilat, E.E. and Downar, T.J., "THE LINEAR REACTIVITY MODEL FOR NUCLEAR REACTOR FUEL MANAGEMENT," Draft manuscript of monograph (to be published), copy dated January 1984.

E1 Eich, W.J., "ADVANCED RECYCLE METHODOLOGY PROGRAM (ARMP): PROJECT STATUS REPORT," EPRI 118-1, (December 1975).

E2 Electric Power Research Institute, "Technical Assessment Guide," EPRI-P-2410-SR, May 1982.

G1 Garel, Keith and Driscoll, M.J., "FUEL CYCLE OPTIMIZATION OF THORIUM AND URANIUM FUELED PWR SYSTEMS," MITNE-204, MIT-EL 77-018, (1977).

G2 Graves, H.W., "NUCLEAR FUEL MANAGEMENT," John Wiley & Sons, Inc., (1979).

G3 Gharamani, K. and Driscoll, M.J., "ORE PRICE ESCALATION IN FUEL CYCLE ECONOMIC ANALYSIS," Trans. Am. Nucl. Soc., 28, 383-384, (1978).

H1 Hafele, W. et al, "MEDIUM AND LONG RANGE ENERGY STRATEGIES," IIASA, (1979).

H2 Hsieh, H., "LONG RANGE FUEL MANAGEMENT FOR LWR STUDIES," NE/SM thesis, Dept. of Nucl. Eng., MIT, (August 1979).

I1 INFCE, "INTERNATIONAL NUCLEAR FUEL CYCLE EVALUATION," IAEA, ISP534-1, (1980).

I2 IIASA, "ENERGY IN A FINITE WORLD: PATHS TO A SUSTAINABLE FUTURE," Report by the Energy Systems Program Group of IIASA, (1981).

K1 Koch, L. and Schoof, S., "THE ISOTOPE CORRELATION EXPERIMENT," ESARDA Final Report, EUR 7766 EN, KfK 337, ISPRA, Italy, (July 1982).

L1 Lapillonne, B., "MEDEEZ: A MODEL FOR LONG-TERM ENERGY DEMAND EVALUATION," RR-78-17, IIASA, (1978).

L2 Lan, J.S., "ASSESSMENT OF THE PREVAILING PHYSICS CODES: LEOPARD, LASER, AND EPRI-CELL," Trans. Am. Nucl. Soc., 38, p685-687, (June 1981).

L3 Loh, W.T., Driscoll, M.J. and Lanning, D.D., "THE USE OF BURNABLE POISON TO IMPROVE URANIUM UTILIZATION IN PWR'S," DOE/ET/34022-3, (May 1982).

M1 MANAGE, "A CODE FOR MANAGEMENT ANALYSIS OF NUCLEAR ALLOCATION FOR THE GENERATION OF ELECTRICITY," EPRI-RP298-1

M2 Montaldo-Volachec, E.M., "COMPUTATION OF SEQUENTIAL BATCH INTERACTIONS IN NUCLEAR FUEL MANAGEMENT," NE thesis, Dept. of Nucl. Eng., MIT, (February 1984).

M3 Mosteller, R.D., et al, "PLUTONIUM ISOTOPIC CALCULATIONS FOR A MODERN LIGHT WATER REACTOR," Nucl. Tech., Vol. 44, p192-196, (June 1979).

M4 Morris, C.J., Wescott, R.I., and Forbes, I.A., "A CODE TO ASSIST IN TEACHING NUCLEAR FUEL MANAGEMENT," Trans. Am. Nucl. Soc., p99-100, (June 1977).

N1 Neff, T.L., "THE INTERNATIONAL URANIUM MARKET," Ballinger, Cambridge, Mass., (1984).

N2 "NUCLEAR PROLIFERATION AND CIVILIAN NUCLEAR POWER," Report of the Nonproliferation Alternative Systems Assessment Program (NASAP), DOE/NE-0001, (June 1980).

P1 Parvez, A. and Becker, M., "RELATIVE WORTH OF U-233 AND U-235 IN LIGHT WATER REACTOR FUEL CYCLES," Nucl. Tech., 63, 176, (1983).

P2 Parvez, A. "RECYCLE VALUE OF DISCHARGED FUEL BY SUBSTITUTION METHOD," Trans. Am. Nucl. Soc., Vol. 46, (June 1984).

S1 Specker, S.R. and Forkner, S.L., "SCOPING - A SIMULATION WITH CYCLING OPTIMIZATION FOR PLANNING AND INTEGRATING NUCLEAR GENERATION INTO A POWER SYSTEM," TVA/FES-041, (1972).

S2 Smith, G.W., "ENGINEERING ECONOMY; ANALYSIS OF CAPITAL EXPENDITURES," 3rd ed., Iowa State University Press, (1973).

S3 Spinrad, B.I., "EFFECTS OF ACCOUNTING RULES ON UTILITY CHOICES OF ENERGY TECHNOLOGIES IN THE UNITED STATES," RR-80-27, Laxenburg, Austria, IIASA, (July 1980).

S4 Sefcik, J.A., Driscoll, M.J. and Lanning, D.D., "ANALYSIS OF STRATEGIES FOR IMPROVING URANIUM UTILIZATION IN PWR S," DOE/ET/34022-1, (January 1981).

T1 Thomas, C.R., et al, "A SURVEY OF NUCLEAR FUEL CYCLE CODES," ORNL/TM-7747, (April 1981).

T2 Turnage, J.C., et al, "THE OAK RIDGE SYSTEM INTEGRATION MODEL (ORSIM) FOR OPTIMIZATION UTILITY GENERATION PLANNING," ORNL-TM-4506, (1975).

W1 Wolfe, B., and Judson, B.F., "CLOSING THE FUEL CYCLE," Nuclear News, (January 1984).

W2 White, M.K. and Dodd, L.R., "PARAMETRIC ANALYSIS OF THE ECONOMIC INCENTIVE FOR INDIVIDUAL REACTOR TO REPROCESS FOR RECYCLE," Trans. Am. Nucl. Soc., Vol. 46, (June 1984).

Z1 Zimmermann, M.W., "A CRITIQUE AND SIMPLIFICATION OF NUCLEAR FUEL CYCLE ECONOMICS CALCULATIONS," SM thesis, Dept. of Nuclear Engineering, MIT, (August 1983).